

Physical and Computational Models of the Gloss
Exhibited by the Human Hair Tress. A Study of
Conventional and Novel Approaches to the Gloss
Evaluation of Human Hair.

A thesis submitted to The University of Manchester for the degree
of Doctor of Philosophy in the Faculty of Engineering and Physical
Sciences

2013

Syed Naveed. I. H. Rizvi

School of Materials

Table of Contents

Abstract	17
Declaration	18
Copyright Statement	19
Acknowledgements	21
Chapter 1 Introduction	24
1.1 Aims and Objectives.....	25
1.2 Thesis outline	28
Chapter 2 Literature Review	31
2.1 Light.....	32
2.2 How Objects modify light.....	32
2.2.1 Laws governing the reflection of light.....	33
2.3 How light is measured.....	34
2.3.1 Radiometry.....	34
2.3.2 Photometry	34
2.3.3 Colorimetry	35
2.4 What is Gloss?.....	41
2.4.1 Hunter's contribution in defining Gloss	42
2.4.2 Standardized Method for measuring Gloss.....	45
2.4.3 Limitations using conventional Glossmeters.....	47
2.4.4 Goniophotometer	48
2.5 Optical properties of the Human Eye.....	50
2.6 Detectors (Image capture devices)	54
2.6.1 Digital SLR Camera	54
2.6.2 Dynamic range	57
2.6.3 High Dynamic range	58
2.7 BRDF (Bi-directional Reflectance Distribution Function)	59
2.8 Psychophysics.....	62
2.8.1 Evolution of Psychophysics	62
2.8.2 Measurement scales	63
2.8.3 Classes of Visual psychophysics experiments	63
2.9 Human Hair	66
2.10 Hair types.....	66
2.11 General Structure and Hair Growth	67
2.11.1 The Cuticle	69
2.11.2 The Cortex.....	71
2.11.3 The Medulla	72
2.12 The Chemical Composition of Human Hair	73
2.12.1 Bonding in Keratin.....	74
2.13 Physical properties of the human Hair	76
2.13.1 Elastic and Tensile Properties	76
2.13.2 Bending and fibre stiffness	78
2.13.3 Torsion and Fibre rigidity	79

2.13.4	Porosity	79
2.13.5	Friction	80
2.13.6	Hair Colour	80
2.14	Hair Cosmetics	81
2.14.1	Shampoos	81
2.14.2	Hair Conditioners	81
2.14.3	Styling Aids	82
2.15	Hair-shine Models (Computational models)	83
2.15.1	Introduction	83
2.15.2	Evolution of Gloss evaluation models for the human hair.....	89
2.16	Summary	103
Chapter 3 Methodology.....		106
3.1	Methodology	107
3.2	Overview	107
3.3	Sample preparation.....	109
3.3.1	Hair treatment methods to create different level of hair shine.....	109
3.3.2	Application Methods for Commercial Products	112
3.4	Visual assessment of Heat, Mechanically, and Chemically treated hair tresses in an unconstrained viewing environment	116
3.4.1	Problems with the visual assessment of human hair gloss	118
3.5	On-Screen Gloss assessments of human hair tresses	118
3.5.1	Method	119
3.5.2	Tress-Gloss 2.0 (GUI) Overview	120
3.6	Hair tress Image Capture setup for hair tresses.....	122
3.6.1	Problems using Colour-Matching booth	124
3.7	Gonio Image Capture Setup	124
3.7.1	Arc	125
3.7.2	Capture device and device holder.....	125
3.7.3	Light Source.....	126
3.7.4	Sample holder (cylinder)	127
3.7.5	Tensioner (spring / clip)	127
3.8	Image-Capture process	128
3.9	Summary	131
Chapter 4 The Optical Properties of Human Hair Tresses and the Development of Novel Human Hair Gloss Evaluation Models		133
4.1	Overview	134
4.2	Effect of different levels of Shine on the Lightness (L^*) and Chroma (C^*) of Blonde, European-Brown and Oriental Hair tress images.....	135
4.3	Effect of different levels of Shine on the Lightness (L^*) and Chroma (C^*) distributions of Blonde, European-Brown and Oriental hair tress images.....	138
4.4	High Dynamic Range Imaging.....	140
4.4.1	Effect of different shine levels of hair tresses on the averaged L^* area of a hair tress at higher shutter speeds.....	142

4.5	Understanding the properties of Human Hair Tress reflection bands	146
4.6	Colour Gradient on hair tresses	146
4.7	The Chroma-Specular effect.....	147
4.8	Separating reflection bands	148
4.9	Separating the shine-band from the hair tress image	148
4.10	Separating Chroma bands.....	152
4.10.1	Separating the Chroma Specular Band from the Hair Tress Images	152
4.10.2	Separating the Chroma Diffuse Bands from the Hair Tress Images	154
4.11	Plotting each reflection band.....	155
4.12	Effect of different treatments on their reflection bands	156
4.12.1	Effect of different treatments on the shine area of the tress.....	156
4.12.2	Effect of different treatments on the Chroma Specular (C_s) Region.....	157
4.13	Effect of the different treatments on FWHM of the Shine curve	159
4.14	Differences in the L^* value and C^* values.....	160
4.15	Effects of different treatments on the contrast ratio (L^* area / C^* area).....	161
4.16	Quantifying human hair gloss	162
4.17	Results and discussion	164
4.17.1	Quantifying the gloss of the European-Brown hair tresses	164
4.17.2	Quantifying gloss of Blonde hair tress	166
4.17.3	Quantifying the gloss of Oriental hair tresses.....	167
4.18	Repeatability of the Model	169
4.19	Summary	177

Chapter 5 A Psychophysical Study of the Perceived Gloss in Images of Human Hair Tresses..... 181

5.1	Overview	182
5.2	Method of constant stimuli (forced choice – pair comparison) Psychophysical experiment	184
5.2.1	Tress Images used in the psychophysical experiment	184
5.2.2	Tobii TX 300 Eye-Tracking system	185
5.2.3	Creating and editing the Psychophysical test using Tobii Studio	187
5.2.4	Participants information	190
5.2.5	Evaluation selection of the Psychophysical experiment	191
5.3	Data analysis of Blonde hair tresses.....	192
5.3.1	Blonde Virgin – Blonde Wax.....	192
5.3.2	Blonde Virgin – Blonde SLES.....	197
5.3.3	Blonde Virgin- Blonde Shine spray	202
5.3.4	Comparisons of Tresses treated with same products	207
5.4	Data analysis of European Brown and Oriental hair tresses	212
5.4.1	Virgin–Wax comparison (European Brown and Oriental)	212
5.4.2	Virgin–SLES Comparison.....	217
5.4.3	Virgin-Shine spray	223
5.4.4	Conclusion	229

Chapter 6 Conclusions and Future Work..... 234

6.1	Conclusions	235
6.1.1	Development of methods to produce different hair tress shine levels	236
6.1.2	Development of the hair tress Image Capture System	236
6.1.3	Psychophysical study and development of the Graphical User Interfaces (GUIs) – Tress Gloss 1.0 and Tress Gloss 2.0	237
6.1.4	A new interpretation of the reflection band on the hair tress, Chroma-Specular (C_s)	237
6.1.5	Segmentation of the reflection bands of the human hair tress.....	238
6.1.6	Development of the novel human hair gloss models.....	239
6.2	Psychophysical study.....	241
6.2.1	Paired image comparisons used in the psychophysical study.....	241
6.2.2	Participants' gaze analysis.....	241
6.2.3	Average decision duration of the participants.....	242
6.2.4	Areas on the tress images used by the participants to evaluate hair shine and the importance of the Chroma area.....	243
6.3	Comparison between the participant's choices and the gloss evaluation models	244
6.4	Future work.....	246
6.4.1	Tress Preparation	246
6.4.2	Tress Evaluation Models	246
6.4.3	Tress Gloss Capture System	247
6.4.4	Virtual Tress Presentation.....	248
6.4.5	Psychophysical Evaluations of Gloss	248
6.5	References:	250

Word-Count: 57,195

List of Figures

Figure 2-1 Fundamental properties of light: intensity, spectrum and polarization (Lefaudeux <i>et al.</i> 2008).....	32
Figure 2-2 CIE standard observer photopic luminous efficiency curve (Reinhard <i>et al.</i> 2006b).	34
Figure 2-3 Colour-matching experiment (Rigg 1997).	35
Figure 2-4 Stiles and Burch (1959) 10° colour-matching functions(Reinhard <i>et al.</i> 2006b).	37
Figure 2-5 CIE 1931 2-degree XYZ colour-matching functions(Reinhard <i>et al.</i> 2006b). ...	37
Figure 2-6 CIE 1931 x, y Chromaticity diagram (Reinhard <i>et al.</i> 2006b).....	39
Figure 2-7 CIELAB colour space (Gonnet 1998).....	40
Figure 2-8 Goniophotometric curves of the total reflectance factor with the decomposition of the reflectance (specular and diffuse) (Barkas 1939).....	42
Figure 2-9 Reflectance function of Specular gloss (Hunter 1975b).....	43
Figure 2-10 Reflectance function of Sheen (Hunter 1975b).....	43
Figure 2-11 Reflectance function of Contrast gloss or Lustre (Hunter 1975b).....	44
Figure 2-12 Reflectance function of absence of bloom (Hunter 1975b).....	44
Figure 2-13 Diagram of Hunterlab Lustermeter (Hunter 1975a).....	46
Figure 2-14 A schematic diagram of the measurement of gloss (Silvennoinen <i>et al.</i> 2007).	47
Figure 2-15 (a) Effect of waviness on the measurement of the gloss of the surface (b) Effect of curved surface on the measurement of the gloss of a surface (Silvennoinen <i>et al.</i> 2007)	48
Figure 2-16 Schematic of Goniophotometer (Silvennoinen <i>et al.</i> 2007).....	49
Figure 2-17 Goniophotometer curve of a dark-brown human hair (Stamm <i>et al.</i> 1977b).....	49
Figure 2-18 Horizontal section of the human eye (Hill 1997).....	50
Figure 2-19 Resolving power of the eye (Hill 1997)	52
Figure 2-20 Rods and Cones (Hill 1997).....	52
Figure 2-21 Absorption spectra of the four-receptor types (Hill 1997).....	53
Figure 2-22 Rods and Cones receptor density distribution across the retina (Hill 1997).	53
Figure 2-23 Typical arrangement of an SLR digital still camera (Toyoda 2006)	54
Figure 2-24 Image processing involved in a Digital Still Camera (modified from (Ramanath <i>et al.</i> 2005)).....	55
Figure 2-25 The Bayer arrangement of colour filters (Re-drawn from (Bayer 1976))	56
Figure 2-26 Test image with contrast ratio 10:1 (Bloch <i>et al.</i> 2007)	58
Figure 2-27 Virgin-Oriental Human Hair tress at 1s, 1/3s, 1/20s shutter speed.	59
Figure 2-28 Virgin-Oriental Human Hair tress images captured at various shutter speeds (1s-1/200s)	59
Figure 2-29 BRDF geometry (Tribble 2000).	60
Figure 2-30 Conventional gonireflectrometer with movable light source and photometer (Ward 1992)	60
Figure 2-31 Luminous intensity according to the angle of observation (in degrees) of a European- brown hair (Guiolet <i>et al.</i> 1987).	61
Figure 2-32 Schematic illustrating the three stages of growth of the human hair (Robbins 2002b).	68

Figure 2-33 Schematic diagram of a cross section of a human hair fibre (Redrawn (Robbins 2002b)).	69
Figure 2-34 Scale lifting caused by fatiguing chemically undamaged hair (Robbins 2002b)	70
Figure 2-35 Layers between Cuticle cell membrane(Rushton 2006).	70
Figure 2-36 Schematic anatomical arrangement of human scalp hair (Rushton 2006) ...	72
Figure 2-37 General amino acid structure (R represents a chemical group) (Robbins 2002a).	74
Figure 2-38 Hydrogen Bonding (= represents hydrogen bonding) (Rushton 2006)	75
Figure 2-39 Ionic bond (Rushton 2006).	75
Figure 2-40 Disulphide Bond (Rushton 2006).	76
Figure 2-41 Load-elongation curves for human hair fibres (Robbins 2002c)	77
Figure 2-42 Modification of the structure of keratin in an elongated hair before it breaks when the fibre is stretched (L'Oreal, 2005).	78
Figure 2-43 Schematic diagram of a bent hair fibre (Robbins 2002c).	79
Figure 2-44 Appearance of a Hair tress with the Shine, Chroma and Diffuse band.	83
Figure 2-45 Lustre is considered to depend on three parameters. (a) Increase of the amount of light reflected. (b) Reduction of the width of the specular light band. (c) The background on which the reflection is observed (Lefaudeux <i>et al.</i> 2008)	84
Figure 2-46 Reflection of light from front and back face of idealized cylindrical fibre (Modified and redrawn from (Stamm <i>et al.</i> 1977a)).	85
Figure 2-47 Possible reflection of incident light by a hair fibre (1) Reflection by cuticle (2) Reflection by cortex cells (3) Reflection by some smoothening substance (4) Reflection by cuticle after entering the fibre. (Re-drawn and modified from (Czepluch <i>et al.</i> 1993)).	86
Figure 2-48 Method employed for illuminating a planar array of parallel oriented hair fibres in order to obtain reflectance curve from a goniophotometer (Stamm <i>et al.</i> 1977a).	86
Figure 2-49 Rudimentary diagram of a goniophotometer experiment (Reich and Robbins 1993).	87
Figure 2-50 Optical model of an individual Hair Fibre (Modified and redrawn from (Stamm <i>et al.</i> 1977a)).	87
Figure 2-51 Diagram of the Goniophotometer built by Guiolet (Guiolet <i>et al.</i> 1987).....	92
Figure 2-52 Luminous intensity re-emitted according to the angle of observation in degrees by a brown hair. Angle of incidence 30° (Guiolet <i>et al.</i> 1987)	93
Figure 2-53 Decomposition of the goniophotometric (GP) curve into its three components - Specular reflection(s), Internal reflection (ir) and Diffuse reflection (d) (Guiolet <i>et al.</i> 1987).	94
Figure 2-54 Definition of gloss (GP curve of a dark brown hair) (Guiolet <i>et al.</i> 1987).	94
Figure 2-55 A typical light scattering curve for a virgin Oriental hair. D is the diffuse reflectance, S is the specular reflectance and W is the width of the curve at half height (Reich and Robbins 1993).	95
Figure 2-56 A typical goniophotometric curve broke down into specular and diffuse components (Keis <i>et al.</i> 2004a).	96
Figure 2-57 Goniophotometric curve of a standard black mirror (Keis <i>et al.</i> 2004a).	97
Figure 2-58 Schematic diagram of an apparatus to measure the lustre of hair (Re-drawn (McMullen and Jachowicz 2003)).	98

Figure 2-59 Image of Human hair tress showing dot-like reflection	98
Figure 2-60 Luminosity analysis horizontal to the fibre axes with a plot of luminance vs. distance for one of the horizontal lines. (Re-drawn(McMullen and Jachowicz 2004))	99
Figure 2-61 Optical set-up of the polarization imaging system (Lefaudeux <i>et al.</i> 2008)	100
Figure 2-62 (a) sample positioned on the cylinder (b) Complete angular distribution with a single image (Lefaudeux <i>et al.</i> 2008)	101
Figure 2-63 3 images are acquired from SAMBA: an intensity image showing the normal view of the hair a specular image showing only the reflections (shine and Chroma) and a diffused light image showing the diffused light only (Lefaudeux <i>et al.</i> 2008).	101
Figure 2-64 Angular profiles computed from the images acquired by averaging along the width of the sample (Lefaudeux <i>et al.</i> 2008).....	102
Figure 2-65 Lustre is considered to depend on three parameters. (a) Increase of the amount of light reflected. (b) Reduction of the width of the specular light band. (c) The background on which the reflection is observed	104
Figure 3-1 Schematic diagram of heat treatment experiment.....	110
Figure 3-2 Combing tester for mechanical treatment.....	111
Figure 3-3 Schematic of the spray-based product application method	114
Figure 3-4 Schematic of how wax is applied onto the hair tresses	115
Figure 3-5 Presentation of Hair tresses Set A is heat treated hair tresses, Set B is hair tresses treated mechanically and Set C is hair tresses treated chemically	117
Figure 3-6 Main window of the Tress-Gloss 1.0	119
Figure 3-7 Observer information form (screen-shot from Tress Gloss 1.0 GUI)	120
Figure 3-8 Observer information form (screen-shots from Tress Gloss 1.0 GUI)	121
Figure 3-9 Main window of the Tress-Gloss 2.0, paired comparison forced choice test	122
Figure 3-10 Image capture setup (pilot study)	123
Figure 3-11 Cylinder used in the pilot study.....	123
Figure 3-12 Image of a European Brown Hair Tress captured in the colour-matching booth under cool white lighting.....	124
Figure 3-13 Gonio-Image Capture Setup.....	125
Figure 3-14 Distance between the capture device and sample in the image capture setup	126
Figure 3-15 Front-view of the light-box	126
Figure 3-16 Schematic diagram of the cylinder.....	127
Figure 3-17 Hair tress mounted on the cylinder with standards.....	127
Figure 3-18 Hair clip and spring.....	128
Figure 3-20 Image captured by the camera and Cropped image of the hair tress.....	130
Figure 4-1 Average L* values of virgin Blonde, virgin European-Brown and virgin Oriental hair tresses	136
Figure 4-2 Average L* and C* curve of the Virgin Blonde hair tress image.....	137
Figure 4-3 Average L* and C* curve of the Virgin European Brown hair tress image	137
Figure 4-4 Average L* and C* curve of the Virgin Oriental hair tress image.....	138
Figure 4-5 Average L* and C* distribution curves of virgin Blonde tress, Blonde tress treated with wax, Blonde tress treated with shine-spray and Blonde tress treated with SLES.	139

Figure 4-6 Average L* and C* curves of virgin European-Brown tress, European-Brown tress treated with wax, European-Brown tress treated with shine-spray and European-Brown tress treated with SLES.....	139
Figure 4-7 Average L* and C* curves of virgin Oriental tress, Oriental tress treated with wax, Oriental tress treated with shine-spray and Oriental tress treated with SLES	139
Figure 4-8 Images of Oriental Hair tresses captured at different shutter speeds a) Hair tress treated with shine enhancing product (shine spray - top), b) Virgin Hair tress (middle), c) Hair tress treated with Wax to achieve dull effect (3% Wax-bottom)	141
Figure 4-9 Images of European-Brown Hair tresses captured at different shutter speeds a) Hair tress treated with shine enhancing product (shine spray - top), b) Virgin Hair tress (middle), c) Hair tress treated with Wax to achieve dull effect (3% Wax - bottom)	141
Figure 4-10 Images of Blonde Hair tresses captured at different shutter speeds a) Hair tress treated with shine enhancing product (shine spray - top), b) Virgin Hair tress (middle), c) Hair tress treated with Wax to achieve dull effect (3% Wax - bottom)	142
Figure 4-11 Areas under the averaged L* value curves of Blonde hair tresses treated with different products (Virgin, Wax, SLES and Shine-spray) at different shutter speeds.	143
Figure 4-12 Areas under the averaged L* value curves of European-Brown hair tresses treated with different products (Virgin, Wax, SLES and Shine-spray) at different shutter speeds.....	143
Figure 4-13 Areas under the averaged L* value curves of Oriental hair tresses treated with different products (Virgin, Wax, SLES and Shine-spray) at different shutter speeds.	144
Figure 4-14 Areas under the average C* value curves of Blonde hair tresses treated with different products (Virgin, Wax, SLES and Shine-spray) at different shutter speeds.	144
Figure 4-15 Areas under the average C* value curves of European-Brown hair tresses treated with different products (Virgin, Wax, SLES and Shine-spray) at different shutter speeds.....	145
Figure 4-16 Areas under the average C* value curves of Oriental hair tresses treated with different products (Virgin, Wax, SLES and Shine-spray) at different shutter speeds.	145
Figure 4-17 The Chroma band of the SLES-washed Blonde hair tress (top half), segmented into two parts and the CIE L*a*b* colour coordinates are adjacent to each part.	146
Figure 4-18 The Chroma band of the SLES-washed European -Brown hair tress (top half), segmented into two parts and CIE L*a*b* colour coordinates are presented adjacent to each part.	147
Figure 4-19 The Chroma band of the SLES-washed Oriental hair tress (top half), segmented into two parts and CIE L*a*b* colour coordinates are presented adjacent to each part.	147
Figure 4-20 Recreation of the Chroma-Specular effect. (a) Shows blur effect on each side of the white band, (b) no blur effect, (c) shine band, as it appears on the hair tress,	

overlaid on a plain colour background with added blur on each side (d) shine-band without blur.....	148
Figure 4-21 Typical L* curve of an European-Brown Human hair tress. The maximum of the averaged L* profile values corresponds to the brightest part of the human hair tress.....	149
Figure 4-22 The shine area was selected and cropped. The frequency of L* and C* values of the area are plotted in the histogram (this sets the limits in order to separate the shine band from the image).	150
Figure 4-23 Shine-band separation from images of European-Brown, Blonde and Oriental Hair tresses (a), (d), (g) Original images, (b), (e), (h) Shine-band separated and overlay on the original image (confirmation of separation), (c), (f), (i) Separated Shine-band.	151
Figure 4-24 Histograms of the L* and C* values in the Chroma-Specular area	152
Figure 4-25 Chroma-Specular separation from images of European-Brown, Blonde and Oriental hair tresses. (a), (d), (g) Original hair tress images, (b), (e), (h) C _s separated and overlaid onto the original image (confirmation of separation), (c), (f), (i) Separated Chroma-Specular, C _s	153
Figure 4-26 Chroma-Diffuse separation from images of European-Brown, Blonde and Oriental hair tresses. (a), (d), (g) Original images, (b), (e), (h) C _d separated and overlaid onto the original image (confirmation of separation), (c), (f), (i) Separated Chroma-Diffuse, C _d	154
Figure 4-27 European Brown, Oriental and Blonde virgin hair tresses Lightness (L*) and Chroma (C*) profiles, Shine band (shine), Chroma-Specular (C _s) and Chroma-Diffuse (C _d) plots.....	155
Figure 4-28 Average Shine-areas (cumulative L*) of the Blonde, European Brown and Oriental tresses treated with Wax, SLES and Shine-spray.....	157
Figure 4-29 Chroma-Specular areas of the Blonde and European Brown hair tresses treated with Wax, SLES and Shine Spray	158
Figure 4-30 Chroma-Specular area of the Oriental hair tress treated with Wax, SLES and Shine spray.	159
Figure 4-31 FWHM of the shine curve of the tresses treated with Wax, SLES and Shine spray.....	160
Figure 4-32 Difference between Shine value (L* value in the shine-area) and the Chroma values (C* value in the Chroma-specular-area) of the tresses treated with Wax, SLES and Shine spray	161
Figure 4-33 L* and C* area ratio of the European Brown tress.	162
Figure 4-34 The gloss of European Brown hair tresses with different treatments	165
Figure 4-35 A comparison of the normalised shine values of the treated European Brown hair tresses, generated by four different gloss evaluation models.....	165
Figure 4-36 Images of Blonde hair tress with different treatments.....	166
Figure 4-37 A Comparison of the normalised shine values, of the Blonde hair tress images, generated by different models	167
Figure 4-38 Oriental hair tresses applied with different treatments	168
Figure 4-39 A graphical representations of the normalised shine assessment values of an Oriental hair tress generated by different gloss evaluation models.....	168
Figure 4-40 Blonde hair tresses, taken from same batch, treated with 3% wax.....	169

Figure 4-41 Repeats of Blonde hair tress comparisons and shine values generated by models	171
Figure 4-42 Normalised shine assessment values of the Blonde hair tresses treated with different products.	171
Figure 4-43 Repeats of European-Brown tress for comparison of the shine values generated by the different models.	173
Figure 4-44 Average shine values, of the European Brown hair tress treated with different products, generated by different models.	174
Figure 4-45 Repeats of European-Brown tresses. A comparison of the shine assessment values generated by the different models.	176
Figure 4-46 Average shine values, of the Oriental hair tresses treated with different products and generated by different models.	176
Figure 4-47 The effect of a blurring effect on the appearance of an object (reproduced and edited from Section 4.3).....	177
Figure 4-48 Reflection band separation of a Virgin Blonde hair tress. (a) Virgin Blonde tress image, original image, (b) Shine-band separated and overlaid on the original image (in green), (c) Chroma-Specular band separated and overlaid on the original image, (d) Chroma-Diffuse band separated and overlaid on the original image, (e) Separated shine-band (in grayscale), (f) Separated Chroma-Specular band, (g) Separated Chroma-Diffuse band.	178
Figure 5-1 Screen shot of the Tress-Gloss 2.0 GUI as displayed on the Tobii eye tracker monitor (along with stimuli specifications)	185
Figure 5-2 Calibration of the Tobii Eye-Tracker (Tobii Eye-Tracker Mannual)	186
Figure 5-3 Calibration result.....	187
Figure 5-4 Flow diagram of the Tobii-eye tracker process (modified, Tobii Technology 2010)	187
Figure 5-6 AOIs (Area of interest) defined on the GUI screen shot.....	190
Figure 5-7 Participant performing the tress gloss psychophysical comparison experiment using the Tobii eye-tracker TX300.....	191
Figure 5-8 Gaze plot of all the participants (each colour is associated with a participant) on the Virgin tress (left) - Wax tress (right) evaluation screen.	192
Figure 5-9 Heat map (time spent attending to AOIs, red represents high frequency, green low and yellow medium) of all the participants on Virgin-Wax evaluation screen of GUI.....	193
Figure 5-10 Average-time taken by each participant to record their decision, when the virgin (Blonde) – Wax (Blonde) hair tress appeared on the screen.....	194
Figure 5-11 Average fixation-count of each participant during virgin-wax (blonde hair tresses) evaluation on the whole screen.....	194
Figure 5-12 Average gaze duration spent by each participant attending to the shine area of the tresses.....	195
Figure 5-13 Average number of fixation counts of the participants in the shine areas of the Virgin-Wax blonde hair tress.....	196
Figure 5-14 Gaze plots of all of the participants (each colour is associated with a participant) on the Virgin tress (left) - SLES tress (right) screen shot.....	198
Figure 5-15 Heat map (time spent on the screen, red represents high frequency, green low and yellow medium) of all the participants on Virgin-SLES evaluation screen of GUI.....	198

Figure 5-16 Average duration taken to record the decision by each participant during the Virgin-SLES (Blonde) evaluation process	199
Figure 5-17 Average fixation count of each participant during Virgin-SLES evaluation process	199
Figure 5-18 Average times spent by the participant within the Shine areas of the hair tress.....	200
Figure 5-19 Average number of fixations within the Shine areas of the hair tresses	201
Figure 5-20 Gaze plot of all of the participants (each colour is associated with a participant) on the Virgin tress (left) - Shine Spray (right) screen shot.....	203
Figure 5-21 Heat map (duration spent gazing at AOIs on the screen, red represents high frequency, green low and yellow medium) of all the participants on Virgin-Shine spray evaluation screen of GUI	203
Figure 5-22 Average times taken to record the choice, by each participant during the Virgin–Shine Spray (Blonde) evaluation process	204
Figure 5-23 Average fixation count by each participant during Virgin-Shine Spray evaluation process	205
Figure 5-24 Average time spend by each participants in the Shine area of the tresses	205
Figure 5-25 Average fixation frequency of the participants in the Shine areas of the Virgin-Shine Spray blonde hair tress	206
Figure 5-26 Gaze plots of all of the participants (each colour is associated with a participant) on the (a) Virgin – Virgin, (b) Wax-Wax, (c) SLES-SLES and (d) Shine Spray-Shine spray screen shot.	208
Figure 5-27 Heat map (time spent on the screen, red represents high frequency, green low and yellow medium) of all of the participants viewing areas on a (a) Virgin – Virgin, (b) Wax-Wax, (c) SLES-SLES and (d) Shine Spray-Shine spray screen shot..	208
Figure 5-28 Average times taken by the participants to record their decision.	209
Figure 5-29 Average number of fixations by the participants in the AOIs on the screen shot of the pair tress comparison of similar tresses.	210
Figure 5-30 Total number of fixations in the Chroma areas of both images (top and bottom) in 33 evaluations.	210
Figure 5-31 Percentage increase or decrease of shine value between the left image and right image. (a) Virgin-Wax comparison, (b) Virgin–SLES comparison, (c) Virgin–Shine spray comparison, (d) Virgin–Virgin comparison, (e) Wax–Wax comparison, (f) SLES–SLES comparison, (g) Shine Spray–Shine Spray comparison.	211
Figure 5-32 Gaze plots of all of the participants (each colour is associated with a participant) on the (a) Virgin-Wax comparison European Brown hair tress, (b) Oriental hair tress.....	212
Figure 5-33 Time spent attending to the tresses by the participants in the form of heat maps (a) European Brown, (b) Oriental hair tress.....	212
Figure 5-34 Average decision durations taken by each participant during the Virgin-Wax (for both European-Brown evaluations and Oriental hair tress evaluations) evaluation process	213
Figure 5-35 Average fixation counts for each participant during the Virgin-Wax evaluation process for European Brown and Oriental hair tresses.....	214
Figure 5-36 The average times spent by the participants fixating within the shine areas of the European Brown hair tresses (Virgin-wax comparison).....	215

Figure 5-37 The average times spent by the participants fixating within the shine areas of the Oriental tresses (Virgin-Wax comparison)	215
Figure 5-38 Average number of gaze count of the participants in the shine areas of the tresses.	216
Figure 5-39 A gaze plot of all of the participants' gaze patterns (each colour is associated with a participant) on the Virgin tress (left)-SLES tress (right) screenshot. (a) European Brown hair tress paired comparison, (b) Oriental hair tress paired comparison.....	218
Figure 5-40 Heat map (time spent viewing areas of the screen, red represents high frequency, green low and yellow medium) of all of the participants, overlaying a Virgin-SLES evaluation screen. (a) European Brown hair tress paired comparison, (b) Oriental hair tress paired comparison.....	218
Figure 5-41 Average-decision time of each participant during the Virgin-SLES evaluation process	219
Figure 5-42 Average fixation counts by each participant during the Virgin-SLES evaluation process	219
Figure 5-43 Average-time spent by the participants viewing the shine areas of the European Brown hair tresses (Virgin-SLES comparison).	220
Figure 5-44 Average-time spent by the participants viewing the shine areas of the Oriental hair tresses (Virgin-SLES comparison).	220
Figure 5-45 Average gaze frequency of the participants in the Shine areas of the European Brown tresses	221
Figure 5-46 Average gaze frequency of the participants in the Shine areas of the Oriental tresses	221
Figure 5-47 Gaze plot for all of the participants on the Virgin tress (left) – Shine Spray tress (right) screenshot (a) European Brown hair tress, (b) Oriental hair tress	223
Figure 5-48 Heat map (time spent on the screen, red represents high frequency, green low and yellow medium) of all of the participants on Virgin-SLES evaluation screen of GUI (a) European Brown hair tress, (b) Oriental hair tress	223
Figure 5-49 Average decision duration of each participant during the Virgin–Shine Spray (EB) evaluation process	224
Figure 5-50 Average fixation count of each participant during the Virgin-Shine Spray evaluation process	225
Figure 5-51 Average time spend by each participant viewing the shine area of the European Brown tresses	226
Figure 5-52 Average time spend by each participants in the shine area of the Oriental tresses	226
Figure 5-53 Average fixation count of the participants viewing the shine areas of the Virgin-Shine Spray (European Brown hair tress)	227
Figure 5-54 Average fixation count of the participants viewing the shine areas of the Virgin-Shine spray (Oriental hair tress)	227
Figure 5-55 Gaze plots of all the participants on the Virgin-Wax comparison, (a) European-Brown, (b) Oriental, (c) Blonde.....	230
Figure 5-56 Average decision times taken by the participant panel.	230
Figure 5-57 Screen shots of the paired comparisons; highlighted areas are where participants were most attentive, during the shine evaluation process.....	231

Figure 5-58 Percentage increase or decrease in shine values generated by different models and the participants' choice, between the left image and right image of the hair tresses.	233
Figure 6-1 Reflection band separation of a virgin blonde hair tress. (a) Virgin blonde tress image, original image, (b) Shine-band separated and overlaid on the original image, (c) Chroma-specular-band separated and overlaid on the original image, (d) Chroma-diffuse-band separated and overlaid on the original image, (e) Separated shine-band, (f) Separated Chroma-specular-band, (g) Separated Chroma-diffuse-band.	239
Figure 6-2 Gaze plots of all the participants viewing the Virgin-Wax comparison, (a) European-Brown, (b) Oriental, (c) Blonde.	242
Figure 6-3 Average times taken by the participants to record their decision.	242
Figure 6-4 Screen shots of the pair comparison images; the highlighted areas are where participants most frequently fixated during the shine evaluation process.....	243
Figure 6-5 Percentage increase or decrease in shine values generated by the different models and participants' choice, between the left and right images of the hair tresses.	245

List of Tables

Table 2-1 Typical dimensions of Terminal hair in humans (Vogt <i>et al.</i> 2008)	67
Table 2-2 Terminal hair diameter (Vogt <i>et al.</i> 2008).	67
Table 2-3 Individual Amino Acids found in Hair (Robbins 2002a)	73
Table 2-4 Surfactants types and characteristics	81
Table 2-5 Results for Maximum - Minimum Analysis for various types of human hair (McMullen and Jachowicz 2004)	99
Table 3-1 List of the hair tresses exposed to heat using GHD IV Hair Straighteners	109
Table 3-2 Combing cycles applied to each hair tress	111
Table 3-3 Hair tresses dipped in SLES solution	112
Table 3-4 Commerical products used in the study	113
Table 3-5 Details and products applied onto the Oriental tresses used in sampling to create different level of hair shine	116
Table 4-1 Average L* curve's peak value and average C* value under the peak of the L* curve and their differences	140
Table 4-2 The shine values of four European Brown tresses with different treatments applied, generated by the different models	165
Table 4-3 Shine values, of the Blonde hair tresses, generated by different models	166
Table 4-4 Shine values of Oriental hair tresses generated by different models	168
Table 4-5 Shine values of the Blonde hair tresses and percentage differences	170
Table 4-6 Shine values of the European Brown hair tresses with percentage differences.	172
Table 4-7 Shine values of the Oriental hair tresses and percentage differences.	175
Table 5-1 Tress images used in the Psychophysical Eye Tracking Study	183
Table 5-2 Generic Breakdown of the images used in the study	185
Table 5-3 Generic structure of the tress comparisons analysed in this section	191
Table 5-4 Average values from different models and participants' choice. Highlighted value is the closest to the participants' choice	197
Table 5-5 Average shine values of Virgin and SLES tresses generated by different models and participants' choice. Highlighted value is the closest to the participants' choice	202
Table 5-6 Average shine values of Virgin and SLES tresses generated by the different models and the participants' choices	207
Table 5-7 Average shine values of European Brown Virgin and Wax tresses generated by different models and participants' choice. The highlighted value is the closest to the participants' choice	217
Table 5-8 Average shine values of Oriental Virgin and Wax tresses generated by the different models and the participants' choice. The highlighted value is the model closest to the participants' choice	217
Table 5-9 Average shine values of Virgin and SLES tresses generated by different models and the participants' choices. The highlighted value is the closest to the participants' choice	222
Table 5-10 Average shine values of the Virgin and SLES tresses generated by different models and the participants' choice. The highlighted value is the closest to the participants' choice	223

Table 5-11 Average shine values of Virgin and Shine Spray tresses generated by different models and participants' choice. Highlighted value is the closest to the participants' choice	228
Table 5-12 Average shine values of Virgin and Shine Spray tresses generated by different models and participants' choice. Highlighted value is the closest to the participants' choice	228

Abstract

The evaluation of the gloss of human hair, following wet/dry chemical treatments such as bleaching, dyeing and perming, has received much scientific and commercial attention. Current gloss analysis techniques use constrained viewing conditions where the hair tresses are observed under directional lighting, within a calibrated presentation environment. The hair tresses are classified by applying computational models of the fibres' physical and optical attributes and evaluated by either a panel of human observers, or the computational modelling of gloss intensity distributions processed from captured digital images.

The most popular technique used in industry for automatically assessing hair gloss is to digitally capture images of the hair tresses and produce a classification based upon the average gloss intensity distribution. Unfortunately, the results from current computational modelling techniques are often found to be inconsistent when compared to the panel discriminations of human observers.

In order to develop a Gloss Evaluation System that produces the same judgements as those produced from both computational models and human psychophysical panel assessments, the human visual system has to be considered. An image based Gloss Evaluation System with gonio-capture capability has been developed, characterised and tested.

A new interpretation of the interaction between reflection bands has been identified on the hair tress images and a novel method was developed to segment the diffuse, chroma and specular regions from the image of the hair tress. A new model has been developed, based on Hunter's contrast gloss approach, to quantify the gloss of the human hair tress.

Furthermore, a large number of hair tresses have been treated with a range of hair products to simulate different levels of hair shine. The Tresses have been treated with different commercial products. To conduct a psychophysical experiment, one-dimensional scaling paired comparison test, a MATLAB GUI (Graphical user interface) was developed to display images of the hair tress on calibrated screen. Participants were asked to select the image that demonstrated the greatest gloss. To understand what users were attending to and how they used the different reflection bands in their quantification of the gloss of the human hair tress, the GUI was run on an Eye-Tracking System.

The results of several gloss evaluation models were compared with the participants' choices from the psychophysical experiment. The novel gloss assessment models developed during this research correlated more closely with the participants' choices and were more sensitive to changes in gloss than the conventional models used in the study.

Declaration

I declare that no portion of the work referred to in the thesis has been submitted in support of an application for another degree or qualification of this or any other university or other institute of learning

Copyright Statement

- I. The author of this thesis (including any appendices and/or schedules to this thesis) owns certain copyright or related rights in it (the “Copyright”) and he has given The University of Manchester certain rights to use such Copyright, including for administrative purposes.
- II. Copies of this thesis, either in full or in extracts and whether in hard or electronic copy, may be made only in accordance with the Copyright, Designs and Patents Act 1988 (as amended) and regulations issued under it or, where appropriate, in accordance with licensing agreements which the University has from time to time. This page must form part of any such copies made.
- III. The ownership of certain Copyright, patents, designs, trademarks and other intellectual property (the “Intellectual Property”) and any reproductions of copyright works in the thesis, for example graphs and tables (“Reproductions”), which may be described in this thesis, may not be owned by the author and may be owned by third parties. Such Intellectual Property and Reproductions cannot and must not be made available for use without the prior written permission of the owner(s) of the relevant Intellectual Property and/or Reproductions.
- IV. Further information on the conditions under which disclosure, publication and commercialisation of this thesis, the Copyright and any Intellectual Property and/or Reproductions described in it may take place is available in the University IP Policy (see <http://www.campus.manchester.ac.uk/medialibrary/policies/intellectualproperty.pdf>), in any relevant Thesis restriction declarations deposited in the University Library, The University Library’s regulations (see <http://www.manchester.ac.uk/library/aboutus/regulations>) and in The University’s policy on presentation of Theses

It must be remembered that there is nothing more difficult to plan, more doubtful of success nor more dangerous to manage than the creation of a new system. For the initiator has the enmity of all who profit by the preservation of the old institution and merely lukewarm defenders in those who would gain by the new one.

Niccolò Machiavelli (1513)

Acknowledgements

First and foremost thanks to the Almighty, without his blessings I am nothing.

It would not have been possible to write this doctoral thesis without the help and support of the kind people around me, to only some of whom it is possible to give particular mention here.

This project has been the result of a long journey, which started from a meeting in Dr. Huw Owens's office back in December 2008. It was a journey filled with excitement, craziness, happiness, and loneliness, and amongst all of these emotions we had our "eureka moments". This project would not have been possible without the full support and valuable advice from my supervisors Dr. Huw Owens and Prof. Chris Carr. I can't thank them enough especially Dr. Huw Owens who not only guided me in my research but also supported me when I was going through tough times. I am grateful and deeply indebted.

I would like to acknowledge the financial and technical support from Croda, especially the guidance I received from Mike Hindley and Grant Mitchell.

I would like to extend my deepest gratitude to my family: my parents Iqbal and Rukhsana Rizvi, my brothers Saeed and Junaid and sisters-in-law Yasmeen, Mehwish, my lovely sister Zehra and Brother-in-law Raza. They were always there whenever I needed them. Thank you! My family has been the backbone of my support system and always have provided unwavering love and encouragement. Thank you for believing in me.

I am thankful to all my friends, for everything from technical support to emotional support. It is impossible to cover everyone by name but I will make an exception for some of whom I wish to thank in particular: Mohsin, Sarah, Katie, Ghada, Robert, Tjasa, Mbonea, Ruth, Ali, Taha, Rolan, Shariq, Sarang and Juveria. I could not have done it without you. Thank you for being there for me from the very beginning. I finally did it!

When I started this project I was single and now as I am writing these lines I have been married for three years to an amazing person, Raziat, and together we have a son, Taqi, who just learned how to say Baba (dad). I am thankful for their patience and support. They have given me their unequivocal support throughout, as always, for which my mere expression of thanks likewise does not suffice.

For any errors or inadequacies that may remain in this work, of course, the responsibility is entirely my own.

This thesis is dedicated to the next generation of my family,
my nephews Abid, Hasnain, Abbas, Danial
and my Son Taqi.

Chapter 1

Introduction

1.1 Aims and Objectives

The principle aim of the project was to produce an instrumental system that would automatically quantify the amount of gloss present on a human hair tress in a way that produced similar decisions to a human panel.

The research was undertaken with the hypothesis that an image based computational gloss evaluation system can quantify gloss of a human hair tress as human observers; in order to produce such a system five principal areas were investigated:

- Human Hair Tress Sample Preparation;
- Human Hair Tress Gloss Evaluation Models;
- Human Hair Tress Gloss Capture System;
- Image Processing and Analysis of Gloss Bands;
- Psychophysical Eye-Tracking Study of Hair Tress Gloss.

The aims and Objective of this research may be summarised as follows:

1. To determine how conventional gloss evaluation systems quantify the gloss of human hair.

Objectives:

- 1-a Produce a Literature Review of Gloss Evaluation Systems
- 1-b Identify and classify the different types of Gloss Evaluation System
- 1-c Identify the most successful and popular models used in Industry

2. To produce a novel dataset of sample hair tresses demonstrating a range of gloss intensities to be used for instrumental and psychophysical evaluation

Objectives:

- 2-a Develop shine enhancing / reducing treatment techniques for the human hair tress
- 2-b Create a range of hair tresses exhibiting different levels of hair shine

3. To build a Human Hair Tress Image Capture System

Objectives:

- 3-a Identify the limitations associated with conventional Glossmeters
- 3-b Design a Gonio-image capture system, in order to capture calibrated images of human hair tresses, consisting of an image capture device, light source and sample holder
- 3-c Calibrate, test and validate the components of the Gonio-image capture setup
- 3-d Use Sofortbild camera control software to automate and link the Image Capture Device of the Gonio-Capture setup, with the computer, and to import the tress images into the MATLAB software package for image processing

4. To separate reflection bands from the images of the hair tresses

Objectives:

- 4-a Identify the reflection bands as they appear on the image of the hair tress
- 4-b Develop code using the MATLAB software package to segment the reflection bands in the image of the hair tress
- 4-c Validate the image segmentation by overlaying the segmented band onto the tress image

5. To determine whether the reflection bands are monochromatic, as they appeared on the hair tress under a fixed light source.

Objectives:

- 5-a Calculate and Examine the CIELAB value population statistics of each component of the reflection bands
- 5-b Evaluate the interaction of Lightness (L^*) and Chroma (C^*) in the reflection bands of the hair tress images

6. To create novel gloss quantification models of images of human hair tresses

Objectives:

- 6-a Identify the most important CIELAB statistical populations for each type of hair tress
- 6-b Calculate the average area under the CIELAB value curves of each reflection band
- 6-c Measure the Full Width Half Maximum (FWHM) value of the shine band L* pixel distribution.
- 6-d Calculate the most occurring value in the chroma band.
- 6-e Formulate and test gloss evaluation equations based on the statistical properties of the shine and chroma bands

7. To compare the current gloss evaluation models and novel gloss assessment models with the gloss discriminations of human observers;

Objectives:

- 7-a Develop a Graphical User Interface (GUI), using the MATLAB software package, capable of displaying a paired comparison forced choice psychophysical test
- 7-b Develop an experimental information sheet, to brief the participants about the psychophysical experiment
- 7-c Conduct a paired-comparison forced-choice psychophysical experiment to quantify the gloss discriminations of human observers using human hair tresses images
- 7-d Compare the human observer gloss discrimination results with those generated by current and novel gloss evaluation models

8. To investigate the gloss discriminations made by human observers viewing images of Human hair tresses.

Objectives:

- 8-a Conduct a forced-choice paired-comparison psychophysical experiment on an eye-tracking system (Tobii TX300)

- 8-b Record the gaze movements of each participant during the forced choice psychophysical experiment
- 8-c Analyse the number and duration of fixations of each participant during each comparison
- 8-d Identify the most frequently visited areas on the images of the hair tresses
- 8-e Examine the gaze patterns generated by the participants during comparisons of similar as well as different types of hair tress (e.g. Blonde, European-Brown and Oriental)

1.2 Thesis outline

A brief summary of the project and a thesis outline is provided in this section.

Chapter 1: Introduction. Chapter one outlines the research question. Although the quantification of gloss and other optical properties of skin and hair are important to the Cosmetics Industry there is currently no standard method of evaluating the gloss of human hair.

Chapter 2: Literature review. Chapter two reviews previous work related to human hair and hair gloss evaluation systems. The basics of colour science have been included (interaction of light with objects, measurement of light, CIE colour spaces). There are several definitions of gloss, which have been explained along with the Hunter classifications of gloss and the problems associated with obtaining accurate gloss measurements. An outline of the Human Visual System and Image Capture devices (such as the digital camera) has been discussed. In this study psychophysical experiments have been conducted and to give an introductory understanding of psychophysics, the evolution of psychophysics has been explained. A brief history of human hair is provided along with its structure, physical and chemical properties. Previous workers have attempted to produce physical models of the gloss produced by single hair fibres as well as hair tresses. Several of the gloss evaluation models suggest that there are separate Specular, Chroma and Diffuse reflectance bands observed on the human hair tress and

attempt to use the intensities of each of these reflection bands independently in order to quantify the perceived gloss. These types of gloss evaluation models have been presented, and these models including those by Stamm, Guiolet, Reich and Robbins, TRI, McMullen and Bossa Nova models have been discussed.

Chapter 3: Methodology. Chapter three describes the methods used in this study, including several new methods, developed by the author, to create different levels of hair shine on the tresses. Two techniques have been used to create different levels of gloss:

- 1) Damage of the hair tress using heat, chemical or mechanical techniques; and
- 2) By the application of commercial products to the hair tresses.

Development of a gloss image capture system along with sample holder and a novel technique to mount and align the sample on the sample holder has been explained. A novel, never been applied to a human hair gloss study, HDR imaging technique to quantify the gloss has been discussed. Two graphical user interfaces (GUIs), Tress-Gloss 1.0 and Tress-Gloss 2.0, have been developed by the author using the software package MATLAB. The GUIs display the hair tress images for a particular type of psychophysical gloss evaluation. Chapter 3 also describes the image-capture process and how different exposure ranges affect the reflection properties of the tress images.

Chapter 4: The Optical Properties of Human Hair Tresses and the Development of Novel Human Hair Gloss Evaluation Models. Chapter four identifies the different reflection bands on the hair tress suggested by previous authors. A new interpretation of these reflection bands has lead to the Chroma-Specular band being identified on the hair tress. This novel approach seems to provide a model that quantifies differences in gloss in a similar way to the discriminations made by human observers. This chapter explains a new method, developed by the author, used to segment the reflection bands from the image of the hair tress. The effect of several different cosmetic treatments on the reflection bands of hair tresses has been discussed. A new model was developed by the author in order to quantify the gloss of human hair tresses. The results generated by the new models (ROC_1 and ROC_2) have been compared with some conventional hair gloss models used in the Cosmetics Industry.

Chapter 5: Assessing the Perceived Gloss of Human Hair Tress Images using A Paired Comparison Forced Choice Test using Eye-Tracking Technology. (A Psychophysical Study). Chapter Five describes a psychophysical study of perceived hair tress gloss. The study used images of treated and untreated hair tresses. The Tress-Gloss 2.0 GUI was run on an eye-tracking device (Tobii Eye Tracker, TX-300) and displayed pairs of tress images and collected subject response data. Eye tracking has not previously been used in hair gloss studies. The gaze data of the participants was captured while they evaluated which of the two hair tress images appeared to have more gloss. Data generated by the eye tracker and the participants' decisions were compared with the gloss values produced by the different hair tress gloss evaluation models. The results have been discussed in this chapter.

Chapter 6: Conclusions and Future work. Chapter six summarises all the findings from the experimental chapters and suggests directions for future work.

Chapter 2

Literature Review

2.1 Light

Radiation we can see is called light; it is part of the family that includes X-rays and radio waves, as well as infrared and ultraviolet radiation. The property of these radiations that gives them their particular characteristics is their wavelength. Radio waves have long wavelengths, they are in the range from about a metre to several kilometres, whereas X-rays have extremely short wavelengths, typically about a millionth of a millimetre or shorter. Light wave has wavelengths in between, ranging from marginally above to marginally below a half a millionth of a metre. To attain convenient numbers for the wavelengths of light, the unit used for expressing light is the nanometre (nm), which is 10^{-9} metre (Hunt 1998). The relative insensitivity of the eye limits the visible part of the spectrum to a very narrow band of wavelengths between 380nm and 780nm (Roy 2000). Light can be characterized by three main properties as shown in Figure 2-1:

- **Intensity:** intensity of light is related to the amplitude of the light vibration. The higher the amplitude more intense light will be.
- **Spectrum:** it is related to the frequency or wavelength of the light vibration. In the case of visible spectrum, red has longer wavelength than blue.
- **Polarization:** it is related to the spatial orientation and coherence of the light vibration. Light can be either polarized, i.e. the light vibration has a defined orientation, or depolarized, i.e. Light vibrates randomly.



Figure 2-1 Fundamental properties of light: intensity, spectrum and polarization (Lefaudeux *et al.* 2008).

2.2 How Objects modify light

When light strikes an object, four major outcomes are attained:

- Specular reflection at the surface of the object (associated with gloss)
- Scattering (associated with diffuse reflection and diffuse transmission)
- Absorption within the object (largely responsible for colour)
- Transmission directly through the object (associated with clarity)

2.2.1 Laws governing the reflection of light

When a ray of light, incident at the angle θ on an air-object interface, hits a surface that is optically polished, the scattering is negligible, and the ray is partly reflected at an angle θ and partly transmitted after refraction at an angle r . The angle of refraction can be calculated by Snell's law;

$$\sin r = \frac{(\sin \theta)}{n} \quad \text{Equation 2-1}$$

Where n is the refractive index of the object.

Knowing the polarization of the incident light, reflectance of the reflected (R_s , R_p) and transmitted (T_s , T_p) rays relative to the incident can be calculated by using Fresnel's equation:

$$R_s = \left[\frac{\sin(\theta_t - \theta_i)}{\sin(\theta_t + \theta_i)} \right]^2 = \left[\frac{n_1 \cos(\theta_i) - n_2 \cos(\theta_t)}{n_1 \cos(\theta_i) + n_2 \cos(\theta_t)} \right]^2 \quad \text{Equation 2-2}$$

$$R_p = \left[\frac{\tan(\theta_t - \theta_i)}{\tan(\theta_t + \theta_i)} \right]^2 = \left[\frac{n_1 \cos(\theta_t) - n_2 \cos(\theta_i)}{n_1 \cos(\theta_t) + n_2 \cos(\theta_i)} \right]^2 \quad \text{Equation 2-3}$$

The transmission coefficient is given by

$$T_s = 1 - R_s \text{ and } T_p = 1 - R_p \quad \text{Equation 2-4}$$

If the incident light is un-polarised, the reflection coefficient is:

$$R = \frac{(R_s + R_p)}{2} \quad \text{Equation 2-5}$$

Where n_1 and n_2 are the refractive indices of the mediums. Fresnel's equation (Fresnel's laws of reflection) describes amplitude and phase relationship between the incident and reflected light. The incident light can be considered as comprises of two polarised beams, one parallel to the plane of incidence (p-polarized) and the other perpendicular to the plane of incidence (Stamm *et al.* 1977a).

2.3 How light is measured

2.3.1 Radiometry

Light may reflect when it interacts with an object. The ability of materials to reflect light is called “reflectance” (Reinhard et al. 2006b). Radiometry is the science concerned with measuring light. Light is radiant energy, and is often measured in joules. Radiometry is the derived quantities that measure how light propagates through media such as space, air and water. These include radiant energy measured over time (measured in joules per second or watts), space (measured in watts per square metre), or angle (measure energy per unit of time per unit of direction) (Palmer and Grant 2010).

2.3.2 Photometry

Light reflecting from a surface gives information about both the light source illuminating the surface and the reflectance of the surface. The human eye is sensitive to wavelengths between approximately 380 to 770 nm (Sinclair 1997). Within this range, the human eye is not equally sensitive to all wavelengths. The range of sensitivity can be approximated with a single curve (difference in sensitivity in individuals is small enough that the spectral sensitivity of any human observer with normal vision may be approximated). Such a curve is standardized by the Commission Internationale de l’Eclairage (CIE) and is known as the $V(\lambda)$ curve or the CIE Photopic Luminous Efficiency curve (Figure 2-2).

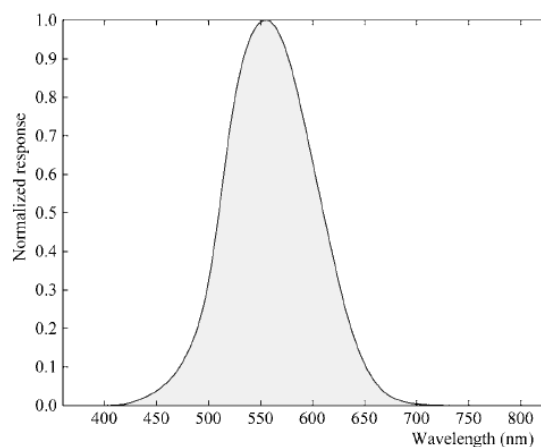


Figure 2-2 CIE standard observer photopic luminous efficiency curve (Reinhard et al. 2006b).

The science of measuring light in units that are weighted according to $V(\lambda)$, or how humans perceive light, is called photometry.

2.3.3 Colorimetry

The field of colorimetry is concerned with assigning numbers to physically defined stimuli such that stimuli with the same specification look alike (Reinhard *et al.* 2006b).

Almost all-modern colour measurement is based on the CIE system of colour specification (Rigg 1997). One of the main results from colour-matching experiments is that over a wide range of conditions almost all colours may be visually matched by adding light from three suitably pure stimuli (Hunt 2004). These three fixed stimuli are called primary stimuli.

The optical primaries are red, green and blue spectrum colours. Although mixtures of these give the widest possible range of colours, however, there is no set of real primary colours that can be used to match all colours using positive amounts of the primaries. In other words, no set of real primaries exists that will eliminate negative tristimulus values entirely.

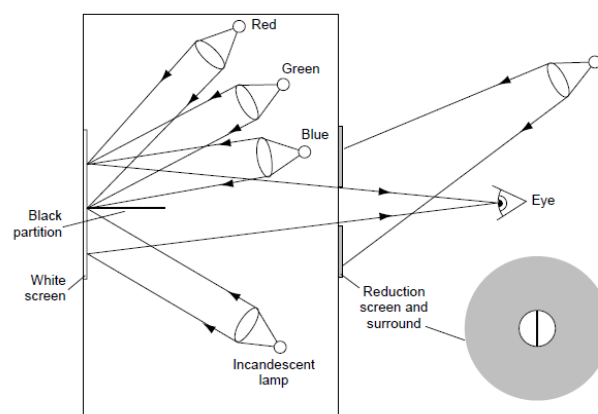


Figure 2-3 Colour-matching experiment (Rigg 1997).

It is possible to determine the tristimulus values for any given stimulus using a device known as a split-field or bipartite colorimeter shown in Figure 2-3. In such a device an observer views a bipartite field. On one side of the field the stimulus is displayed, on the other side the additive mixture of the three primaries is displayed. The observer adjusts the intensities of each of the three primaries and if necessary adds a primary to the stimulus displayed until the additive mixture is indistinguishable from the stimulus. By recording the intensities of the three primaries for each target wavelength, three functions $r(\lambda)$, $g(\lambda)$, and $b(\lambda)$ may be created. These are called colour-matching functions. The amounts required depend on the observer, and results for an average (or standard observer) are required.

Colour-matching experiments were carried out by Wright and Guild (CIE 1931 standard observer) and later in 1959 by Stiles and Burch. Stiles and Burch used primary light sources that were nearly monochromatic with peaks centred on $\lambda_R = 645.2 \text{ nm}$, $\lambda_G = 525.3 \text{ nm}$, and $\lambda_B = 444.4 \text{ nm}$ (Stiles and Burch 1959). Colour-matching function obtained by Stiles and Burch are plotted in the Figure 2-4. In these experiments they used a 10° field of view instead of 2° , which was used by Wright and Guild. Due to this difference in angles, these functions are called 10° colour-matching functions. They were adopted by the CIE to describe the CIE 1964 standard observer.

“There is little to choose between the two observers” (1931 and 1964 standard observer) (Rigg 1997).

CIE 1964 standard observer can be represented as:

$$Q_\lambda = \bar{r}(\lambda)R + \bar{g}(\lambda)G + \bar{b}(\lambda)B \quad \text{Equation 2-6}$$

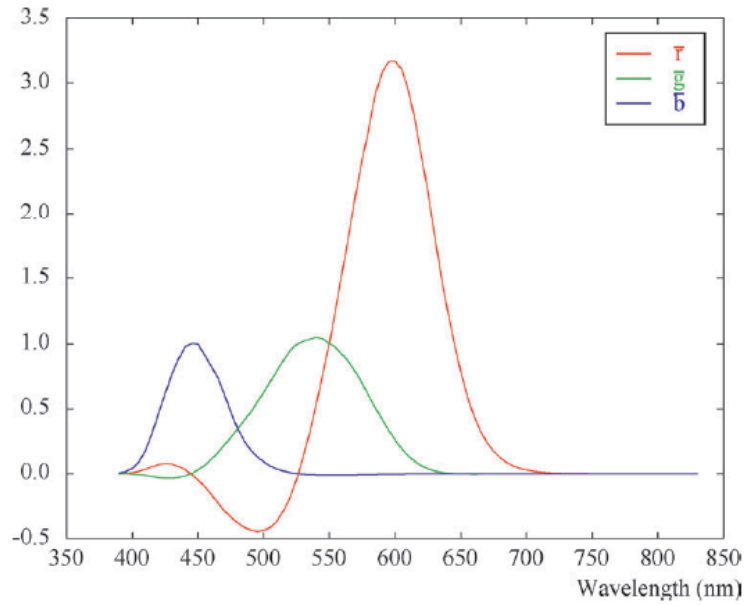


Figure 2-4 Stiles and Burch (1959) 10° colour-matching functions(Reinhard *et al.* 2006b).

Since R, G, and B were real primaries, some of the values were negative as shown in the Figure 2-4. In that it is simpler to deal with a colour space whose tristimulus values are always positive. The CIE has defined alternative colour-matching functions chosen such that any colour may be matched with positive values.

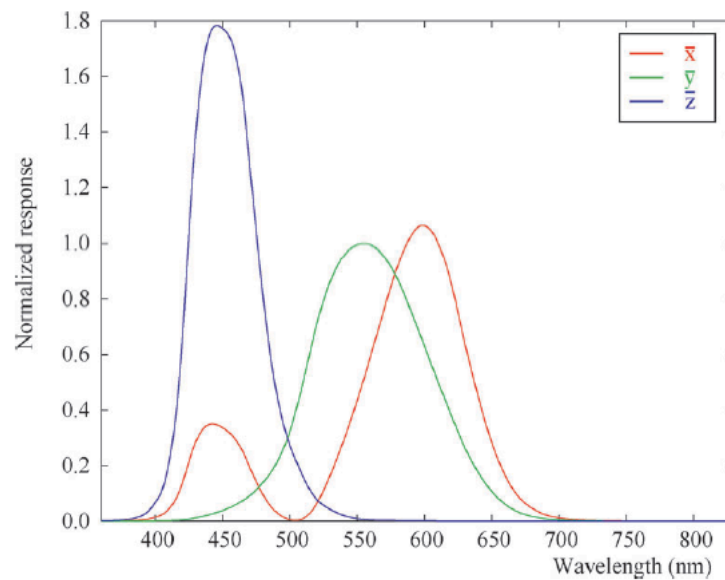


Figure 2-5 CIE 1931 2-degree XYZ colour-matching functions(Reinhard *et al.* 2006b).

These colour-matching functions are named $\bar{x}(\lambda)$, $\bar{y}(\lambda)$ & $\bar{z}(\lambda)$, and are plotted in Figure 2-5. These functions are the result of experiments of the 2°-viewing field and are

therefore known as the CIE 1931 standard observer. A spectral stimulus may now be matched in terms of these colour-matching functions, as follows:

$$Q_{\lambda} = \bar{x}(\lambda)X + \bar{y}(\lambda)Y + \bar{z}(\lambda)Z \quad \text{Equation 2-7}$$

2.3.3.1 Calculation of tristimulus values from measured reflectance values

Suppose R_{λ} is the fraction of light reflected at each wavelength of a sample, these values will be completely independent of the light shone on the sample because they are given in terms of a percentage. For example, a white object reflects at least 90% of incident light under strong daylight or weak tungsten light.

Suppose light shone on the sample emits light at each wavelength is E_{λ} . Then the amount reflected at each wavelength will be $E_{\lambda} \times R_{\lambda}$. If we consider only light of wavelength λ , one unit of energy λ can be matched by an additive mixture of \bar{x}_{λ} units of X together with \bar{y}_{λ} units of Y and \bar{z}_{λ} units of Z:

$$1[\lambda] \equiv \bar{x}_{\lambda}[X] + \bar{y}_{\lambda}[Y] + \bar{z}_{\lambda}[Z] \quad \text{Equation 2-8}$$

This can be represented as

$$E_{\lambda} R_{\lambda}[\lambda] \equiv E_{\lambda} \bar{x}_{\lambda} R_{\lambda}[X] + E_{\lambda} \bar{y}_{\lambda} R_{\lambda}[Y] + E_{\lambda} \bar{z}_{\lambda} R_{\lambda}[Z] \quad \text{Equation 2-9}$$

The total amount of energy reflected over the visible spectrum is the sum of the amounts reflected at each wavelength. This can be represented as:

$$\sum_{380}^{760} E_{\lambda} R_{\lambda} \quad \text{Equation 2-10}$$

Where Σ means that the $E_{\lambda} R_{\lambda}$ values for each wavelength through the visible region should be added together, and the limits of $\lambda = 380$ and 760 nm are the boundaries of the visible region.

2.3.3.2 CIE Colour Space

The tristimulus values XYZ are useful for defining colour, but the results are not easily visualised. Because of this, the CIE defined a colour space in 1931, representing colour in two dimensions independent of lightness, known as the Yxy colour space. CIE Y represents the Lightness scale and is equal to $V(\lambda)$ and x and y are the chromaticity coordinates calculated from the CIE tristimulus values, as shown in Equation 2-11.

$$x = \frac{X}{X+Y+Z}, \quad y = \frac{Y}{X+Y+Z}, \quad z = \frac{Z}{X+Y+Z} \quad \text{Equation 2-11}$$

(x + y + z = 1)

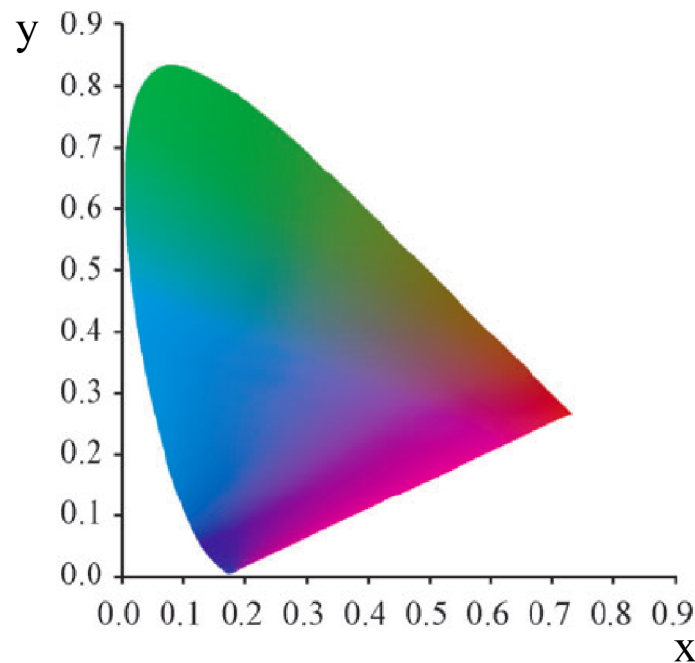


Figure 2-6 CIE 1931 x, y Chromaticity diagram (Reinhard et al. 2006b)

CIE x, y chromaticity diagram for Yxy colour space is shown in Figure 2-6. All monochromatic wavelengths map to a position along the curved boundary, called the Spectral Locus, which is of horseshoe shape. The line between red and blue is called the “purple line”.

*L*a*b* Colour Space*

The 1931 CIE xyY chromaticity diagram was not perceptually uniform, that is, the distance between two points located in one part of the diagram may correspond to a different perceived colour difference than two points located elsewhere in the diagram (Berns et al. 2000). This non-uniformity has given rise to alternative colour space. L*a*b* colour space (also known as CIELAB) is the uniform colour space defined by CIE in 1976. In this colour space L* is lightness and a* and b* are the chromaticity coordinates. Figure 2-7 shows the CIELAB chromaticity diagram. L*, a* and b* are defined by Equations 2-12 to 2-14

$$L^* = 116 \left(\frac{Y}{Y_n} \right)^{1/3} - 16 \quad \text{Equation 2-12}$$

$$a^* = 500 \left[\left(\frac{X}{X_n} \right) - \left(\frac{Y}{Y_n} \right) \right] \quad \text{Equation 2-13}$$

$$b^* = 200 \left[\left(\frac{Y}{Y_n} \right) - \left(\frac{Z}{Z_n} \right) \right] \quad \text{Equation 2-14}$$

where X_n , Y_n and Z_n are the tristimulus values, for the particular standard illuminant and observer, for a sample reflecting 100% of the light at all wavelengths (McDonald 1997).

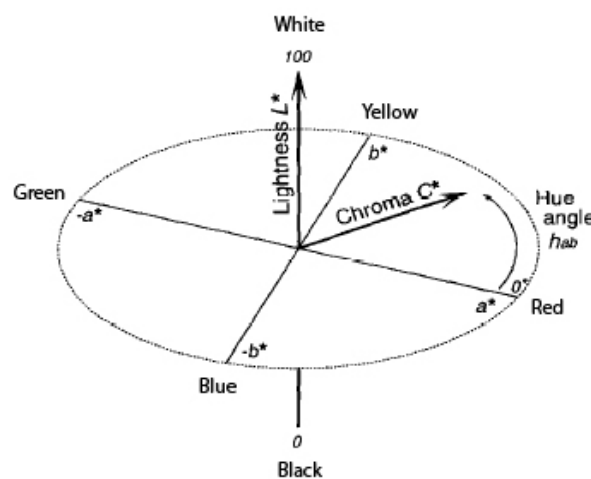


Figure 2-7 CIELAB colour space (Gonnet 1998)

2.4 What is Gloss?

Gloss is the attribute of surfaces that causes them to have a shiny appearance. It is generally associated with specular reflection. In 1760 Bouguer proposed a model to define the optical air mass and sunbeam penetration through the atmosphere, two years after Bouguer's death, Lambert published classical calculation methods determining indoor illuminance from a planar source (Kittler 2007). For at least two hundred and fifty years serious efforts have been made to characterize the phenomenon of gloss, but it is still difficult to objectively predict or to perceptually evaluate gloss (Lindstrand 2002). One reason for this is the lack of a clear definition of gloss. CIE first define gloss as *"directionally selective reflection properties responsible for the degree to which reflected highlights, or the images or objects, may be seen as superimposed on the surface"* (CIE 1970). In 1979 CIE fine-tuned the definition; CIE changed it from physical one to a perceptual one and the definition was changed to *"perceived surface brightness associated with the luminous specular (regular) reflection from a surface"*. ASTM 'standard Terminology of Appearance' defines gloss as, *"n-angular selectivity of reflectance, involving surface-reflected light, responsible for the degree to which reflected highlights or images of objects may be seen as superimposed on a surface"*.

The variables involved in visual gloss are mentioned, but the characterization of gloss is not specified. It possible to give a physical definition for gloss, in terms of the ability of a surface to reflect light in the specular direction in relation to that of e.g. a polished glass surface with a well-defined optical property such as the refractive index, and their reflection can be described in a simpler way.

Barkas (1939) developed the idea based on Bouguer's (1760) proposed model (Barkas 1939). He simplified reflection by assuming surface showing gloss consists of different types of reflections and they may be divided into two types,

- One being a diffused component which can be explained by Lambert's law (if a parallel beam of light of a finite cross section falls at any angle of incidence on to an optically rough surface, the total flux scattered at any angle of view is proportional to cosine of that angle); and

- Other reflecting, at the specular angle, according to the geometrical optics and Fresnel's equation (it describes what fraction of the light is reflected and what fraction is refracted).

On these assumptions formulae are obtained whereby the reflection flux can be resolved into its diffuse and specular components Figure 2-8 shows goniophotometric curves of the total reflectance factor (image is modified and 2 out of 8 angles of incidences from the original image are shown).

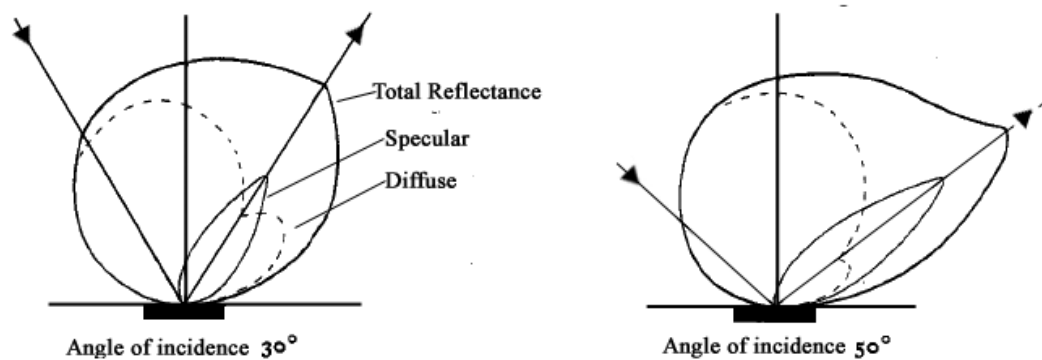


Figure 2-8 Goniophotometric curves of the total reflectance factor with the decomposition of the reflectance (specular and diffuse) (Barkas 1939)

However defining gloss for human hair, the detailed physical description is complicated and consequently there is a lack of descriptive models and theory, although a number of research works are well worth mentioning (described in more detail in Section 2.15.2).

2.4.1 Hunter's contribution in defining Gloss

In the early 1930s Hunter studied gloss and discovered that specular reflection can vary from one surface to another. He concluded that variation in specular reflection depends upon, the fraction of light reflected in the specular direction, the manner and extent to which light is spread to either side of the specular direction, and the change of fractional reflectance as specular angles changes. Hunter, in 1934, while designing a glossmeter to compare the capacities of materials to reflect light specularly at 45° from the

perpendicular, found a problem that values of relative specular reflectance as measured on the glossmeter did not correlate with the visual rankings. Analysis of the problem revealed that the image-reflecting capacity of a surface was not what specular glossmeter was measuring. During the remainder of the decade Hunter studied many different materials and their glossiness rankings. During the course of these investigations it became apparent that there were at least six different visual criteria by which glossiness rankings are made.

1. **Specular gloss**; is the shininess and highlight brilliance that occurs. The ratio of the light reflected from a surface at a specified angle to that incident on the surface at the same angle on the opposite side of the surface normal. Equation 2-15 and Figure 2-9 shows the reflectance function of specular gloss. Where S represent specular and I represent incident light

$$G_s = \frac{S}{I}$$

Equation 2-15

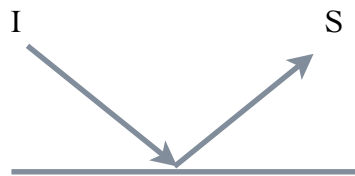


Figure 2-9 Reflectance function of Specular gloss (Hunter 1975b)

2. **Sheen**; is the shininess arising at almost grazing angles of incidence. Equation 2-16 and Figure 2-10 shows the reflectance function of sheen.

$$G_{sh} = \frac{Sh}{I}$$

Equation 2-16



Figure 2-10 Reflectance function of Sheen (Hunter 1975b)

3. **Contrast gloss or lustre**; is the ratio of the specularly reflected light to that diffusely reflected. Equation 2-17 and Figure 2-11 shows the reflectance function of contrast gloss or lustre.

$$G_c = \frac{S}{D} \quad \text{Equation 2-17}$$

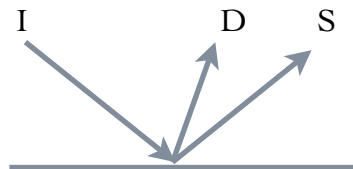


Figure 2-11 Reflectance function of Contrast gloss or Lustre (Hunter 1975b)

4. **Absence of bloom**; is a measure of the absence of haze or the milky appearance adjacent to the specularly reflected light.

$$G_b = \frac{B - D}{I} \quad \text{Equation 2-18}$$

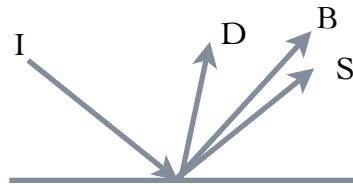


Figure 2-12 Reflectance function of absence of bloom (Hunter 1975b)

5. **Distinctness of image**; the sharpness of the specularly reflected light.
6. **Surface uniformity**; is a measure of the freedom from surface non-uniformities such as texture.

John S. Christie described the physical phenomena responsible for gloss and classifies the various appearance attributes responsible for gloss of objects (Christie 1979). Christie's definitions of these geometric attributes of reflectance are as follows:

- **Lightness**: is the attribute of surface appearance by which an object appears whiter than black.

- Specular gloss: is the appearance attribute corresponding to the illuminance with which lights are observed to be specularly reflected.
- Distinctness of image (DOI): the sharpness that outlines are reflected by the surface of an object (mirror like quality of surface).
- Haze: the scattering of light that produces a cloudy appearance adjacent to a bright beam of reflected light.
- Directionality: the extent to which the appearance of a surface, and particularly its glossiness, changes with rotation of the surface in its own plane.
- Lustre: the appearance characteristic of an object associated with the change in illuminance of reflected light when the angle of view is changed.
- Sheen: shininess in otherwise matte surface when light can be seen to be specularly reflected at near grazing angles.
- Uniformity: freedom from texture, freedom from markings or other visible clue with which the eye can identify position of the surface.

2.4.2 Standardized Method for measuring Gloss

Although there have been many attempts for the photometric measurement of gloss only a few have been standardized (Czepluch *et al.* 1993). The major reason that there are few standard methods to measure gloss is due to a lack of correlation with subjective evaluation. Ingersoll in the early 1900s established the first method for gloss measurement (Ingersoll 1914, Ingersoll 1921). His instrument, the 'Glarimeter', was the first commercial glossmeter. It was actually a contrast-gloss meter (Hunter 1975a). The measurement principle of the glarimeter was based on the polarization of light. The angle of incidence and angle of detection were 57.5° . Gloss was evaluated by a contrast method using a polarizing element that subtracted the specular component from the total reflection.

Extensive work on gloss by Hunter in the early 1930s led him to developed first photoelectric-based glossmeter (Richard S. Hunter 1937, Hunter 1975a). Hunter's glossmeter employed a measuring geometry of 45° . Figure 2-13 shows the beam axes of

a lustermeter designed by Hunterlab. The formula developed to express this relationship is:

$$Lustre = 100 \left(1 - \frac{\text{diffuse reflectance factor}}{\text{specular reflectance factor}} \right)$$

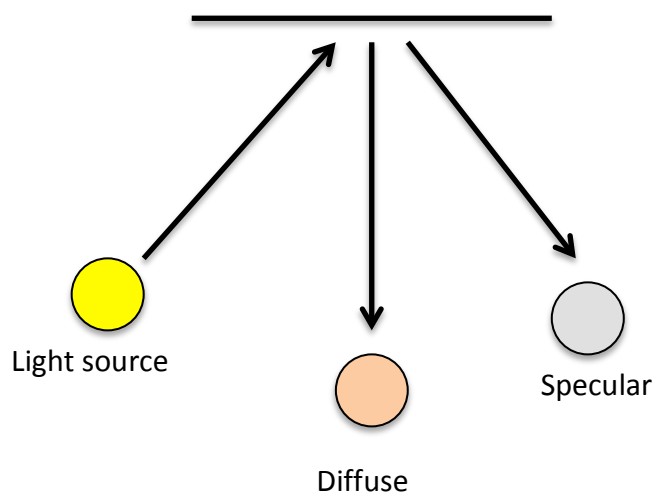


Figure 2-13 Diagram of Hunterlab Lustermeter (Hunter 1975a).

In 1951, Hunter's advancement in the gloss measurement led to the first standardized test method to determine gloss of high-gloss and also low-gloss surfaces. According to the test method of American Society for Testing and Materials (ASTM) D523, the measurement of gloss of high-gloss surfaces should be measured with 20° and low-gloss surfaces (such as textiles) with 85° geometry. Specular gloss measurement of a surface is determined in ASTM D523 and International Standards of Organization (ISO) 2813 standards. There are standards similar to ISO 2813 and ASTM D523 standards. Standards relating to visual evaluation of appearance are listed in the Appendix A.

Glossmeter measurements are based on very simple methods; the surface is illuminated by a light source at an angle and a detector is located at the same but opposite angle. Figure 2-14 shows a schematic diagram of a glossmeter. Ideally the glossmeter should measure irradiance of the specular reflection but in reality, when the surface is rough,

the light is scattered, and the scattered light may also be detected. Glossmeter sensitivity strongly depends on the measurement geometry. Fixed one or two angles will not cover different surfaces having different level of shine (from matte to high gloss). Commercial glossmeters have measuring geometries 20° , 45° , 60° , 75° and 85° with respect to surface normal.

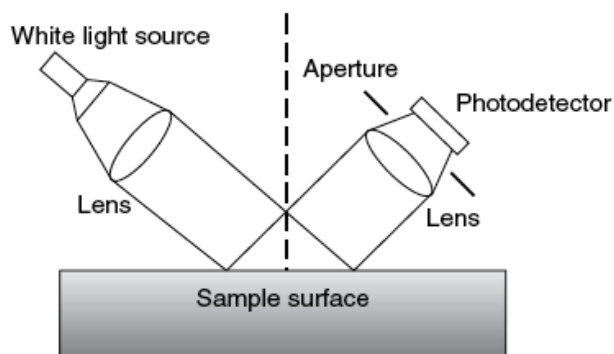


Figure 2-14 A schematic diagram of the measurement of gloss (Silvennoinen *et al.* 2007).

Gloss calculations are based on the ratio between luminous flux of light, reflected in specular direction from an object to the light reflected from a highly polished black glass in the specular direction. The refractive index of black glass should be 1.567 at the wavelength of the sodium line D (589.2nm), and it has to be ideally flat (Silvennoinen *et al.* 2007). For all angles of incidence this standard reference plate made of black-coloured glass, has given specular gloss value of 100 gloss units (GU). “Specular gloss value”, typically ranges from 100 (high gloss) to 0 (low gloss).

2.4.3 Limitations using conventional Glossmeters

Conventional glossmeters are effective for samples having smooth and flat surfaces. Usually, the size and shape of the sample causes difficulties in measuring gloss. Another problem is having 5 different measuring geometries because of the limited sensitivity of conventional glossmeters (Aims and Objective Section 1.1, Objective 3-a). If the surface is uneven or curved glossmeters might give erroneous gloss readings. Figure 2-15 shows the effect of different surfaces on the measurement of gloss.

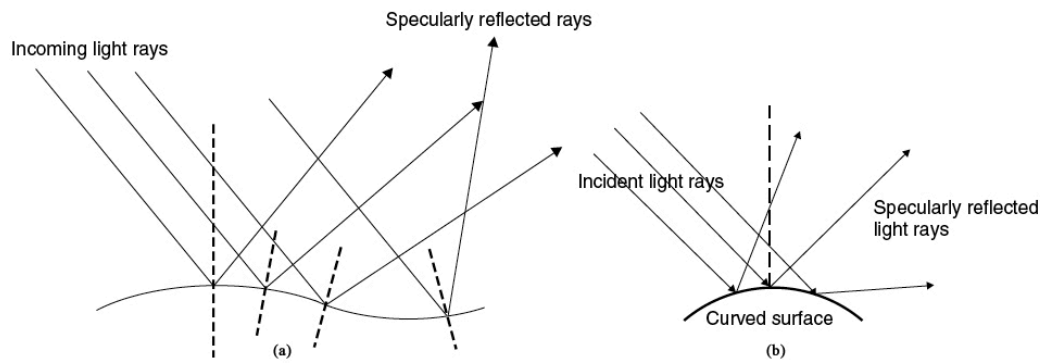


Figure 2-15 (a) Effect of waviness on the measurement of the gloss of the surface (b) Effect of curved surface on the measurement of the gloss of a surface (Silvennoinen *et al.* 2007)

2.4.4 Goniophotometer

As mentioned in the previous section, (Section 2.4.3), a glossmeter does not specify the optical properties of a reflecting surface. The only way of specifying the optical properties of a reflecting surface is by means of the polar intensity distribution curves (Harrison 1945). Curves should be three-dimensional measuring intensities at all angles of incidence. Instruments suitable for determining these polar curves are termed Goniophotometers. The foundation of goniophotometry were provided by Bouguer (Harrison 1945). These devices produce photometric measurements of a sample. Figure 2-16 shows as schematic of a goniophotometer, where the light source with a distance l_s is projected toward the sample, S , and reflected light is detected by the detector in a specific direction with a distance l_d . Both light source and detector and even the sample, can be moved in position so that the reflected light can be detected at different angles around the specular direction, where, θ_i illumination angle and θ_r is the detection angle. The light detected by the detector is normally weighted according to the $V(\lambda)$ spectral response. This response is converted into an electrical signal and plotted as a curve. Figure 2-17 show a typical goniophotometer curve of a dark-brown human hair (actual figure from the source consists of two curves one measured intensity from root to tip and second from tip to root of a human hair, but for the sake of explanation one curve has been removed).

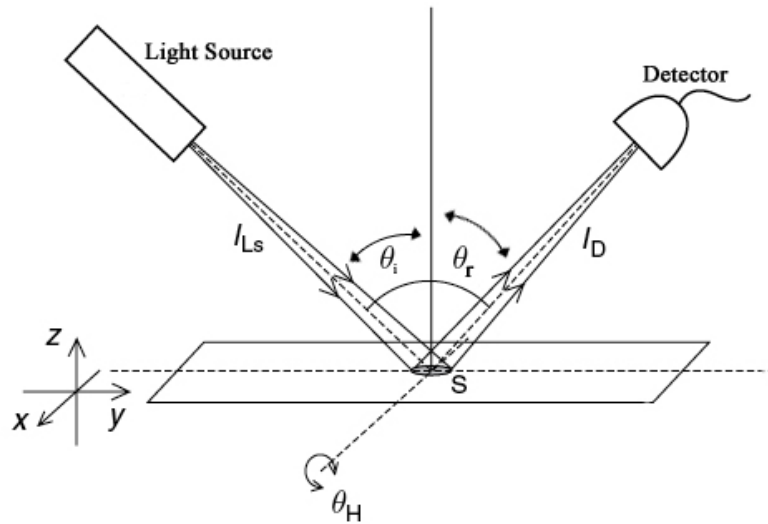


Figure 2-16 Schematic of Goniophotometer (Silvennoinen *et al.* 2007)

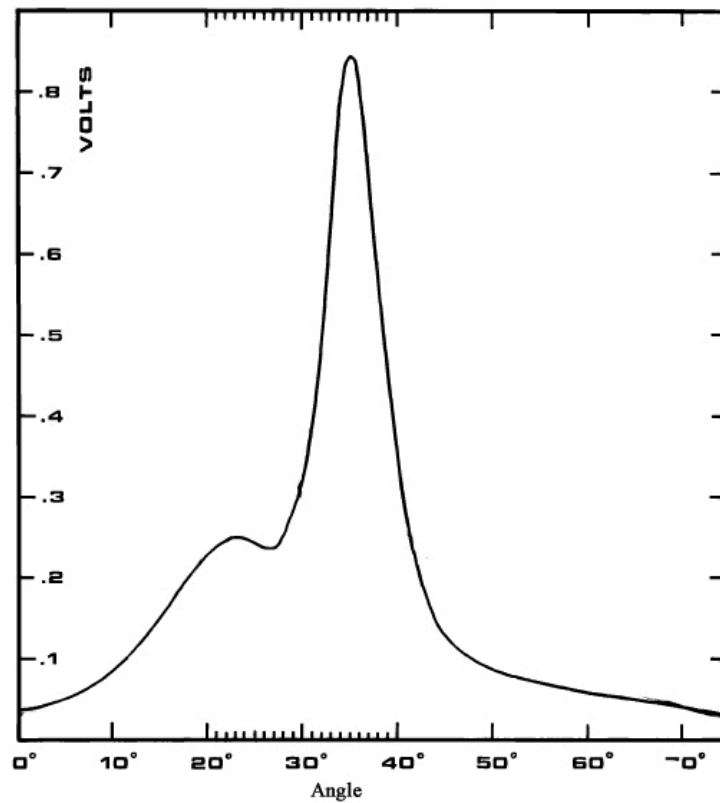


Figure 2-17 Goniophotometer curve of a dark-brown human hair (Stamm *et al.* 1977b)

Conventionally, the detectors in goniophotometers are light sensors similar to those in spectrophotometers. With advancements in digital imaging, the use of a digital camera as the light detector to predict gloss has been proposed for several years (Kumar and MacDonald 2006, Marschner *et al.* 2000). In human hair, image-based techniques have been shown to give a good prediction of visual results for gloss (Lefaudeux *et al.* 2008).

2.5 Optical properties of the Human Eye

In visual processing the eye works as a transducer. It provides the means of converting one form of energy (electromagnetic energy), in the form of light, into nerve impulses (Hill 1997). The human eye acts like a camera. The outer layer, the cornea, and lens act together like a camera lens to focus an image at the back of the eye. The Retina, acts like a film or a sensor of a camera (Fairchild 2005a). Following initial coding by nerve cells in the retina, the nerve impulses transmit along the optic nerve and relay, via nerve fibres, to terminate in a part of the brain (Occipital cortex). Somewhere in between the photoreceptors in the retina and the occipital cortex, information about lightness, colour, shape, movement and depth of scene or objects are coded and decoded to provide sight (Hill 1997). Figure 2-18 shows a horizontal section of the human.

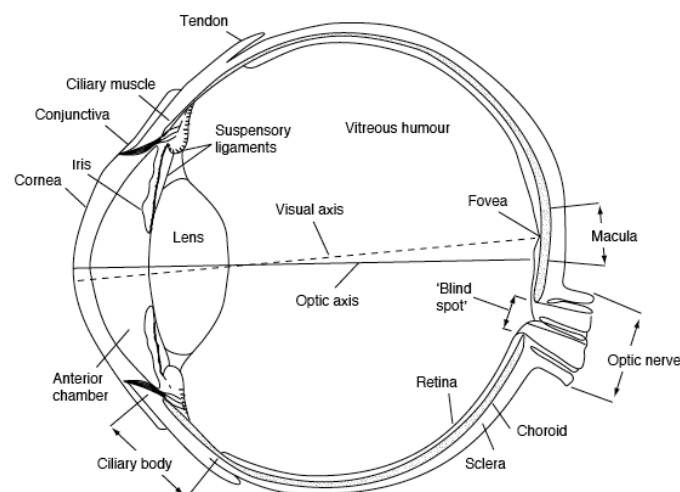


Figure 2-18 Horizontal section of the human eye (Hill 1997)

2.5.1.1 Cornea

The cornea is a transparent, dome-shaped surface that covers the front of the eye. It has two primary functions (a) to refract and (b) transmit light. The thickness of the cornea is not uniform; the central thickness is approximately 530 μm (Acharya et al. 2008) it has mean refractive index of about 1.376 (David A and George 2000). The cornea serves as the most significant image-forming element of the eye (Fairchild 2005a).

2.5.1.2 The Lens

The lens is a layered, flexible structure and its function is to focus objects. It varies in refractive index, higher in the centre than at the edges. This feature serves to reduce aberrations (the failure of rays to converge at one focus because of limitations or defects in a lens). Ciliary muscles control the shape of the lens (Fairchild 2005a).

2.5.1.3 Iris and Pupil

The Iris is a muscle, which has a circular aperture, the pupil, and is positioned just in front of the lens. The Iris controls the amount of light entering the eye. In darkness the pupil expands to its maximum diameter of about 8mm, while in high illumination it reduces to 1.5mm. Focal length of the eye is about 17mm; the effective aperture of the pupil can vary between f2.5 and f13. The f-number is the ratio of a focal length of a lens to its diameter (Hill 1997).

2.5.1.4 The Retina

The Retina is the light-sensitive tissue of the eye and consists of a number of cellular, pigmented and nerve fibres layers. The thickness of the retina varies from 50 μ m (0.05mm) at the foveal centre to about 600 μ m (0.6mm) near to the optic disc (David A and George 2000). The outermost layer of the retina contains photosensitive receptors called rods and cones, which transduce the information of the image projected onto the retina into chemical and electrical signals. The signals are then processed by a network of cells and transmitted to the brain through the optic nerve.

There are two special areas that exist in the Retina, which are known as the fovea and the blind spot (junction area of the optical nerve). The Fovea is responsible for sharp central vision. The Fovea is divided in concentric areas: foveola, fovea and macula, whose respective angular diameters are 1°, 5° and 20° (Silvennoinen *et al.* 2007). The resolving power of the eye will decrease as a function of angular distance from the foveola. Figure 2-18 shows the resolving power of the eye.

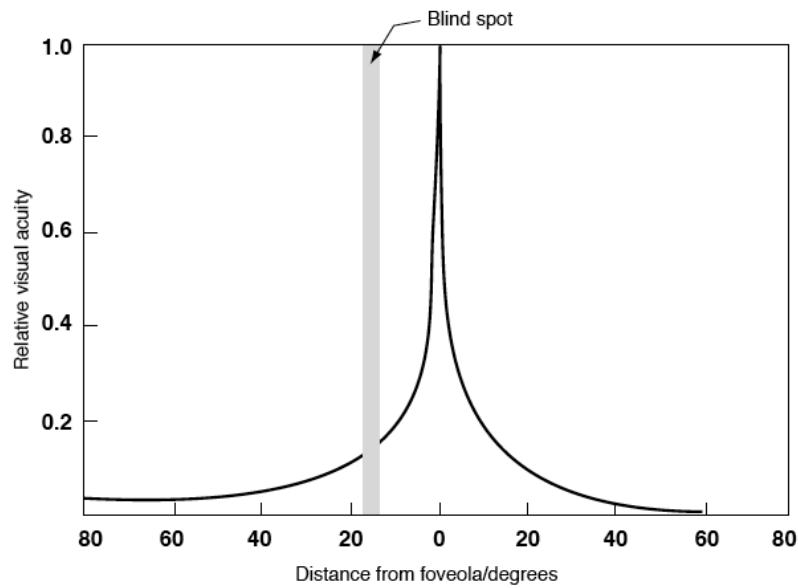


Figure 2-19 Resolving power of the eye (Hill 1997)

2.5.1.5 Rods and Cones

Rods and cones, the photoreceptors, are so named because of their physical shapes. Figure 2-20 shows a schematic of a single Rod and a single Cone. Rods operate optimally at low luminance levels while cones are most efficient at higher luminance levels. At high levels of luminance only cones are active. In the intermediate levels, both cones and rods are active. Rod-only vision is known as scotopic vision. Vision served only by cones is referred as photopic vision, whereas mesopic vision is referred to the vision served by both photoreceptors.

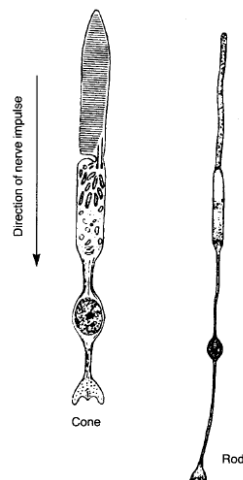


Figure 2-20 Rods and Cones (Hill 1997)

There is only one type of rod receptor with a peak at 510 nm in spectral responsivity. However there are three types of cones each sensitive to different part of the spectrum shown in Figure 2-21. The three types of cones are most properly known as L, M, S cones. These names refer to the long-wavelength, middle-wavelength and short wavelength cones. They are also known as RGB cones (Red, Blue and Green).

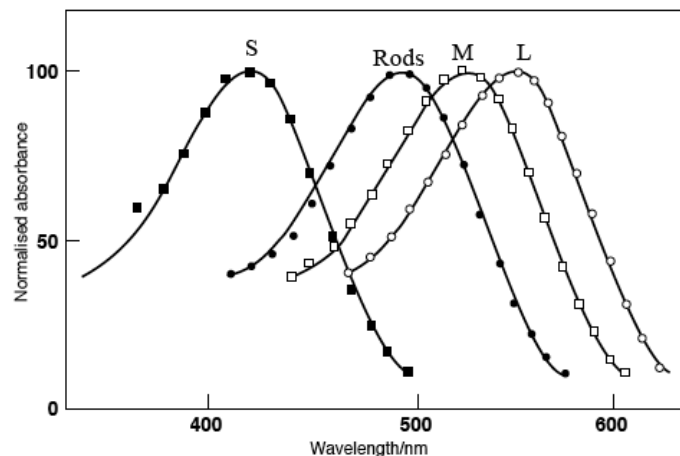


Figure 2-21 Absorption spectra of the four-receptor types (Hill 1997)

The spatial distributions of these cones are not even. S cones are not present in most central area of fovea and S cones are not densely populated in the retina. There are far more L and M cones than S cones and there are approximately twice as many L cones as M cones. The relative populations of the L:M:S cones are approximately 12:6:1 (Fairchild 2005). Figure 2-22 shows the spatial distributions of rods and cones across the retina.

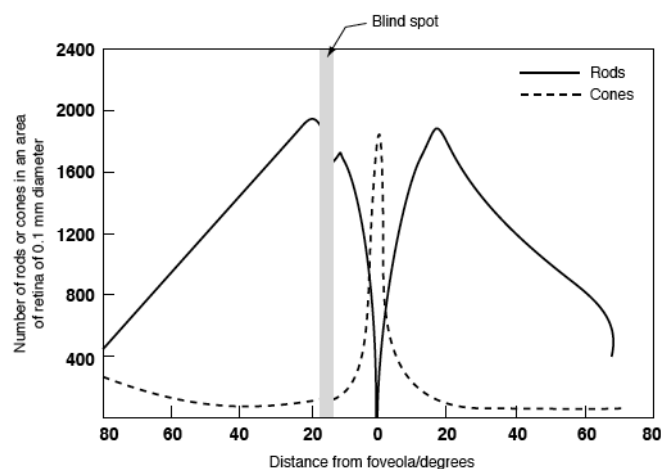


Figure 2-22 Rods and Cones receptor density distribution across the retina (Hill 1997)

2.6 Detectors (Image capture devices)

In this study, the main devices used to capture images of the hair tresses have been Digital cameras. A digital camera is an imaging device that takes still photographs or video, or both, digitally by recording images on a light-sensitive sensor. With advancements in image capture technology, these devices (digital cameras) are being used in quantifying gloss in different areas; they range from cosmetic industry to agriculture to understanding the behaviour/health of animals (McMullen and Jachowicz 2003), (Lefaudeux *et al.* 2008), (Mendoza *et al.* 2010), (Toomey *et al.* 2010).

2.6.1 Digital SLR Camera

Digital still cameras of the single lens reflex (SLR) type have an interchangeable lens system; Figure 2-23 shows a digital still camera. DSLR cameras have instant return mirror mechanisms like ordinary SLR cameras. The major difference is that they have image sensors in place of film and they have LCD monitor displays (Toyoda 2006). Figure 2-24 briefly summarizes the digital camera's image processing.

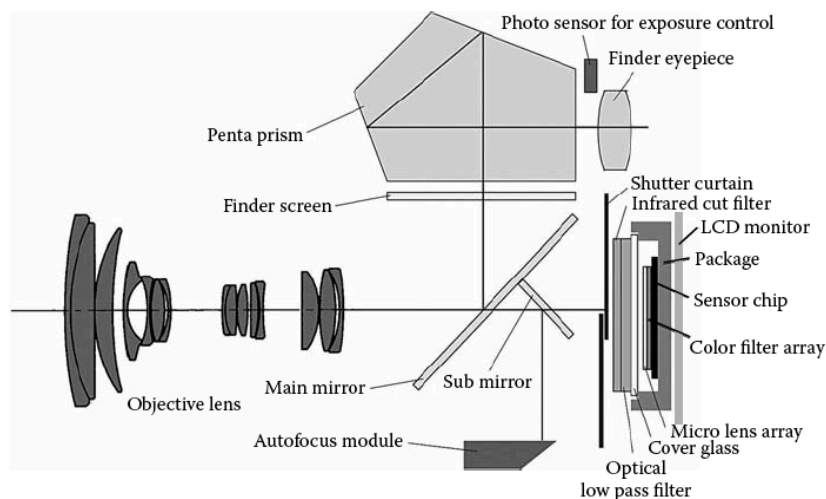


Figure 2-23 Typical arrangement of an SLR digital still camera (Toyoda 2006)

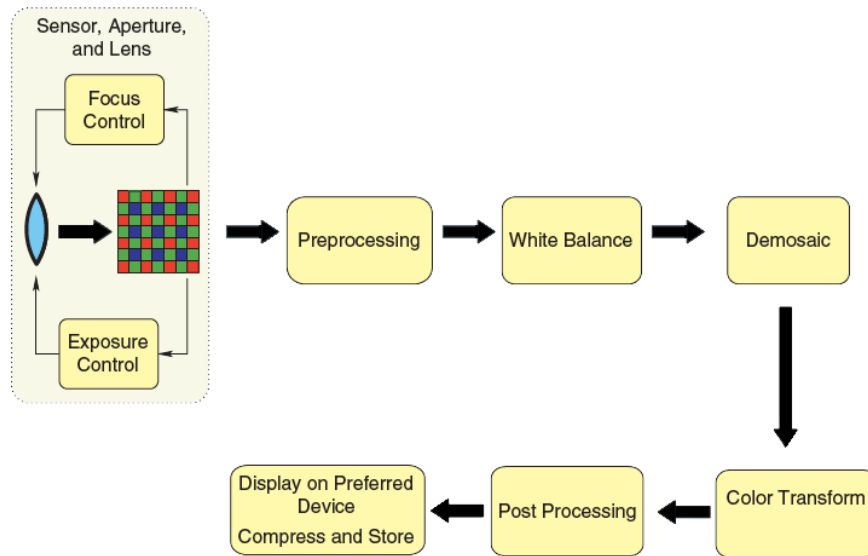


Figure 2-24 Image processing involved in a Digital Still Camera (modified from (Ramanath *et al.* 2005))

2.6.1.1 Image sensors

A device that converts an optical image that is formed by an imaging lens into electronic signals is known as an image sensor. They are predominantly used in digital cameras and other imaging devices. Charge-coupled devices (CCDs) are the most popular image sensors for digital still cameras. However, CMOS (complementary metal-oxide Semiconductor) sensors are beginning to be used in SLR cameras (Toyoda 2006). An image sensor is basically a monochrome sensor, so it would only be able to create grey-scale images. To capture a colour image a colour filter array is placed in front of the each individual sensor. By breaking up the sensor in to variety of red blue and green pixels, an accurate image can be predicted (by retrieving information from each pixel). These processes are called demosaicing and interpolation. The most commonly used primary colour filter pattern is the 'Bayer' pattern (Bayer 1976). This pattern configuration has twice as many green filters as red or blue filters. The reason behind this configuration is that the human visual system derives image details primarily from the green portion of the spectrum. That is, luminance differences are associated with green whereas colour perception is associated with blue and red (Nakamura 2006).

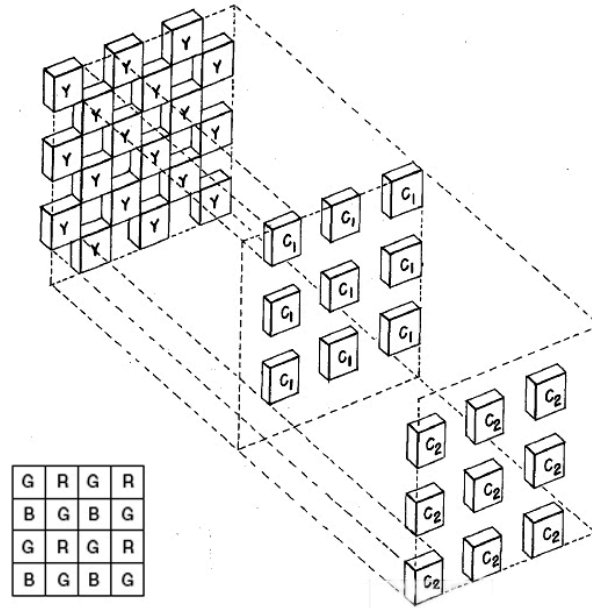


Figure 2-25 The Bayer arrangement of colour filters (Re-drawn from (Bayer 1976))

2.6.1.2 White Balance

The Human visual system has the ability to map “white” colours to the sensation of white, even if the object is illuminated under different light sources. This phenomenon is known as “colour constancy”. However, digital cameras do not have a highly sensitive system like the human eye (Zaraga and Langfelder 2010). One method of ensuring white balance is to assume that white patch must induce maximal camera responses in the three channels. In other words Red, Green and Blue channels of the image, the white balanced image has signals given by R/R_{max} , G/G_{max} and B/B_{max} . However, using the maximum output of all three channels is very often a poor estimate of the illuminant (Ramanath *et al.* 2005). It is not always the case that white balance must be performed automatically in digital cameras. Some cameras, such as the one used in this study, have the ability to select or set the white balance manually using a standard white balance card for calibration.

2.6.1.3 Colour transformation

Digital cameras are not colorimetric, given that the spectral sensitivities of the camera are not identical to the human colour matching functions. The data captured by the sensor is in the colour space (un-rendered colour space) of the camera and has little to do with colorimetric (human) values. One means of obtaining colorimetric values of an image is to transform the image from the sensor's colour space to the CIE XYZ colour space.

Most capture and display devices have their own colour space, generically referred to as device-dependent RGB. Although it is possible to convert an image between two device-dependent colour spaces, it is more convenient to define a single standard colour space. The negative aspect of such standards is there is not one single standard but several standards (Reinhard *et al.* 2006a). Most of the encodings are divided into two types a) *Output-referred*: they employ a colour space corresponding to a particular output device rather than original scene they are meant to represent. b) *Scene-referred*: they represent the original captured scene values as closely as possible. Display on a particular output device then requires some method of mapping the pixels to the device's gamut. This process is known as tone mapping.

2.6.2 Dynamic range

The Dynamic Range (DR) is the highest overall contrast that can be found in an image. It is also known as contrast ratio. A test image is shown in Figure 2-26 with a contrast ratio 10:1. In photography, dynamic range is measured in Exposure Value (EV) (also known as Stops), which is the amount of light that reaches the sensor (Bloch *et al.* 2007). EV is controlled by combination of a camera's shutter speed and aperture of the lens, also known as *f*-number. *f*-number is given by:

$$N = \frac{f}{D}$$

Where, *f* is focal length and *D* is the diameter of the aperture.

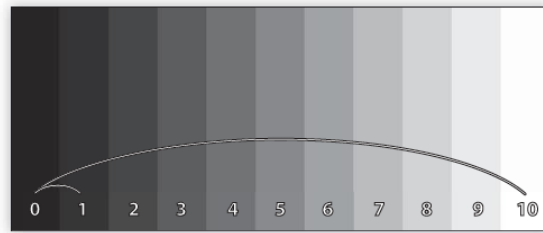


Figure 2-26 Test image with contrast ratio 10:1 (Bloch et al. 2007)

2.6.3 High Dynamic range

The Dynamic range (DR) is dependent on two factors: the overall range of brightness and the smallest steps. High Dynamic Range (HDR) imaging is achieved by increasing the brightness steps or adding an extra level of brightness. This can be done by capturing multiple standard images, often using different exposures, and then merging them into an HDR image. Most HDR images are scene-referred, in that their pixels have a direct relation to radiance in some scene (Reinhard et al. 2006a).

2.6.3.1 HDR Imaging and the Shine Band

Using HDR imaging techniques, taking images of a sample at different shutter speeds, to measure gloss is a relatively new idea. Only Kumar and MacDonald (Kumar and MacDonald 2006) used this method to evaluate the gloss of papers (six paper samples were used in the study, having different gloss values). However, this technique has never been used to evaluate the gloss of a human hair tress. Figure 2-27 shows three images of a single human hair tress (Oriental-virgin) captured at different shutter speeds and Figure 2-28 shows images of a single human hair tress (Oriental-virgin) at various shutter speeds (1s -1/200s).



Figure 2-27 Virgin-Oriental Human Hair tress at 1s, 1/3s, 1/20s shutter speed.

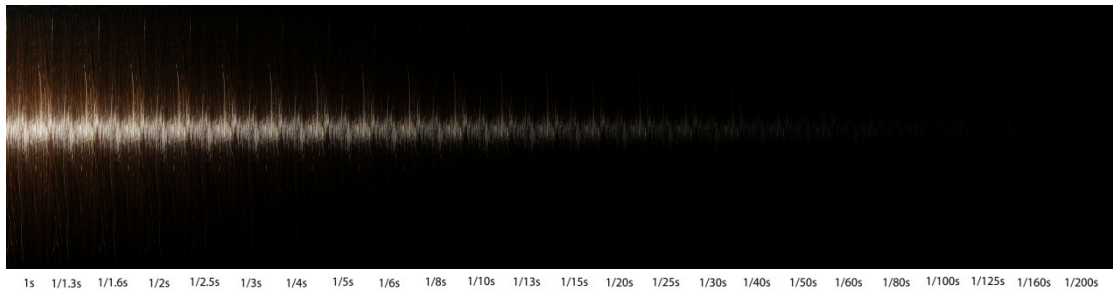


Figure 2-28 Virgin-Oriental Human Hair tress images captured at various shutter speeds (1s-1/200s)

2.7 BRDF (Bi-directional Reflectance Distribution Function)

One of the major goals of an image-based gloss evaluation system is to synthesize realistic images of the sample. To measure gloss, a description of reflectance is needed for each reflective surface of the sample. The interaction of light with a surface can be expressed as a single function, called a bi-directional reflectance distribution function, or BRDF (Nicodemus 1965). Bi-directional Reflectance Distribution Functions (BRDF) describe the directional dependence of the reflected energy. This is a function of four angles, two incidents and two reflected, as well as the wavelength and polarization of the incident light. Figure 2-29 shows the geometry of a BRDF and it can be defined as the ratio of reflected light L in a particular direction $(\theta_s \phi_s)$ to the incident light I from another direction $(\theta_i \phi_i)$, as shown in following equation;

$$BRDF = f_s(\theta_i, \phi_i, \theta_s \phi_s) = \frac{dL_s(\theta_s \phi_s)}{dI_i(\theta_i \phi_i)}$$

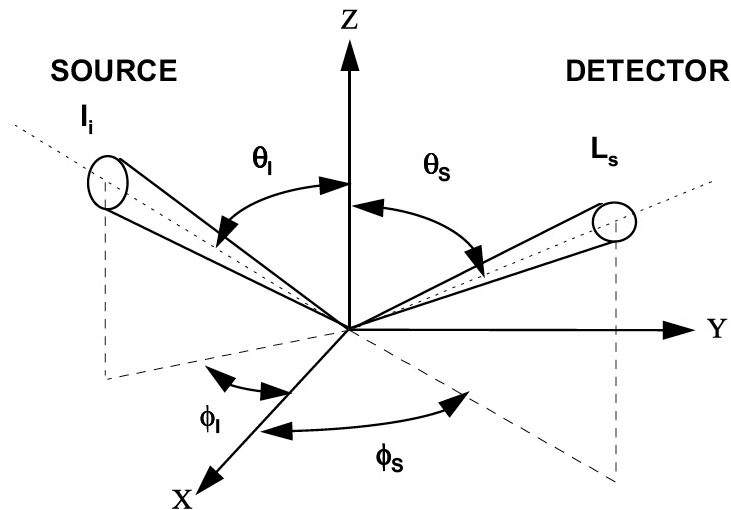


Figure 2-29 BRDF geometry (Tribble 2000).

BRDF may either be calculated from mathematical functions derived from analytical models or can be measured by empirical measurements of the sample. Traditionally BRDF is measured with a gonireflectometer, positioning a source and detector with respect to a flat sample (Marschner *et al.* 2000). Figure 2-30 shows conventional gonireflectometer. In a typical setup of BRDF capture, three or four angular dimensions are handle by specialized mechanisms that position a light source and detector at various directions from a sample. The final measurement is performed either by measuring the entire spectrum at once or by recording multiple measurements.

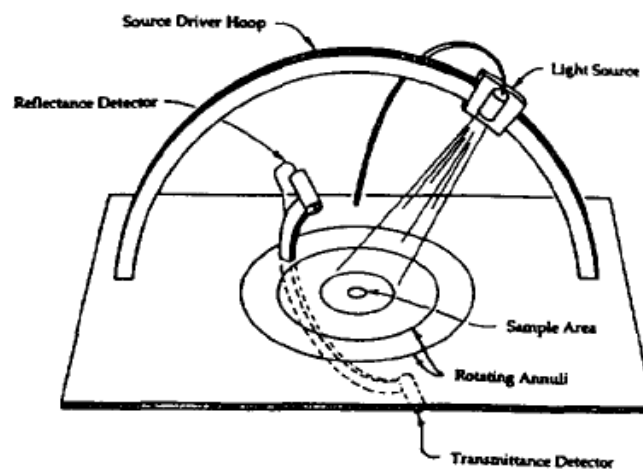


Figure 2-30 Conventional gonireflectometer with movable light source and photometer (Ward 1992)

Ward (Ward 1992) used a curved mirror to gather light scattered from a flat sample into a camera (CCD) with a fish-eyed lens. Lu *et al.* (Lu *et al.* 1998) used photographs of a cylinder covered with their sample (velvet). The cylinder was used to give broad angular coverage in the incidence plane. They took multiple images with different light source positions to cover all angles. Marschner (Marschner *et al.* 2000) used a similar method to present measurements to produce the full isotropic BRDF.

Since the BRDF is a function of four angles, it is too complex to be practical for most measurements. Conventionally, from the three dimensional BRDF domain, two-dimensional data is extracted with an assumption that ϕ_i and ϕ_s are constant (eg. $\phi_i = \phi_s = 90^\circ$) in a restricted section of the hemisphere (Luo 2008, Fan and Gijbels 1996). Only the incident angle θ_i and the reflected angle θ_s are considered. Figure 2-31 shows the light intensity at different angles of a European brown human hair. The first peak indicates how glossy the fibre is and the second peak is associated with the colour. The height and width (full width at half maximum) of the luminous intensity profile indicates the glossiness of the hair fibre (more details in the Section 2.15.2).

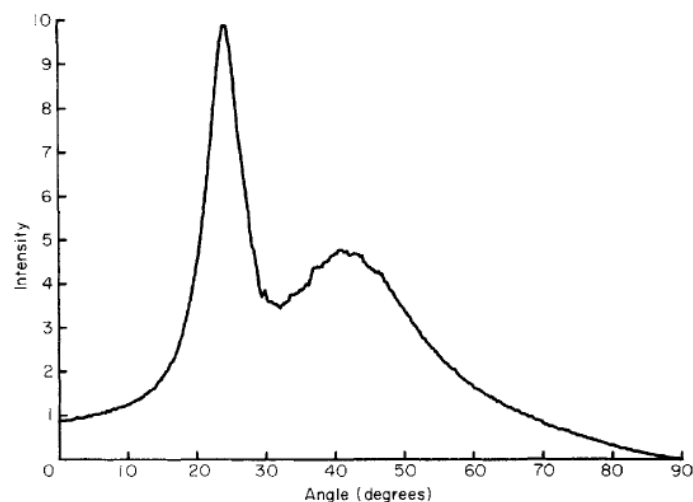


Figure 2-31 Luminous intensity according to the angle of observation (in degrees) of a European- brown hair (Guiolet *et al.* 1987).

2.8 Psychophysics

Psychophysics is the scientific study of the relationships between the physical measurements of stimuli and the sensations and perceptions of those stimuli (Johnson and Fairchild 2003).

2.8.1 Evolution of Psychophysics

The formal discipline of psychophysics is less than 150 years old. Major events in the field of psychophysics can be represented in the work of Weber, Fechner and Stevens (Fairchild 2005b). In the early nineteenth century, E.H. Weber investigated the perception of the heaviness of lifted weights. He asked observers to lift a given weight and then he increased the weight until the observer noticed a change in weight. This is a measurement of threshold for change in weight. Weber concluded that, for a given initial weight, I , the change in weight necessary to produce a perceptual difference, ΔI , followed a constant ratio, $\Delta I/I$. This stimulus change is often referred to as a “Just Noticeable Difference”, or a JND. This relationship is known as Weber’s Law.

Later in the nineteenth century, Fechner (known as the father of psychophysics) built on the work of Weber to derive a mathematical relationship between stimulus intensity and perceived magnitude. Fechner made the following assumptions:

- a) Weber’s law is indeed valid for all stimulus intensity and,
- b) JNDs are indeed a valid unit of sensation and all JNDs are perceived as being equal. It means that the perceived magnitude of a stimulus is proportional to the logarithm of the intensity of the physical stimulus, $S = k \log(I)$, where S is the perceived sensation, k is constant, and I is the measured physical intensity (Fechner 1966). This solution is known as Fechner’s law.

Almost 100 years later, Stevens questioned the generality in the Fechner’s results. Stevens studied the relationships, for over 30 different types of perception, between physical stimulus intensity and perceptual magnitude. Stevens concluded that the relationships between physical stimuli and their corresponding perceptual scales could be defined as power functions. The general form of Steven’s Power Law is the function

$S = kI^\gamma$, where S is perception, k is constant and γ is the exponential power value (Johnson and Fairchild 2003).

2.8.2 Measurement scales

In general there are four types of measurement scales for psychophysical experiments. These scales are nominal, ordinal, interval, and ratio (Kantowitz *et al.* 2008).

2.8.2.1 Nominal Scales

Nominal scales are a simple form of scale, where scale numbers are used as names of objects. An example of nominal scale would be the numbers on a One Day International (ODI) cricket player's T-shirt. They don't hold any value but are used to identify the player.

2.8.2.2 Ordinal Scales

In Ordinal scales objects can be sorted or ranked, either in ascending or descending order based on whether they have a greater or lesser amount of a particular attribute.

2.8.2.3 Interval Scales

An interval scale has equally spaced units, or intervals. For-example if a sample is judged two units away from the target and a second sample is also judged two units away from the sample but in a different direction, the differences between the target and two samples will be perceptually equal.

2.8.2.4 Ratio Scales

Ratio scales have all the properties of the Nominal, Ordinal and Interval scales plus a meaningfully defined zero point. Ratio scales are normally applied in basic physical measurement systems like length and weight.

2.8.3 Classes of Visual psychophysics experiments

To measure perceptions of stimuli, there are many different experimental techniques. For visual experiments e.g. studying images and colour appearance, Psychophysics experiments are divided into two classes

- Threshold and matching experiments: these experiments measure the change in sensitivity required for the observer to detect a particular stimuli.
- Scaling experiments: these experiments are used in order to determine relationships between the physical and perceptual magnitudes of a stimulus.

2.8.3.1 Threshold Techniques

Threshold experiments are designed to measure the JND (just-noticeable difference) in the experiment; Weber's weight experiment is an example of a threshold experiment. The threshold technique is used to measure the observer's sensitivity to changes in a given stimulus. Threshold techniques are useful for defining visual tolerances such as those for perceived colour differences (Kantowitz *et al.* 2008).

Threshold techniques include the following:

- *Method of adjustment*: in this technique, the observer controls the stimulus magnitude and adjusts it to a point that is just perceptible.
- *Method of limits*: in this method, predefined discrete intensity levels of stimuli are presented (in either ascending or descending order) and the observer responds 'yes' or 'no' dependent upon their perception.
- *Method of constant stimuli*: in this method, numbers of stimulus intensity levels (typically 5 to 7), around the level of the threshold, are presented multiple times in random order. The observer's sensitivity of each stimulus is determined.

2.8.3.2 Scaling technique

This technique is designed to generate relationships between physical measures of stimulus intensity and how they are perceived. Usually the scale and scaling method of the experiment are decided before any visual data is collected. The scaling techniques are divided in two types a) one-dimensional scaling and b) multidimensional scaling (Fairchild 2005b).

2.8.3.2.1 One-dimensional scaling

In one-dimensional scaling observers are asked to judge a single perceptual attribute e.g. how glossy the hair tress is, or what the difference is in shine between a pair of hair tresses.

Several One-dimensional scaling psychophysical scales have been devised, which are as follows:

- *Rank order*: an observer is asked to arrange a group of samples either increasing or decreasing magnitudes of a particular perceptual attribute.
- *Graphical rating*: A scale is given and the observer is asked to judge where sample lies on that scale.
- *Category scaling*: an observer is asked to separate a large number of samples into different categories.
- *Paired comparisons*: in this technique, all samples are presented pair-wise and the observer judges them, usually one pair at a time.
- *Partition scaling*: in this method, two different samples are presented and observer is asked to find another sample with the same difference.
- *Magnitude estimation or production*: in this method, the observer is asked to assign ranks (numbers) to the stimuli according to their magnitude of perception or observers are given a number and they have to produce a stimulus with that perceptual magnitude.

2.8.3.2.2 Multidimensional scaling

Multidimensional scaling (MDS) is a method similar to one-dimensional scaling, but it requires more than one scaling attribute (Fairchild 2005b).

2.9 Human Hair

Aristotle, in the fourth century BC, suggested that hair is formed from sooty vapours exhaled through the body's pores that hardened when they came into contact with air. Saint and scientist Albertus Magnus, in eleventh century AD, believed that scalp hair fibres were the product of bodily fluid and phlegm excreted from the brain (Vogt *et al.* 2008). William Derham, in early sixteenth century, used a microscope to study human hair and saw medullae. This led him to believe that hair fibres were tubules for the evacuation of bodily fluids (Derham 1713). Only, in the nineteenth century, careful study of the skin and hair follicle structure was fully defined and the mechanism of human hair fibre growth was explained as it is considered in today (Beigel 1869).

2.10 Hair types

The human body is diversely covered with hair. Human hair can be classified, based on the shape, structure, and time of appearance on the body. Major types of hair are a) lanugo-hair, b) vellus-hair and, c) terminal-hair (Rook 1965).

Lanugo-Hair is prenatal hair. They are soft, fine and are either lightly pigmented or contains no pigments. They usually shed before birth or soon thereafter (Robbins 2002b). The diameter of lanugo-hair is less than 30 μ m and the length greater than 2mm (Vogt *et al.* 2008).

Vellus-Hair is fine and poorly pigmented. They grow on all areas of the human body with the exception of the palm of the hands and the soles of the feet. The diameter of vellus-hair is less than 30 μ m and the length is less than 2mm.

Terminal-Hair has a larger cross-section as compared to other hair types. They are pigmented. The shape and size of terminal-hair varies with human body location, some examples of terminal hair fibre length found on human body are tabulated in Table 2-1. The shape of the cross-section and terminal hair diameter varies from person to person, but it can be approximated by ethnicity and hair colour. The diameter of the cross-

section of Caucasian scalp hair ranges from as low as 40µm in blonde-haired to 90µm in dark-haired individuals. The shape of the cross-section also varies with ethnicity; Asian hair is typically circular in cross-section, while Caucasian hair typically has an elliptical cross-section shape. In contrast, African hair has an elliptical (even ribbon like) cross-sectional shape. Diameters of terminal hair fibres are tabled in Table 2-2.

Table 2-1 Typical dimensions of Terminal hair in humans (Vogt *et al.* 2008)

Area (Hair type)	Length –typical range (mm)
Scalp	100-1000
Eyebrow and eyelash	5-10
Beard and moustache	50-300

Table 2-2 Terminal hair diameter (Vogt *et al.* 2008).

Hair type	Diameter (typical range) µm
Blonde-haired Caucasians	40-80
Dark-Brown/Black haired Caucasians	50-90
Red-haired Caucasian	50-90
African (African-American)	60-100
Asian (far-East)	80-120

2.11 General Structure and Hair Growth

Human hair grows in three distinct stages called anagen (growing stage), catagen (transition stage), and telogen (resting stage) (Reiger 2000) Figure 2-32 shows different stages of human hair growth.

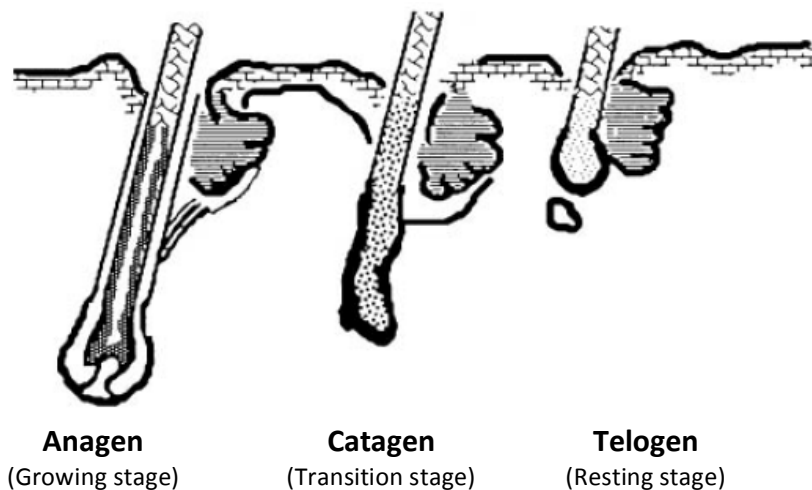


Figure 2-32 Schematic illustrating the three stages of growth of the human hair (Robbins 2002b).

The anagen stage; the growing stage, is characterized by intense metabolic activity in the hair bulb which lies inside the hair follicle. Hair-bulb is a tiny cup-shaped pit buried deep in the scalp. It is a structure of actively growing cells, which eventually produce the long fine cylinder of a hair. For scalp hair, this activity generally lasts for two to six years, producing hair that grows to approximately 100 cm in length.

The catagen stage; the transition stage, lasts for only a few weeks. During the catagen stage, metabolic activity slows down and the base of the bulb migrates up-wards through the skin toward the epidermal surface.

The telogen stage; the resting stage, also lasts only for a few weeks. This relatively uneventful period (no growth) dramatically changes as a new hair begins to grow beneath the telogen follicle, pushing the old telogen fibre out. The telogen fibre is eventually shed.

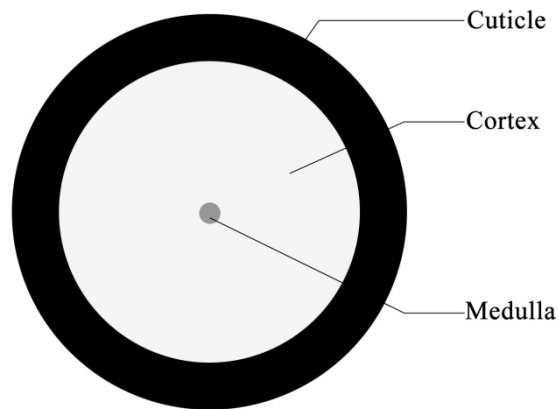


Figure 2-33 Schematic diagram of a cross section of a human hair fibre (Redrawn (Robbins 2002b)).

Morphologically, a fully formed hair fibre contains three or sometimes four different units of structures. Figure 2-33 shows a representation of the cross section of a human hair fibre. At the surface, the hair contains a thick protective covering consisting of layers of flat overlapping saclike structures called the cuticle. The cuticle layers surround the cortex and the cortex contains the major part of the fibre mass. The thicker hair often contains one or more loosely packed porous regions called the medulla, which is located near the centre of the fibre. The fourth unit is the cell membrane complex that glues or binds the cells together.

2.11.1 The Cuticle

The outermost structure of hair is called the cuticle. This forms a protective coating that envelops the delicate cortex and helps protect it from damage. The cuticle consists of flat overlapping scales, which are attached to the cortex at the root end (proximal end) of the fibre and they point toward the tip end (distal end) of the hair fibre, like shingles on a roof. In human hair, the cuticle layer is generally five to ten scales thick, with each scale being approximately $0.5\ \mu\text{m}$ thick. Each scale has approximately $5\ \mu\text{m}$ of exposed surface and is approximately 45 to 60 μm long. Smooth, unbroken scale edges can be found near the scalp, however as we move downward towards the tip end they often become more damaged; for example scale lifting, shown in Figure 2-34, due to normal

grooming actions, such as combing, brushing, and shampooing.

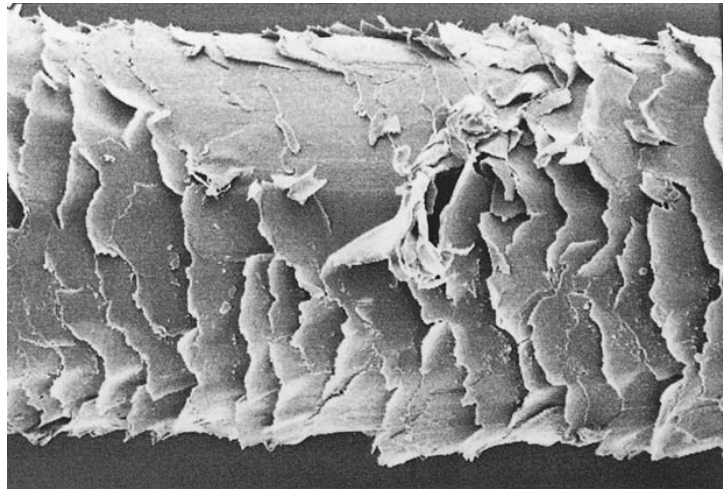


Figure 2-34 Scale lifting caused by fatiguing chemically undamaged hair (Robbins 2002b)

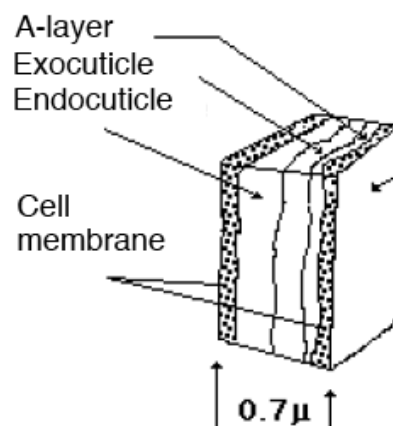


Figure 2-35 Layers between Cuticle cell membrane(Rushton 2006)

Each cuticle scale contains an outer membrane, the epicuticle. Within the cuticle cell membrane there are three distinct layers, illustrated in Figure 2-35:

- *The A-layer*, a resistant layer with high cystine content of approximately 30%.
- *The exocuticle*, sometime called the B-layer, also rich in cystine (content approximately 15%).
- *The endocuticle*, low in cystine (content approximately 3%).

The Endocuticle is the weakest component of the cuticle, when compared with the A-layer and exocuticle, due to its low cysteine content. This difference in composition means the endocuticle can absorb more water than the other cuticle layers (Swift 1997), this gives rise to the increased swelling in water and chemical sensitivity.

The cuticle and cortical cells are held tightly in place by intercellular lipids, including ceramides and they are protected by a fatty layer consisting of materials such as 18-methyl-eicosanoic acid (18-MEA). These materials naturally protect hair from surface damage; together they form a cell membrane complex, which is the only continuous part of the fibre.

2.11.2 The Cortex

The cortex of a hair fibre, consists of cells bound together with intercellular material or a cell membrane complex, constitutes the major part of the fibre mass and gives the fibre its elasticity, strength and colour. Cortical cells are generally 1 to 6 μm thick and approximately 100 μm long. Human hair contains a symmetrical cortex, unlike wool fibres. Most wool fibres contain two or three types of cortical cells. These wool fibre types are:

- *Orthocortex*: contains less matrix between the intermediate filament and a lower sulfur content.
- *Paracortex*: are smaller in diameter and have higher sulphur content.
- *Mesocortex*: contains an intermediate cystine content.

The cortical cells from human scalp hair are all similar to the orthocortical cells of wool, but they have high-sulphur content.

The major portion of the cortical cell comprises of spindle-shaped macrofibrils. In human hair the macrofibrils are approximately 0.1 to 0.4 μm in width. Each macrofibril consists of filaments called microfibrils (intermediate filaments) and a matrix. Hundreds of microfibrils twist together to form a macrofibril. Within the microfibrils is a substructure,

the protofilament (protofibrils), which consists of keratin proteins with a spiral-shaped α -helix structure twisted together to form a rope-like structure as illustrated in Figure 2-36. Together with the matrix proteins, the microfibril and matrix composite structure forms a tear resistant, elastic, highly cross-linked structure.

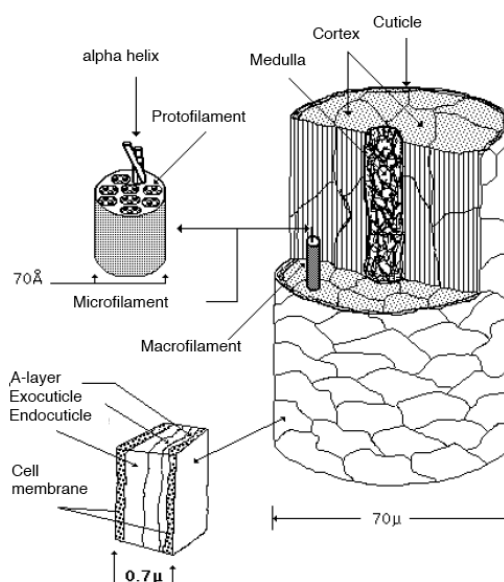


Figure 2-36 Schematic anatomical arrangement of human scalp hair (Rushton 2006)

The cortex is also the major site where natural colour pigments occur. There are two primary types of pigments: eumelanin and pheomelanin. Eumelanin produces hair shades of brown to black and pheomelanin produces the auburn hues.

2.11.3 The Medulla

The Medulla is not always present in hair but when present it is most commonly found in thicker, coarser hair (Jones 2001). In human hair medulla is vestigial but in wool and other animal hairs the medulla is a central air-canal, which provides insulation (Hashimoto 1988). Medullary cells are loosely packed and during formation they leave a series of vacuoles along the fibre axis. Medullary cells are spherical and hollow inside and are bound together by a cell membrane. The Medulla forms only a small proportion of the total fibre mass making its contribution to the chemical and mechanical properties of the hair negligible (Halal 2002), but the medulla may influence the colour and gloss of light brown and blonde hair due to the scattering of light.

2.12 The Chemical Composition of Human Hair

Human hair is a complex tissue comprising of amino acids, water, lipids and trace elements gathered in several morphological components (the cuticle, cortex, and medulla). Chemically, individual human hair fibre vary depending upon its moisture content and it consists of approximately 65 – 95% proteins (Robbins 2002a). Approximately, 91% of hair's dry weight is protein, 4% is lipid, 4% melanin and the remainder is made up of sugars, ash and zinc. The ash content varies from 0.55 to 0.94% (Dutcher 1951). The trace elements reported in human hair are Ca, Mg, Sr, B, Al, and Na. Amino acids are molecules containing an amino group, a carboxylic acid group and a side chain that varies between different amino acids Figure 2-37 shows general structure of an amino acid. Amino acids are the building blocks of proteins. Proteins are straight chain polymer made from the 21 naturally occurring amino acids linked together by peptide bonds (Swift 1997). The protein formed in hair belongs to a group of fibrous proteins known as Keratins. Keratins are insoluble, cross-linked proteins which contain the amino acid cystine. Typically these protein chains contain hundreds of amino acids. The individual amino acids found in hair are given in Table 2-3.

Table 2-3 Individual Amino Acids found in Hair (Robbins 2002a)

Amino Acid
Alanine
Arginine
Aspartic Acid
Cystine
Glutamic acid
Glycine
Histidine
Isoleucine
Leucine
Lysine
Methionine
Phenylalanine
Proline
Serine
Threonine
Tyrosine
Tryptophan
Valine

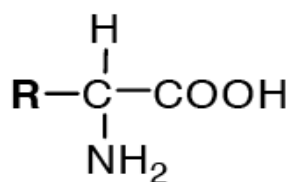


Figure 2-37 General amino acid structure (R represents a chemical group) (Robbins 2002a)

Amino acids are characterized by the chemical properties of their side chain group and the side-groups determine whether the amino acid is hydrophilic or hydrophobic and neutral, acidic or basic. Amino acids are linked together by a peptide bond (–CONH–), the group CONH is not a strong combination and can be broken by oxidation and acid / alkali hydrolysis.

2.12.1 Bonding in Keratin

In hair proteins, individual peptide chains are linked together with several types of cross-linking bonds.

Hydrogen Bonding

Hydrogen bonds are formed between two atoms, one of which is hydrogen, with partial but opposite electrical charges. These bonds are weak non-covalent bonds. In the human hair hydrogen atom of the NH group of one amino acid in a polypeptide chain can form a hydrogen bond with the oxygen atom of the CO group of another amino acid as shown in the Figure 2-38. Hydrogen bonds are essential to the stability of the helical structure formed by the hair protein. They break when hair becomes wet and then reforms when it dries. Even though they are weak bonds they account for one third of the fibre's total strength and this is due to the high number of Hydrogen bonds (Halal 2002).

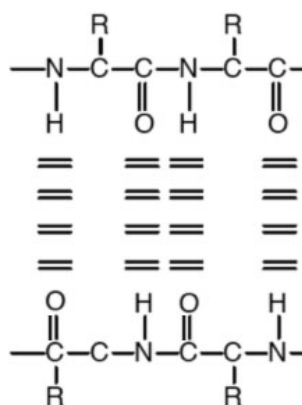


Figure 2-38 Hydrogen Bonding (= represents hydrogen bonding) (Rushton 2006)

Ionic bonds

Ionic bonds are formed by the attractions between the positively charged amino group (NH_3^+) and the negatively charged acid group (COO^-) of another as shown in the Figure 2-39. This type of bond is affected by pH and can be broken by strong acidic or alkaline solutions.

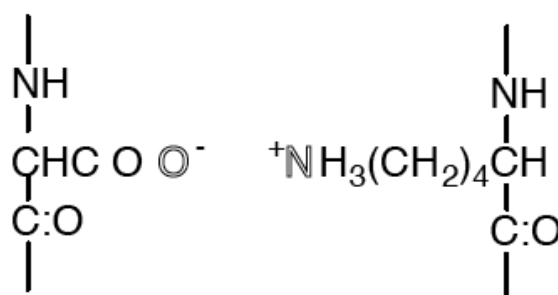


Figure 2-39 Ionic bond (Rushton 2006)

Disulphide bonds

Keratin is the most important hair protein. There are many different types of keratins and their properties vary from soft and flexible to hard and inflexible. The presence of cysteine gives keratin its structure stability. These cysteine molecules are situated on a polypeptide chain in such a way that one half of the Cystine molecule is situated in one polypeptide chain and the other half in the adjacent chain. They are linked with a disulphide bond which is covalent and the strongest type of bond ($-\text{CH}_2-\text{S}-\text{S}-\text{CH}_2-$) as shown in the Figure 2-40. Even though there are fewer disulphide bonds than hydrogen

or ionic bonds, disulphide bonds account for one third of the hair's total strength (Halal 2002); they give hair high degree of physical and chemical stability (Swift 1997)

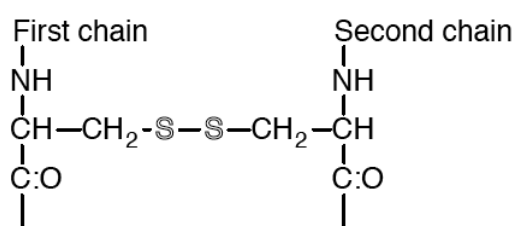


Figure 2-40 Disulphide Bond (Rushton 2006)

The overall shape of a protein is determined by the number and type of bonds between the amino acids. The number and type of these bonds determines the fibre's properties including the strength of the hair fibre.

2.13 Physical properties of the human Hair

The perception of hair appearance provides an almost instant recognition of the interplay of diverse physical parameters (Wolfram 2003). Physical properties can be divided into stiffness, elasticity, cross-sectional area, shape and density (Erik *et al.* 2008). For the cosmetic appearance of hair not all of the physical properties are equally important. Strength and elasticity, colour, shine and porosity are among the most important properties to the hair care industry (Tomes 2008).

2.13.1 Elastic and Tensile Properties

The 'strength' of human hair resides in the cortex (Berivan *et al.* 2008), which is a composite structure in which spindle-shaped microfibrils are embedded in a sulphur-rich matrix ((Nikiforidis 1992); The Cortex, section 2.11.2).

The stretching of hair can cause damage to the cuticle and the cortex, by producing transverse cracks in the cuticle and cortex, which if continued results in fibre breakage. When it comes to elastic deformation and stretching, most research has been focused on the whole fibre (Rushton); this involves strain (longitudinal), bending, stiffness,

twisting and rigidity. For every strain (deformation) of an elastic substance, there is a corresponding stress (the tendency to recover to its normal position). Stress is measured in force per unit area, such as Newtons (Robbins 2002c).

The most common types of strain are stretching or elongation (the ratio of an increase in length to the original length), linear compression (the ratio of decrease in length to original length), shear (the ratio of displacement of one plane relative to an adjacent plane), bending, and torsion. Each type of stress and strain has a modulus (the ratio of stress to strain) that also has units of F/A , force per unit area (Robbins 2002c).

Tensile and longitudinal testing provides information about the hair's strength and elasticity and on the mechanisms of hair breakage. The stress generated in human hair during longitudinal stretching depends on the history of the applied strain (Nikiforidis 1992). Thus, the stress response $\sigma(\epsilon, t)$ is a function of two variables, the strain ϵ and the time t (Nikiforidis 1992). The elongation of a hair fibre can be represented by a conventional stress-strain curve as shown in Figure 2-41. Stress or force is plotted against strain or percentage elongation. The curve for hair fibres consists of three regions (Hookean region, Yield region, Post-yield region).

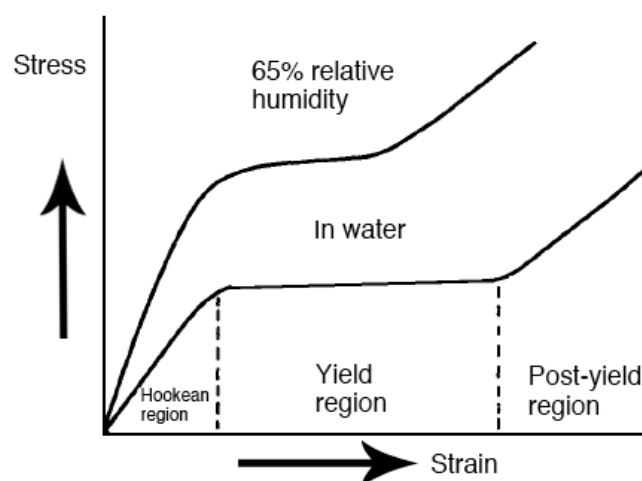


Figure 2-41 Load-elongation curves for human hair fibres (Robbins 2002c)

A hair fibre's behaviour differs depending on the amount that the fibre is stretched. Up to 5% elongation, which is the Hookean region, the fibre is elastic and it returns to its

normal position when the force is released (Erik et al. 2008). Keratin in the fibre is normally responsible for the elasticity. Keratin molecules form helices, and are known as α -Keratin. When a fibre is stretched these α -Keratin uncoil to form β -Keratin and a stretching of the H-bonds occurs. If the elongation is less than 5%, within the Hookean region, they reform the helical α -Keratin form, when the stretching force is removed. The width of the region and the shape of the load-elongation curve are affected by the moisture content of the fibre, pH and temperature.

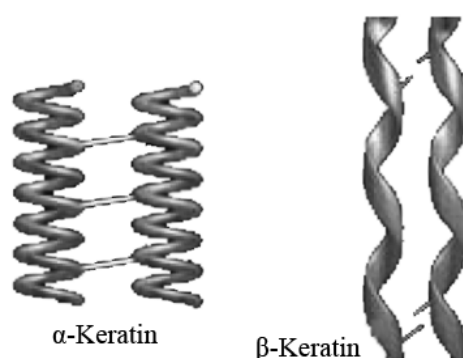


Figure 2-42 Modification of the structure of keratin in an elongated hair before it breaks when the fibre is stretched (L'Oreal, 2005)

When the elongation of the fibre extends between 5% and 25%, the fibre is said to be in the yield region; in this region the fibre does not return to its original length. When the hair fibre is extended a further 5%, α -Keratin unwinds to β -Keratin and fibre enters in a condition known as flowing. In flowing condition a hair fibre can be stretched by up to 25% but the β -Keratin will not change to α -Keratin when the stretching force is removed and the hair fibre will not return to its original length.

When the fibre is stretched by more than 25% it enters the post yield region. The post-yield region extends from a stretching of the fully extended helix (from 25% elongation), leading eventually to rupture of the fibre (the breaking point of the fibre). In general, the larger the fibre diameter the greater the breaking force required.

2.13.2 Bending and fibre stiffness

When a fibre is bent, the outer layers of the fibre are stretched, and inner layers are compressed. The region in the centre of the hair fibre is unchanged, Figure 2-43 shows schematic diagram of a bent hair fibre. The stiffness is the resistance to bending (Scott and Robbins 1978) and is the fundamental fibre property. The stiffness of the fibre

varies with relative humidity; for example, the stiffness of human hair decreases with increasing relative humidity (Robbins 2002c).

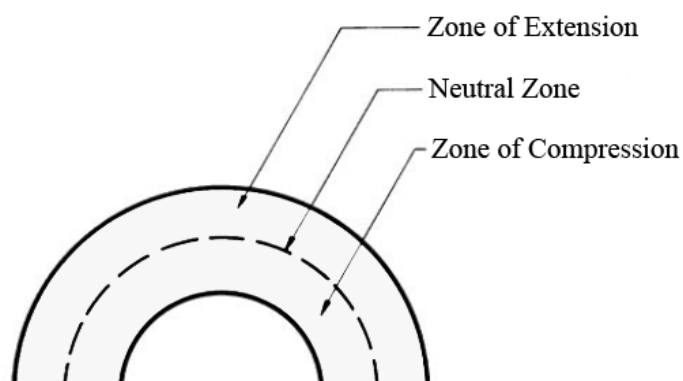


Figure 2-43 Schematic diagram of a bent hair fibre (Robbins 2002c).

2.13.3 Torsion and Fibre rigidity

Rigidity is the torque required to produce a twist of one turn per centimeter (Robbins 2002c, Guthrif *et al.* 1954). Hair fibres are routinely twisted during combing, brushing and setting. The resistance to twisting is the torsional rigidity.

Water has a greater effect on the torsional properties than on either stretching or bending, because it twists more easily than it stretches or bends. It is believed that in water, hair becomes less elastic and more plastic (Rushton 2006).

2.13.4 Porosity

The water content in dry hair is approximately 15% by weight (Wolfram 2003). Hair fibres are very porous and are permeable to water vapour in the atmosphere and in humid weather the water content of hair fibres increases and the fibre swells. The hair's outer layer (cuticle) is the main barrier to the water entry and water penetration is dependent upon the condition of the cuticle. If the fibre absorbs too much water it can crack and in extreme cases the swelling can cause the fibre to break. If the hair's moisture content drops below 15% the hair becomes dry (Schueller 1999). Hair fibres swell when they absorb water and this is due to hydrogen bonding. The Amino acids form new hydrogen bonds with water instead of with each other, this causes polypeptides to move apart which causes swelling (Halal 2002). The swelling of the

fibres is not uniform and the non-keratinous regions, the cell membrane and endocuticle, swell the most (Tomes 2008). Swelling also causes the edge of the cuticle to lift resulting in increased friction between fibres and a further increase in porosity (Wolfram 2003).

2.13.5 Friction

Friction is the force that resists motion when one body slides over another. The frictional force necessary to slide one surface over another is proportional to the load pressing the two surfaces together, and appears to be independent of hair diameter. This generally applies to dry, unlubricated surfaces but not to hydrodynamic lubricants, such as fluid layers that separate the moving surface (Robbins 2002c, Howell *et al.* 1959)

However, surface lipids provide a reduction in friction and are present even in a dry state. Hair exhibits a directional frictional effect because of the orientation and overlap of cuticle cells. It is easier to move a surface over hair in a root to tip direction than from tip to root.

2.13.6 Hair Colour

The colour of hair is due to the presence of melanin in the pigment cells known as melanocytes. Melanin is a natural pigment present in animals and plants and regardless of colour all humans except albinos, have melanin in their hair (Zviak 1986). The colour difference in hair is due to the chemical composition of melanin, there are two type of melanin. (a) Eumelanin, which is responsible for the dark brown-black shades and (b) Pheomelanin, which is responsible for lighter red-yellow shades (Liu *et al.* 2005).

Eumelanin and pheomelanin are primarily found in the cortical cells and medulla, and comprise approximately 3-4% of the total fibre mass. The actual shade of hair colour depends not only on which melanin is present but also the amount, shape and location of the pigment (Zviak 1986). In some cases only one of these pigments is present and if there is no pigment present then the hair looks white. Hair colour does not remain constant throughout life because melanin formation is not constant. As people age the production of pigment slows and may stop altogether (Zviak 1986).

2.14 Hair Cosmetics

Hair cosmetics are designed to maintain the hygiene of the scalp hair and to beautify the head. They include hair shampoos, conditioners, hair styling aids like wax and hair sprays.

2.14.1 Shampoos

The primary function of shampoo is to remove unwanted elements like sebum, styling products, environmental dirt etc., from the scalp and hair. They function by employing surfactants (detergents). Surfactants are amphiphilic compounds that contain a lyophilic (solvent loving) group and a lyophobic (solvent hating) group. The detergents are divided into four basic types: anionic (they have a negative charge on their lyophobic group), cationic (they have a positive charge on their lyophobic group), amphoteric (they possess both charges on their lyophobic group) and non-ionic (they have no charge). Types of surfactants are listed in Table 2-4. Anionic surfactants are most popularly used in shampoos.

Table 2-4 Surfactants types and characteristics

Surfactant type	Chemical class	Characteristics
Non-ionic	Polyoxyethylene fatty alcohols, polyoxyethylene sorbitol esters, alkanolamides	Mildest cleansing
Anionic	Lauryl sulphates, laureth sulphates, sarcosines, sulposuccinates	Deep cleaning, may leave hair harsh
Cationic	Long chain amino esters, ammonioesters	Poor cleaning, poor lather.
Amphoteric	Betaines, sultaines, imidazolinium derivatives	Mild cleaning, non-irritating to eyes.

2.14.2 Hair Conditioners

Sebum is an ideal hair conditioner but it is associated with a greasy appearance and dirty feel (Draelos 2008). As stated in the previous section (Section 2.14.1), shampoos are designed to remove sebum but the excessive removal of sebum creates the need for a

synthetic substitute. Hair conditioners were developed to mimic sebum and to apply the positive attributes of sebum like a decrease in hair static electricity, and an improvement in lustre. Hair conditioners are categorised as cationic detergent, film former (polymers) and silicones (dimethicone, cyclomethicone).

2.14.3 Styling Aids

Styling aids are designed to enhance the appeal of the hair. They include hair gels, waxes, hair sprays, shine sprays and mousses.

Hair Sprays: usually in an aerosolized liquid form, they employ copolymers, such as PVP (polyvinylpyrrolidone), which stiffens the hair, and creates a temporary bond between hair shafts. They are water-soluble and can easily be removed by shampooing.

Styling Gel and waxes: Gels are similar to hair sprays. The only difference is that they are in the form of a gel. Gels can be formulated to give very strong holds. There is a whole range of non-aqueous based products, which might include waxes, putty etc. Waxes also employ modified polymers and they soften at body temperature (Draelos 2008).

2.15 Hair-shine Models (Computational models)

2.15.1 Introduction

Visually, lustre is observed as a contrast between the specular and diffuse reflections from an object. However the relationship between the appearance of lustre and the light reflected from the hair is complex (Keis *et al.* 2004b). The way hair scatters light determines its shine and this scattering depends on the condition of the fibre (Bustard and Smith 1990). Figure 2-44 shows three different bands of reflection formed when light is shone on the hair tress.

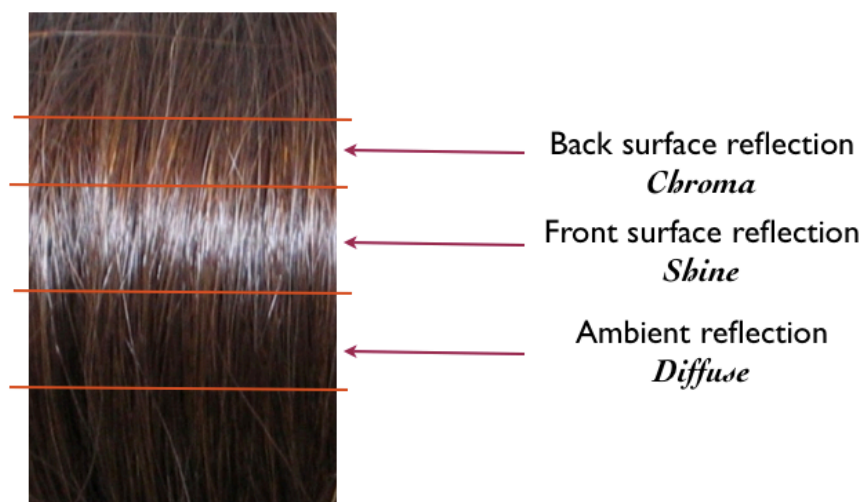


Figure 2-44 Appearance of a Hair tress with the Shine, Chroma and Diffuse band.

Shine or lustre is perceived when an object scatters much more light at a particular angle or in a particular direction than in other directions (Reich and Robbins 1993). Under these conditions, surface highlights or brightness contrasts appear and the object is seen to be shiny.

Lustre is generally considered to depend on 3 main parameters (Lefaudeux *et al.* 2008);

- **The amount of reflected light.** (Directly proportional to the incident light; the more the reflected light there is, the higher the lustre will be). As shown in Figure 2-45 Part a: a glossy sample under two different intensities of light. When the incident light is higher in intensity, a higher gloss is perceived.

- **The distribution / width of the reflected light.** For the same amount of reflected light, the more prominent and more defined the reflected light is, the higher the perceived lustre will be. When light is shone onto the hair tress three different bands of reflection have been identified: Chroma, Shine and Diffuse. If these bands appear more defined and more concentrated the lustre is perceived to be greater (Figure 2-45 Part b).
- **The background on which, the reflection is observed.** The darker the background, the greater the contrast between background and foreground and this leads to a higher perceived lustre (Figure 2-45 Part c).

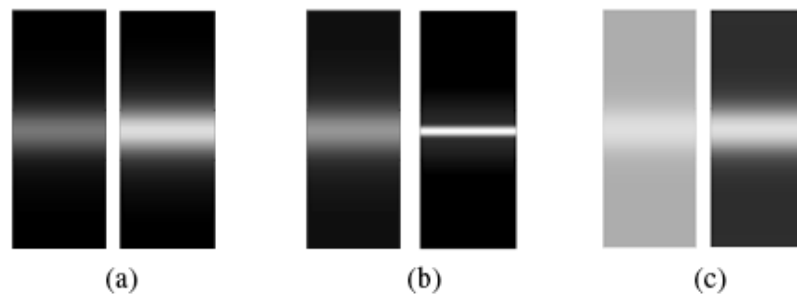


Figure 2-45 Lustre is considered to depend on three parameters. (a) Increase of the amount of light reflected. (b) Reduction of the width of the specular light band. (c) The background on which the reflection is observed (Lefaudeux *et al.* 2008)

A hair fibre can only reflect light symmetrically to the incident direction when its outer surface, mainly the cuticle, is covered with a smooth layer for example a spray or liquid. Figure 2-46 shows a theoretical cylinder, representing a horizontal human hair fibre, held under slight tension. The cylinder is assumed to be ideally optical, that is, it has a smooth external surface, a circular cross-section, is colourless, transparent and optically isotropic. When light is shone onto the cylinder, a reflection will occur from both sides of the cylinder wall, the front face (near side) and the back (far side) and all of the reflected rays in both sets would be parallel to one another (thus the angle of reflection would be equal and opposite to the angle of incidence). This situation is found to be the case with glass or synthetic fibres.

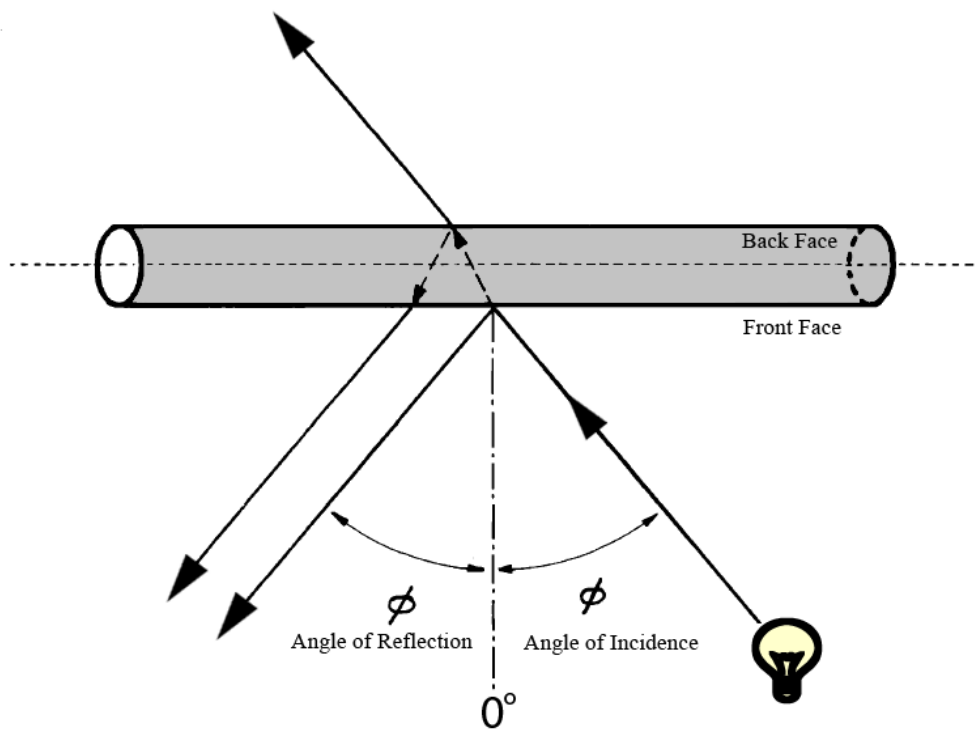


Figure 2-46 Reflection of light from front and back face of idealized cylindrical fibre (Modified and redrawn from (Stamm *et al.* 1977a)).

The surface of a human hair is not smooth but features cuticle cells in a tile-like arrangement. They produce around 10 layers of scales (cuticle), each layer possessing a radial thickness of $\sim 0.5\mu\text{m}$ (Stamm *et al.* 1977a). It is the presence of the scales, which increases the difficulty in measuring the light reflected by the external surface of hair fibres. Figure 2-47 shows possible reflections of light when it interacts with hair fibre. Glossmeters will not be effective in measuring reflection in different directions (as shown in Figure 2-47) as the head of the photometer is fixed. In order to measure the reflection created by the hair Goniophotometer was used Figure 2-49 shows a rudimentary diagram of the instrument.

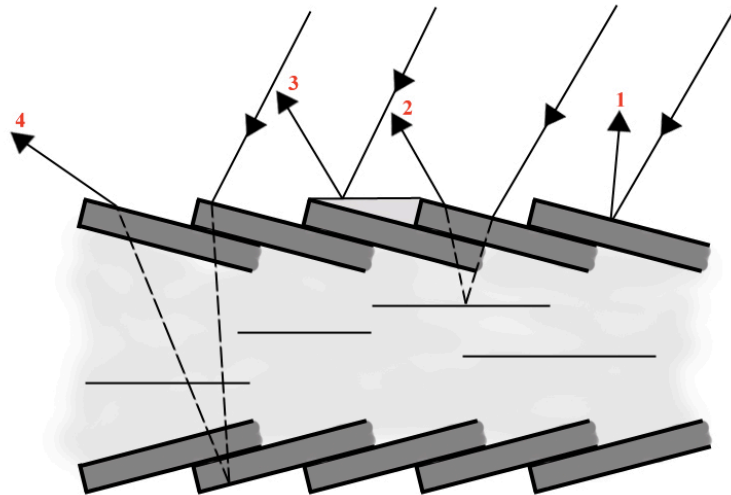


Figure 2-47 Possible reflection of incident light by a hair fibre (1) Reflection by cuticle (2) Reflection by cortex cells (3) Reflection by some smoothening substance (4) Reflection by cuticle after entering the fibre. (Re-drawn and modified from (Czepluch *et al.* 1993))

Stamm *et al.* states that the results of a gloss evaluation study on a single hair fibre are not as precise as those obtained from monolayers of parallel oriented hair fibres (Stamm *et al.* 1977b). To obtain improved results they designed a holder on which a number of fibres could be strung. Normally they worked with 21 single hair fibres. Figure 2-48 is showing a beam of light, coming from the lower right, illuminating a planar array of hair fibres held under slight tension, parallel to one another.

The intensity of the light, which is specularly reflected and scattered by the hair fibres, is detected at various angles and recorded using a goniophotometer.

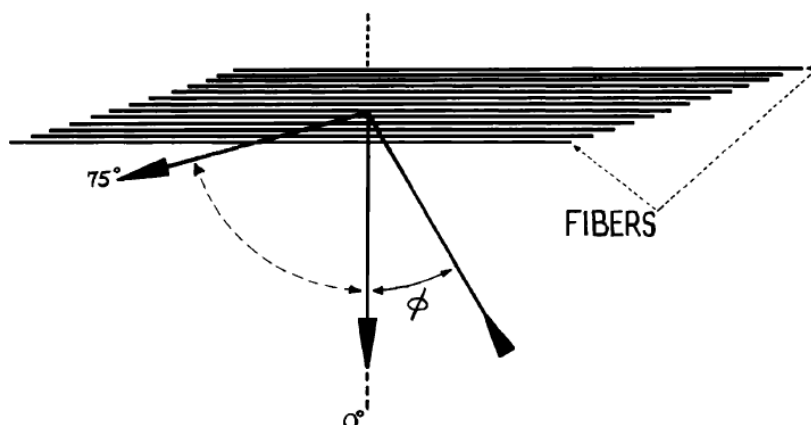


Figure 2-48 Method employed for illuminating a planar array of parallel oriented hair fibres in order to obtain reflectance curve from a goniophotometer (Stamm *et al.* 1977a).

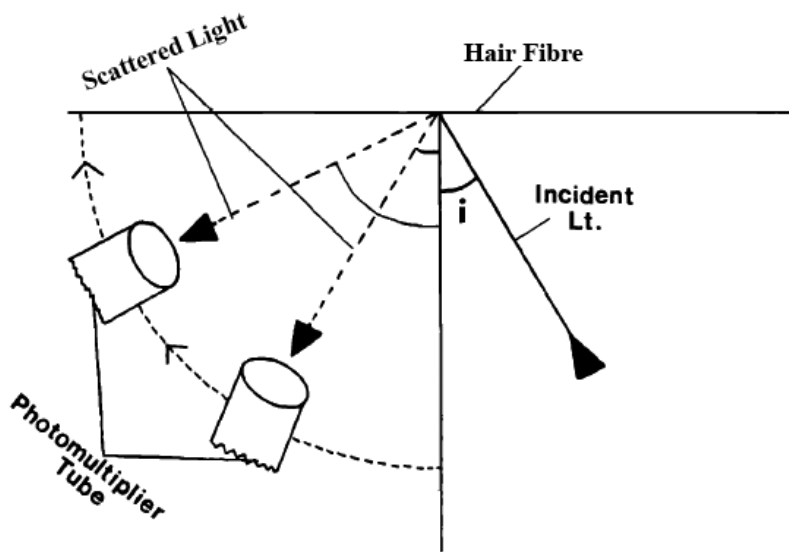


Figure 2-49 Rudimentary diagram of a goniophotometer experiment (Reich and Robbins 1993).

In view of the surface and overall morphological structure of human hair the light was optically modified in three main ways as schematically shown in Figure 2-50. Such a three component model has been proposed and investigated by Stamm and subsequently by Guiolet (Guiolet *et al.* 1987).

The differences in the refractive indices of the morphological components are considered as being of minor importance.

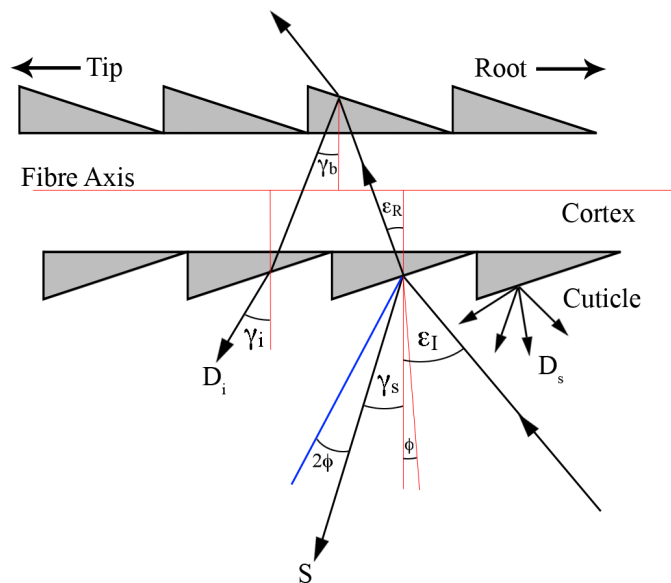


Figure 2-50 Optical model of an individual Hair Fibre (Modified and redrawn from (Stamm *et al.* 1977a)).

An incident light beam hits the fibre surface in the root-to-tip (RT) direction at an incident angle ε , which is given with respect to the direction normal to the fibre axis.

First component of light S is specularly reflected at the receptor angle γ_s :

$$\gamma_s = \varepsilon - 2\phi \quad \text{Equation 2-19}$$

Whereas ϕ is the tilt angle of the cuticle cell with respect to the fibre axis.

Second component of light D_s is diffusely scattered and reflected at and near the fibre surface. When the hair is coloured, the intensity of light reflected from within the hair is diminished, leading to a decrease of intensity of diffusely reflected light with the darkness of the hair. When light is transmitted through the surface layer, Melanin absorbs the light, thus reducing the diffuse reflectance. This is the reason why darker coloured hair produces brighter gloss bands than lighter coloured hair.

Due to the random nature of the scattering and reflection process that leads to diffuse reflection and due to the non-uniform nature of the effect, the mean receptor angle γ_d for diffusely reflected light might be expected to coincide with the incident angle.

$$\gamma_d = \varepsilon_I \quad \text{Equation 2-20}$$

A further fraction of the incident beam is refracted into the fibre according to Snell's law. Taking the cuticle angle in account

$$n_k = \frac{\sin(\varepsilon_I - \phi)}{\sin(\varepsilon_R - \phi)} \quad \text{Equation 2-21}$$

so that:

$$\varepsilon_R = \sin^{-1} \left[\frac{1}{n_k \sin(\varepsilon_I - \phi)} \right] + \phi \quad \text{Equation 2-22}$$

Where ε_R is the refraction angle, n_k is the refractive index of the keratin fibre.

When light penetrates into the fibre it is partly scattered and partly absorbed by the hair pigment and thus wavelengths are preferentially filtered. In less pigmented hair (very blond or white hair) a significant amount of light may be reflected at the back-wall (back-side) of the fibre, as a fraction of light coming out from the fibre the interference will be Hair/Air opposite to the point of incidence. Assuming the light passes through the fibre and taking the opposite tilt direction of the reflecting surface into account, the back-wall reflection will occur at an angle described by: Equation 2-23

$$\gamma_b = \varepsilon + 2\phi \quad \text{Equation 2-23}$$

This beam emerges after refraction at an angle (Snell's law, under the principle of Equation 8);

$$\gamma_i = \sin^{-1} \left[\frac{1}{n_K \sin(\gamma_b + \phi)} \right] - \phi \quad \text{Equation 2-24}$$

Where γ_i is the receptor angle for the internally reflected light. When this **third component** of light re-emerges from the fibre it has the colour of the hair and is experimentally observed as a separate peak in the Goniophotometer curve. The location of this peak is shifted to higher angles by 10%, the peak shift was constantly observed (Stamm et al. 1977a).

2.15.2 Evolution of Gloss evaluation models for the human hair

In the last thirty years or so there have been a number of studies published on measuring the gloss of human hair (Aims and Objective Section 1.1, Objective 1-b). Stamm (Stamm *et al.* 1977b) employed a goniophotometer and multiple fibres to record the light distribution curves necessary to calculate lustre parameters. Guiolet's (Guiolet *et al.* 1987) model was based on Stamm's 3-component model of a single hair fibre using goniophotometer. Czepluch (Czepluch *et al.* 1993) later expanded this work by constructed a computerized goniophotometer. Reich-Robbins (Reich and Robbins 1993) and Bustard-Smith (Bustard and Smith 1991) also utilised goniophotometric reflectance

measurements, to study the effect of shampooing and dyeing on the lustre, of single hair fibres. Keis (Keis *et al.* 2004b) used a standard high gloss black tile to normalise the goniophotometer curve of a single hair fibre. Wortmann (Wortmann and Schulze 2003) in their study mentioned recording data from a goniophotometer takes a “painstakingly long time” (approx. 15 min) and to overcome this problem they used a multi-channel instrument, to measure reflected light from a single hair fibre. Maeda measured lustre by using a colour image processor, which analysed the reflected light by a natural-hair wig on a mannequin head. This work was later expanded by Rennie (Rennie *et al.* 1997) by taking an image of a head with a video camera and measuring the intensity of the light. McMullen (McMullen and Jachowicz 2003) used a high resolution camera to take images of hair tresses mounted on a cylinder, which were then analysed by scanning across dark and highlighted areas of the resultant image using image analysis software. They claim that the intensity curves were similar to goniophotometric scattering curves. Lefaudeux (Lefaudeux *et al.* 2008) further extended the image capture study and used a three element setup similar to McMullen (1. digital camera, 2. light source, 3. cylinder) but their analysis of images was different from McMullen.

There have been as many as 10 (major) models proposed that quantify lustre in the last 20 years and this number is increasing. This demonstrates that although imaging technology is improving that a system to measure the gloss of human hair has not been discovered that correlates with the human perception of gloss.

Major gloss models, which lead us to the current gloss evaluation model, mentioned in this section, are explained in detailed below:

2.15.2.1 Stamm's Model of Gloss (Stamm *et al.* 1977b)

Stamm's definition of Gloss is based on Hunter's contrast gloss (RS Hunter 1937) which is defined as the contrast existing between the intensity of the specularly reflected light (s), measured at the angle of direct specular reflection, and that of the diffusely scattered light (d), measured at an angle of emergence of 0° that is along the normal to the interface. Thus for Hunter's gloss, we have;

$$G_c = \frac{s}{d} \quad \text{Equation 2-25}$$

This function tends to infinity as d approaches zero. To correct this shortcoming Nickerson (Nickerson 1957) suggested;

$$G_c = \frac{(s - d)}{s} \quad \text{Equation 2-26}$$

For hair, spot values for s (specular reflection) and d (diffuse scattering) were measured using GP (Goniophotometer) curves at the top of the front-face specular peak and from the background value at 0°. Substituting the values in to Equation 2-26 Stamm *et al.* determined that the function G_c has high precision in measuring lustre in various kinds of hair but has only a narrow range of values.

From the recorded GP curve, Stamm *et al.* obtained directly the integrated area between the GP curve and the baseline. This area is the sum of the specular reflection and diffuse scattering (S+D). An imaginary line between the ordinate values at 0° and 75° (the extreme limits of the angular region scanned) is drawn and it is assumed that the area under the line is the diffuse scattering, D. Knowing (S+D) and D they obtained S by taking the difference between S and D thus producing a function for lustre, Equation 2-27:

$$\text{Lustre} = G_c = \frac{(S - D)}{S} \quad \text{Equation 2-27}$$

2.15.2.2 Guiolet's Model of Gloss (Guiolet *et al.* 1987)

Guiolet *et al.* designed a Goniophotometer principally for the study of hair fibres (Figure 2-51). The illumination telescope allows the user to adjust the angle of incidence from 0 to 90° and in their experiments they chose a fixed angle of incidence of 30°. Standard sample holders take five hairs 5cm long, mounted in parallel 2mm apart. Measurements of the hair fibres were taken at the root end.

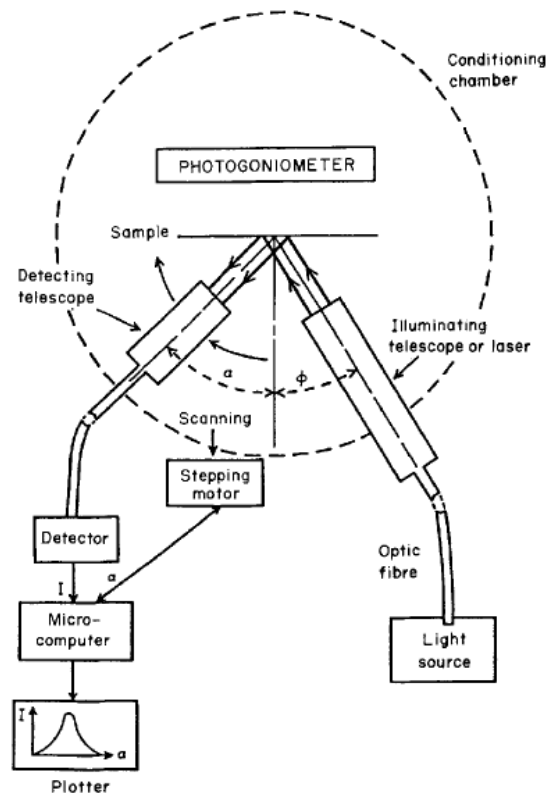


Figure 2-51 Diagram of the Goniophotometer built by Guiolet (Guiolet *et al.* 1987)

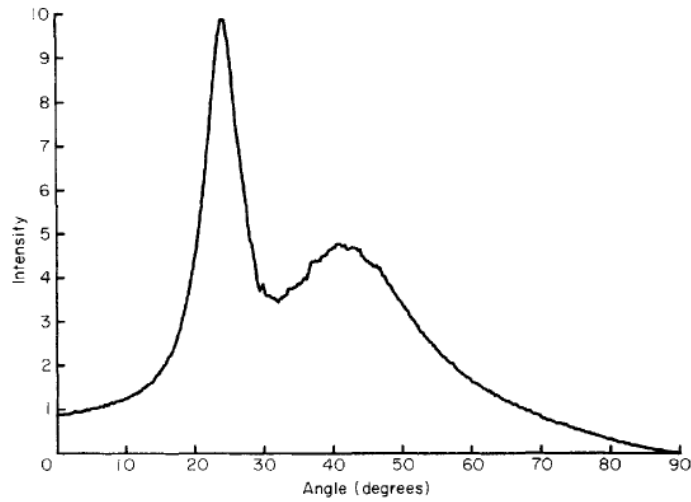


Figure 2-52 Luminous intensity re-emitted according to the angle of observation in degrees by a brown hair. Angle of incidence 30° (Guioulet *et al.* 1987)

Guioulet's gloss model is based on Stamm's 3-component model. Figure 2-52 shows a GP curve of brown hair. In order to obtain the required optical parameters Guioulet breaks down the GP curve as shown in Figure 2-53 into a specular reflection (s) curve, internal reflection (ir) curve and diffuse curve (d) as shown in Figure 2-54 and evaluates gloss using the following relationship, Equation 2-28;

$$\text{Gloss} = G = \frac{s}{d} \quad \text{Equation 2-28}$$

This is defined as the ratio between the maximum intensity of the specular reflection peak and the maximum intensity of the diffuse band, d, measured at 0° according to Hunter's formula.

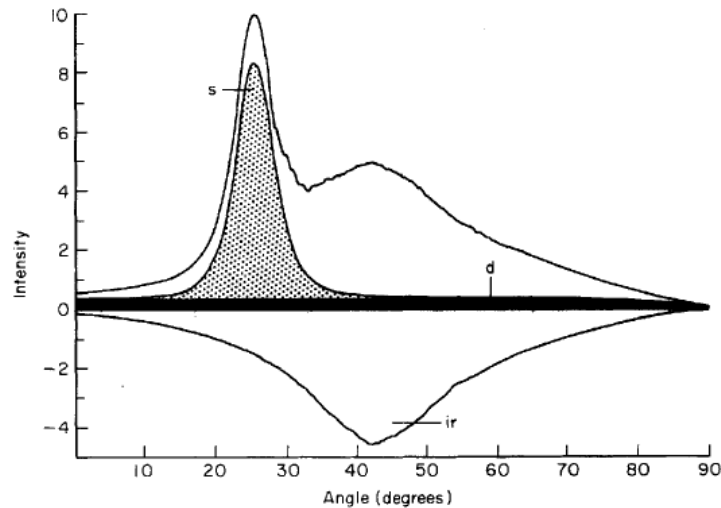


Figure 2-53 Decomposition of the goniophotometric (GP) curve into its three components - Specular reflection(s), Internal reflection (ir) and Diffuse reflection (d) (Guiolet et al. 1987).

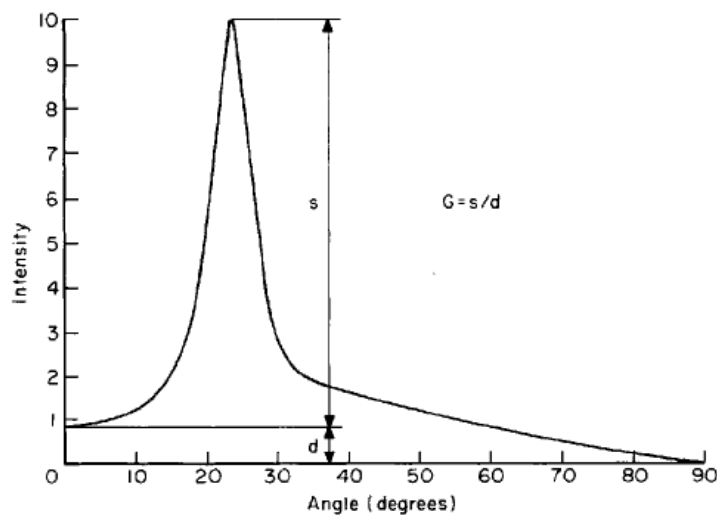


Figure 2-54 Definition of gloss (GP curve of a dark brown hair) (Guiolet *et al.* 1987).

2.15.2.3 The Reich-Robbins Model of Gloss (Reich and Robbins 1993)

Reich and Robbins slightly modified the Stamm and Guiolet models by using polarizers (having the directions of polarization perpendicular to the plane of incidence) in order to maximize the accuracy of the diffuse scattering measurement.

A sample hair fibre was secured at one end and kept under constant tension by attaching a 2-gram alligator clip to the other end. A Goniophotometer with a rotating

light detector, from 0° to 75°, measured the intensity of the incident light that was scattered by the hair. The angle of incidence was set at 30°. Specular reflection was measured from the GP curve near this angle. Light is also scattered at angles other than specular (diffuse reflection).

Reich and Robbins tested several functions and the best agreement with subjective evaluations was found using the relationship shown in Equation 2-29:

$$L = \frac{S}{DW_{(\frac{1}{2})}} \quad \text{Equation 2-29}$$

Where L equals lustre or shine. D is the integrated diffuse reflectance and is obtained, as in Stamm's model, by collecting the scattered light intensities at 0° and 75° and measuring the area under the resulting line. S is the integrated specular reflectance and is obtained by measuring the area of the specular peak, while $W_{(\frac{1}{2})}$ is the width of the specular peak at half-height of the specular curve. Figure 2-55 shows a goniophotometer curve of a single hair fibre.

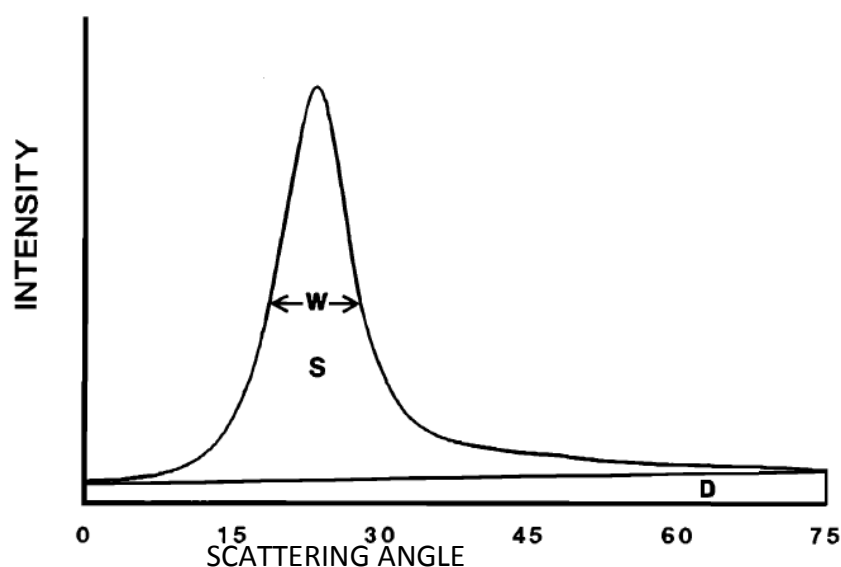


Figure 2-55 A typical light scattering curve for a virgin Oriental hair. D is the diffuse reflectance, S is the specular reflectance and W is the width of the curve at half height (Reich and Robbins 1993).

It has been mentioned in a previous section (Stamm's model of gloss, Section 2.15.2.1) that the use of Hunter's expression, Equation 2-25, that the function tends to infinity as

D approaches zero. For most cases involving hair, however, scattering of light off the scale edges insures a minimum value for D, so that Equation 2-25 is broadly applicable.

2.15.2.4 TRI (Textile Research Institute) Model of Gloss (Keis et al. 2004a)

The TRI (Textile Research Institute) model of gloss uses goniophotometric measurements of single hair fibres to evaluate hair shine. Single fibres are mounted horizontally in a sample holder and held in place by clips. The measurements of gloss are performed in the root-to-tip direction of the hair fibres at an angle of incidence of 45°. The reflected light is detected by a photomultiplier as a function of angle and the GP curve is split into specular and diffuse components, as shown in Figure 2-56.

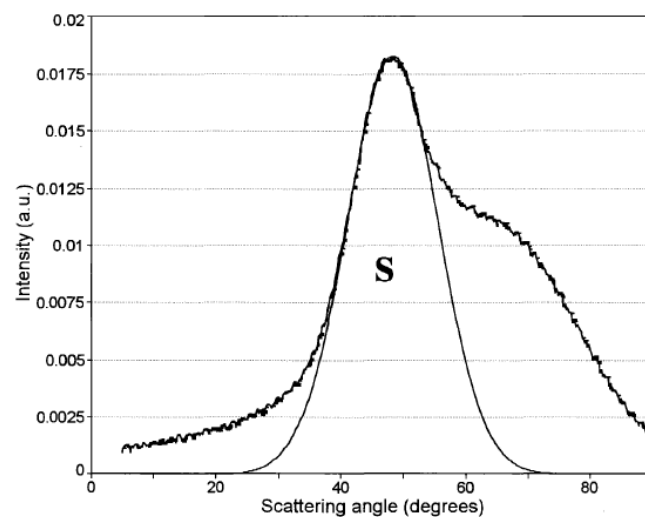


Figure 2-56 A typical goniophotometric curve broke down into specular and diffuse components (Keis et al. 2004a).

Keis and Ramaprasad modified the Reich-Robbins model by incorporating the peak width at half height of a standard specular reflector; Figure 2-57 shows the goniophotometer curve of the standard black mirror. This gives following the relationship (Equation 2-30):

$$L = \frac{SW_{(\frac{1}{2})_{\text{standard}}}}{(S + D)W_{(\frac{1}{2})_{\text{sample}}}} \quad \text{Equation 2-30}$$

Where S is the specular peak area obtained from the goniophotometric curve, $(S+D)$ is the total area under the intensity curve, $W_{(\frac{1}{2})standard}$ is peak width at half height of the standard and $W_{(\frac{1}{2})sample}$ is peak width or a fit at half height of the sample.

$W_{(\frac{1}{2})standard} / W_{(\frac{1}{2})sample}$, is a normalization factor and the standard used by Keis *et al.* was a polished black-mirror provided by Hunter Lab (Keis *et al.* 2004a).

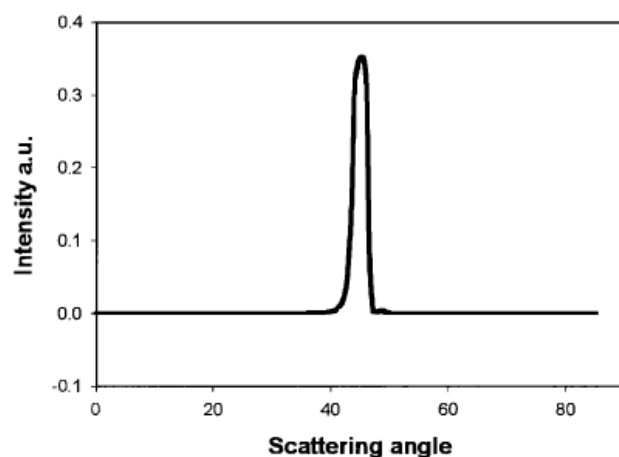


Figure 2-57 Goniophotometric curve of a standard black mirror (Keis *et al.* 2004a).

2.15.2.5 McMullen – Jachowicz Model for Lustre evaluation (McMullen and Jachowicz 2003, McMullen and Jachowicz 2004)

McMullen *et al.* used an image capturing setup to evaluate the gloss of a human hair tress. Figure 2-58 shows a schematic diagram of apparatus used by McMullen to measure the lustre of human hair tress. While performing their analysis they noticed that the specular reflection band on a hair tress consists of a series of discrete micro-reflections arising from individual hair fibres and corresponds to the structural elements located along the fibre length. They concluded that specular reflection band that appeared on the hair tress is not a continuous and uniform plane of light but possesses a dot-like or striped appearance and this effect is easily detectable by the naked eye. Figure 2-59 shows the dot-like highlights on an image of a hair tress. (Image was captured in our lab to explain McMullen’s dot-like reflection effect)

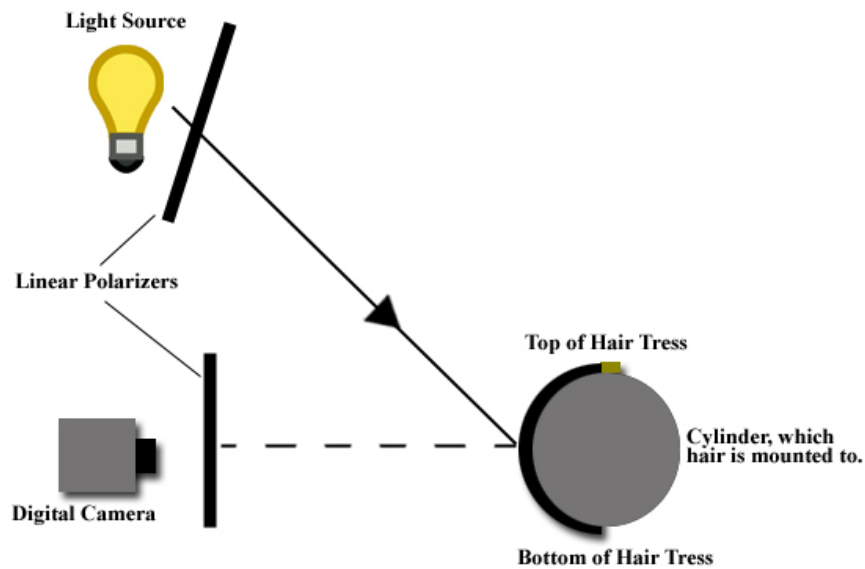


Figure 2-58 Schematic diagram of an apparatus to measure the lustre of hair (Re-drawn (McMullen and Jachowicz 2003))

In order to quantify the micro-contrast effects arising from the presence of highlights and neighbouring shadows (diffuse reflection areas) in the specular reflection band of the hair tress, McMullen *et al.* measured light intensity as a function of distance in the horizontal direction (relative to hair fibre axis). Figure 2-60 is replica of McMullen's graph.

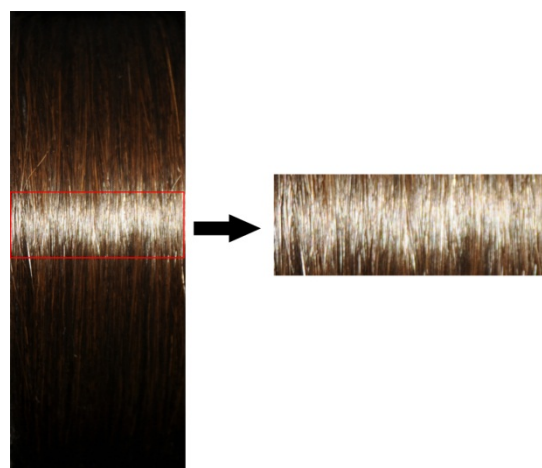


Figure 2-59 Image of Human hair tress showing dot-like reflection

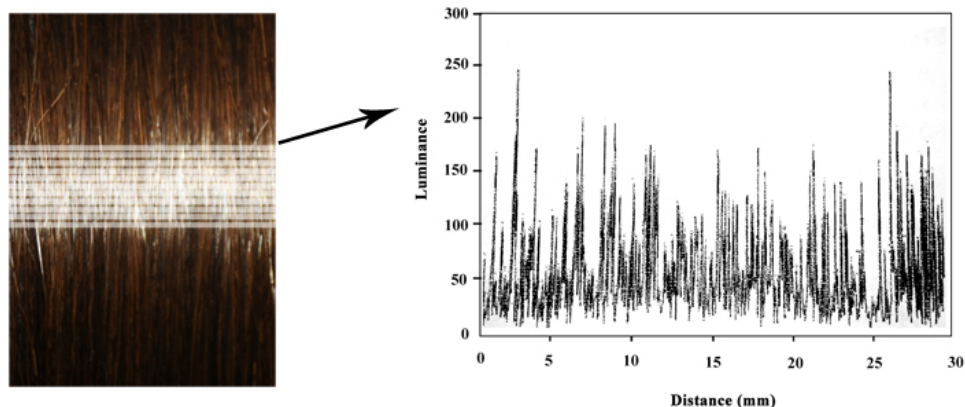


Figure 2-60 Luminosity analysis horizontal to the fibre axes with a plot of luminance vs. distance for one of the horizontal lines. (Re-drawn(McMullen and Jachowicz 2004))

Luminous values, maxima and minima, were recorded for each line. Taking the difference between the peak maxima and peak minima curves gave an indication of the micro-contrast related to the dot-like appearance of the specular reflection band observed on a human hair tress. They calculated the difference between maxima and minima and compared the results with Stamm and Robbins's model; some of the data are tabulated in Table 2-5. McMullen & Jachowicz suggested that the contrast calculated for dot-like highlights and shadows within the specular band follows the same trend and could be valuable for the assessment of the lustre of human hair.

Table 2-5 Results for Maximum - Minimum Analysis for various types of human hair (McMullen and Jachowicz 2004)

	Oriental	Medium Brown	Light brown	Light blond	Natural white
Max area	13780	15860	19020	26140	46600
Min area	428	4131	7369	17380	40020
Max - Min	13350	11730	116650	8765	6586
L (stamm)		0.72	0.70	0.65	0.32
L (Reich-Robbins)		0.67	0.32	0.19	0.06

2.15.2.6 Bossa Nova Technologies, BNT, (SAMBA) Model of Gloss (Lefaudeux *et al.* 2008)

Instead of using a goniophotometer the Bossa Nova team designed a system consisting of three main elements: a polarized illumination, a polarization camera and a cylinder on which the sample is positioned as shown in Figure 2-61.

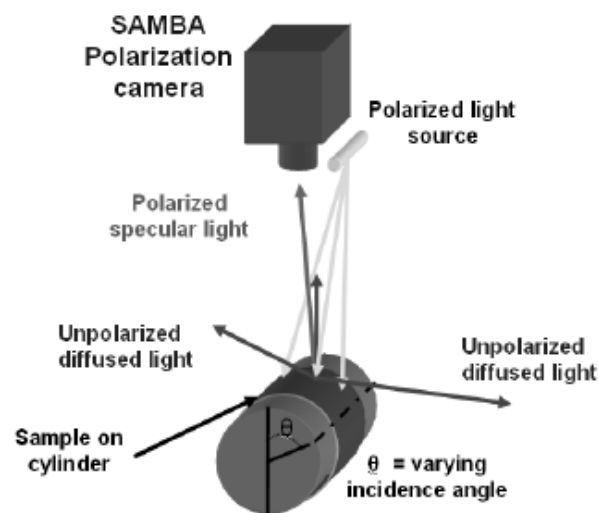


Figure 2-61 Optical set-up of the polarization imaging system (Lefaudeux *et al.* 2008)

Combining a camera with a cylinder allows the recording of the angular distribution of light reflected from the sample without the need for any moving parts. The orientation relative to the illumination and observation changes according to the point on the surface of the cylinder that is considered as shown in Figure 2-62. The main difference between a polarization imaging system and a goniophotometer is that the goniophotometric measurement only gives the profile of the intensity of light while polarization imaging provides the profile of intensity, specular and diffused light, as well as the corresponding images that can be used as a visual control and this provides a better understanding of the numerical data (Lefaudeux *et al.* 2008).

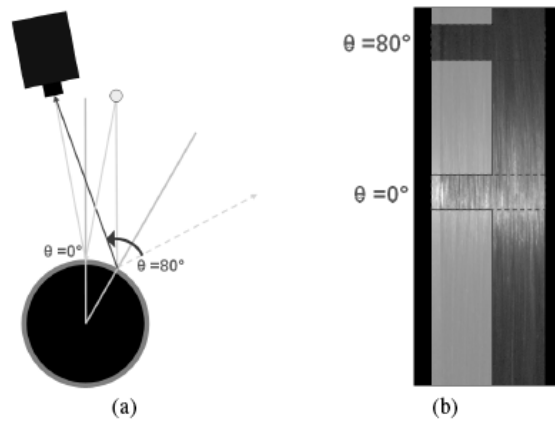


Figure 2-62 (a) sample positioned on the cylinder (b) Complete angular distribution with a single image (Lefaudeux *et al.* 2008)

The use of both a polarized illumination and a polarization camera allows the capture of three types of images as shown in Figure 2-63:

- A normal intensity image representing what a human eye would see ("Intensity", Figure 2-63).
- A specular image representing the light that is polarized ("Specular", Figure 2-63).
- A diffused light image representing the light that is un-polarized ("Diffused", Figure 2-63).

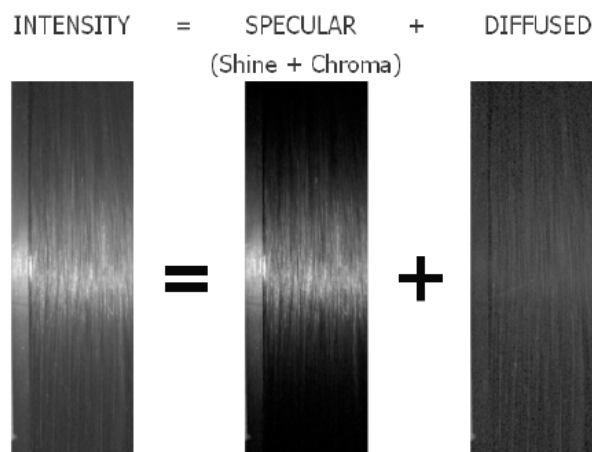


Figure 2-63 3 images are acquired from SAMBA: an intensity image showing the normal view of the hair a specular image showing only the reflections (shine and Chroma) and a diffused light image showing the diffused light only (Lefaudeux *et al.* 2008).

The BNT (Bossa Nova Technologies) system is angularly calibrated with its geometric properties so that the real angles are known for each line of the image. The computation

of the angular profiles is achieved by averaging the images along the transverse direction Figure 2-64. These angular profiles are similar to those provided by goniophotometers. From these profiles and images, relevant parameters characterizing the light distribution are computed (Lefaudeux *et al.* 2008). Polarization imaging provides the profile of intensity, specular and diffused light of the human hair tress. Having these profiles separately allows a better understanding of the effect of treatments. Further processing on the specular profiles using RGB information allows the system to separate the shine band from the Chroma band. This separation is based on the assumption that the shine band is white. Figure 2-64 shows angular profiles of the image.

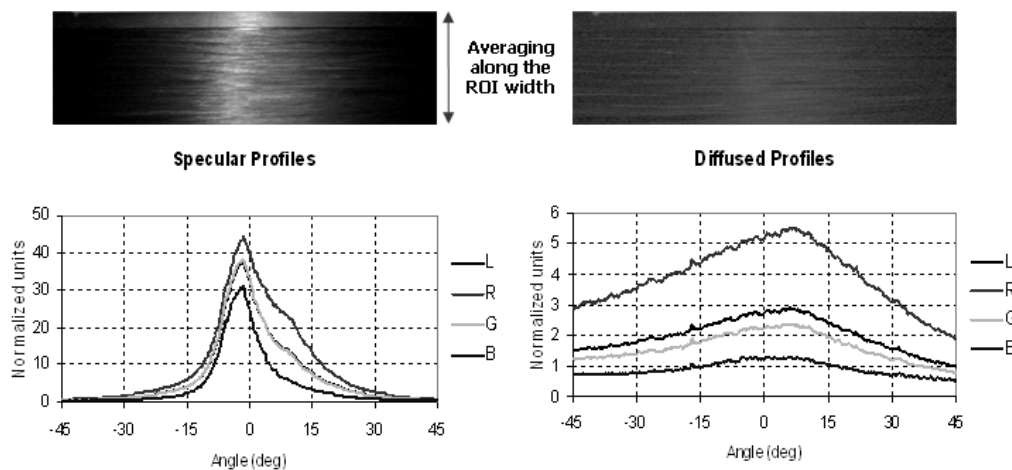


Figure 2-64 Angular profiles computed from the images acquired by averaging along the width of the sample (Lefaudeux *et al.* 2008).

BNT modified the TRI equation; they divided the specular light band into two parts S_{in} and S_{out} . S_{in} corresponds to the peak of the specular light and contributes to an increase of the lustre. S_{out} corresponds to the wings of the specular light (high angles) distribution and contributes to a decrease in the apparent lustre. In addition to measuring the width of the specular peak at half height they measured the width on the image. This gives the following relationship:

$$L_{BNT} = \frac{S_{in}}{(D + S_{out})W_{visual}} \quad \text{Equation 2-31}$$

2.16 Summary

Gloss is the feature of surfaces that causes them to have a shiny or lustrous appearance. It is generally associated with reflection of light from the tress in the specular direction. In the early 1930s Hunter studied gloss and determined that specular reflection can vary from one surface to another. He divided gloss into six different types, 1) Specular gloss, 2) Sheen, 3) Contrast gloss or lustre, 4) Absence of bloom, 5) Distinctness of image, and 6) Surface uniformity. Although there have been many attempts to measure gloss only a few have been standardized (Czepluch *et al.* 1993). Extensive work on gloss by Hunter led to the development of the first photoelectric-based glossmeter. The standardized methods used for measuring gloss are described in Section 2.4.2 (Aims and Objectives Section 1.1, Objective 1-a). The problem with conventional glossmeters is that they are only effective for samples that have a smooth and flat surface (Aims and Objectives Section 1.1, Objective 3-a). Thus, Glossmeters do not specify the optical properties of a reflecting surface. Polar intensity distribution curves provide the only way of specifying the optical properties of a reflecting surface. Instruments suitable for determining these polar intensity distribution curves are termed Goniophotometers.

With advancements in image capture technology, digital cameras are being used in quantifying gloss in different areas; they range from application in the cosmetic industry to agriculture and the understanding of the behaviour/health of animals (McMullen and Jachowicz 2003), (Lefaudeux *et al.* 2008), (Mendoza *et al.* 2010), (Toomey *et al.* 2010). In this study, a digital SLR camera was used to capture the images of the hair tresses and these images are then analysed (using MATLAB) to quantify the gloss of the tress.

To understand how humans make gloss judgements, psychophysical experiments were conducted (Chapter 5). Psychophysics is the scientific study of the relationships between the physical measurements of stimuli and the sensations and perceptions of those stimuli (Johnson and Fairchild 2003). A brief outline of psychophysical methods is provided in Section 2.8.1.

Human hair has been discussed in Section 2.9. As well as a brief history of human hair knowledge, human hair types, structure such as the cuticle, the cortex and the medulla

have been explained in Section 2.11. The chemical and physical properties of human hair have been discussed in Sections 2.12 and 2.13.

Lustre or Contrast-Gloss is visually observed as a contrast between the specular and diffuse reflections from an object. However, when observing human hair the relation between the lustre and reflected light from the hair is complex. The way the hair fibre or hair tress scatters light determines its shine and the surface scattering depends on the condition of the hair fibre or hair tress. When light is incident to the surface of the hair fibre or hair tress it has been suggested that the reflection can be divided into three different reflection bands: 1) Front surface reflection (the Shine band); 2) Back surface reflection (the Chroma band); and 3) Ambient reflection (the Diffuse band), (Aims and Objectives Section 1.1, 4-a). Lustre or shine is perceived when an object scatters more of the incident light at a particular angle or in a particular direction than in other directions (Reich and Robbins 1993). Shine or Lustre is generally considered to depend upon three main parameters (Lefaudeux *et al.* 2008); 1) The amount of reflected light, 2) The width of the shine band; and 3) the background on which the reflection is observed. Figure 2-65 the lustre parameters (the figure has been reproduced from the section 2.15.1).

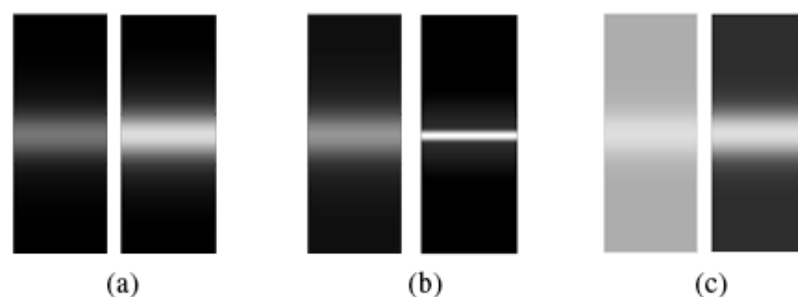


Figure 2-65 Lustre is considered to depend on three parameters. (a) Increase of the amount of light reflected. (b) Reduction of the width of the specular light band. (c) The background on which the reflection is observed

Over the last thirty years there have been a number of studies published on measuring the gloss of human hair. The evolution of the gloss evaluation models applied to the human hair tress can be traced to Stamm's work in 1977. Stamm used a goniophotometer to record the light distribution curves of multiple hair fibres. In the last twenty years there have been as many as 10 major human hair gloss evaluation models

proposed and the number is increasing. This suggests that although the instrumental methods of capture technology have improved that no system of measuring the gloss of human hair has been discovered that correlates with the human perception of gloss to the satisfaction of Industry. The Evolution of human hair gloss models is described in Section 2.15.2.

Chapter 2 provides a review of previous studies relevant to the work presented in this thesis, along with the chemical and morphological properties of human hair. In the Chapter 3 the various methods used in this research are discussed. These include aspects of sample preparation, the development of the gonio-image capture setup and the image capture process.

Chapter 3

Methodology

3.1 Methodology

3.2 Overview

Appearance is an important property of human hair and in specifying hair appearance gloss should be taken into consideration. There are several problems involved in the definition and measurement of the gloss of human hair. Measurements may be affected by many factors such as the hair colour, the lighting environment (ambient illumination), surface smoothness, hair morphology, hair mass density on scalp and hair fibre alignment (Gao *et al.* 2009). In addition to the technical challenges, the very nature of the lustre/shine question itself changes drastically with context (Kaplan *et al.* 2010); so gloss and its measurement has been the subject of extensive investigation, in both theoretical and practical aspects. There have been several devices and methods developed to measure gloss (Section 2.15.2) but no one method has been adopted as an Industry Standard. The most popular technique, used in the Cosmetics Industry, for the automatic assessment of hair gloss is to digitally capture images of the hair tresses and produce a gloss classification based upon the average gloss intensity distribution. Unfortunately, current computational modelling techniques are often found to be inconsistent when compared to the panel discriminations of human observers (Lefaudeux *et al.* 2008).

To investigate the hypothesis that an image based computational gloss evaluation system can quantify the gloss of a human hair tress in a similar way to human observers, Stated in Chapter 1 Section 1.1, certain aspects of the human visual system are required to be modelled, in order to develop a Gloss Evaluation System that will satisfy both computational modelling and the subjective evaluation system (panel system). Chapter 3 focuses on the sample preparation methodology (Aims and Objectives Section 1.1, Objective 2-a), the development of a gonio-image capture experimental setup (Aims and Objectives Section 1.1, Objective 3-b) and on-screen evaluation methods (Aims and Objectives Section 1.1, Objective 7-a). In order to produce different levels of hair shine, hair tresses were treated using heat, chemical and mechanical techniques. It was noted that these techniques do not necessarily produce a range of shine that can be detected by human observers. To overcome this problem hair tresses were treated with different commercial products. Currently there are no agreed commercial standards, which

outline application methods, available to apply commercial products to the hair tress. In order to achieve consistency the author has developed new application methods to apply products to the hair tresses (as stated in Aims and Objectives Section 1.1, Objective 2-a). These methods are described in Section 3.3.2. A discussion of the image-capture issues when the images were captured in a colour-matching booth is provided in Section 3.4.1. To overcome some of these issues the author has developed a Gonio image capture setup (as stated in Aims and Objectives Section 1.1, Objective 3-b). This system includes a bespoke sample holder (cylinder), which incorporates tress alignment and enhanced tress-presentation properties. The sample holder and tress mounting techniques are novel and have not been previously described in the literature. The Gonio image capture setup is outlined in Section 3.9. A High Dynamic Range (HDR) imaging technique was used to capture the hair tress images. This technique, capturing hair tress images at different shutter-speeds, has not previously been applied to human hair gloss evaluation. Thus, this research is the first time that HDR Imaging has been used as part of a hair tress gloss evaluation system. MATLAB code has been written, adapted and developed in order to convert the captured images, from sRGB colour space to the CIELAB colour space. The effect on each component of the colour space on different shutter-speeds was examined. In order to relate the computational methods to human gloss evaluation of the hair tress, psychophysical experiments have been conducted. A graphical user interface (GUI) has been developed by the author (Aims and Objectives Section 1.1, Objective 7-a), using the software package MATLAB, and this was used for the magnitude estimation psychophysical test on the images of the hair tress (Section 3.5). The Tress-Gloss 1.0 GUI displays an image of a hair tress on a calibrated screen, and participants were asked to rate the tress image, on a scale of 1 (least glossy) to 9 (very glossy), in terms of gloss. It was noted that participants were reluctant to give extreme values. To overcome this problem the author modified the Tress-Gloss 1.0 GUI (called Tress-Gloss 2.0) and changed the magnitude estimation test to a method of constant stimuli (forced choice – pair comparison) psychophysical test.

3.3 Sample preparation

3.3.1 Hair treatment methods to create different level of hair shine

To produce different levels of gloss on European Brown hair tresses, 15 Dark Brown European hair tresses were randomly selected from the Croda holdings. The tresses were of an unknown history. The tresses were arranged according to their similarity of appearance (by an expert at Croda plc.) and a sample number was given to each hair tress. The hair tresses were divided into three groups of five, one for each type of treatment. Each group had a different treatment applied; one group was heat-treated, one group was chemically treated and one group mechanically treated. These samples were presented to an untrained panel of observers to rank each tress relative to the other tresses in their particular set based on their gloss appearance, under un-controlled conditions.

3.3.1.1 Heat treatment of the hair tresses

Six (6) of the fifteen (15) European-Brown hair tresses were selected based on their similarity of appearance. The six hair tresses were washed with water under a constant flow rate of 1500 – 2000 ccm (cubic centimetres) for approximately 2 mins. A 10% Sodium Lauryl Ether Sulphate, SLES, (0.5 ml) solution was applied to each hair tress. Each hair tress was rubbed constantly by hand for 2 mins, working the applied solution into the tress. Post washing, the tresses were left to dry under controlled environmental conditions (50 % relative humidity (RH)).

Table 3-1 List of the hair tresses exposed to heat using GHD IV Hair Straighteners

Hair Tress number	Heat Exposure (seconds)
1462	10 sec.
1456	20 sec.
1460	30 sec.
1457	40 sec.
1461	50 sec.
1459	60 sec.

To mimic heat treatment, a ceramic flat iron / Hair straightener (GHD IV Styler) was applied to the hair tresses. Currently there is no standard heat treatment test adopted by the cosmetic industry. For this reason, a new test was developed. Instead of running a pair of tongs (in our case the GHD IV) in the root to tip direction we divided the hair tresses into segments, where each segment's height was equal to that of the tongs height as shown in Figure 3-1. At each segment location, the hair straightener was compressed onto the hair tress for one of the durations listed in Table 3-1 (this was dependent on the test parameter e.g. 30 sec). To create a range of heat treatment, 6 hair tresses were selected and each tress was exposed to heat at one of the durations as shown in Table 3-1.

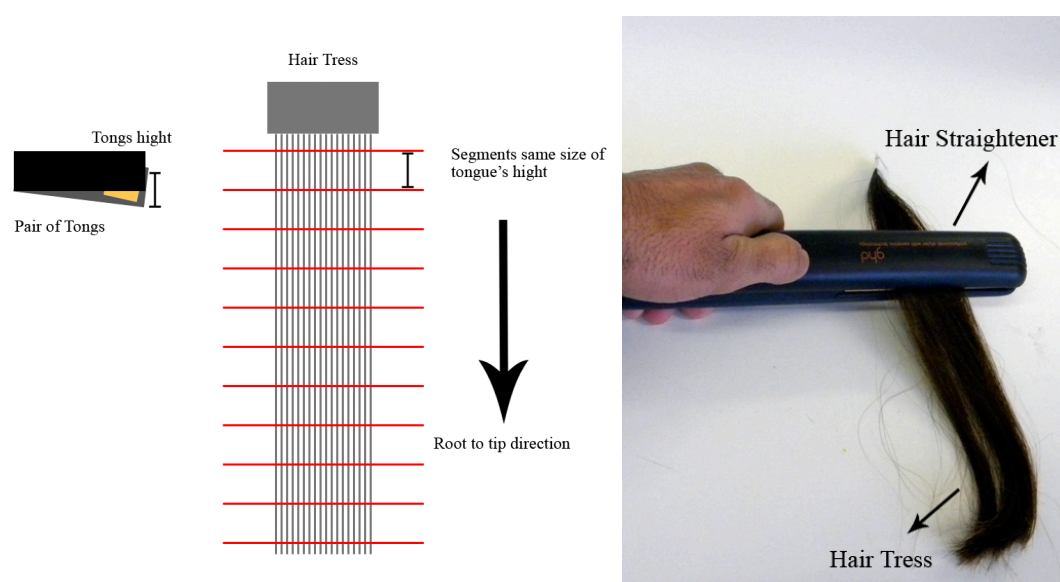


Figure 3-1 Schematic diagram of heat treatment experiment

3.3.1.2 Mechanical treatment Methodology

A set of four European Brown hair tresses of similar original appearance were treated mechanically using the UMIST Combing Tester. This device comprises of six combs attached at equal intervals to a cylinder; the hair tress is clamped at the top of the cylinder and as the cylinder rotates the combs pass through the hair tress, mimicking manual combing action (as shown in Figure 3-2). To create a range of mechanical treatment, 4 tresses were selected and they were washed in the same manner (see

Section 3.3.2.2) as the heat-treated tresses. Once the treated hair tresses were left to dry under controlled environmental conditions (50% relative humidity). Post drying, the combing frequency cycle was varied as outlined in Table 3-2.

Table 3-2 Combing cycles applied to each hair tress

Hair Tress ID Number	Combing Cycles
1412	1000 cycles
1410	6000 cycles
1409	12000 cycles
1411	18000 cycles



Figure 3-2 Combing tester for mechanical treatment

3.3.1.3 Chemical treatment Method

Five hair tresses were selected. To chemically treat the surface of the hair, a 28% Sodium Lauryl Ether Sulphate (SLES) solution was applied to each hair tress. Each hair tress was submerged in the solution for certain duration (see Table 3-3). The tresses were washed using the same procedure as that used for the heat-treated tresses (Section 3.3.1.1) but instead of being treated with a 10% SLES solution, they were submerged in a 28% SLES solution. One hair tress was removed immediately from the solution and acted as a control sample. The remaining samples were submerged in the 28% SLES solution for varying periods of time as outlined in Table 3-3. For example, hair tress 1479 was submerged in the SLES solution for 2 hours. Once the sample had been

submerged for the allotted time it was removed from the SLES solution and the post treatment schema applied (each tress was left to dry in environmentally controlled conditions with 50% relative humidity).

Table 3-3 Hair tresses dipped in SLES solution

Hair Tress ID Number	Time dipped in the 28% SLES
1477	Control
1479	2 hrs
1478	3 hrs
1476	4 hrs
1475	20 hrs

3.3.2 Application Methods for Commercial Products

3.3.2.1 Hair Samples

Several virgin hair tresses of Blonde, European Brown and Oriental hair were obtained from Croda plc. Each hair tress was 15mm +/- 0.5 wide and 260mm +/- 1 long. Tresses were kept in a conditioned room for 24 hours (20 °C +/- 2 temperatures and 50% +/- 2% humidity) before the treatment, in order to attain the humidity equilibrium. Hair tresses were weighed in their dry state and then washed with 10% SLES solution. Croda's washing protocol was adopted in washing hair tress.

3.3.2.2 Washing procedure

Each tress was fully wetted under water of a constant flow (the flow rate and temperature of the water was 1.5 litres per minute and 35 °C respectively). After wetting, a 0.5mL SLES, 10% (w/w) concentrated solution was applied using a syringe to the hair tress. The solution was massaged into the tress using the thumb and fingers for two minutes. The tress was then rinsed under flowing water for 30 seconds with manual rubbing. Post washing, tresses were air dried under the controlled environmental conditions.

3.3.2.3 Shine levels

The goal was to apply different commercial products to human hair tresses in order to produce three different appearance levels of gloss or shine. To produce these levels commercial products were used are tabulated in the Table 3-4;

Table 3-4 Commerical products used in the study.

Product	Active ingredient
Spray Products	
Schwarzkopf pro styling silky shine styling spray 150ml	Cyclomethicone
Tesco Hairspray 300ml	PEG-12 Dimethicone, PPG-12 Dimethicone, VA/Crotonates/ Vinyl Neodecanoate Copolymer
Pantene pro V Ice shine ultimate Hold Hair spray 300ml	PEG-12 Dimethicone
Wella Shockwave boost it! Heat defence volumising mousse 200ml	VP/VA Copolymer
Gel Products	
Alberto V05 styling Gel Mega hold 175ml	PVP/VA Copolymer
Wax	
Alberto Vo5 styling Wax 75ml	Beeswax
Alberto vo5 extreme style matt wax 75ml	VP/VA Copolymer, Microcrystalline Wax, Cera Alba (Beeswax, Cire D'Abeille)
Shampoo and Conditioners	
John Frieda brilliant brunette liquid shine conditioner 250ml,	Dimethiconol
Pantene ice shine conditioner 200ml	Bis-Aminopropyl Dimethicone
Charles Worthington takeaways brilliant shine conditioner 75ml,	Dimethacone, Stearamidopropyl Dimethacone
Tesco everyday shampoo apple and Aleo-vera 750ml.	Sodium Laureth Sulfate

3.3.2.4 Product application methods

There are currently no standard application procedures for applying commercial products to hair tresses (products mentioned in the Section 3.3.2.4). In order to achieve consistent application a series of product application methods were developed.

3.3.2.4.1 Application Method for Spray-based products

For the application of spray products, the tress was held vertically and the product was sprayed on to the tress, at a distance of approximately 15cm, from root to tip in one motion and preferably in less than 10 sec. After each dispensed spray a comb was used to spread the product evenly onto the tress. For holding spray products, the hair tress was presented on a cylinder (sample holder) and product was sprayed approximately 15cm away; Figure 3-3 shows a schematic of the spray product application method.

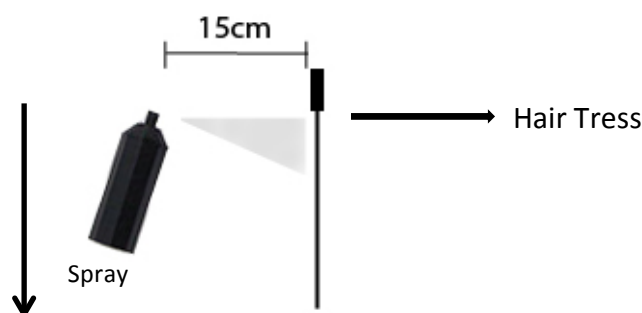


Figure 3-3 Schematic of the spray-based product application method

3.3.2.4.2 Application Method for Waxes

To achieve evenness, a known amount of wax (3% w/w by weight of the tress hair) was placed on a comb. The root end of the tress was placed at the top edge of a hair dryer blower opening. The dryer was set to a medium heat (approx. 45⁰C) with a low airflow. Using these settings, a comb was gently run through the tress until all the wax was transferred onto the hair tress (the tress exposure to the hair dryer did not exceed 40 sec.). Figure 3-4 shows a schematic of the wax application method. A Fransen 1200-watt hair dryer was used in the study.

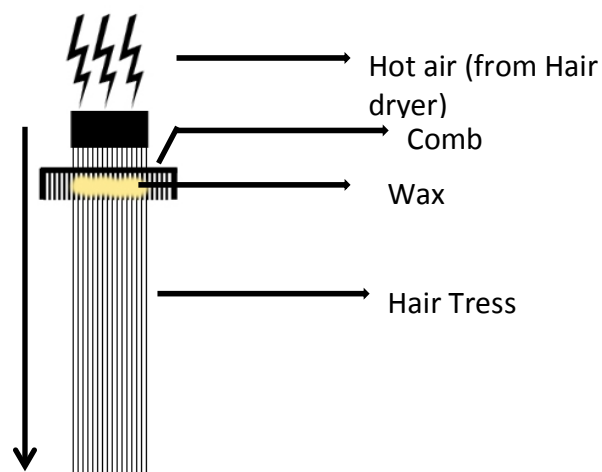


Figure 3-4 Schematic of how wax is applied onto the hair tresses

3.3.2.4.3 Application Method for Gel and liquid-based products

A known amount of product (see Table 3-4 for details) was taken in hand and applied onto the hair tress. To produce an even application the tress was manually massaged (using thumb and fingers) for 1 min in root to tip direction. Post massage a comb was used to align the hair fibres.

Table 3-5 shows the application details of the Oriental hair tresses used in the sample preparation (the same products were applied to Blonde and European brown hair tresses). Two products were selected in order to give the maximum difference in shine. These two products along with virgin (tress with no treatment) and SLES washed tress were used in the gloss evaluation study. Tresses selected were:

- Virgin hair tress (No treatment)
- Tress washed with 10% SLES
- Tress treated with wax 3% w/w of the tress hair
- Tress treated with Schwarzkopf pro styling silky Shine spray

Table 3-5 Details and products applied onto the Oriental tresses used in sampling to create different level of hair shine

Oriental						
Tress ID No.	Dry Weight	3% weight	5% weight	10% weight	20% weight	Application
101	5.1	0.153	0.255	0.51		Wax matt look vo5 3% (extreme style)
102	6.2	0.186	0.31	0.62		Wax matt look vo5 5% (extreme style)
103	5.9	0.177	0.295	0.59		Vo5 Styling Gel 10% (mega hold)
104	6.2	0.186	0.31	0.62	1.24	Vo5 Styling Gel 20% (mega hold)
105	6.4	0.192	0.32	0.64		Shine spray twice both side
106	4.19	0.125	0.209	0.419		Pantene pro v ice shine both side (15cm away from the tress)
107	6.09	0.182	0.304	0.609		Tesco Hair spray both side
108	5.18	0.155	0.259	0.518		Pantene Pro V twice both sides
109	5.76	0.172	0.288	0.576	1.152	Wella mousse 20%
110	5.68	0.170	0.284	0.568		Wella mousse 10%
111	6.12	0.183	0.306	0.612		Styling Wax vo5 3%
112	6.67	0.200	0.333	0.667		Styling wax vo5 5%
113	5.91	0.177	0.295	0.591		Pantene ice shine conditioner 10%
114	6.23	0.186	0.311	0.623		Pantene ice shine conditioner 50%
115	5.39	0.161	0.269	0.539		Charles Worthington 10%
116	6.57	0.197	0.328	0.657		Charles Worthington 50%
117	6.6	0.198	0.33	0.66		John Frieda Collection 10%
118	6.96	0.208	0.348	0.696		John Frieda Collection 50%
119	6.49	0.194	0.324	0.649		Matte Wax (extreme style) 4%
120	7.06	0.211	0.353	0.706		Vo5 Styling Gel 15% (mega hold)

3.4 Visual assessment of Heat, Mechanically, and Chemically treated hair tresses in an unconstrained viewing environment

To evaluate the perceived gloss of the treated and untreated European-Brown hair tresses (Section 3.3), a panel of naïve observers was assembled at Croda in Cowick Hall. The gloss panel was conducted at an interview room at Croda with diffuse but unknown artificial lighting. For this pilot study three sets of samples of European-Brown hair tresses were prepared that consisted of 15 hair tresses in total. Each set was treated differently, to represent different forms of hair-treatments. The samples were presented on large cardboard tubes on a table. Both the cardboard tubes and table were covered with white paper.

Each observer was given an Experiment Instruction Sheet outlining the experimental paradigm. They were also asked to complete a gloss evaluation form, which contained questions outlining aspects such as age, gender and handedness, which have all been

related to a bias in colour perception. The gloss evaluation form also contained a data-capture section that allowed each observer to make ranked gloss evaluations on each hair tress (see Appendix B).

The treated hair tresses were presented to individual observers and placed over a cylinder covered with white paper under uncontrolled lighting, as shown in Figure 3-5. The treated hair tresses were presented along the cylinder in three sections. Section A contained the heat-treated hair tresses, section B contained the mechanically treated tresses and section C contained the chemically treated tresses. The hair tresses were placed onto the cylinder without applying further tension. Observers' viewing distance and viewing angle were unconstrained and they were discouraged from touching any of the samples or discussing their observations with other participants.

A gloss evaluation sheet was developed by the author (Appendix B) in order to capture the judgements of each observer. The gloss evaluation sheet was presented to each individual within the untrained panel to allow the capture of information relating to the gloss of each hair tress. A gloss ranking range of 1 to 6 was set for the heat-treated tresses, 1 to 4 for the mechanically treated tresses and 1 to 5 for the chemically treated tresses (where 1 was the rating for the least glossy sample within the set and the largest number in the gloss range (4, 5 or 6) was the rating for the most glossy sample in the set). The task of the observer was to rank each sample within the test set. For example, for the heat-treated samples there were 6 samples. The observer would rank the sample they perceived to be the least glossy, as rank 1 and the glossiest would be ranked six. The remaining samples would be assigned a ranking relative to the other samples in the set.

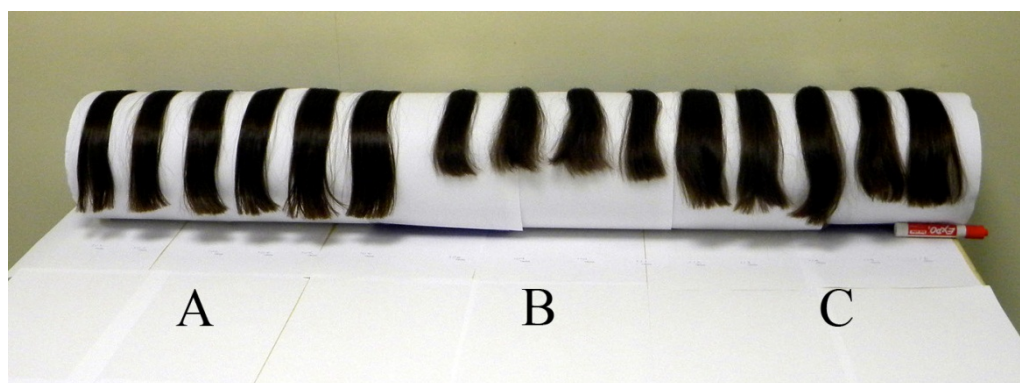


Figure 3-5 Presentation of Hair tresses Set A is heat treated hair tresses, Set B is hair tresses treated mechanically and Set C is hair tresses treated chemically

Observers were instructed to assign a gloss ranking with a gloss ranking range that differed dependent on the size of each of the hair tress sets. The observers were not given any example gloss rankings or practice in their discriminations.

3.4.1 Problems with the visual assessment of human hair gloss

It was assumed prior to the gloss ranking experiments that the gloss ranking for a particular sample would be dependent on the amount of physical damage sustained by the hair tress (either thermal, chemical or mechanical). This assumption was based on the premise that each hair tress had identical surface properties prior to the treatment. Although the tresses were selected on their similarity of appearance they were unlikely to have identical surface properties. For example, the set of 6 heat-treated hair tresses were ranked by the panel and did not show the expected trend (the hair tresses ranked as the least glossy to have been heat treated for a greater duration with the hair straighteners). There are many reasons why the panel ranking results were not as expected. Tress presentation may have been a contributing factor to the inconsistent rankings. It is well known that texture or spatial structure has an effect on the perception of colour and this may mean that the hair alignment of the tresses should have been more adequately constrained.

Having so many variables in physical gloss evaluation system and limited number of tresses available, it was thought that it would be feasible to digitally capture the images of the tresses in a controlled environment and display the images randomly on a calibrated screen for the tress gloss evaluation. To create an on-screen evaluation system, there was a need to develop an image capture setup to capture images of the tresses within a controlled environment and a computer program that could display images of the hair tresses on screen and collect experimental data.

3.5 On-Screen Gloss assessments of human hair tresses

Two Graphical user interfaces (GUIs) were developed, Tress-Gloss 1.0 and Tress-Gloss 2.0, for the purpose of on-screen evaluation. The GUIs were developed using MATLAB (R2010a) and have never before been employed in any other similar studies. Tress-Gloss 1.0 is based on Magnitude estimation psychophysical test, using Tress-gloss 1.0, a

number of observers visually ranked the apparent gloss of a series of samples (Hair tresses) observed on a calibrated LCD screen. The Tress-Gloss 1.0 displayed these images randomly; one at a time, and each observer ranked the hair tress. This test continued until each image was ranked three times (in our case images appeared 45 times, 15x3). On completion of the test, the data was gathered and analysed Figure 3-6 shows the screen shot of the main window of the Tress-Gloss 1.0.

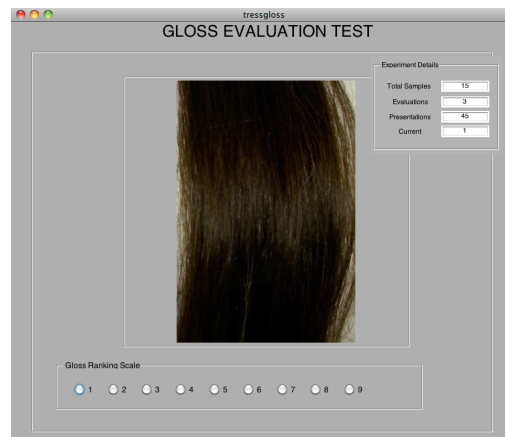


Figure 3-6 Main window of the Tress-Gloss 1.0

It was noted that in using the Magnitude Estimation method (a one-dimensional scaling method), observers were reluctant to provide extreme rankings. This may be due to a lack of context in making the ranking choice (e.g. there is no anchor or standard for comparison). For this reason, Tress-Gloss 1.0 was modified and the test was changed from a Magnitude Estimation method to a 'Paired Comparison Forced Choice' test. In Tress-Gloss 2.0 (a modified version of Tress-gloss 1.0), a pair of equally sized images of hair tresses appeared on a calibrated display and observers were asked to choose which tress appeared glossier/shinier.

3.5.1 Method

Images of hair tresses were imported into the MATLAB-GUI. As this test was a psychophysical experiment, the subject details needed to be recorded. A form was developed that appeared at the start of the test, which accepted user information. A pair of equally sized images of hair tresses appeared the screen and the user was asked

to choose which tress image appeared shinier. As soon as the observer registered their decision the next image pair appeared and this continued until all of the images had been displayed. At the end of the test all the data was saved to a CSV file (Comma-Separated Values file) that was then exported to Microsoft Excel for further data processing. This MATLAB GUI generated two types of CSV file. The first type recorded all of the data and other type holds user information (Appendix C). These files were saved by default into the same folder where GUI had been saved.

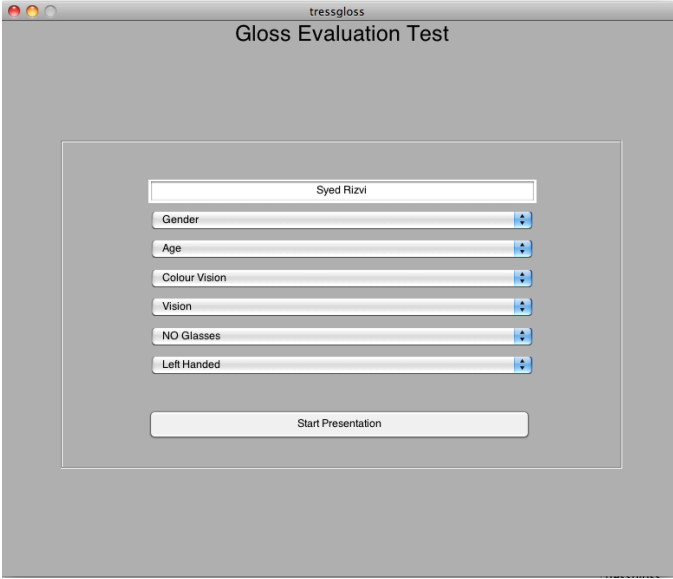
The image is a screenshot of a MATLAB GUI window titled 'tressgloss' with a subtitle 'Gloss Evaluation Test'. The window has a light gray background. In the center, there is a white rectangular box containing a form for observer information. The form consists of a text input field at the top with the name 'Syed Rizvi' entered. Below this are six dropdown menus, each with a label and a blue arrow icon on the right: 'Gender', 'Age', 'Colour Vision', 'Vision', 'NO Glasses', and 'Left Handed'. At the bottom of the white box is a 'Start Presentation' button.

Figure 3-7 Observer information form (screen-shot from Tress Gloss 1.0 GUI)

3.5.2 Tress-Gloss 2.0 (GUI) Overview

At the start of the test, a window appeared that requests the observer's details, as shown in Figure 3-7. The observer information is collected, collected information includes name in a text box (observer will click the text box and input his/her name using keyboard), pop-up menus are provided for other information including gender, age, colour vision, vision, Figure 3-8.

Figure 3-8 Observer information form (screen-shots from Tress Gloss 1.0 GUI)

With ageing, the quality of vision changes, some properties of the eye change roughly linearly with age (including the yellowing of the lens).

As there is little information linking colour deficiency and gloss, the option was added to see if there is any difference in assessing gloss for colour-deficient observers. Prior to the start of the test, each observer performed a colour deficiency assessment (using Ishihara Pseudo-Isochromatic plates).

Visual assessment is related to psychophysics. Information about the observer's dominant-eye (left or right) can allow a better understanding of how people with different dominant eyes perceive gloss. The observer's vision (near-sighted or farsighted) and eye correction methods were also taken in consideration. If the observer's vision was corrected they were asked to provide their vision prescription.

In Tress-Gloss 2.0 (a modified version of Tress-gloss 1.0), a pair of equally sized images of hair tresses appeared on a calibrated display, and was surrounded by a mid grey background. The grey background colour was chosen to be neutral in order to anchor the observer's judgements. Once the pair of tress images appears on the screen the observers were asked to choose which tress appeared glossier/shinier. Comparisons were only made for hair tresses of the same type (for example European Brown). To

avoid distractions the dialog box containing the experiment details, in the Tress-Gloss 1.0, was removed from the main evaluation body of the Tress-Gloss 2.0 GUI. This produced an interface with fewer distractions and helped the observers to concentrate on the comparison instead of the number of remaining trials. Figure 3-9 shows the main window of the Tress-Gloss 2.0 GUI. The observer recorded their choice by pressing the number key 1 or 2. Number key 1 represented the tress image on left whereas the number key 2 represented the tress image on right of the screen.

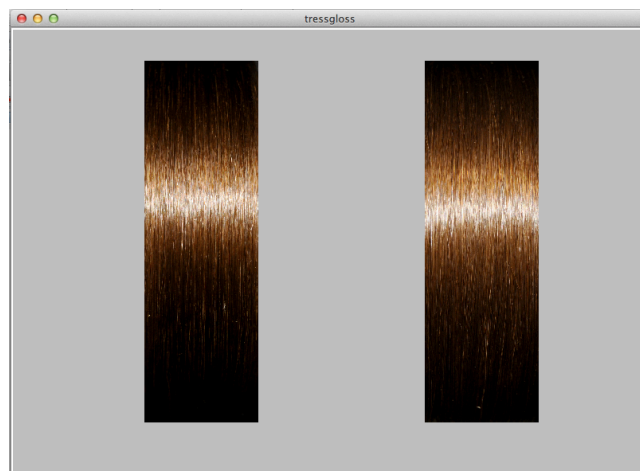


Figure 3-9 Main window of the Tress-Gloss 2.0, paired comparison forced choice test

3.6 Hair tress Image Capture setup for hair tresses

Initially, the hair tress images were captured in a colour-matching booth (Macbeth Spectra Light II). The image capture setup consisted of three main elements: illumination (light source), a 10MP digital camera and a cylinder on which the hair sample was mounted. The digital camera was placed at a distance of 40 cm away from the sample and was at a 45⁰-degree angle relative to the cylinder; Figure 3-10 shows the image capture setup used for the initial study.

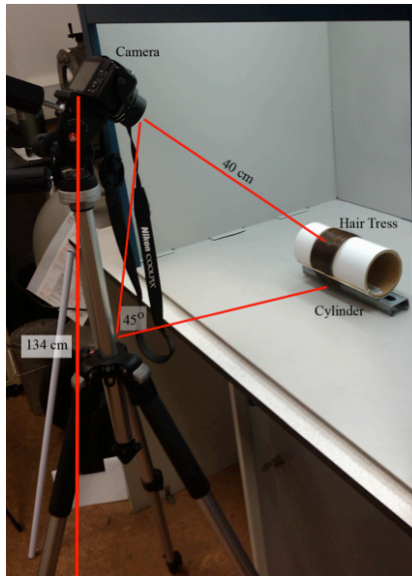


Figure 3-10 Image capture setup (pilot study)

A cylinder with a diameter of 8.5 cm, covered with grey paper, was used to hold the hair tress; an aluminium base was attached to the cylinder to allow it to be fixed onto any flat surface. A clamp was attached to one end of the cylinder so that the root end of the hair tresses, usually the wax-covered part could be clamped and on the other side of the cylinder an elastic band was fixed across the cylinder to hold the tip-end of the hair tress. Figure 3-11 shows different views of the cylinder used as a sample holder in the pilot study experiment.

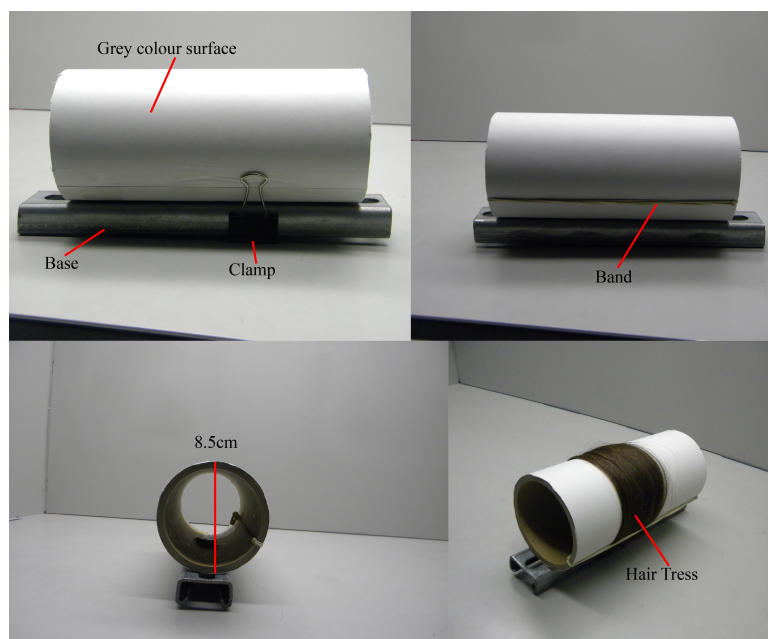


Figure 3-11 Cylinder used in the pilot study.

3.6.1 Problems using Colour-Matching booth

Initially it was thought that using a colour-assessment booth, as a constrained lighting environment, for the image capture of hair tresses would be an ideal solution. The images could be captured under different light sources but it was noted that there was no flexibility in capture angles and more than one shine band was visible on the hair tress due to the light source (tube-lights). Figure 3-12 shows the two shine bands on the hair tress; image capture in the colour-matching booth under cool white fluorescent lighting.



Figure 3-12 Image of a European Brown Hair Tress captured in the colour-matching booth under cool white lighting

3.7 Gonio Image Capture Setup

In order to overcome the problems faced in the hair tress image capture setup used to capture the images of the hair tresses, a prototype Gonio-image capture system was developed. The Gonio image capture system consists of five main elements; 1-Light source, 2-Image capture device (Digital SLR Camera), 3-Sample holder (cylinder with grooves on), 4-Arc, 5-Tensioner (Spring). Figure 3-13 shows the Gonio capture setup.

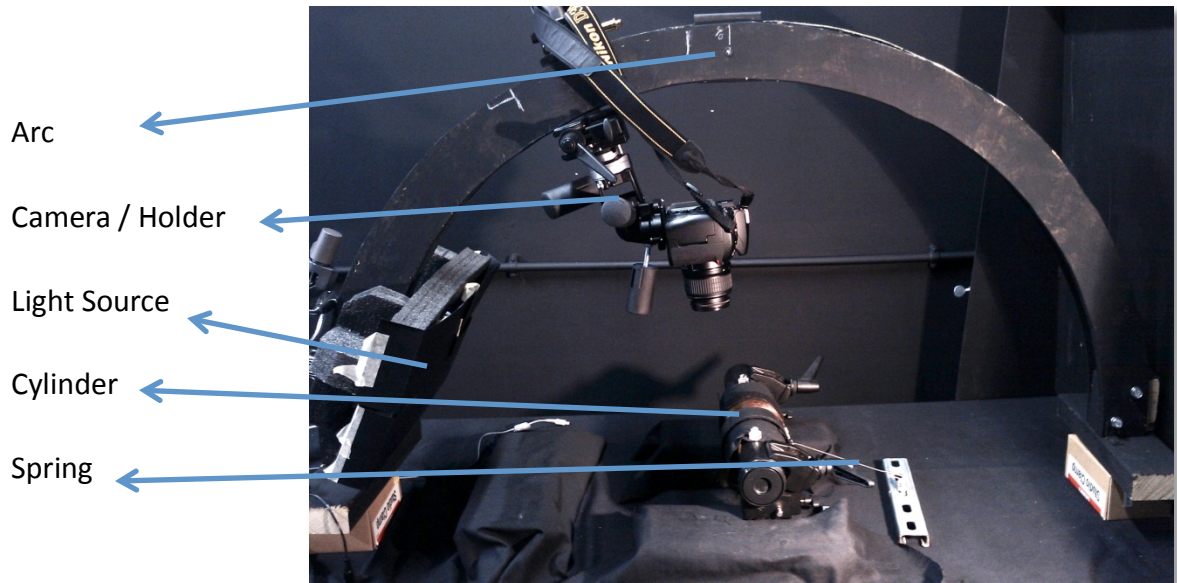


Figure 3-13 Gonio-Image Capture Setup

3.7.1 Arc

A 120 cm diameter semi-circular arc was designed to accommodate the image capture device holder. This allowed the camera or other measuring devices to be easily moved along the path of the arc and at a set distance from the sample. This allowed the capture of images of the sample from 0° to 90° but also the flexibility to measure at angles greater than 90° to the sample.

3.7.2 Capture device and device holder

A tripod-head was fixed on an aluminium bar and was attached to the arc. The bar could be moved along the arc's path and could be fixed at any point. Using a tripod-head provided flexibility in adjusting the angle from the camera to the sample along the path of the arc. To capture an image of a hair tress a Nikon D300 digital SLR camera was used, with a Nikkor lens having a focal length range of 18 mm to 55 mm. The distance between the sample and image capture device (camera) was 26 cm. All the images were captured at zero degrees to the sample, in this study. Figure 3-14 shows the experimental setup including the distance between the tress and camera and the distance between the base of setup and camera lens.

The aim of this system was to create an image capture system, develop an image-processing model that can separate the hair tress reflection bands and create a novel

method to measure the shine of the human hair tresses. Variation in shine and spatial movement of shine band related to the image capture angle will be analysed in future studies.

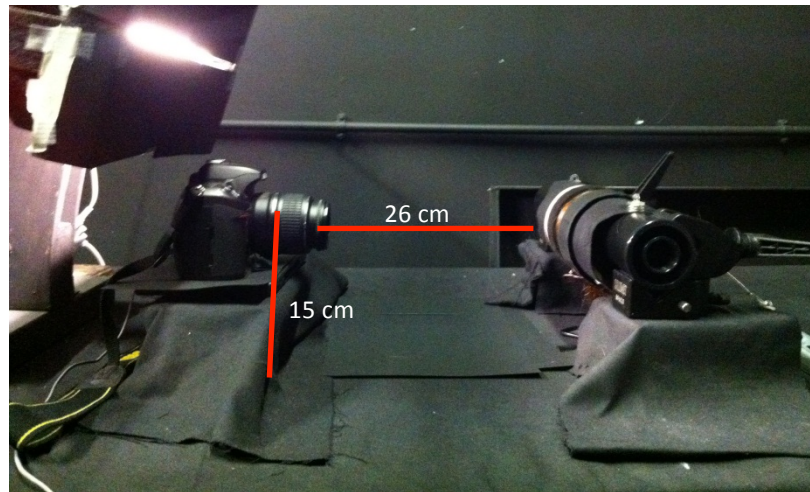


Figure 3-14 Distance between the capture device and sample in the image capture setup

3.7.3 Light Source

A fluorescent tube was used to illuminate the sample in this study. The fluorescent tube was fitted in a box with a horizontal opening, or slit, of 0.5 cm. The purpose of the light box and baffle was to produce a bar of light that would be as homogenous as possible. The light box was produced in order to reduce further diffusion of the light source and the distance between the light source and cylinder was 45 cm. The box was fixed at an angle of 20° ($\pm 4^{\circ}$) relative to the sample. Figure 3-15 shows the front view of the light box fixed on the arc.



Figure 3-15 Front-view of the light-box

3.7.4 Sample holder (cylinder)

A cylinder with the diameter of 8.5cm and grooves 1.5 cm wide and 0.5 cm deep was produced to hold the sample. Grooves were made in the sample holder in such a way that hair tress is sandwiched between two standards (shine and diffuse standards) and this was incorporated into the design to provide known limits while evaluating the shine. Figure 3-16 shows schematic diagram of the cylinder and Figure 3-17 shows hair tress mounted on the cylinder with both standards on each side.

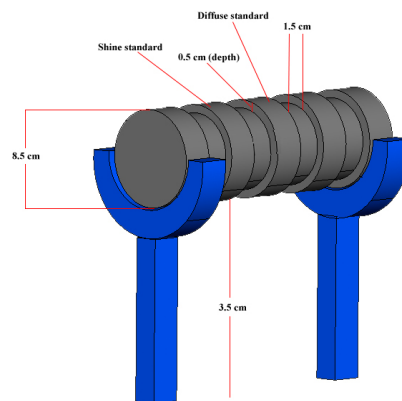


Figure 3-16 Schematic diagram of the cylinder

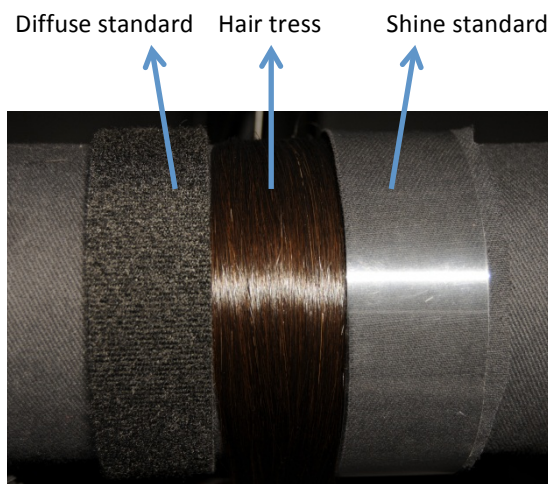


Figure 3-17 Hair tress mounted on the cylinder with standards

3.7.5 Tensioner (spring / clip)

Different techniques were tried to secure the sample on the cylinder. The method that gave best possible outcome was a combination of a hair clip and a spring. The hair clip produces a dual benefit; firstly it holds the fibres (hairs) under tension and secondly it provides an alignment mechanism. The spring attached to the clip provides a set tension

and the combination of both properties created an aligned hair fibres wrapped around the cylinder at a set tension. Figure 3-18 shows the clip-spring combination used in the study.



Figure 3-18 Hair clip and spring

3.8 Image-Capture process

Pre-processing of the hair tress images was undertaken in order to produce a standardised cropped image captured from the calibrated capture system, ready to be analysed further using MATLAB. Figure 3-19 shows flowchart of the process.

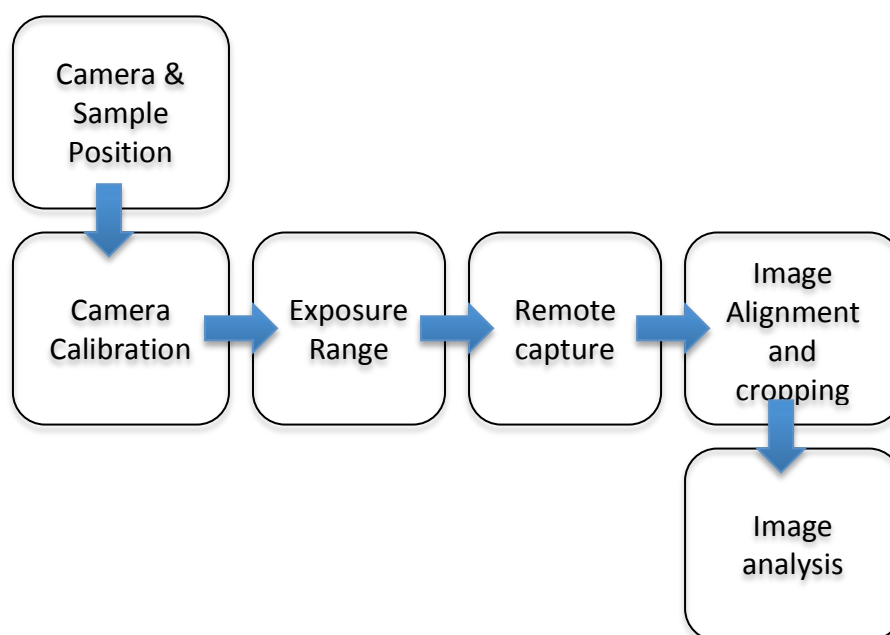


Figure 3-19 Flow diagram of image pre-processing

Camera calibration: Prior the start of the experiment, the digital camera was colourimetrically calibrated. As Nikon D300 is a professional level digital camera there were numerous image-capture settings for this device but on the whole these features are designed purely to take sharp, vibrant pictures. The goal of the gloss image capture system was different as the imaging of the hair tresses was only to measure and quantify the gloss. The D300 was switched to manual mode as this gave more control over the device. As images were captured in a low light environment ISO200 was selected. An X-rite White Balance Card was used to calibrate the white balance of the D300 camera. The X-rite white balance card provides a white reference point and a uniform surface that is spectrally neutral in commonly used lighting conditions and is used for white balance calibration. White-Balance and other camera features are described in the previous chapter (Section 1.6.1 Digital SLR camera).

Exposure range and remote capture: Macintosh software Sofortbild (version 1.2.4) was used to control the camera remotely. The Nikon D300 was connected to a laptop computer (MacBook 3.1 late 2007 model) using a USB cable. Sofortbild automatically recognizes the camera and shows camera model, lens name, focal length, focus mode, exposure value and battery status in a status bar. All major camera settings like shutter speed, aperture, exposure, white balance, ISO, image format and size are shown and can be changed from inside the Sofortbild software. As images of a tress were captured at different shutter speeds, a function called Bracketing was used. Bracketing allows a series of pictures to be captured once the minimum and maximum shutter speeds are selected. For this study a minimum shutter speed of 1 second and maximum shutter speed was 1/200 second was selected. These shutter speeds had been determined from a pilot study of a range of glossy materials. 24 images of a single hair-tress were captured at shutter speeds between 1 second and 1/200 of a second and saved to the hard disk of the laptop computer.

Image Alignment and Cropping; Even though extra care was taken in mounting the sample and placing the camera, alignment of the image can vary from sample to sample and when camera takes an image it captured the whole cylinder, which include shine and diffuse standards as well as the tress. To align and crop the image of the image Adobe Photoshop (CS3 Version 10.0) was used. Figure 3-20 shows a typical image from the system and the pre-processed cropped image of a hair tress.

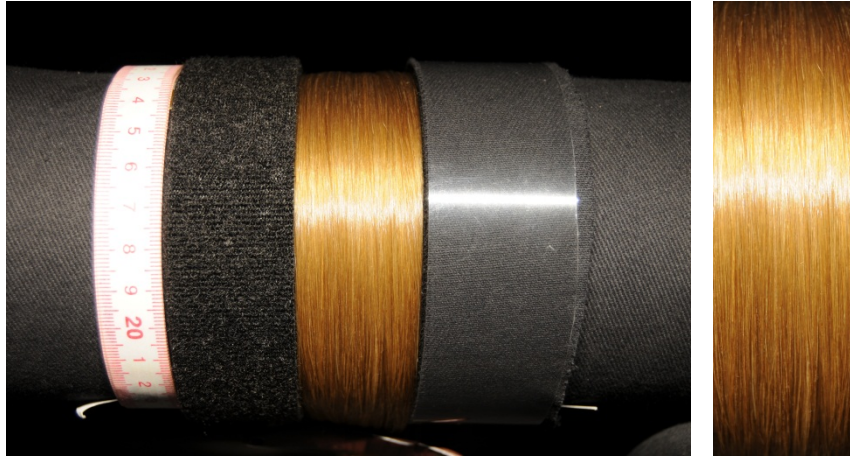


Figure 3-20 Image captured by the camera and Cropped image of the hair tress

Image analysis: Once the hair tress images were aligned and cropped they were imported into the MATLAB. For colourimetric analysis the images were converted from sRGB to CIELAB colour space. The transformation was applied using the MATLAB functions 'makecform' and 'applycform' with transform specified as 'srgb2lab'. This resulted in three planes of MxN dimension being calculated from the original RGB image. The first plane represented CIE L* (lightness), the second a* (red-blue) and third b*(yellow-green). The L* array was averaged by using 'mean' function, this will convert MxN metrics of L* into one-dimensional array in order to produce a profile of average lightness along the length of the tress. To calculate the Chroma (C*) of the tress image, Equation 3-1 was used:

$$Chroma = C^* = \sqrt{a^{*2} + b^{*2}} \quad \text{Equation 3-1}$$

The C* metric was averaged using the same method that was used in averaging the L* metric. Both L* and C* averaged arrays were plotted and their areas under the curves were calculated by using MATLAB's trapezoid function 'trapz'.

3.9 Summary

In order to develop an automated model of hair shine, which can be related to the human gloss evaluation system, tresses with different levels of hair shine were produced. To achieve the different levels of hair shine, tresses were treated using heat, chemical and mechanical techniques. A novel method was developed to heat treat a hair tress by dividing a hair tress into segments, where each segment's height was equal to that of the tongs height (hair-straightener). At each segment location, the hair-straightener was compressed on the hair tress for a certain duration. For chemical treatment, tresses were submerged in the 28% SLES solution for a certain duration and to treat hair tress mechanically the UMIST Combing Tester was used. It was thought with an increase of combing cycle on the hair the shine of hair tress would decrease. Unfortunately excessive combing did not produce a range of shine differences that could be discriminated by a panel of naive observers. To produce different levels of shine on the hair tresses, a second approach was taken. European Brown, Blonde and Oriental hair tresses were treated with different commercially available products. Due to the unavailability of commercial application standards, which was discussed in the application methods section, the author has developed new application methods to apply products such as waxes and sprays to the hair tresses. The application of a semisolid product to a tress to produce an even coating was achieved using a combination of a comb and a hair-dryer. A known amount of wax was deposited onto the comb and under a hair-dryer a comb was gently "run" through the tress until all of the wax was transferred onto the hair tress. This method is novel and has never been reported in the literature. The different commercial hair products used in the study are listed in Section 3.8.4. Two products were selected which gave a maximum difference in shine (wax samples were diffuse and shine spray samples were glossy) when compared to virgin tresses. These two sorts of treated tresses along with virgin and SLES washed tresses were used in the gloss evaluation study.

A Gonio image capture setup has been developed that consists of five main elements (Light source, image capture device, sample holder, arc and tensioner). The sample holder and tress mounting techniques are novel and have never been reported in published experiments. For hair shine evaluation, the author has used HDR (high

dynamic range imaging), which is the first time that it has been applied to hair shine in such studies. Pre-processing methods have been developed in order to produce a standardised cropped image of a hair tress. These steps include, camera and sample position, camera calibration, exposure range, remote capture, image alignment and cropping and finally image analysis. These steps are explained in section 3.10. A series of MATLAB scripts and functions were written by the author to convert the sRGB image captured by the camera into CIELAB colour planes. The effect of each component of the colour space on different shutter-speeds has been examined. It should be noted that when the average L^* area under the curve of HDR images of hair tresses treated with wax, shine-spray, SLES, were compared their difference remains the same throughout the HDR range, Section 3.11.1 explains the effect on average L^* area of a hair tress image at higher shutter speeds.

To relate the automated gloss-evaluation system to the human gloss-evaluation system, psychophysical experiments were conducted. A GUI (graphical user interface), Tress-Gloss 1.0, has been developed by the author. Tress-Gloss 1.0 was a magnitude estimation test in which a single image of a hair tress appears on the screen and the observers were asked to rate the gloss on a scale of 1-9. It was noted that the participants were reluctant to give extreme values, as there was no standard displayed. For this reason, the author changed the magnitude estimation psychophysical experiment to a method of constant stimuli (forced choice, paired comparison) psychophysical experiment. The Tress-Gloss 2.0 GUI was produced whereby a pair of images of hair tresses appeared on the screen and participants were asked to choose which hair tress looked shinier.

Chapter 3 has explained the methods that have been used to quantify hair gloss in this study. In Chapter 4 the optical properties of the human hair tress will be discussed along with an analysis of the effects on the optical properties of the tress of different treatments.

Chapter 4

The Optical Properties of Human Hair Tresses and the Development of Novel Human Hair Gloss Evaluation Models

4.1 Overview

Chapter 4 focuses on the optical properties of the human hair tress and the development of the human hair gloss model (as stated in Aims and Objectives Section 1.1, Objective 6-e). Three different types of hair tresses were used in the study (Blonde, European Brown, and Oriental). The visual appearance of each hair type differs due to the pigmentation present within the hair fibre; Blonde hair tresses reflect more light as they absorb less light whereas Oriental hair tresses absorb more light. To understand the effect of lightness and Chroma reflected by the different types of hair tress, the average values of L^* and C^* of the tress images were examined (as stated in Aims and Objectives Section 1.1, Objective 5-a). The effect of average L^* and C^* values on the tress images, prepared with different commercial products (explained in sample preparation Section 3.3), were also examined. Images of Tresses treated with different commercial products were captured at different shutter speeds, the effect on the area under the curves of the average L^* and C^* values was examined. It should be noted that even though the shutter speed increases the difference between the shine-levels remains the same (shine difference invariance). Images captured at a 1 second shutter speed were selected for further analysis of the reflection characteristics of the hair tresses.

Through image analysis it was noted that the Chroma band (Section 4.2) is not uniform. The colour of the hair tress changes from light to dark, producing a colour gradient, as we move upward from the shine band. A new interpretation of the reflection band, called Chroma-Specular (C_s), was identified in this study that has not been suggested in the literature for human gloss evaluation models.

Furthermore a new method was developed by the author to separate the reflection bands (Shine, Chroma-Specular and, Chroma-Diffuse band) from the hair tress images (As stated in Aims and Objectives Section 1.1, Objective 4-b). The separation was performed by selecting the shine area on the image of the tress and calculating the most frequent value (MFV) of L^* and C^* in the shine area (the reflection band separation method is explained in Section 4.4). Once each band was separated, the effect of each reflection band on the different levels of hair shine was examined.

With the novel interpretation of the reflection bands, C_s , and a novel method that separates the reflection-bands successfully, two new gloss evaluation models were

successfully produced, ROC_1 (Rizvi-Owens-Croda) and ROC_2 , were developed by the author (Aims and Objective Section 1.1, Objective 6-e). The performance of the ROC models was compared with conventional gloss evaluation models. The ROC gloss-evaluation-models are explained in Section 4.12 and comparisons with other models are provided in Section 4.13.

4.2 Effect of different levels of Shine on the Lightness (L^*) and Chroma (C^*) of Blonde, European-Brown and Oriental Hair tress images

Three different types of hair tresses were used in the study (Blonde, European Brown and Oriental). The visual appearance of each hair type is different because of coloured pigments present in the hair fibre. An initial research question was (as stated in Aims and Objective Section 1.1) could an image based gloss evaluation system be sensitive enough to distinguish between different intensities of reflection from the hair tresses? To understand this question, images of the hair tresses (Blonde, European-Brow and Oriental) were captured and imported into the image processing software (MATLAB), (Aims and Objectives Section 1.1, Objective 3-d). The tress images were transformed from sRGB to CIELAB colour space. The L^* and C^* values of the image were averaged out vertically across the image length and were plotted in a chart (the image capture process is explained in section 3.9). Figure 4-1 shows the average L^* values of the three virgin hair tresses (Blonde, European Brown and Oriental). It can be noted that the area under the average L^* values curve is high in blonde hair tresses when compared with European brown and oriental L^* curves, this is because less of the light is absorbed by the light-coloured hair tresses.

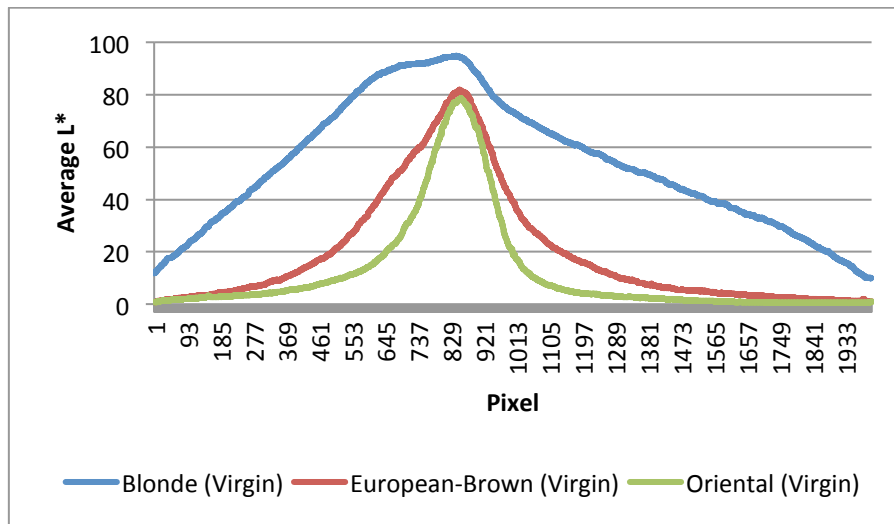


Figure 4-1 Average L* values of virgin Blonde, virgin European-Brown and virgin Oriental hair tresses

It was established that the average L* values of the tress image are higher in light-coloured hair tresses and decreases with an increase in the pigmentation of the hair. This led to the next question, what impact does the Chroma distribution values have on the image-based-gloss evaluation system? The C* distribution values were averaged and plotted alongside the averaged L* distribution values. Other than Gao (Gao *et al.* 2010), no published hair gloss evaluation models have used Chroma as a parameter in their models to quantify gloss. Gao mentioned the subject, stating that if the distance between the shine peak (taken from L* curve) and Chroma peak increases the tress is said to be dull when compared with the tress which has less distance between the two peaks. Figures 4-2 to 4-4 show the averaged L* and C* values curves of the virgin hair tresses (Blonde, European-Brown and Oriental). It should be noted that these values show that the average Chroma values curve does not drop to zero at the L* maximum value (Aims and Objectives Section 1.1, Objectives 5-a and 5-b). This finding, by the author, is very important as it suggests that the shine band, on the hair tress, consists of mixture of both C* and L* values. This may suggest that human hair gloss perception is dependent on both L* and C* values at the gloss band.

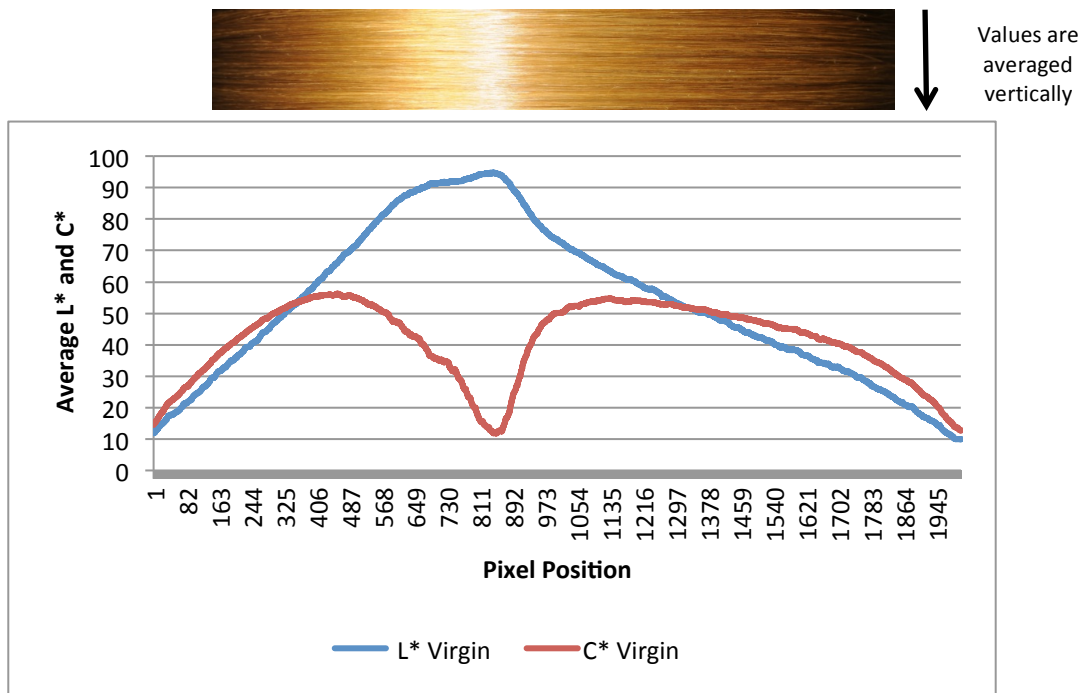


Figure 4-2 Average L* and C* curve of the Virgin Blonde hair tress image

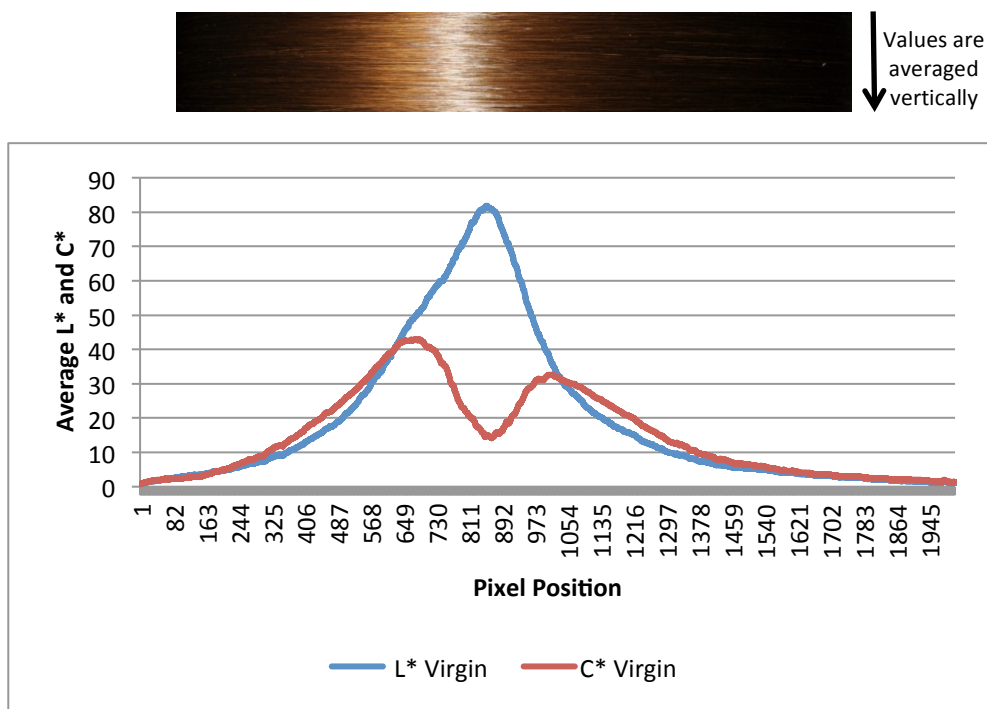


Figure 4-3 Average L* and C* curve of the Virgin European Brown hair tress image

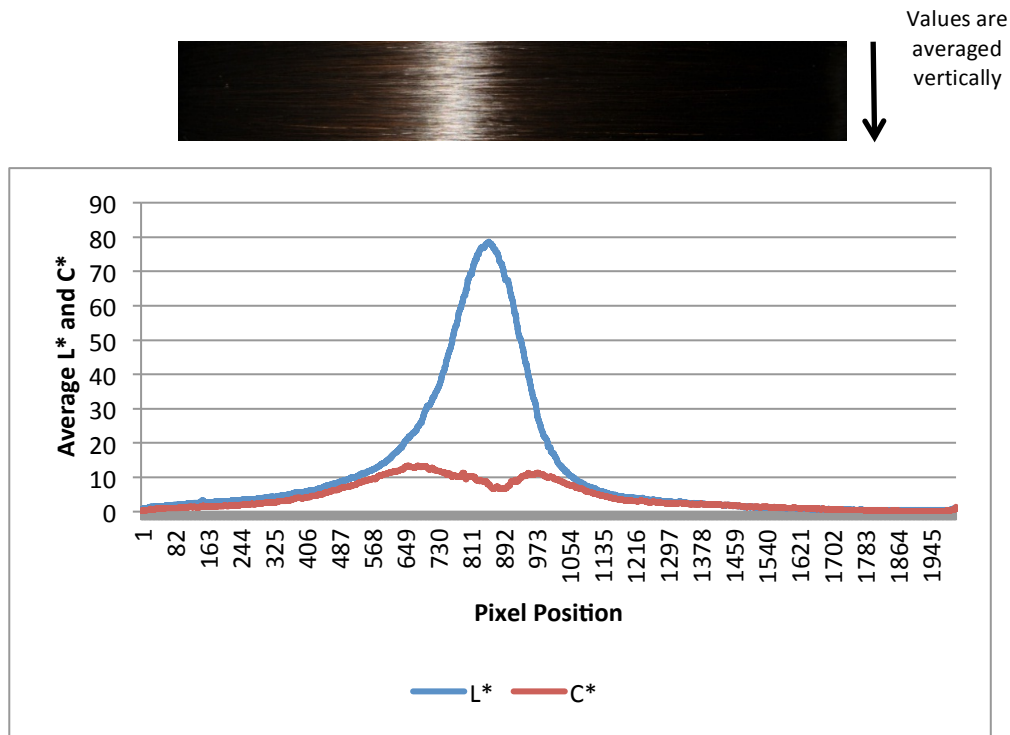


Figure 4-4 Average L* and C* curve of the Virgin Oriental hair tress image

4.3 Effect of different levels of Shine on the Lightness (L*) and Chroma (C*) distributions of Blonde, European-Brown and Oriental hair tress images.

As suggested in Section 4.2 the shine-band on the hair tress consists of mixture of Chroma and lightness properties. Thus, it would be interesting to determine how each of the average L* value- and C* value- curves of the images of same tress but of different shine levels will appear. Several tresses treated with different commercial products were prepared, out of which four levels of shine were selected (tress with no treatment (i.e. virgin), tress washed with SLES, tress treated with wax and tress sprayed with shine spray). Tress preparation is explained in Section 3.3.2. Images of each tress untreated and treated with the different commercial products were captured and analysed. L* and C* values of each image were averaged and are plotted in Figure 4-5, Figure 4-6, and Figure 4-7. Figures 4-5 to 4-7 show the average L* and C* value curves of the Blonde, European-Brown and Oriental hair tresses treated with different products.

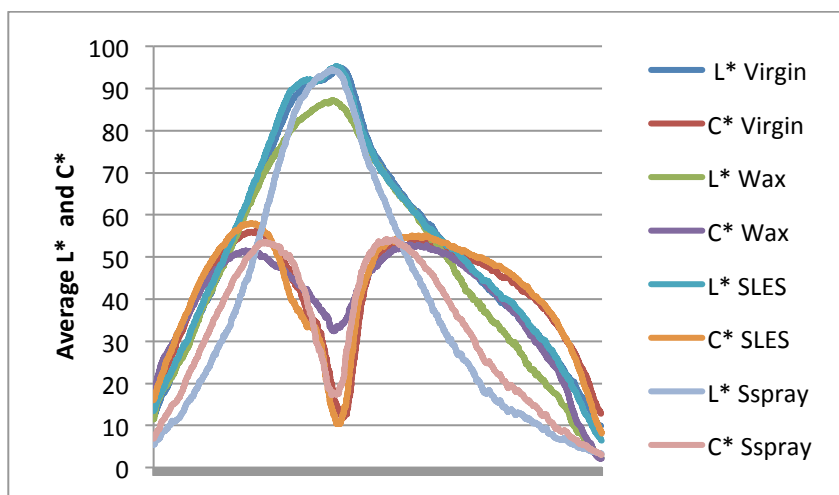


Figure 4-5 Average L* and C* distribution curves of virgin Blonde tress, Blonde tress treated with wax, Blonde tress treated with shine-spray and Blonde tress treated with SLES.

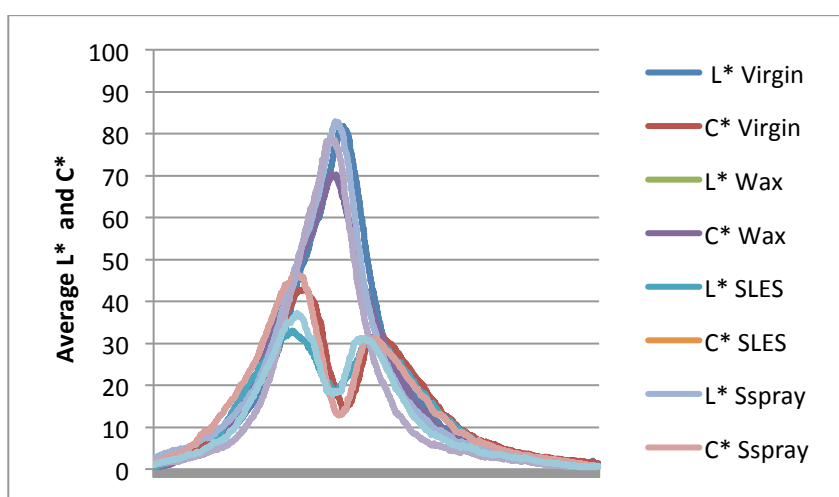


Figure 4-6 Average L* and C* curves of virgin European-Brown tress, European-Brown tress treated with wax, European-Brown tress treated with shine-spray and European-Brown tress treated with SLES

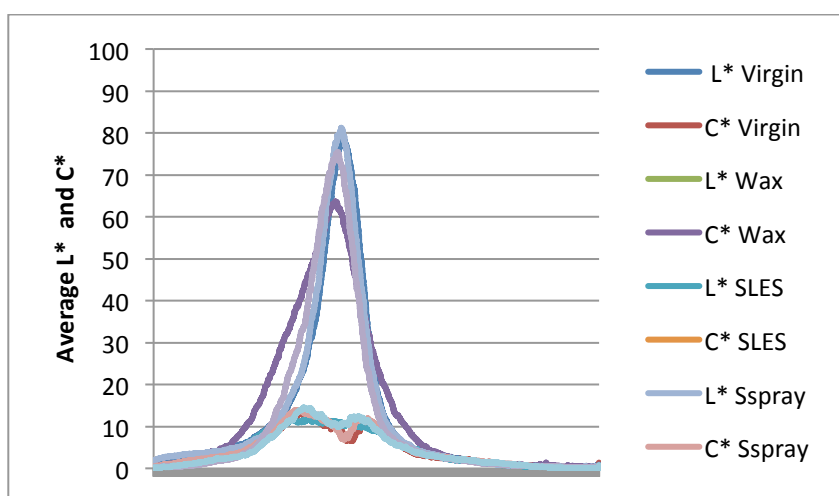


Figure 4-7 Average L* and C* curves of virgin Oriental tress, Oriental tress treated with wax, Oriental tress treated with shine-spray and Oriental tress treated with SLES

It should be noted that as the tress become duller (less shiny) the Chroma value, C^* , at the peak of the averaged L^* values curve increases. This suggests that the shine of the human hair tress is dependent on both the Lightness and the Chroma of the tress. Table 4-1 shows the maximum values of the L^* curves of the virgin (tress with no treatment) and wax treated tresses. As the tress become duller the Chroma value under the peak of L^* curve increases. For the blonde hair tresses the Chroma value increases to approximately 32 from 11 and the European-Brown (EB) hair tresses the Chroma value under the peak increases from approximately 15 to 19. The Oriental hair tresses show an average Chroma value reduction from 11 to 8. The reductions in the Chroma values for the EB and Oriental hair tresses are logical; as the pigmentation increases the absorption of light increases and this results in small increase in the Chroma values in the dull hair tresses. Whereas when the difference between the maximum value of L^* curve and C^* value under the peak of the L^* curve is compared with treated hair a big difference was observed. This confirms that not only lightness is responsible for the shine but also the lightness should be together with Chroma to produce a more complete representation of the shine of the hair tress.

Table 4-1 Average L^* curve's peak value and average C^* value under the peak of the L^* curve and their differences

	Blonde Virgin	Blonde Wax	EB Virgin	EB Wax	Oriental Virgin	Oriental Wax
Average L^* curve's peak value	94.78	87.20	81.89	70.33	78.69	63.71
C^* value under the peak of L^*	11.92	32.49	15.06	19.55	8.03	11.04
Difference	82.86	54.71	66.83	50.78	70.66	52.67

4.4 High Dynamic Range Imaging

As stated previously (Chapter 1 Sections 1.6.3 and 1.6.3.1), High Dynamic Range (HDR) imaging is a relatively new idea when applied to the measurement of gloss. This technique has never been previously published in the literature as a method to evaluate the gloss of human hair tresses. In photography the HDR technique is used to increase

the brightness level and hence contrast level so that images will appear more vibrant but in measuring gloss the goal is entirely different. When images are captured at a higher shutter speed only the brightest elements of the image will be captured. If the object is glossy the gloss band will be visible only on images captured at higher shutter speeds when compared with objects with a matte finish. Figure 4-8, Figure 4-9, Figure 4-10 shows images of hair tresses, treated with different products, captured at different shutter speeds (1 second – 1/200 second).

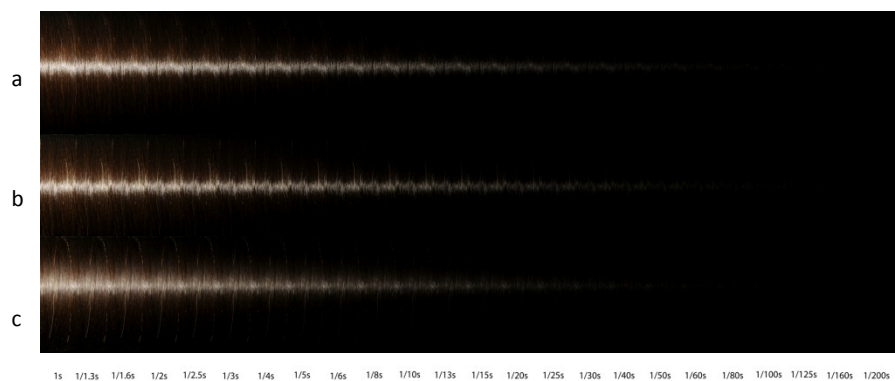


Figure 4-8 Images of Oriental Hair tresses captured at different shutter speeds a) Hair tress treated with shine enhancing product (shine spray - top), b) Virgin Hair tress (middle), c) Hair tress treated with Wax to achieve dull effect (3% Wax-bottom)

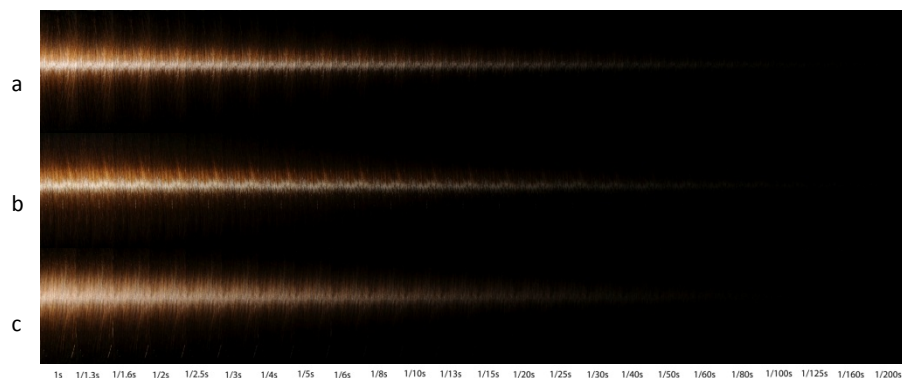


Figure 4-9 Images of European-Brown Hair tresses captured at different shutter speeds a) Hair tress treated with shine enhancing product (shine spray - top), b) Virgin Hair tress (middle), c) Hair tress treated with Wax to achieve dull effect (3% Wax - bottom)

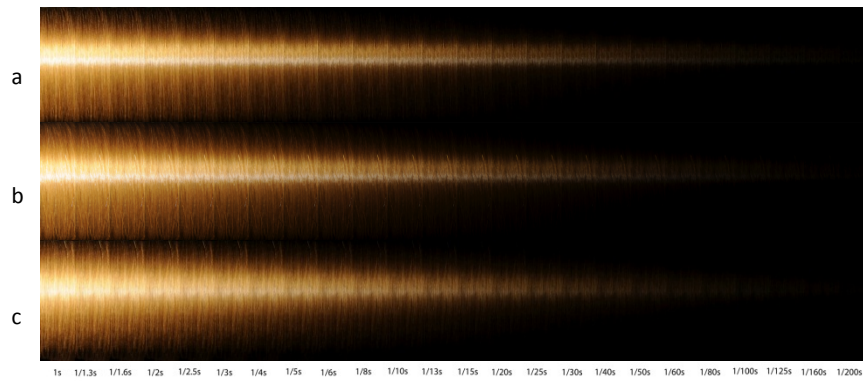


Figure 4-10 Images of Blonde Hair tresses captured at different shutter speeds a) Hair tress treated with shine enhancing product (shine spray - top), b) Virgin Hair tress (middle), c) Hair tress treated with Wax to achieve dull effect (3% Wax - bottom)

4.4.1 Effect of different shine levels of hair tresses on the averaged L^* area of a hair tress at higher shutter speeds

Images of hair tresses (treated with different products) were captured at different shutter speeds. Once the sRGB images were converted into the CIELAB colour space, the average area under the L^* curve showed a predictable pattern. The L^* curve area decreases with an increase in shutter speed but when the L^* curve areas were compared with tresses treated with shine changing products (Wax, Shine-spray) the difference between them remained approximately the same at all shutter speeds. Figure 4-11, Figure 4-12 and Figure 4-13 shows the area under the average L^* values' curve of tresses treated with SLES, Wax, Shine-Spray at different shutter speeds (to show the trend L^* curve area plots are presented separately with different y-axis, average L^* , values). Similar patterns were observed in the Chroma (C^*) areas, as the difference between the tresses treated with shine-changing products remains approximately the same with an increase in shutter speed. Figure 4-14, Figure 4-15 and Figure 4-16 shows the area under the average C^* value curves of tresses treated with SLES, Wax, Shine-Spray at different shutter speeds. This information was important in selecting a shutter speed for further analysis of the reflection bands on the hair tresses. Out of 24 different exposure levels examined, images captured at a 1 second shutter speed gave an optimal representation of the hair tresses. The ROC models used to quantify gloss were based on tress images captured at a 1 second shutter speed.

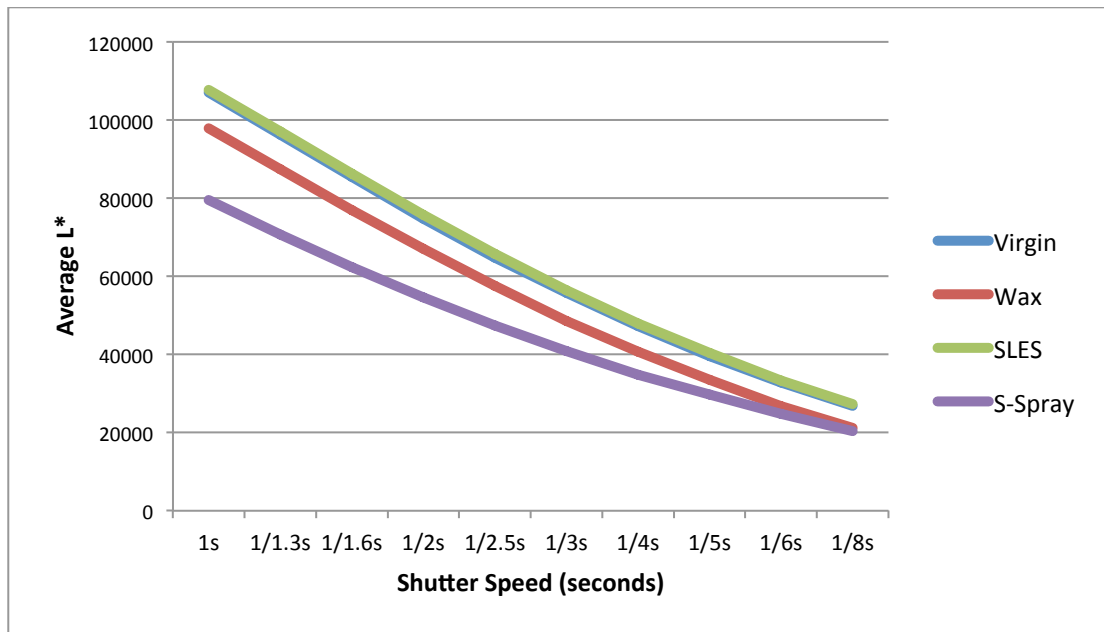


Figure 4-11 Areas under the averaged L* value curves of Blonde hair tresses treated with different products (Virgin, Wax, SLES and Shine-spray) at different shutter speeds.

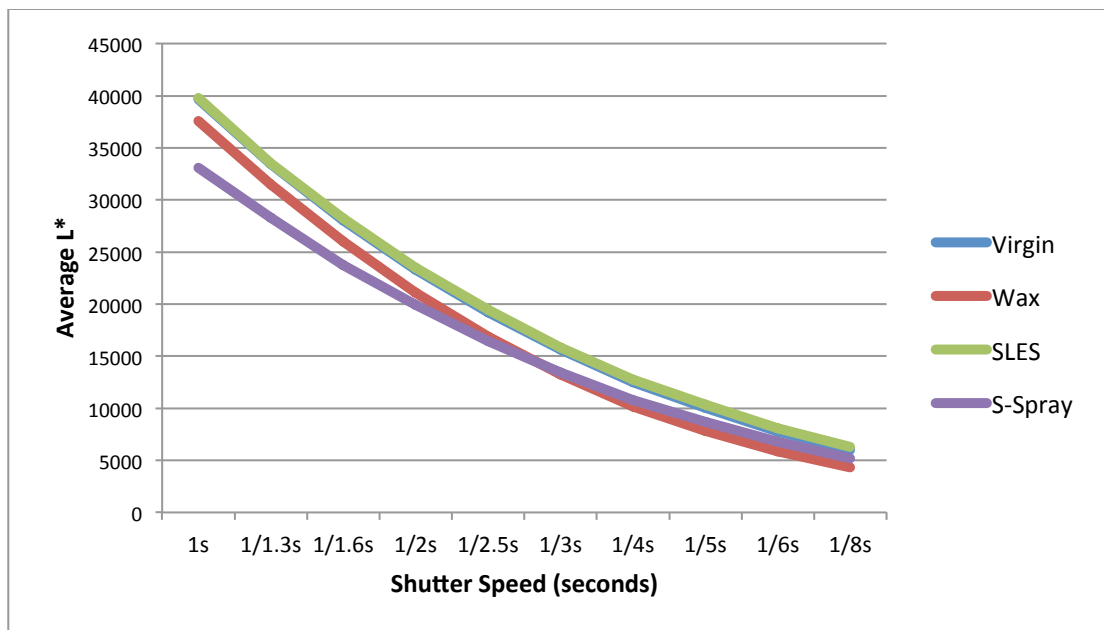


Figure 4-12 Areas under the averaged L* value curves of European-Brown hair tresses treated with different products (Virgin, Wax, SLES and Shine-spray) at different shutter speeds.

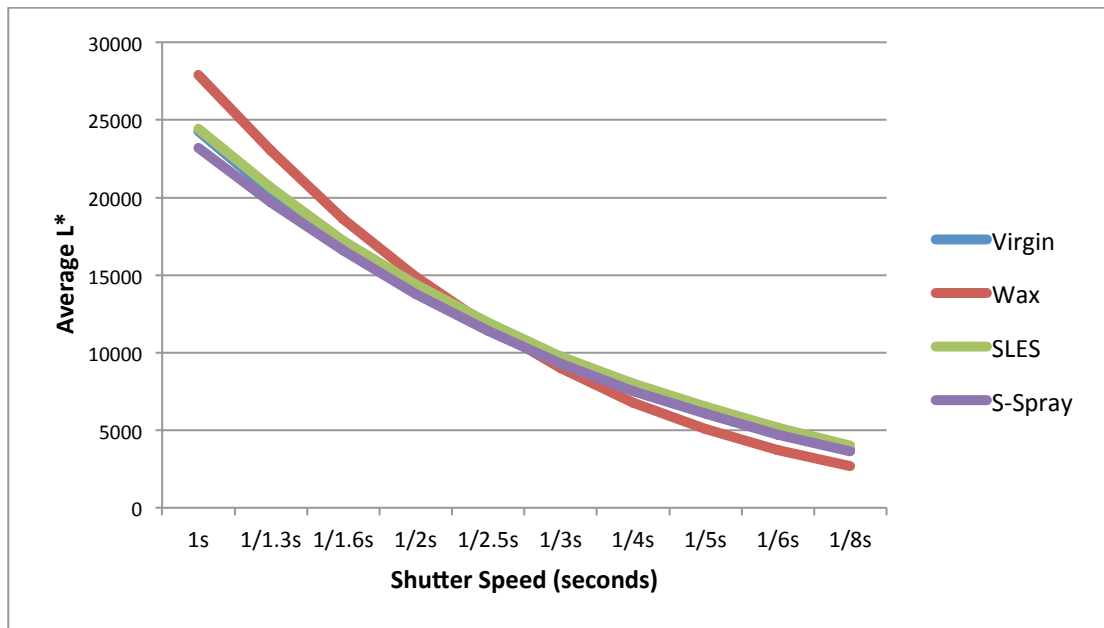


Figure 4-13 Areas under the averaged L* value curves of Oriental hair tresses treated with different products (Virgin, Wax, SLES and Shine-spray) at different shutter speeds.

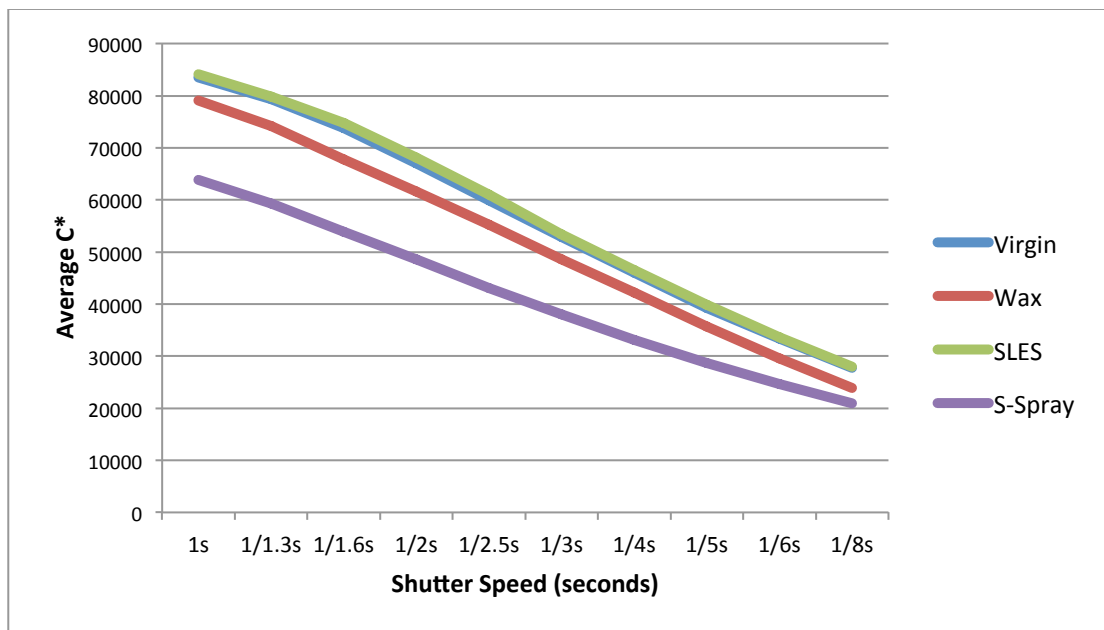


Figure 4-14 Areas under the average C* value curves of Blonde hair tresses treated with different products (Virgin, Wax, SLES and Shine-spray) at different shutter speeds.

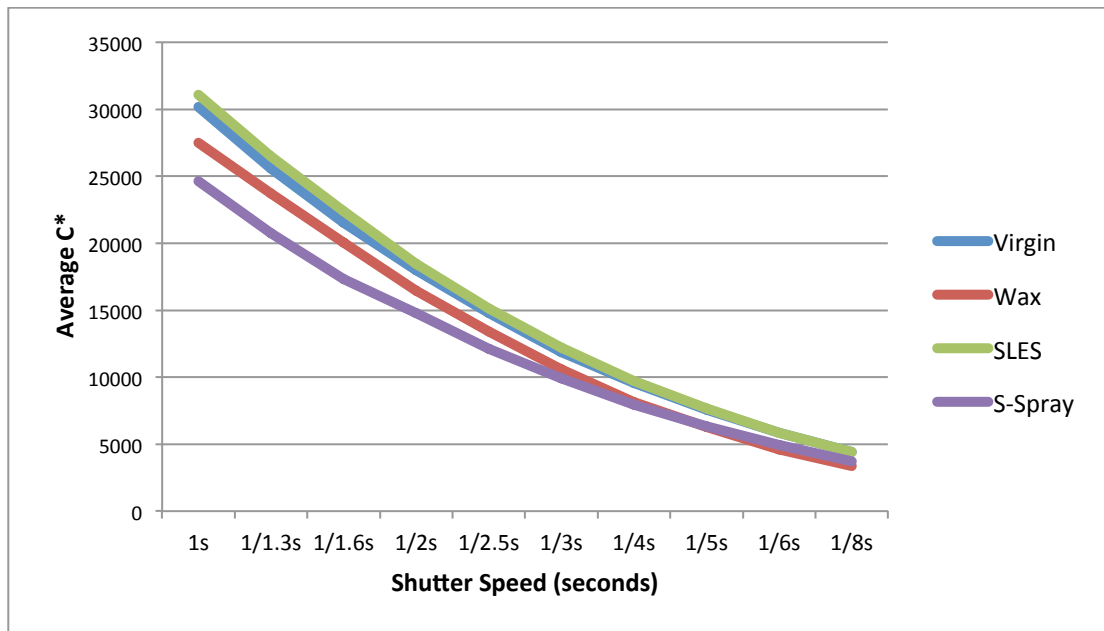


Figure 4-15 Areas under the average C* value curves of European-Brown hair tresses treated with different products (Virgin, Wax, SLES and Shine-spray) at different shutter speeds.

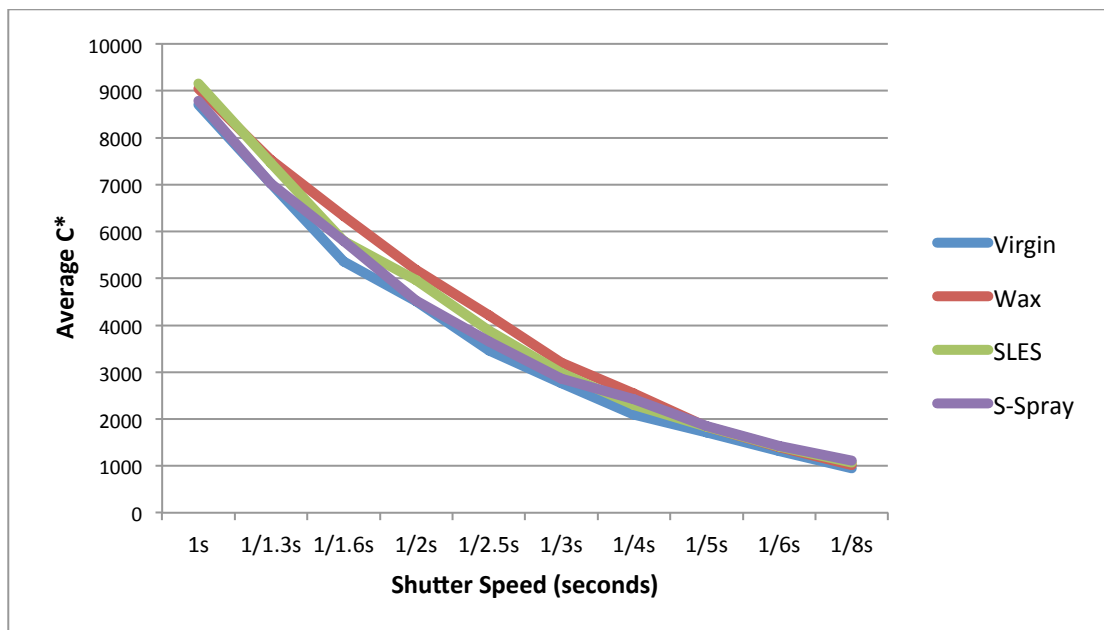


Figure 4-16 Areas under the average C* value curves of Oriental hair tresses treated with different products (Virgin, Wax, SLES and Shine-spray) at different shutter speeds.

4.5 Understanding the properties of Human Hair Tress reflection bands

Most conventional gloss evaluation models are based on Stamm's three component-model, where light interacts with a human hair fibre (or hair tress) its reflection can be broken into three types, shine (the brightest part of the reflection), Chroma (gives the saturation of the colour of the fibre) and diffuse reflection. In the measurement of gloss, Hunter's contrast gloss model is still the conventional method for defining the shine of human hair. Unfortunately the gloss values produced by this model, and its derivatives, do not correlate to the subjective evaluation of a panel of human observers. It can be argued that extracting or separating the shine band and diffuse reflectance from a hair tress varies from one model to another and due to different separation methods large differences in the shine values can be generated. This may be one reason why the shine values do not relate to the subjective evaluations.

4.6 Colour Gradient on hair tresses

During this research it was noticed that the Chroma band (coloured part of the reflection) is not uniform and it changes from bright to dark producing a colour gradient, especially in light colour tresses. This was particularly noticeable for the blonde tresses. Figure 4-17, Figure 4-18, and Figure 4-19 shows different colours in the Chroma band of each type of hair tress. Using this information the Chroma band can be segmented into two main sections, one section representing the light or bright colour of the hair tress mixed with the specular component of the illuminant (C_s - Chroma Specular) and the second section representing the colour of the hair tress mixed with the diffuse component of the illuminant (C_d - Chroma Diffuse).

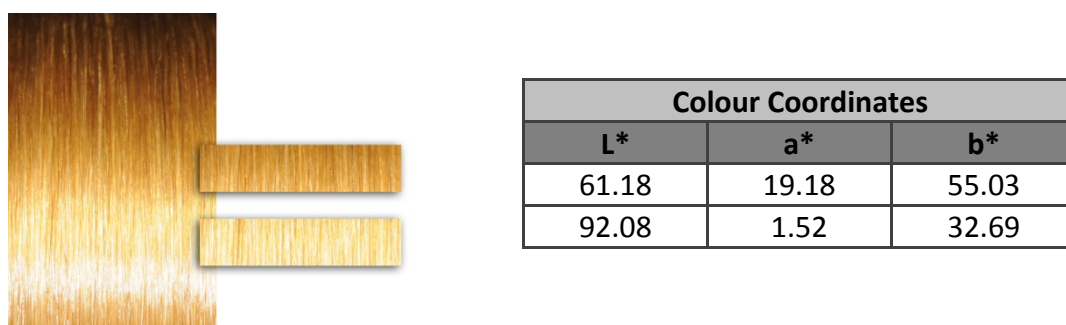


Figure 4-17 The Chroma band of the SLES-washed Blonde hair tress (top half), segmented into two parts and the CIE $L^*a^*b^*$ colour coordinates are adjacent to each part.



Colour Coordinates		
L*	a*	b*
15.49	12.68	16.37
53.11	22.69	40.71

Figure 4-18 The Chroma band of the SLES-washed European -Brown hair tress (top half), segmented into two parts and CIE L*a*b* colour coordinates are presented adjacent to each part.



Colour Coordinates		
L*	a*	b*
7.23	5.38	4.74
17.62	8.03	11.24

Figure 4-19 The Chroma band of the SLES-washed Oriental hair tress (top half), segmented into two parts and CIE L*a*b* colour coordinates are presented adjacent to each part.

4.7 The Chroma-Specular effect

When light and dark regions are perceived adjacent to each other the boundary between the two phases (light and dark) appears to have different lightness gradients. This phenomenon was reported by Ernst Mach, and the effect is hence known as a Mach band (Ratliff 1984). When an observer looks at the hair tress illuminated by a spot source they perceive a similar Mach band-type effect between the Shine and the Chroma band of the hair tress. Section 4.6 (Colour Gradient) explains the colour gradient detected on the image of the hair tress. Using this information width, intensity, and background on which the shine band is perceived are not the only features, as it is believed in gloss evaluation models (Lefaudeux *et al.* 2008), to make an object appear shiny. There is a fourth component, which is equally important in glossy appearance. It is the “blurred” (light colour or desaturated region) region of the light just above and below the shine band. In digital photography to make an object glow, blur is added just above and below the shine, one example is the light-sabres from the movie Star-Wars. Figure 4-20 shows two images; these both have the same background colour and the

same white intensity but slight blur has been added to one image, on each side of the shine.

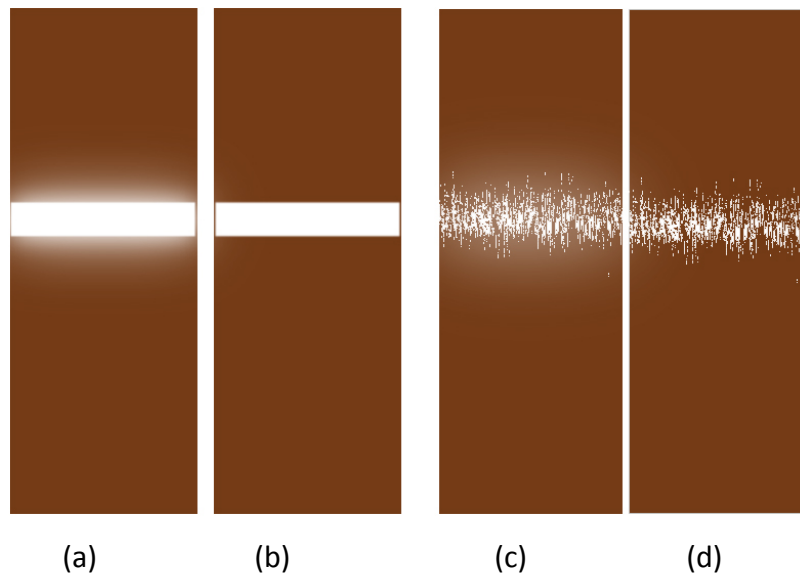


Figure 4-20 Recreation of the Chroma-Specular effect. (a) Shows blur effect on each side of the white band, (b) no blur effect, (c) shine band, as it appears on the hair tress, overlaid on a plain colour background with added blur on each side (d) shine-band without blur.

4.8 Separating reflection bands

It is easy to identify the reflection bands as they appear on the hair tress but separating them is not as simple as detecting them. This is the reason why, to separate reflection bands researchers have used different techniques, which include, polarizers, measuring reflectance at a certain angle (angle of reflection) and curve fitting (explained in Section 2.15.2). Polarizers remain the most popular segmentation technique. The problem with using polarizers is that they reduce the amount of the light. Our goal was to separate the reflection bands in a diffuse environment, which would replicate more closely a normal observer's viewing conditions. The decompositions of the reflection bands were performed using automated selection functions and not fits.

4.9 Separating the shine-band from the hair tress image

Initially, to separate the shine bands a manual selection of the shine area was performed. An image of a hair tress appeared on the screen and the user selected the shine area manually. Once the selection had been made the MATLAB code automatically

cropped the area and ran a series of routines, which resulted in separation of the shine band from the image of the hair tress. The major problem with manual selection was that the selection may vary from person to person; even a slight variation can result in a differing shine value. To overcome this problem an automated selection process was developed (Aims and Objective Section 1.1, Objective 4-b). Firstly the brightest part of the image was identified; this was achieved by converting the sRGB image in to CIELAB values. The transformation between colour spaces was implemented using the MATLAB functions **'makecform'** and **'applycform'** and the specified transform was **'srgb2lab'**. This resulted in three planes of MxN metrics of the image. The first plane represented L* (lightness), the second a* (red-blue) and third b*(yellow-green). To select the brightest part of the image, the L* array was averaged using the MATLAB **'mean'** function. This resulted in a one-dimensional array of lightness, which represented an average profile of Lightness Intensity values (L*) along the tress image. The average L* value array was plotted and the location of the maximum value of the array was identified. The maximum value of the curve was assumed to be the brightest point of the image. Figure 4-21 shows a typical L* curve of a European brown human hair tress, the maximum value of the L* corresponds to the brightest part of the hair tress.

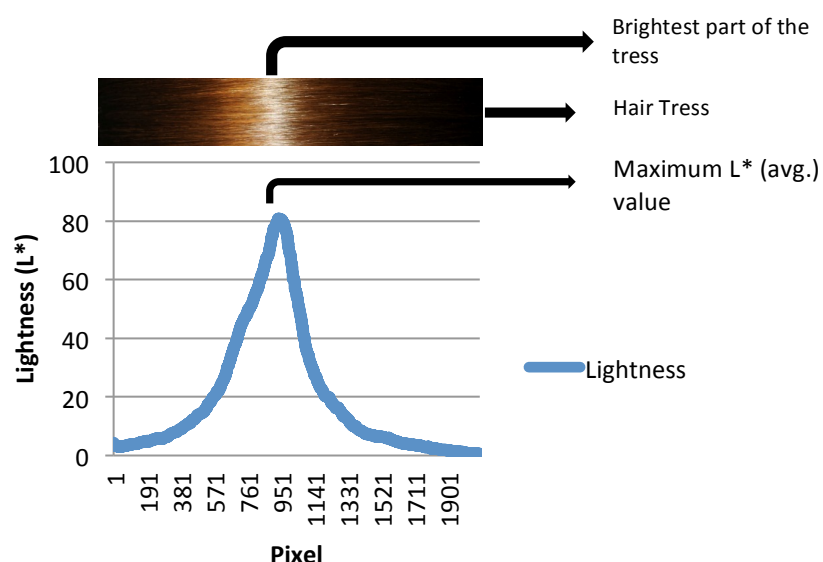


Figure 4-21 Typical L* curve of an European-Brown Human hair tress. The maximum of the averaged L* profile values corresponds to the brightest part of the human hair tress.

With the brightest point identified, different sized selection areas were trialled in order to achieve an optimum selection. In manual selections the size of the selection rectangle ranged from 190 to 218 pixels. It was determined that a selection area having a height of 200 pixels and width the same as the tress width gave optimal separation results. The MATLAB **'imrect'** function was used to select the shine area. The selection area was then cropped using the **'imcrop'** function and converted into CIE L*C*h colour space. Chroma (C*) was calculated using the following MATLAB command:

$$>> C = \text{sqrt}((a.^2) + (b.^2));$$

Once both the L* and C* arrays of the selected area were calculated, MATLAB code was written to create two separate arrays, for each of L* and C*. These arrays contained values greater than zero of L* and C*. L* and C* values of the selected area were then averaged horizontally and a frequency histogram plotted. The most frequently occurring values (MFV) of the L* and C* mean profile distributions were selected (As stated in Aims and Objectives Section 1.1. Objective 6-d). Figure 4-22 shows the cropped selected area and histograms of the L* and C* values of a European Brown hair tress. The MFV of the L* and C* profiles of the shine area were the limits used to separate the shine-band from the hair tress image.

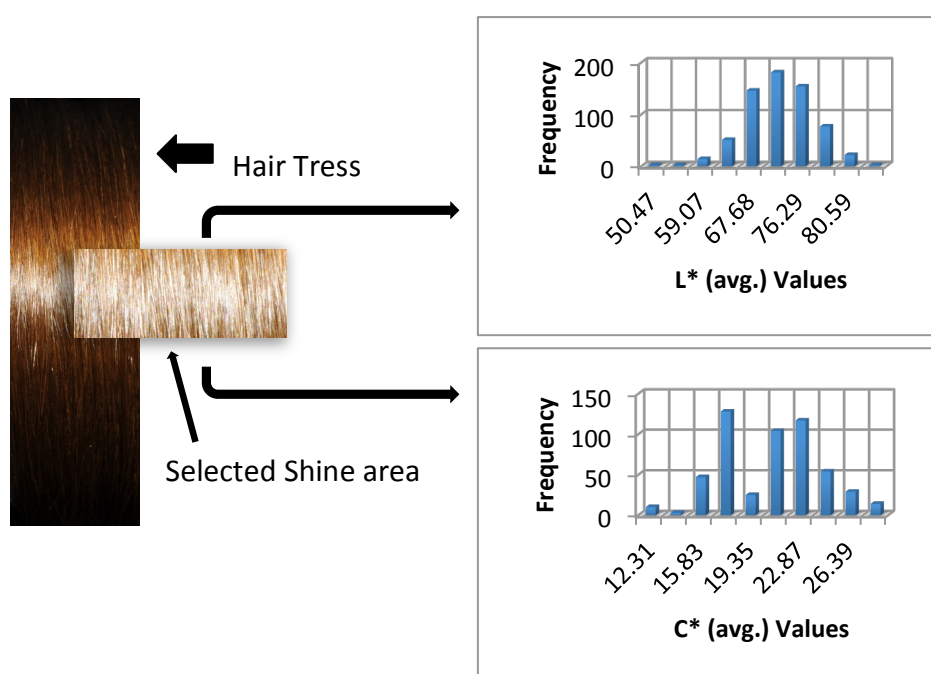


Figure 4-22 The shine area was selected and cropped. The frequency of L* and C* values of the area are plotted in the histogram (this sets the limits in order to separate the shine band from the image).

With the limits selected (for L^* and C^*), MATLAB code was written to create a 3-Dimensional Image array containing only those values which were greater or equal-to the MFV of L^* and less than or equal-to the MFV of C^* of the original image (transformed from 'sRGB' to 'CIE LCh' colour space). This array represents the shine-band. To check the result a mask was overlaid on the original image, this provided confirmation that the shine-band has been separated from the image accurately (Aims and Objectives Section 1.1, Objective 4-c). Figure 4-23 shows separated shine-bands of a European brown (a, b, c), Blonde (d, e, f) and Oriental (g, h, i) hair tresses.

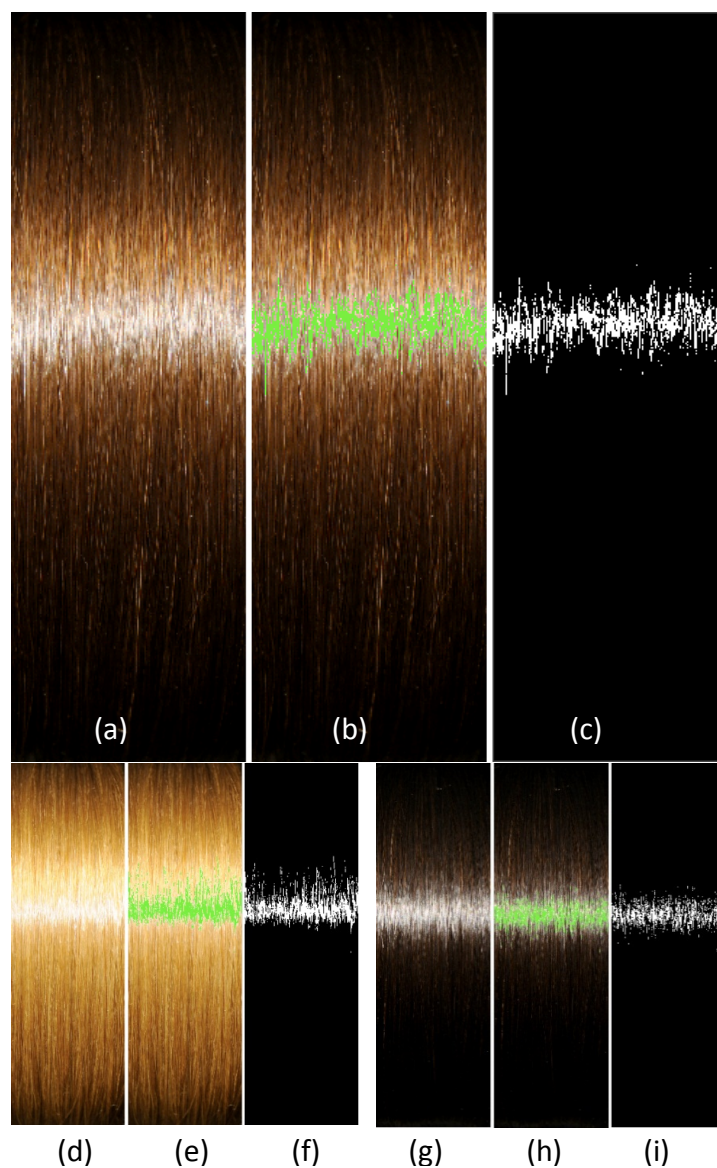


Figure 4-23 Shine-band separation from images of European-Brown, Blonde and Oriental Hair tresses
 (a), (d), (g) Original images, (b), (e), (h) Shine-band separated and overlay on the original image
 (confirmation of separation), (c), (f), (i) Separated Shine-band.

4.10 Separating Chroma bands

As explained in Section 4.6 (Colour Gradients), the Chroma has been divided into two segments C_s (Chroma-Specular), which is just above and below the shine band, and C_d (Chroma-Diffuse).

4.10.1 Separating the Chroma Specular Band from the Hair Tress Images

The C_s areas are located just above and just below the shine band. Once the location of the shine band has been identified (as explained in Section 4.9, Separating the Shine Band), to separate the C_s band the MFV of L^* and the MFV of C^* in the Chroma-Specular region were required. To obtain the most frequent values (MFVs) of L^* and C^* and thus separating the Chroma-Specular band, two approaches were used, one for light coloured hair tresses (e.g. Blonde) and one for dark colour hair tresses (e.g. Oriental and European Brown). For the light colour hair tresses the area under the shine band was selected, because in light colour hair tresses there is chance of backscatter reflection that might produce a second shine-band above the first one. Selecting the area above the shine band can reduce the sensitivity of the selection. For dark coloured hair tresses the area above the shine-band was selected. As in dark colour hair tresses the chances of a second reflection-specular is reduced, due to greater light absorption by the hair fibre. The selected cropped area of the tress image was then converted from sRGB to CIE L^*C^*h colour space. To separate the C_s , the MFV of the L^* and C^* limits were obtained (Section 4.9 Separating the Shine band). Figure 4-24 shows the histograms of the L^* and C^* values of the Chroma area.

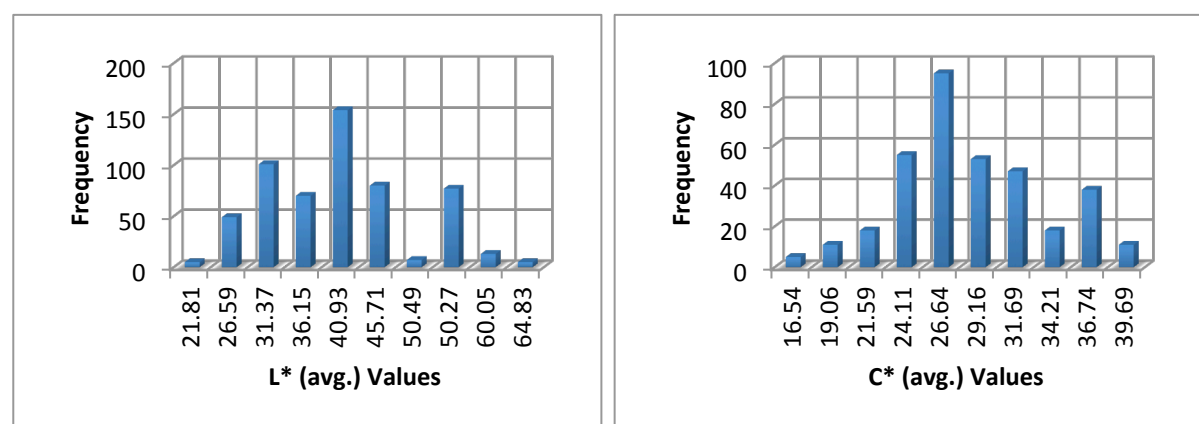


Figure 4-24 Histograms of the L^* and C^* values in the Chroma-Specular area

After obtaining the MFV of L^* and C^* , an array was created which contained only those values which were above & equal-to MFV of L^* and MFV of C^* in the selected Chroma area. To check the result a mask was overlaid on the original image Figure 4-25 shows the separated Chroma-specular (C_s) bands of European brown (a, b, c), Blonde (d, e, f) and Oriental (g, h, i) hair tresses.

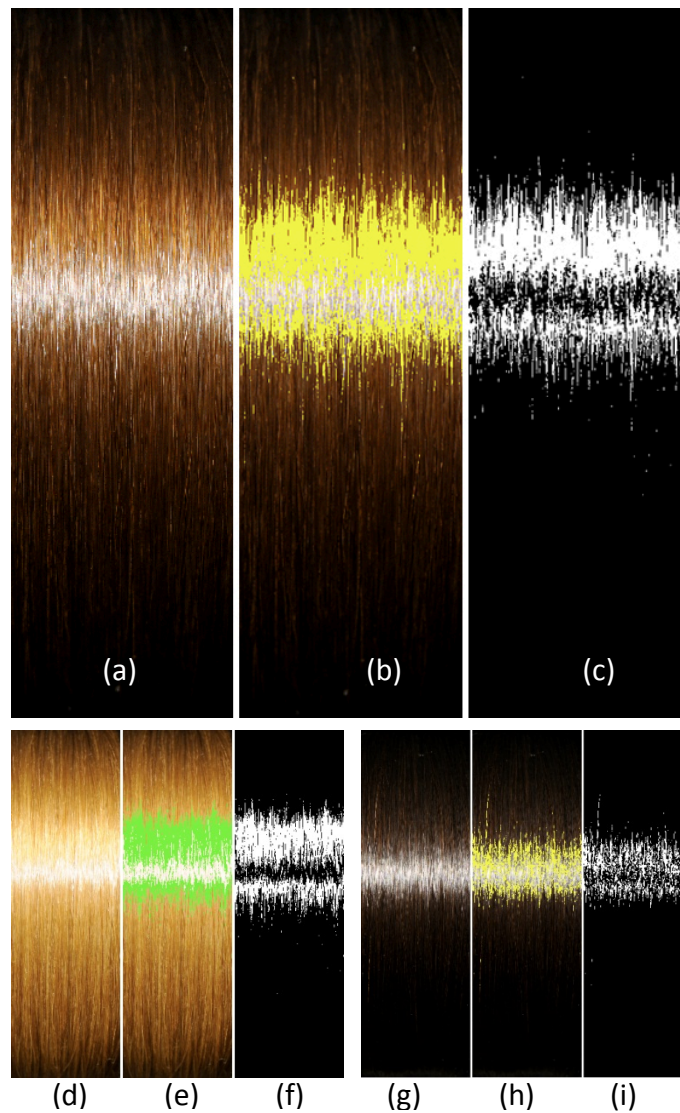


Figure 4-25 Chroma-Specular separation from images of European-Brown, Blonde and Oriental hair tresses. (a), (d), (g) Original hair tress images, (b), (e), (h) C_s separated and overlaid onto the original image (confirmation of separation), (c), (f), (i) Separated Chroma-Specular, C_s .

4.10.2 Separating the Chroma Diffuse Bands from the Hair Tress Images

To separate the Chroma-Diffuse band, C_d , from the original image of the hair tress, an array was created containing the inverse limits of the C_s band, which contains only those values which were below and equal-to the MFV of L^* of the selected C_s area. To check the result a mask was overlaid on the original image. Figure 4-26 shows the separated third component of the reflection of European brown (a, b, c), Blonde (d, e, f) and Oriental (g, h, i) hair tresses.

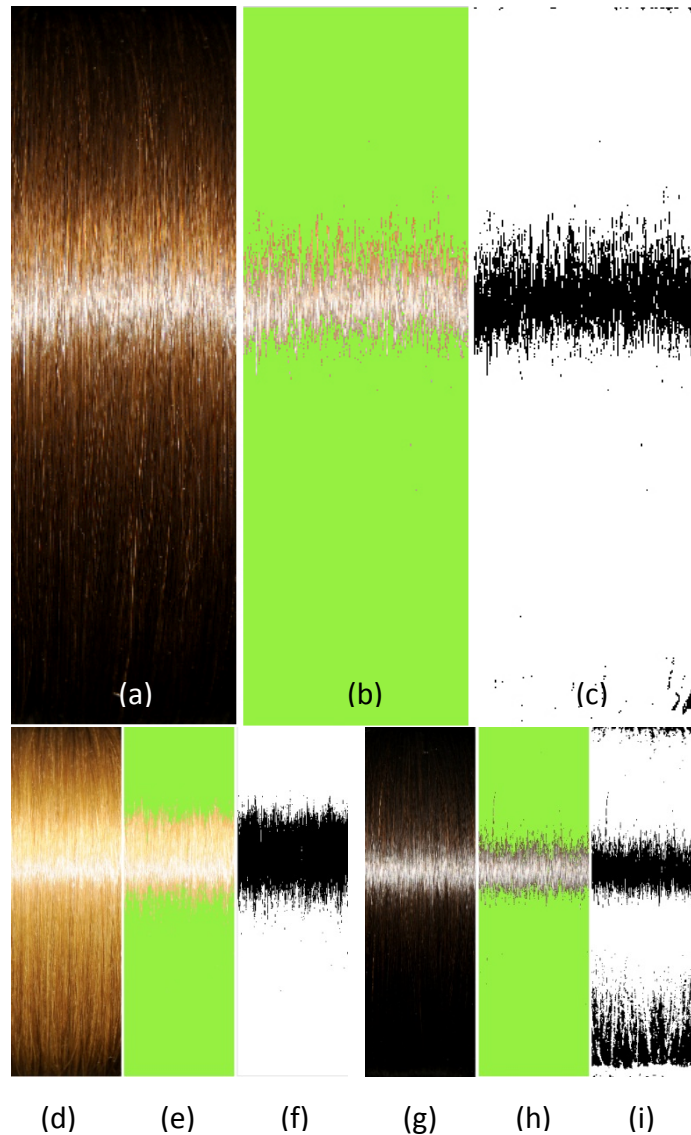


Figure 4-26 Chroma-Diffuse separation from images of European-Brown, Blonde and Oriental hair tresses. (a), (d), (g) Original images, (b), (e), (h) C_d separated and overlaid onto the original image (confirmation of separation), (c), (f), (i) Separated Chroma-Diffuse, C_d .

4.11 Plotting each reflection band

Once each of the reflection bands were separated the values for L^* and C^* of each band were averaged horizontally across the image and plotted in a chart. Figure 4-27 shows plots of each band of European Brown, Oriental and Blonde hair tresses. Area under the curves was calculated to quantify gloss (As stated in Aims and Objectives Section 1.1, Objective 6-b).

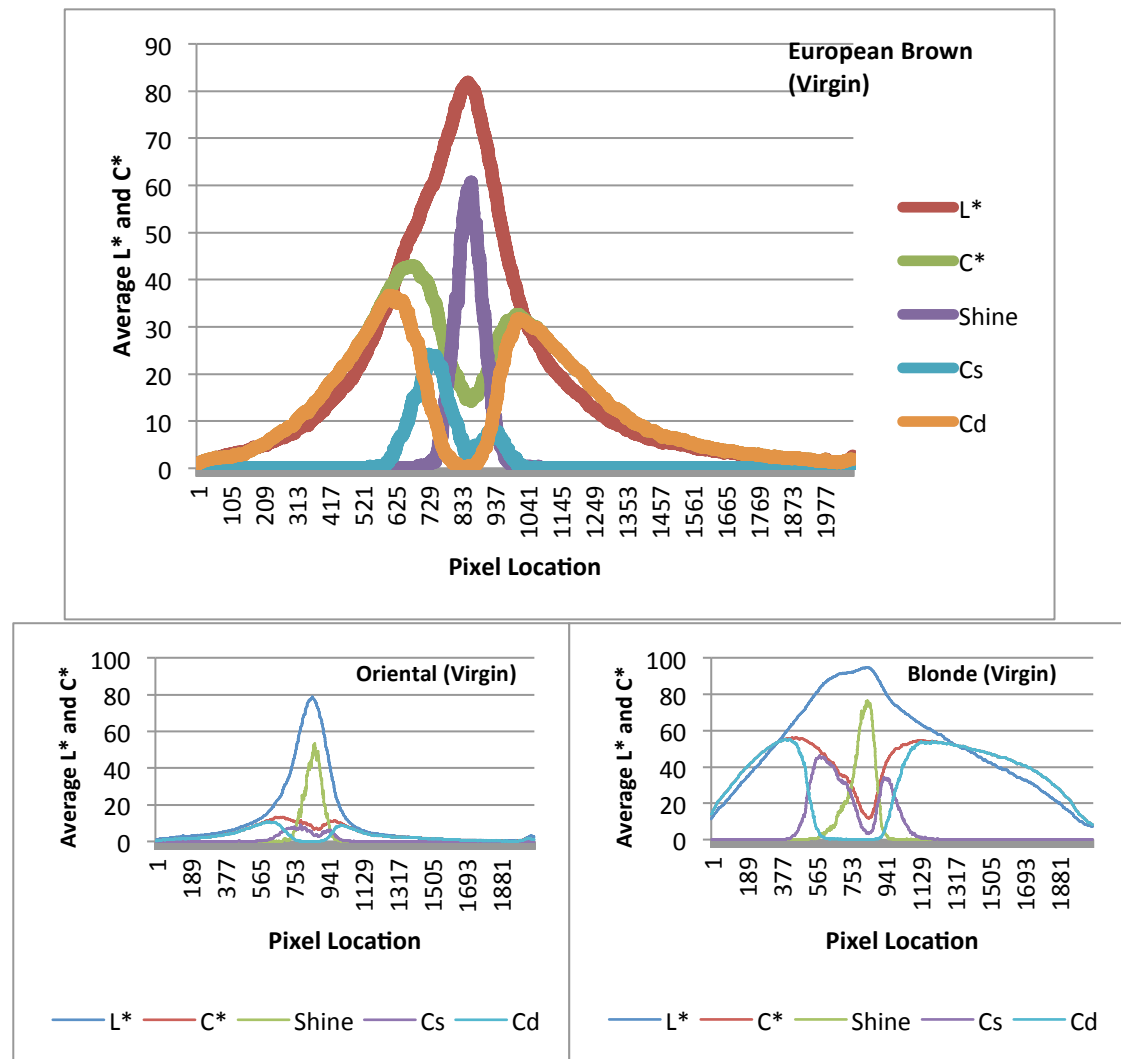


Figure 4-27 European Brown, Oriental and Blonde virgin hair tresses Lightness (L^*) and Chroma (C^*) profiles, Shine band (shine), Chroma-Specular (C_s) and Chroma-Diffuse (C_d) plots

4.12 Effect of different treatments on their reflection bands

When a shine enhancing or reducing product was applied to the tresses, they affected the reflection properties of the tresses. For example, if wax is applied to a tress, the light reflected in the specular direction will reflect less in comparison with the light reflected diffusely and hence the tress appears dull. In this chapter the hair tress reflection bands have been identified and a new method to segment the hair tress images has been introduced. This section provides an analysis of how each band changes when different products are applied to the tresses.

To create different levels of shine three products were selected to be applied to the tresses. Wax was used to make the tresses dull, whereas tresses washed in SLES had an enhanced shine as compared to the virgin hair tress. Shine spray was applied to tresses to determine how much the shine deviates from that exhibited by the virgin hair tresses. Details of the products and application procedure are described in the sample preparation section (Section 3.3). Four tresses of each hair type (Blonde, European brown and Oriental) were prepared and the data captured was averaged.

4.12.1 Effect of different treatments on the shine area of the tress

The shine area of the tresses changes with different product applications, Figure 4-28 shows the average shine areas (area under the shine curve, explained in the section 4.9 Separating the shine-band from the hair tress) of the blonde, European brown and oriental tresses. Shine-area reduces by approximately 25% when the wax is applied to the tress. Increase in shine-area was noted in Blonde and Oriental SLES-washed hair tresses whereas shine-area decreases by 0.8% in SLES washed European brown hair tress. It was interesting to note that SLES washed European brown hair tresses appear shinier if not the same as the virgin hair tresses, this lead to the conclusion that shine is not the only factor involved in quantifying the gloss of a human hair tress. Reduction in shine-area was also observed, when tresses sprayed with shine-spray were compared with virgin tresses.

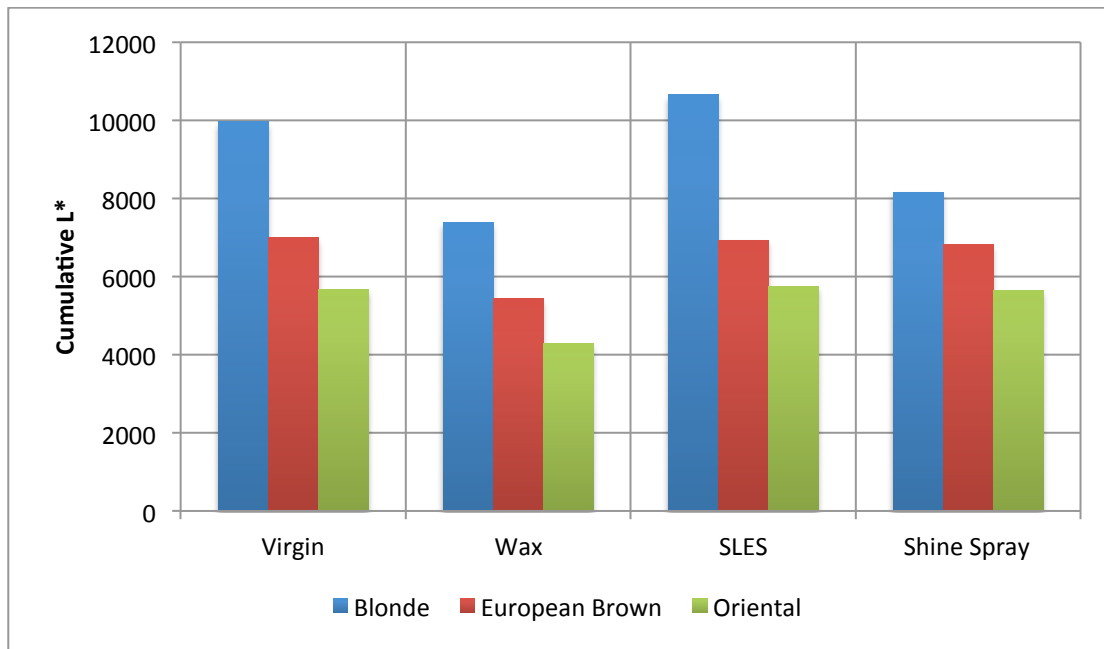


Figure 4-28 Average Shine-areas (cumulative L*) of the Blonde, European Brown and Oriental tresses treated with Wax, SLES and Shine-spray

4.12.2 Effect of different treatments on the Chroma Specular (C_s) Region

As the shine-area increases the common understanding is that the tress will appear shinier but that is not true in all cases. It was noted that the shine-area of a European brown hair tress washed with SLES decreased by 0.8% when compared with the virgin tress, but the tress still appeared shinier than the virgin hair tress when rated by human observers (explained in Participants' choice in the psychophysical Section 5.4). The reduction of the L* area does not correlate with the appearance of the tress; wax treated tresses appear perceptibly duller than the virgin hair tresses but the shine-area was reduced by only 25%. The identification of another reflection band (C_s) on a hair tress (a sub division of Chroma band, discussed in Section 4.10 Separating Chroma bands) appears to help in terms of an increase in the sensitivity of the shine model (in quantifying the gloss of human hair tress). Figure 4-29 and Figure 4-30 show the Chroma-Specular areas of the tresses treated with wax, SLES and Shine Spray (due to the large values produced by Blonde and European brown hair tresses, the C_s areas of Oriental hair tresses are plotted in a separate graph to show the trend). Tresses treated with wax reflected less light in the C_s area, a 42% reduction was calculated for the blonde hair tress when compared with virgin blonde hair tress. Similarly a 35% reduction

was calculated for European brown tresses with applied wax and an 11% reduction Cs area was calculated for oriental hair tresses.

When European Brown tresses were washed in SLES and the Cs area was compared with the virgin tress Cs area a 9% increase in C_s area was calculated. Comparing the Cs areas of Oriental Virgin tresses with Oriental tresses washed with SLES an 18% increase of area was calculated. A 5% reduction in the Cs area was calculated in the Blonde virgin to Blonde SLES hair tresses. Other than the Oriental tress treated with shine spray, all the other shine spray treated tresses showed a decrease in C_s areas; 19% in Blonde and 6% in European brown.

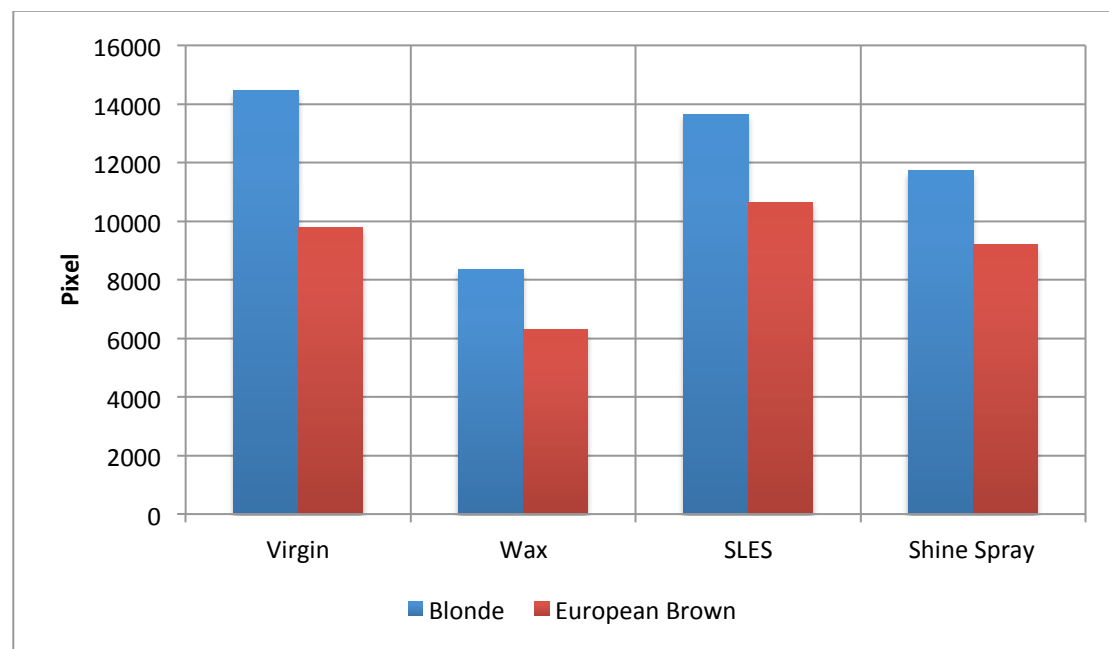


Figure 4-29 Chroma-Specular areas of the Blonde and European Brown hair tresses treated with Wax, SLES and Shine Spray



Figure 4-30 Chroma-Specular area of the Oriental hair tress treated with Wax, SLES and Shine spray.

4.13 Effect of the different treatments on FWHM of the Shine curve

The width of the shine band is another factor that plays an important role in measuring shine; if the band is narrow the object is assumed to appear shinier (Aims and Objective Section 1.1, Objective 6-c). Figure 4-31 shows the full-width-half-maximum (FWHM) of the shine curves of tresses treated with different products (Wax, SLES and Shine-spray). All of the tresses treated with wax showed an increase in the width of the shine curve when they were compared with virgin hair tresses. The Oriental tress showed a 50% increase in shine width, whereas blonde showed an 18% increase and European brown showed a 7% increase in the width.

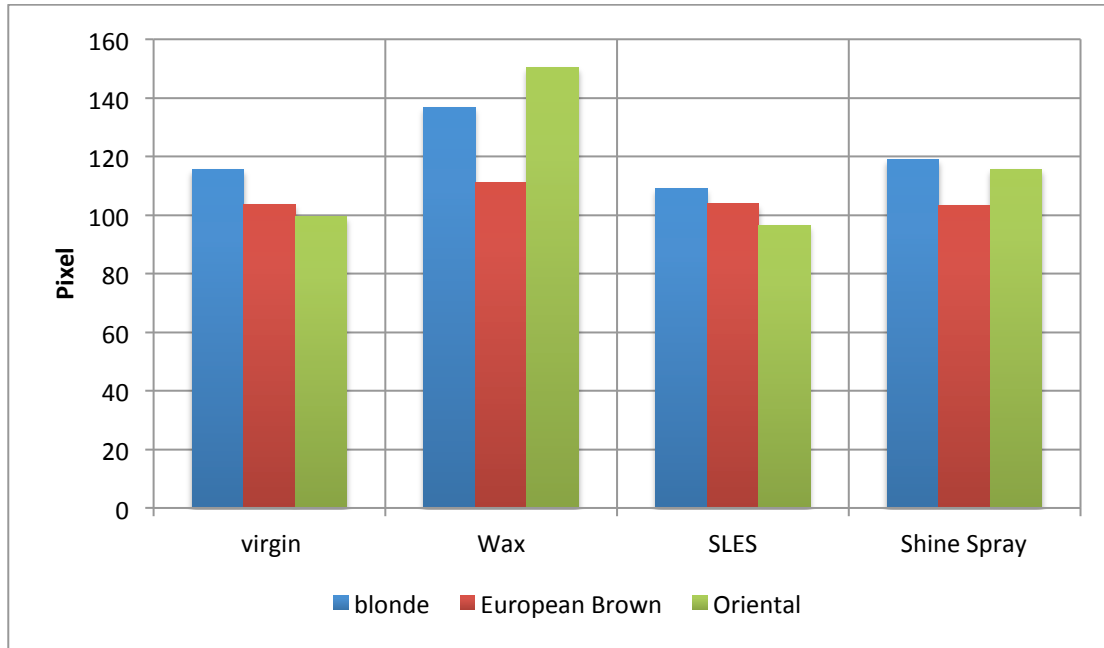


Figure 4-31 FWHM of the shine curve of the tresses treated with Wax, SLES and Shine spray

4.14 Differences in the L* value and C* values

Another factor that appears to play an important role in the sensitivity of the hair gloss model is the difference between the shine value (L* value in the shine area) and Chroma value (C* value in the Chroma-Specular area). As the difference between the shine band and the Cs band increases the contrast between these regions also increases, which causes the tress to appear shinier. When a wax-treated tress is compared with a virgin tress the difference between the shine band values and Chroma band values decreases and this may be a reason why the wax treated hair tress appears dull. The average difference of D_{LC} (difference between the L* and C* values) from virgin tress to wax was -14% for European brown, -6% in Blonde and -23% in Oriental hair tresses. Figure 4-32 shows the differences between the L* and C* values (D_{LC}).

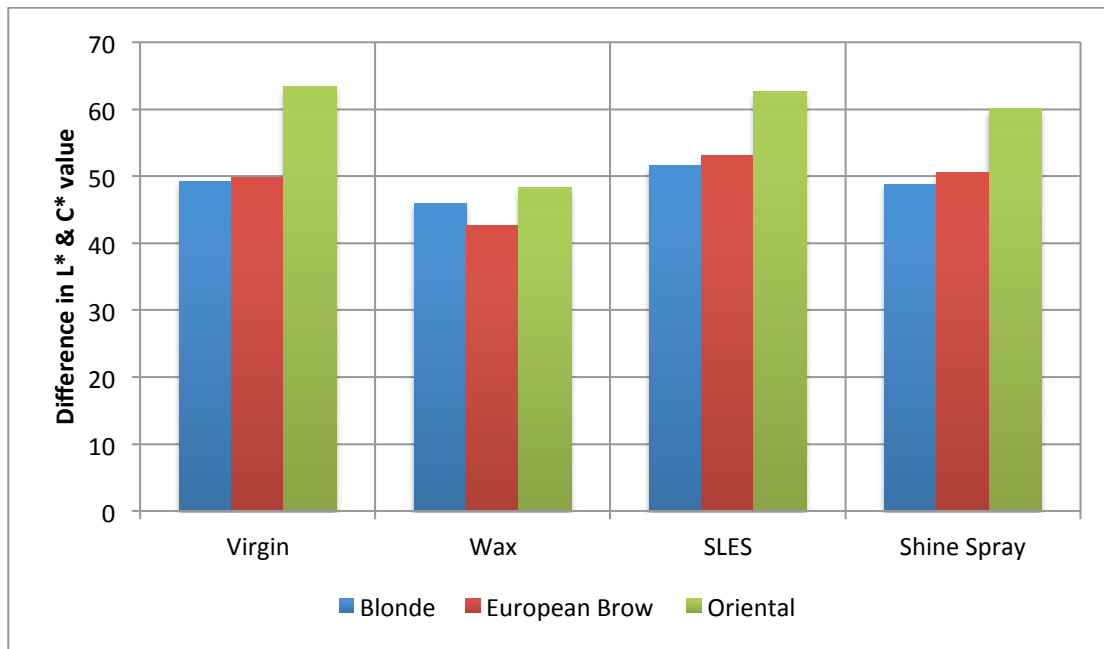


Figure 4-32 Difference between Shine value (L* value in the shine-area) and the Chroma values (C* value in the Chroma-specular-area) of the tresses treated with Wax, SLES and Shine spray

4.15 Effects of different treatments on the contrast ratio (L* area / C* area)

Once the reflection bands are separated, an analysis was performed to determine various ratios produced by the Lightness and Chroma properties of the reflection bands. How much do these ratios change with an increase or decrease in the shine of the tresses? The contrast ratio between the shine band and the background colour of the tress can be obtained by measuring the area under curves of the L* values (for the shine band) and C* (background colour). The ratio between the L* area and the C* area of the European brown and Oriental hair tresses was determined. The ratio was high in wax treated hair tresses whereas the SLES washed hair tress showed lower ratio. The reason behind the higher ratio in wax treated hair tress is, as the L* curve area reduces the C* area also reduces but the reduction in Chroma area is not linear. In order to get a value closer to human perception shine width (FWHM of the curve) has been added to the conventional gloss evaluation models (details of the gloss evaluation models are discussed in the literature review section). Figure 4-33 shows the average ratio between L* area and C* area of European brown tress treated with different products.

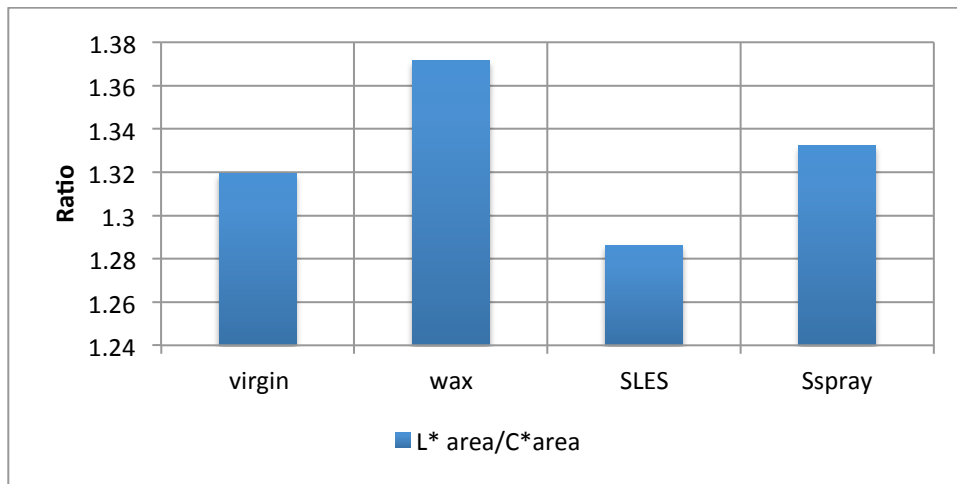


Figure 4-33 L* and C* area ratio of the European Brown tress.

4.16 Quantifying human hair gloss

Different formulae were applied to the data extracted from the hair tress images for the measurement of hair gloss, from a Hunter like approach, which is the ratio between the Specular band and the Chroma band, to a modified Reich-Robbins model. The results generated from these approaches were not sensitive enough to show the small changes in visual perception, which were evident in the images of the hair tresses. Higher intensity in the specular direction and a smaller diffuse area does not guarantee that the image will appear shinier, as results in the psychophysical section show. For example, 100% of the observers chose a virgin tress over the tress treated with wax but the current methods showed only a 20% difference in shine.

Unfortunately current gloss evaluation models, when measuring the gloss of the human hair tress / fibre, do not consider the colour gradient around the shine band. This may be the reason why the gloss values do not correlate to the subjective panel evaluation. The conventional gloss evaluation models are not sensitive enough to identify small changes in the shine of the human hair tress. The colour gradient approach not only complements the shine but also may provide an indication of the condition of the hair tress. If the gradient is smooth the tress appears more visually appealing to the observer. In order to provide a model with outputs closer to human visual discriminations two new approaches were developed to quantify the gloss of a human hair tress. In these formulae, Equation 4-1 and Equation 4-2, Chroma was divided into two segments where:

- C_s (Chroma specular) contributes to increasing the shine
- C_d (Chroma diffuses) contributes to decrease in shine, part of diffuse reflection.

The difference between the MFV of the L^* in the shine band and MFV of C^* in the Chroma-Specular band, D_{LC} , was calculated and incorporated into the model in order to enhance sensitivity. As explained in the previous section (4.14 Differences in the L^* value and C^* value) if the D_{LC} value is high when compared with other tresses, it means that the contrast between the shine and Chroma is high which makes the tress appear shinier. Equation 4.1 shows the first formula to evaluate hair shine of light colour hair tresses, for example blonde or European-Brown, and in the dark colour hair tresses, for example Oriental hair tress, the chroma-diffuse is near negligible due to the light absorption. In order to enhance the sensitivity the ROC model was modified, instead of using Chroma-Diffuse, the difference between the overall L^* area, P_L , and Chroma-Specular was used Equation 4.2 shows the second approach to evaluate hair shine for the dark colour hair tresses.

$$L_{ROC1} = \frac{(S \times C_s) D_{LC}}{C_d \times W_{shine}} \quad \text{Equation 4.1}$$

$$L_{ROC2} = \frac{(S \times C_s) D_{LC}}{(P_L - C_s) W_{shine}} \quad \text{Equation 4.2}$$

Where S is Shine area, C_s (Chroma-Specular reflection) is first part of the Chroma, D_{LC} is difference between L^* and C^* , C_d is Chroma-Diffuse reflection, P_L is the area under the L^* profile of the tress and W_{shine} is FWHM of the shine curve.

Shine is a relative term; a shine value is a meaningless number if it is not compared with another shine value. Keeping this in mind we wanted not to fix any value or any limit in quantifying gloss. Each number generated by the ROC models is image (Hair tress image) dependent. The decompositions of the reflections were made using selection functions and not fits. With the current gonio image capture setup, the new shine formula gives the same order of magnitude as the increase (or decrease) observed by participants.

4.17 Results and discussion

To quantify the appearance of gloss on the human hair tresses four approaches were used. Each hair tress was treated with different products to enhance or reduce their perceived shine and their images were imported into MATLAB for further analysis. Details of the sample preparation and image capture-import procedure are described in Chapter 3 (Methodology). Several approaches were attempted in order to quantify the gloss of a human hair tress, of which two gave superior gloss discrimination and sensitivity. These approaches are labelled as ROC Model 1 (Equation 4-1) and ROC Model 2 (Equation 4-2), (Aims and Objectives Section 1.1, Objective 6-e). Details of these models are explained in Section 4.16 (Quantifying human hair gloss). These two models are compared with two different approaches; modified Robbins and the Profile/width model, which are commonly used in the quantification of gloss in images of human hair tresses.

4.17.1 Quantifying the gloss of the European-Brown hair tresses

Figure 4-34 shows four images of a European-Brown hair tress each of which represents different levels of shine (clearly visible in the images). It can be noted that the tress washed with SLES appears shinier than the rest of the tress images and the tress treated with 3% wax appears the dullest when compared to the other images (in Figure 4-34). The goal of the gloss evaluation model is not only to identify the differences between gloss intensities seen in the images but also to be sensitive enough to represent the difference in shine intensity. Table 4-2 shows the raw values generated by four different gloss assessment models. Each of these models ranked tresses in the right order, which is from shiniest to dullest (SLES-washed – Virgin- Shine Spray- Wax) but their sensitivities were different. The ROC₁ (model 1) and ROC₂ (model 2) models also provide the best results in terms of sensitivity. ROC₂ showed a 73% decrease and ROC₁ showed a 71% decrease in shine whereas the modified Robbins model shows a 26% decrease in shine when the SLES washed hair is compared with the tress treated with wax. Figure 4-35 shows a graphical representation of the normalized values of the models. Values are normalised to provide a fair comparison.



Figure 4-34 The gloss of European Brown hair tresses with different treatments

Table 4-2 The shine values of four European Brown tresses with different treatments applied, generated by the different models

	Virgin	SLES-wash	Shine-spray	Wax (3%)
ROC Model 1	1546	1933	1528	567
ROC Model 2	975	1281	888	357
L*profile/width	108	111	99	84
R Robbins	292	304	264	223

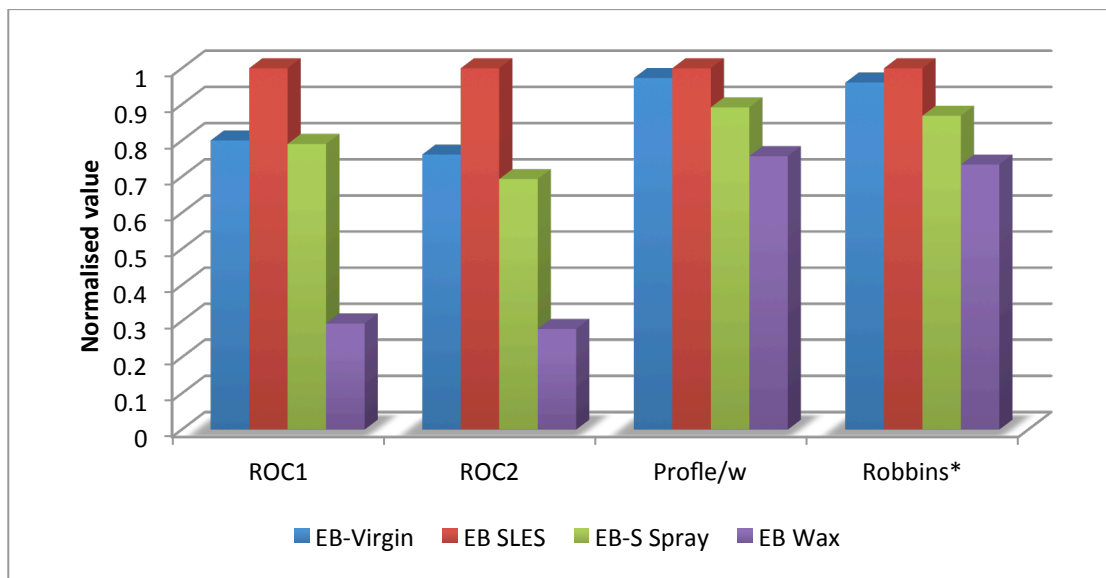


Figure 4-35 A comparison of the normalised shine values of the treated European Brown hair tresses, generated by four different gloss evaluation models

4.17.2 Quantifying gloss of Blonde hair tress

Figure 4-36 shows four images of a Blonde hair tress; each of which represents a different level of shine. There is little difference between the Virgin (untreated) hair tress and SLES-washed hair tress but a large perceptual difference can be observed when comparing the SLES-washed or Virgin hair tress to the Shine-sprayed or Wax treated hair tress. In particular the shine-sprayed hair tress looks unhealthy when it is compared with the SLES-washed hair tress. Table 4-3 shows the raw data generated by the models. The modified-Robbins model predicts that the shine sprayed tress is the shiniest when compared with the other tresses (Figure 4-36) but this does not correlate to the human perceptual evaluation. Shine spray has increased the contrast but the tress does not appear shiny, in fact it looks dull and unhealthy. In the virgin-shine spray comparison our models ROC_1 and ROC_2 show a -32% and -30% decrease in shine, respectively, whereas the Modified Robbins formula predicted a 10% increase in shine. Figure 4-37 shows a graphical representation of the normalised shine values generated by the models.



Figure 4-36 Images of Blonde hair tress with different treatments

Table 4-3 Shine values, of the Blonde hair tresses, generated by different models

	Virgin	SLES-wash	Shine-spray	Wax (3%)
ROC Model 1	988	1041	665	418
ROC Model 2	717	763	501	311
L*profile/width	95	96	110	88
R-Robbins	261	259	289	224

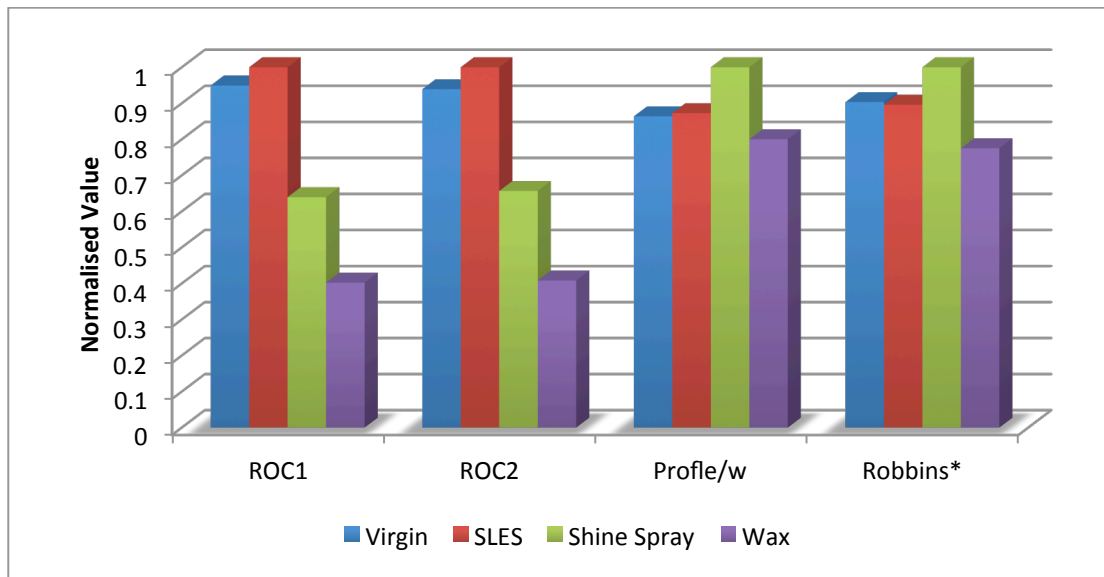


Figure 4-37 A Comparison of the normalised shine values, of the Blonde hair tress images, generated by different models

4.17.3 Quantifying the gloss of Oriental hair tresses

Figure 4-38 shows four images of an Oriental hair tress each of which represent different levels of shine. All of the gloss evaluation models showed a similar trend. The tress washed with SLES was assigned the highest ranking (i.e. the shiniest) by all of the models and wax was rated the dullest in the group as it had the lowest shine value. In terms of sensitivity the ROC₁ and ROC₂ models showed the maximum difference between the virgin tress and tress treated with wax. ROC₁ predicted a -65% decrease and ROC₂ predicted a -82% decrease in shine whereas the modified Robbins model produced a -37% decrease and the Profile/w model showed a -34% decrease in shine. Other than the ROC₁ and ROC₂ models the rest of the models showed a lack of correlation between tress appearance and shine value. The shine values generated by each of the models are tabled in the Table 4-4. It can be concluded that ROC model 1 and ROC model 2 show the best representation in variation of shine on the hair tress.



Figure 4-38 Oriental hair tresses applied with different treatments

Table 4-4 Shine values of Oriental hair tresses generated by different models

	Virgin	SLES-wash	Shine-spray	Wax (3%)
ROC Model 1	1263	1472	1088	434
ROC Model 2	114	132	67	20
L*profile/width	113	115	97	74
R Robbins	308	316	253	192

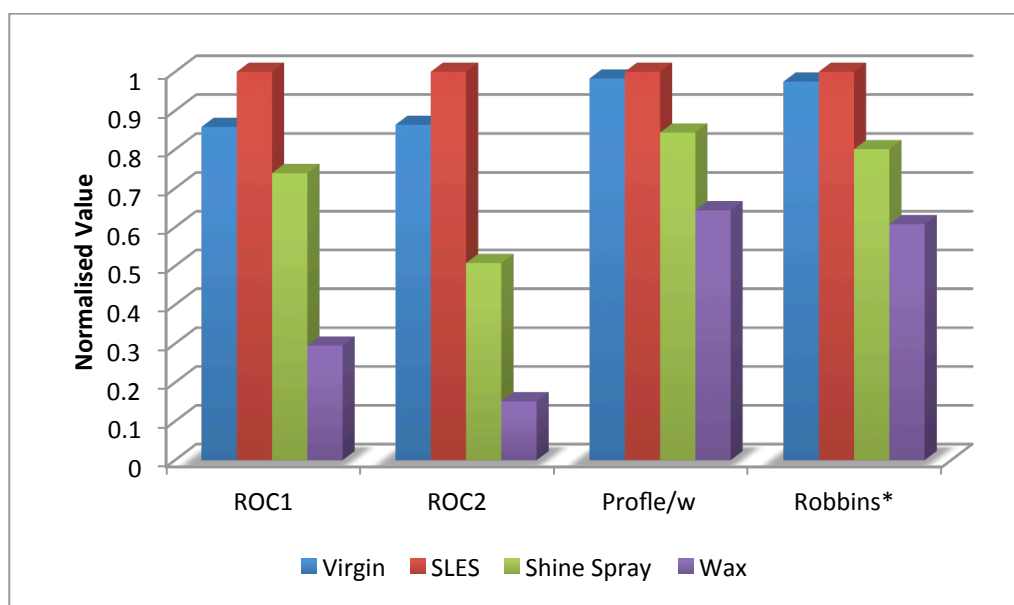


Figure 4-39 A graphical representations of the normalised shine assessment values of an Oriental hair tress generated by different gloss evaluation models

4.18 Repeatability of the Model

Although the tresses were prepared under the same sample preparation conditions (sample preparation Chapter 2 Section 3.3.2), their visual appearance differed when placed on the sample holder. This was due, in part, to the nature of the hair fibres. As these fibres were not connected they could cast a shadow onto each other. For example, when a hair tress is combed, some fibres are pushed inward and others are pulled outwards. The alignment and surface structure of the hair tress may contribute to the creation of a shine band that does not appear smooth on the hair tress. It is extremely difficult to replicate the appearance or surface-texture of the hair tress. Even if the tresses were sampled from the same batch there is no guarantee that the number of hair fibres would be same in each of the tresses. Figure 4-40 shows three blonde hair tresses taken from the same batch and treated with 3% wax. Although similar, there are differences in appearance visible between the images.



Figure 4-40 Blonde hair tresses, taken from same batch, treated with 3% wax

To check the repeatability of the models, three tresses of each hair type (Blonde, European-Brown, and Oriental) were prepared. The values generated by the models ranked the tresses in an order that correlated to the judgement of a human panel and the ROC₁ and ROC₂ models produced a higher sensitivity than other models tested. When the shine assessment values were averaged, the sensitivity of the models changed. This may be because of the nature of the hair tresses. Table 4-5 shows the

shine assessment values of the tresses, generated by each model. The difference in shine value, generated by the ROC₁ model, between the virgin hair tress and the wax treated hair tress was -57% in the first repeat whereas the difference increased to -70% and -75% in the second and third repeat samples of the blonde hair tresses, respectively. This demonstrates the variability of the shine assessment values produced. As the models are image dependent, the variability of the shine assessment values may be significantly different even though the same products have been applied in a standardised way to the same type of hair tresses.

Table 4-5 Shine values of the Blonde hair tresses and percentage differences.

Blonde							
Repeat 1					% Differences		
	Virgin	SLES	Shine Spray	Wax	V-W	V-SLES	V-Sspray
ROC ₁	988.31	1041.12	665.65	418.77	-57.63	5.34	-32.65
ROC ₂	717.05	763.76	501.36	311.74	-56.53	6.51	-30.08
Robbins*	261.00	259.00	289.00	224.00	-14.18	-0.77	10.73
Profile/w	95.00	96.32	110.00	88.00	-7.37	1.39	15.79

Repeat 2					% Differences		
	Virgin	SLES	Shine Spray	Wax	V-W	V-SLES	V-Sspray
ROC ₁	799.94	969.18	610.06	236.63	-70.42	21.16	-23.74
ROC ₂	599.17	715.55	468.12	176.50	-70.54	19.42	-21.87
Robbins*	261.38	253.68	290.57	207.80	-20.50	-2.95	11.17
Profile/w	96.81	93.91	108.73	81.89	-15.42	-3.00	12.31

Repeat 3					% Differences		
	Virgin	SLES	Shine Spray	Wax	V-W	V-SLES	V-Sspray
ROC ₁	891.44	1034.03	878.11	219.01	-75.43	16.00	-1.49
ROC ₂	654.94	764.63	669.48	165.18	-74.78	16.75	2.22
Robbins*	264.91	263.26	288.05	212.55	-19.77	-0.62	8.74
Profile/w	97.83	96.48	108.28	83.16	-14.99	-1.38	10.68

Averages					% Differences		
	Virgin	SLES	Shine Spray	Wax	V-W	V-SLES	V-Sspray
ROC ₁	893.23	1014.78	717.94	291.47	-67.37	13.61	-19.62
ROC ₂	657.05	747.98	546.32	217.81	-66.85	13.84	-16.85
Robbins*	262.43	258.65	289.21	214.78	-18.16	-1.44	10.20
Profile/w	96.55	95.57	109.00	84.35	-12.63	-1.01	12.90

Figure 4-41 shows images of Blonde tresses treated with different products. The normalised shine assessment values generated by each model are shown.

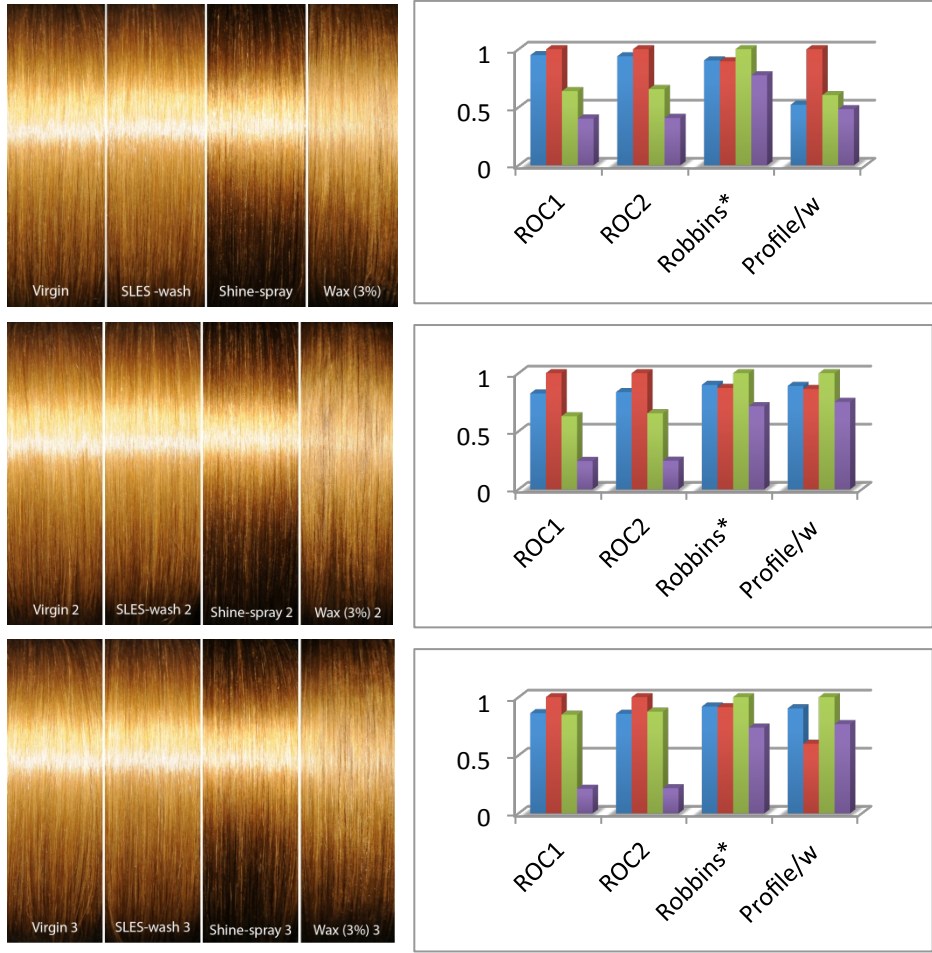


Figure 4-41 Repeats of Blonde hair tress comparisons and shine values generated by models

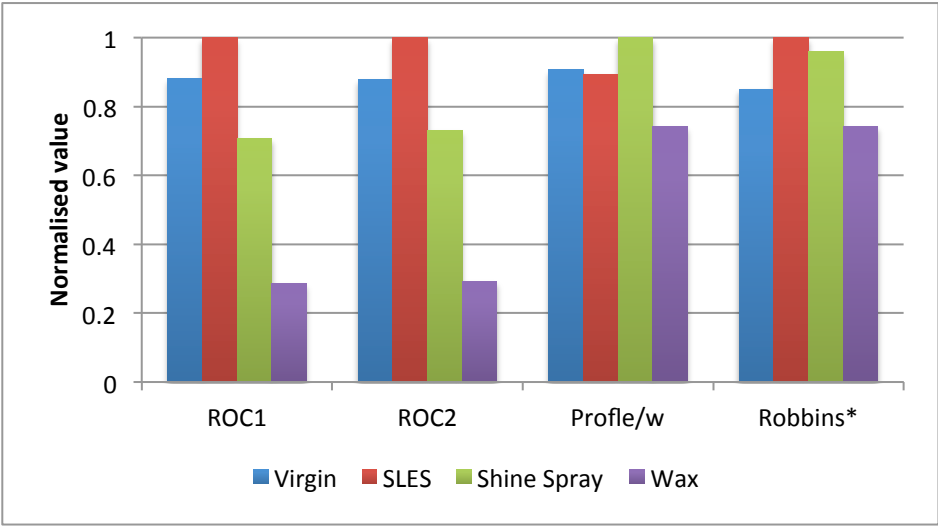


Figure 4-42 Normalised shine assessment values of the Blonde hair tresses treated with different products.

The shine assessment values of the European Brown tresses showed a similar trend with all of the tested models generating high values for SLES washed tresses, in all three repeats. The ROC₁ and ROC₂ models showed the largest maximum difference in shine values when the European-Brown tresses were compared with each other. Table 4-6 shows the raw shine assessment values of the European Brown hair tresses and shine-value differences in percentage terms.

Table 4-6 Shine values of the European Brown hair tresses with percentage differences.

European Brown hair tresses							
Repeat 1					% Differences		
	Virgin	SLES	Shine Spray	Wax	V-W	V-SLES	V-Sspray
ROC1	1546.66	1933.02	1528.11	567.21	-63.33	24.98	-1.20
ROC2	975.00	1281.00	888.00	357.00	-63.38	31.38	-8.92
Robbins*	292.00	304.00	264.00	223.00	-23.63	4.11	-9.59
Profile/w	108.66	111.75	99.71	84.85	-21.91	2.84	-8.24

Repeat 2					% Differences		
	Virgin	SLES	Shine Spray	Wax	V-W	V-SLES	V-Sspray
ROC1	1734.91	1782.80	1699.91	721.64	-58.41	2.76	-2.02
ROC2	1066.79	1182.56	1012.03	456.27	-57.23	10.85	-5.13
Robbins*	282.04	299.30	273.01	217.66	-22.83	6.12	-3.20
Profile/w	106.61	112.29	103.35	83.32	-21.85	5.33	-3.06

Repeat 3					% Differences		
	Virgin	SLES	Shine Spray	Wax	V-W	V-SLES	V-Sspray
ROC1	2163.18	2394.10	2006.81	563.29	-73.96	10.67	-7.23
ROC2	1316.72	1484.84	1250.67	337.73	-74.35	12.77	-5.02
Robbins*	282.74	295.34	285.70	213.24	-24.58	4.46	1.05
Profile/w	106.92	109.49	106.49	81.08	-24.17	2.40	-0.40

Averages					Differences		
	Virgin	SLES	Shine Spray	Wax	V-W	V-SLES	V-Sspray
ROC1	1814.92	2036.64	1744.94	617.38	-65.98	12.22	-3.86
ROC2	1119.50	1316.13	1050.23	383.66	-65.73	17.56	-6.19
Robbins*	285.59	299.55	274.24	217.97	-23.68	4.89	-3.98
Profile/w	107.40	111.18	103.18	83.08	-22.64	3.52	-3.92

As expected each European Brown hair tress had a different visual appearance these differences are evident in the images. Figure 4-43 shows the images of the European Brown hair tresses along with the graphical representation of the normalised shine

values generated by the four gloss evaluation models. Due to the greater sensitivity of the ROC models, small changes in the appearance of the tresses were detected. Figure 4-44 shows the average shine-values (normalised) produced by different models.

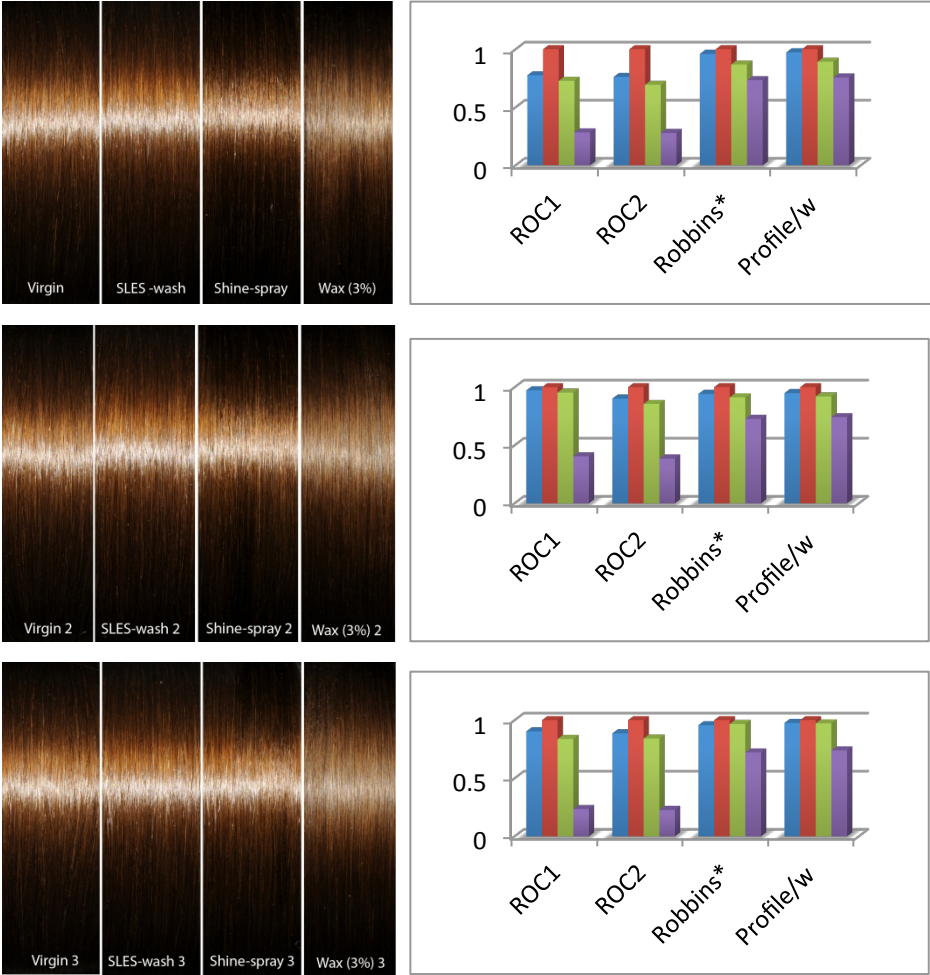


Figure 4-43 Repeats of European-Brown tress for comparison of the shine values generated by the different models.

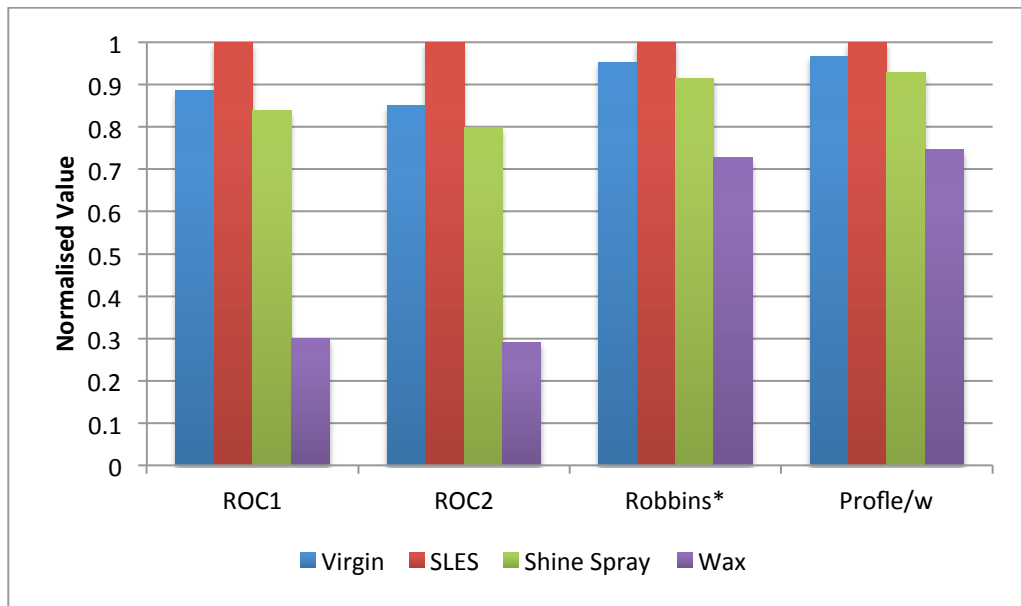


Figure 4-44 Average shine values, of the European Brown hair tress treated with different products, generated by different models.

Perhaps unsurprisingly all of the shine assessment values varied in the repeats of the Oriental hair tresses, these variations are visible on the images of the tresses. Figure 4-45 shows the images of the Oriental hair tresses treated with different products, along with the normalised shine values generated by the different models. Even though variations were noted in the shine-values, all of the models under evaluation rated the SLES treated hair tress as the shiniest. In terms of average difference, for example, from virgin hair tress to wax treated hair tress the ROC models showed the greatest difference in sensitivity. ROC₂ predicted a -71% decrease in shine whereas the modified Robbins formula produced a -41% reduction in shine. Figure 4-46 shows the normalised average shine values generated by the different models.

Table 4-7 Shine values of the Oriental hair tresses and percentage differences.

Oriental							
Repeat 1					% Differences		
	Virgin	SLES	Shine Spray	Wax	V-W	V-SLES	V-Sspray
ROC1	1263.00	1472.00	1088.00	434.00	-65.64	16.55	-13.86
ROC2	114.00	132.00	67.00	20.00	-82.46	15.79	-41.23
Robbins*	308.00	316.00	253.00	192.00	-37.66	2.60	-17.86
Profile/w	113.00	115.00	97.00	74.00	-34.51	1.77	-14.16

Repeat 2					% Differences		
	Virgin	SLES	Shine Spray	Wax	V-W	V-SLES	V-Sspray
ROC1	1240.74	1342.76	972.99	312.95	-74.78	8.22	-21.58
ROC2	108.98	133.69	90.56	12.42	-88.60	22.68	-16.90
Robbins*	310.68	314.16	250.22	173.59	-44.13	1.12	-19.46
Profile/w	115.90	115.60	95.37	68.72	-40.71	-0.27	-17.72

Repeat 3					% Differences		
	Virgin	SLES	Shine Spray	Wax	V-W	V-SLES	V-Sspray
ROC1	1039.77	1495.87	977.45	265.81	-74.44	43.87	-5.99
ROC2	74.13	154.36	85.13	11.88	-83.97	108.24	14.85
Robbins*	293.00	316.43	243.61	168.41	-42.52	8.00	-16.86
Profile/w	108.97	115.83	93.53	66.88	-38.63	6.30	-14.17

Averages					% Differences		
	Virgin	SLES	Shine Spray	Wax	V-W	V-SLES	V-Sspray
ROC1	1181.17	1436.88	1012.81	337.59	-71.42	21.65	-14.25
ROC2	99.03	140.02	80.90	14.77	-85.09	41.38	-18.31
Robbins*	303.89	315.53	248.94	178.00	-41.43	3.83	-18.08
Profile/w	112.62	115.48	95.30	69.87	-37.96	2.53	-15.38

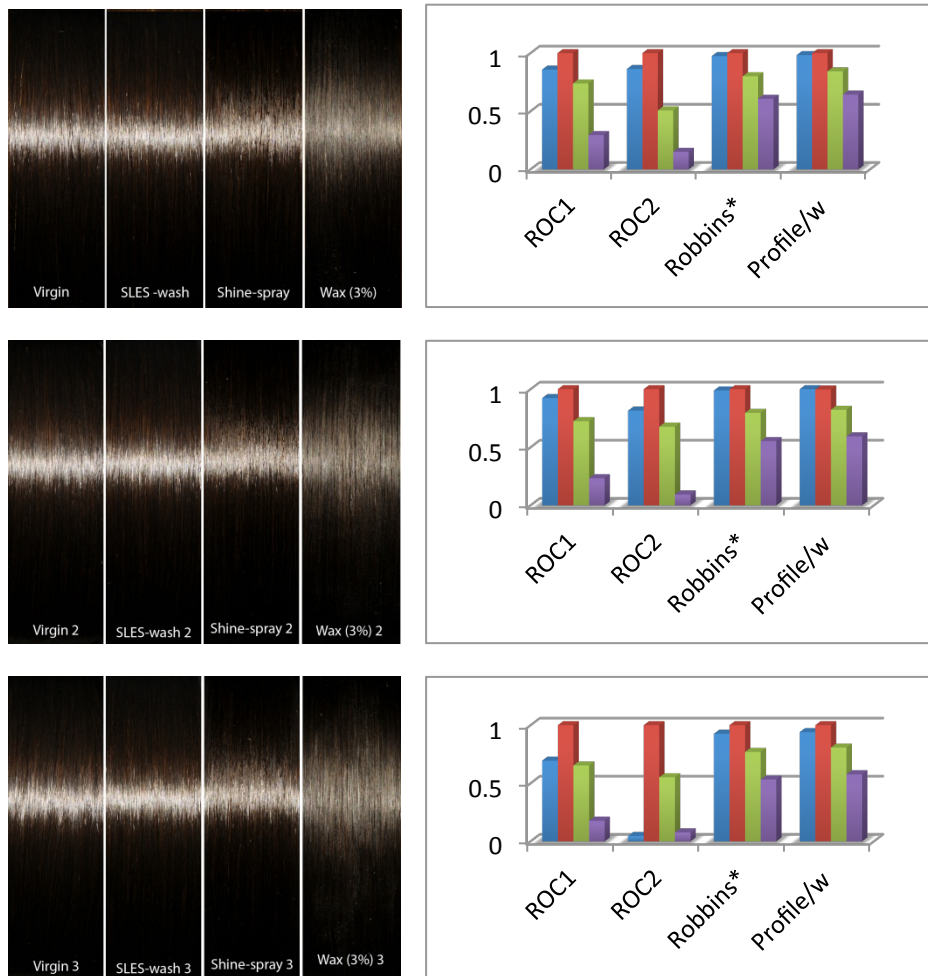


Figure 4-45 Repeats of European-Brown tresses. A comparison of the shine assessment values generated by the different models.

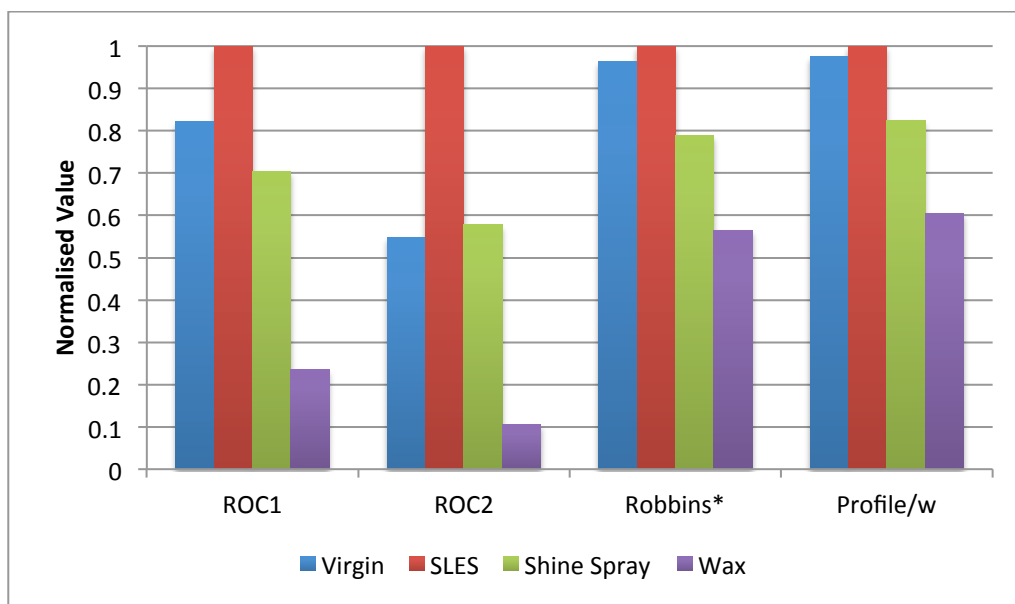


Figure 4-46 Average shine values, of the Oriental hair tresses treated with different products and generated by different models.

4.19 Summary

A number of publications on the subject of hair-shine exist, over the previous 30 years, as explained in Section 2.15.2. Even though the models proposed to evaluate hair-shine are different they work on principles based on Stamm's three-component model. In Stamm's model the incident light reflected from the hair tress or a hair fibre is separated into three distinct reflection bands (Specular, Chroma and Diffuse).

Although the three-band approach almost certainly describes the physical properties of the light reflected from a hair tress this does not mean that the perceptual properties of the hair tress have been adequately described. The perceptual analysis of the light reflected from the hair tress may not be as straightforward as Stamm's three-components model suggests. When images of the hair tresses were analysed it was noted that the Chroma band (coloured part of the reflection) is not uniform and changes gradually with a colour gradient, colour gradients are explained in more detail in Section 4.2.

The Chroma-Specular (Cs) band has been suggested as a novel interpretation of the shine band information. The Chroma-Specular band may be considered in relation to digital photography where the addition of blur creates a glowing effect, for example the light-sabre from the movie Star Wars. Figure 4-47 shows how a blur effect created by the author using Adobe Photoshop CS3 seems to enhance the shine band. In images of human hair tresses the Chroma Specular band may complement or even enhance the perceived shine of the shine band.



Figure 4-47 The effect of a blurring effect on the appearance of an object (reproduced and edited from Section 4.3).

Different techniques have been used to separate the hair tress reflection bands. These techniques include using polarizers, measuring the reflectance at certain angles and curve fitting. An ideal system would separate the reflection bands in a diffusely illuminated environment, which would realistically replicate the viewing conditions of a normal observer.

Once the Chroma-Specular band was identified an automated method of separation was created. Current separation methods do not identify the Chroma-Specular band. The new method of separating the reflection bands from the image of the hair tress was initially to manually select the shine-area on the image and calculate the L^* and C^* limits of that area. The L^* and C^* limits were then used to segment the tress image which resulted in the separation of the shine band. The Author also added a real-time confirmation, which shows the separated band overlaid on the original tress image. Figure 4-32 shows the separated reflection bands and an overlay (in green) on the image of a virgin blonde hair tress. The manual and automated separation methods used to identify the reflection-bands are explained in Section 4.8.

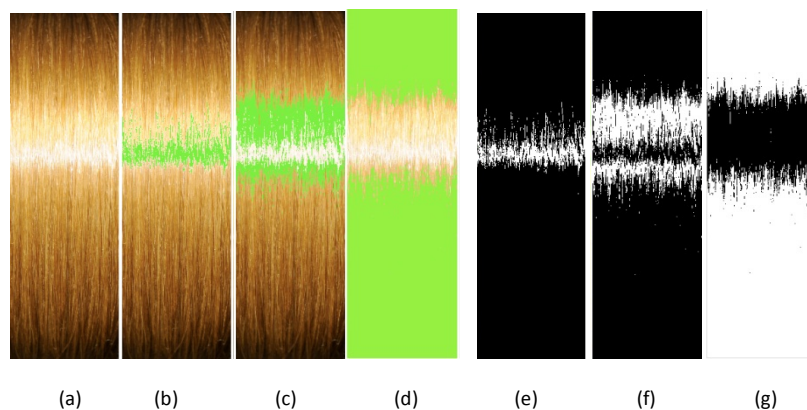


Figure 4-48 Reflection band separation of a Virgin Blonde hair tress. (a) Virgin Blonde tress image, original image, (b) Shine-band separated and overlaid on the original image (in green), (c) Chroma-Specular band separated and overlaid on the original image, (d) Chroma-Diffuse band separated and overlaid on the original image, (e) Separated shine-band (in grayscale), (f) Separated Chroma-Specular band, (g) Separated Chroma-Diffuse band.

Once the reflection bands were separated, the L^* values and the C^* values present in each area were averaged horizontally and plotted as an intensity curve. The area under each of the curves was calculated. The effect of different hair tress treatments on the areas of the reflection bands was examined. It was assumed that if the shine area increased that the tress would appear shinier. It was interesting to note that the European Brown hair tresses appeared shinier if not the same when virgin hair tresses were compared with SLES treated hair tresses but the shine areas calculated showed a 0.8% decrease. This suggests that the areas of L^* profiles are insufficient to assess gloss completely and the relationship between the reflection bands is important for an evaluation of gloss that correlates to human perception. The effects of the different tress treatments on the areas of the reflection bands are explained in Section 4.8.

To quantify the gloss of a human hair tress, the author has developed two new formulas, the ROC_1 (Rizvi-Owens-Croda) and ROC_2 formulas. The ROC_1 formula not only predicts the correct level of shine (in an order that correlated to the judgement of a human panel) but also is sensitive enough to detect similar shine differences to human observers. The ROC_1 formula consists of five main elements; the area of the Shine band, the area of the Chroma-Specular band, the area of the Chroma-Diffuse band, the Shine Band width at half height (FWHM) and to increase the sensitivity difference the height of the L^* curve and the C^* (D_{LC}) curve was also incorporated into the formula. Even though the ROC_1 model produced the correct level of shine to increase the sensitivity of the model when using oriental (black) hair tresses the ROC model was modified and instead of using Chroma-Diffuse, the difference between the Shine profile and the Chroma-Specular was used.

ROC was compared with two conventional hair gloss models. In European-brown hair tresses ROC_1 and ROC_2 predicted an 83% and a 71% decrease in the shine, respectively, whereas the modified Robbins model showed only a 26% decrease when an SLES washed hair tress was compared with a tress treated with 3% wax. ROC_1 was demonstrated to be the most sensitive when compared with other models.

In Blonde hair tress evaluation when shine-spray was sprayed onto the tress, even though the contrast between the shine and background increased the tress appears

greasy and visually less appealing (some observers described this as less healthy). Other than the ROC_1 and ROC_2 models, the conventional models showed an increase in shine when a shine-sprayed blonde tress was compared to a virgin blonde hair tress. The difference in the model outputs would appear to be due to the inclusion of the Chroma-Specular component. It could be tentatively suggested that the ROC_1 and ROC_2 models not only predict the level of shine but could also be indicating a more general indicator of hair “health” or preference of appearance mirrored by human observers of the hair tress. Of the two novel equations produced in this work, the ROC_1 model was the most sensitive in discriminating gloss changes in the blonde hair tresses.

When the Oriental hair tresses were evaluated all of the models predicted the correct shine levels but the ROC_1 and ROC_2 models showed the maximum difference between the virgin hair tress and tress treated with 3% wax. ROC_1 showed a 65% decrease in the shine whereas ROC_2 showed an 82% decrease in shine. The modified Robbins model showed a 37% decrease in shine. Thus the ROC_2 model was the most sensitive to quantifying gloss differences in the Oriental hair tresses.

To relate the ROC models with human perception, a method of constant stimuli (forced choice – pair comparison) psychophysical experiment was conducted. In Chapter 5 there is a comparison of the ROC models with the evaluations made by a panel of human subjects.

Chapter 5

A Psychophysical Study of the Perceived Gloss in Images of Human Hair Tresses.

5.1 Overview

Chapter 5 focuses on the relationship between the hair gloss evaluation by humans and the hair-gloss evaluation models. An attempt has been made to answer the question, can the values from a model of hair gloss determined from digital images correlate to human perception? To answer this question psychophysical-studies were performed. Initially a graphical user interface (GUI), Tress-Gloss 1.0 was developed by the author, which was based on magnitude estimation psychophysical test. In Tress-Gloss 1.0 an image of a hair tress appears on the calibrated screen and participants were asked to rank the tress on the basis of how shiny they appear on a scale of 1 to 9. It was noted that participants were reluctant to give extreme values of rank. To overcome this problem the psychophysical test was changed to a method of constant stimuli (forced choice- pair comparison) test and Tress-Gloss 1.0 was modified. The modified MATLAB GUI was called Tress-Gloss 2.0 and this displayed a pair of hair tresses images on the screen. Participants were asked to choose which tress appeared shinier and were forced to choose one of the images. For further details about the GUIs (Tress-Gloss 1.0 and Tress-Gloss-2.0) please see Section 3.7.6.

To understand how human observers evaluate hair shine, the Tress-Gloss 2.0 GUI was executed on an eye-tracking system (Tobii TX300), which records the eye-movements of the participants while they are evaluating the shine of the hair tress image (Aims and Objective Section 1.1, Objectives 6-a). This type of eye-tracking study has never been reported in the literature and this study is the first to use eye-tracking technology (Tobii TX300) to collect the gaze data of the participants while they are evaluating hair shine.

Tobii Studio 3.0.3 (Tobii Eye Tracker software) was used to automatically collect the gaze data of each participant (Aims and Objective Section 1.1, Objectives 6-b). It was possible using Tobii Studio, to select areas of interest (AOIs) on the screen and calculate how many times a participant gazed in those predefined areas of the screen (Aims and Objective Section 1.1, Objectives 6-c, 6-d). Using Tobii studio the Tress-Gloss 2.0 window was divided into seven segments: 1) Shine-area of the left tress image, 2) Shine-area of the right tress image, 3) Top-Chroma area of the left tress image, 4) Top-Chroma area of the right tress image, 5) Bottom-Chroma area of the left tress image, 6) Bottom-Chroma area of the right tress image and, 7) the whole screen (consisting of both tress images). Readings from the Tobii Eye Tracker can be represented in three graphical formats a)

gaze plots, b) heat maps and c) cluster diagrams. Details of the AOIs and visualizations are explained in Sections 5.2.3.1 and 5.2.3.2. It was interesting to discover that for the range of colours of human hair tress images used in this study all of the participants evaluate hair shine in a similar pattern (Aims and Objective Section 1.1, Objectives 6-e). A group of eleven participants (7 male and 4 female) took part in the psychophysical study. Each participant was briefed about the experiment and was given an experiment information sheet, which described the experimental methodology. Participants were specifically asked to choose the shiniest hair tress from a pair of tress images, which would appear on each side of a calibrated screen.

Four levels of hair shine were prepared (Virgin tress, SLES washed tress, Wax treated tress and tress sprayed with shine spray), tress preparation is explained in Section 3.7, and two repeats of each shine level were used in the psychophysical study. Each image represented an individually prepared tress (e.g. there were 3 different EB SLES treated tresses and therefore three different tress images) and hence 36 tress images in total were used, a breakdown of the tresses used is tabulated in Table 5.1.

Table 5-1 Tress images used in the Psychophysical Eye Tracking Study

Tress image type	Virgin	SLES washed	Shine-sprayed	Wax treated	Total tress images
Blonde	3	3	3	3	12
EB	3	3	3	3	12
Oriental	3	3	3	3	12
Total images					36

Each level of shine was compared with each other making a total comparison for each hair type of sixty-six. The total number of evaluations performed by each participant was 198 (66 comparisons of blonde tress images, 66 comparisons of EB tress images, and 66 comparisons of Oriental tress images). The study was carried out in three sessions, one session for each hair type. This reduced the amount of repeat comparisons and improved the readability of data. Of the sixty-six evaluations of each hair type, there were twenty-one evaluations of the Blonde hair tress images and nine comparisons of each European-Brown and Oriental hair tress. Image presentation is discussed in

Chapter 5 with the breakdown of the evaluation types explained in Section 5.2.5 for Blonde and Section 5.4.1 for European-Brown and Oriental types.

The software package Tobii Studio recorded each session of the experiment as a video that included the gaze data of the participant and the tress images as they had appeared on the screen (Figure 5-1 Tress-Gloss 2.0 screenshots). Each video of a participant's session was segmented on the basis of tress comparison. The areas of interest (AOIs) were manually selected on the video segments and the gaze data of each participant was captured. Once each comparison was segmented, the following data was determined; how many times a participant gazed in a certain area (e.g. Shine area), how much time a participant spent in the areas of interest (AOIs) and how long it took to decide which hair tress image was the glossiest (discrimination time).

The observer selections were recorded and compared with the gloss-evaluation model outputs. Gaze-plots, heat-maps and clustering along with observer choices was compared with other models, as explained in Section 5.3.

5.2 Method of constant stimuli (forced choice – pair comparison)

Psychophysical experiment

Tress Gloss 2.0 was used in a forced choice – paired comparison psychophysical experiment; details of the GUI (Tress-Gloss 2.0) are described in Chapter 3 Section 3.5.2. The experiment was performed in order to understand how human observers quantify gloss and which parts of the tress they attended to most frequently before making their decision. To record their choice, Tress-Gloss 2.0 was executed on the Tobii TX300 eye tracking system. The Tobii TX300 software automatically records the participants' gaze during the experiment.

5.2.1 Tress Images used in the psychophysical experiment

Twelve images of each type of hair tress (12 images of Blonde tresses, 12 images of European-brown tresses, 12 images of Oriental tresses) were used in the study. The experiment consisted of three repeats of each hair type and each image was paired with all the images of the same type (hair colour), which resulted in 66 evaluations of each hair type (66 evaluations for Blonde, 66 evaluations for European-Brown and, 66 evaluations for Oriental). Table 5-2 shows the generic breakdown of the images used in the study.

Table 5-2 Generic Breakdown of the images used in the study

Tress (repeats)	Number of images			
	Virgin	SLES	Shine-Spray	Wax
Tress set 1	1	1	1	1
Tress set 2	1	1	1	1
Tress set 3	1	1	1	1
Total	3	3	3	3
Total images used in the study for each type				12

5.2.2 Tobii TX 300 Eye-Tracking system

The Tobii TX300 Eye Tracker was used to record eye movements, during the experiment. The Tobii TX300 collects gaze data at 300 Hz, the system is designed in such a way that it allows large head movements. Due to the high sampling rate, it is possible to collate the fixation, pupil size changes and blinks. The Tobii TX300 Eye Tracker System at the University of Manchester comprises an eye-tracking unit and a removable 23" wide screen 1920 X 1080 pixel TFT monitor. Figure 5-1 shows a screen shot of the Tress-Gloss 2.0 GUI, displayed on the monitor of the Tobii eye-tracker.

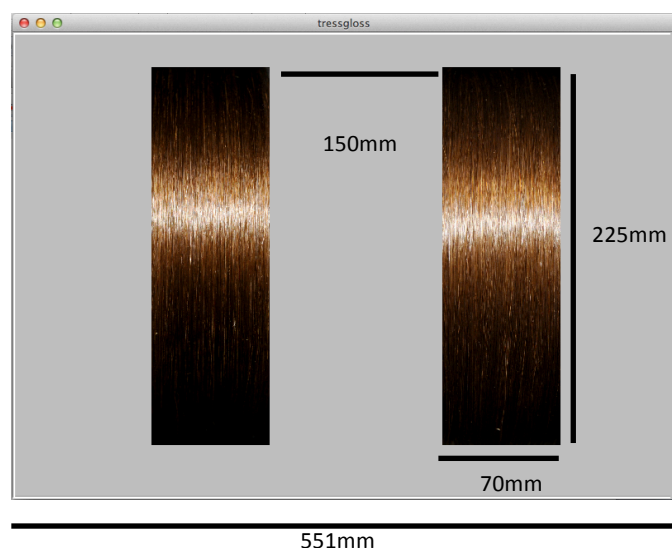


Figure 5-1 Screen shot of the Tress-Gloss 2.0 GUI as displayed on the Tobii eye tracker monitor (along with stimuli specifications)

5.2.2.1 Calibration of Eye-Tracking system

Prior to the test being performed, the observer was asked to sit comfortably in front of the Eye-tracker at an approximate distance of 64 cm. Figure 5-2 shows a schematic of an observer sitting in front of the eye-tracker. The observer performed an eye position calibration procedure, which forms part of the eye tracking software Tobii Studio version 3.0.3.

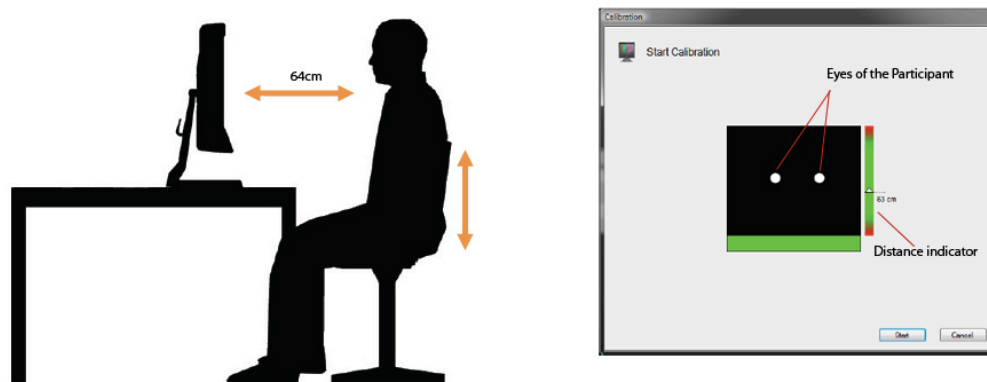


Figure 5-2 Calibration of the Tobii Eye-Tracker (Tobii Technology 2010)

During the calibration procedure the Tobii TX300 measures characteristics of the observer's eyes and uses these characteristics together with an internal, physiological based 3D eye model to calculate gaze data. This model includes information about shape and the reflection properties of different part of the human eye (Tobii User manual). During calibration, the observer was asked to look at specific locations on the screen, also known as calibration dots, while several images of the eyes were taken by the eye-tracker and analysed. The resulting information is then integrated with the eye model and a gaze point for each image sample is calculated. When the calibration was finished, the calibration results were displayed in a dialog box as shown in Figure 5-3.

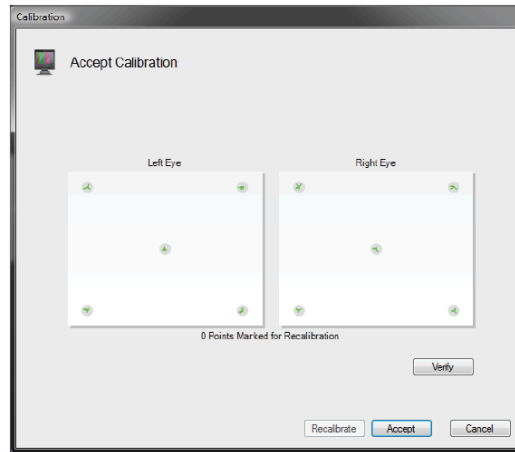


Figure 5-3 Calibration result.

5.2.3 Creating and editing the Psychophysical test using Tobii Studio

Tobii Studio version 3.0.3 (the software provided with the Tobii TX300 system) was used in the psychophysical experiment, to record the participants' gaze data. To record eye gaze data from the MATLAB GUI Tress-Gloss 2.0, an option "Screen Rec", provided by Tobii studio, was used. Screen Rec. records stimuli that are presented by external software, in this case MATLAB. Once Tobii Studio had recorded the gaze data it was further analysis. Figure 5-4 shows a flow diagram of the process.

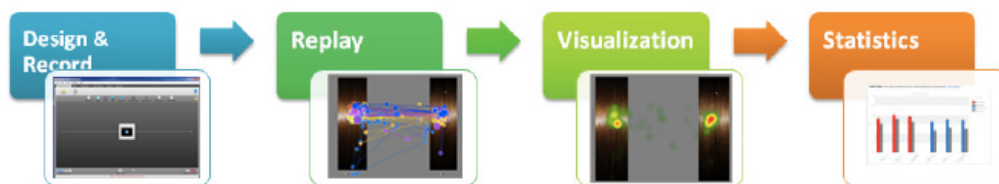


Figure 5-4 Flow diagram of the Tobii-eye tracker process (modified, Tobii Technology 2010)

Once the psychophysical experiment was started, the Tobii TX300 recorded the eye movements of the user during the experiment and saved the session to a video file. Each tress evaluation screen was then segmented out from the video. For example if a participant took 10 minutes to complete 66 comparisons, Tobii studio records the gaze data of the participants in a form of 10 minute long video. The recorded video was then

opened as a time-line in the software Tobii Studio and each comparison was carefully selected and segmented out for further analysis. This analysis included where the observers were looking, when appearance of the hair tress changes in terms of shine. These segments can be replayed to check the segmentation has been done correctly.

5.2.3.1 Visualization

Tobii Studio 3.0.3 has divided visualisation into three main types: a) Gaze plot, b) Heat map and, c) Cluster.

Gaze Plot visualization shows the sequence and position of fixations (dots) on a static media, (in our case the Tress-Gloss 2.0 evaluation screen). The size of the dots indicates the fixation duration and the numbers in the dots represent the order of the fixations. Gaze Plots can be used to illustrate the gaze pattern of a single test participant throughout the entire eye tracking session, or of several participants in a short time interval.

A *heat map* uses different colours to show the number of fixations participants made in certain areas of the image or for how long they fixated within that area. Red usually indicates the highest number of fixations or the longest time, and green the least, with varying levels in between

The *Cluster* visualisation is a graphic representation of areas with high concentrations of gaze data points (clusters), superimposed on a background image. Figure 5-5 shows a screen shot of each type of visualisation along with a screen shot of the GUI image.

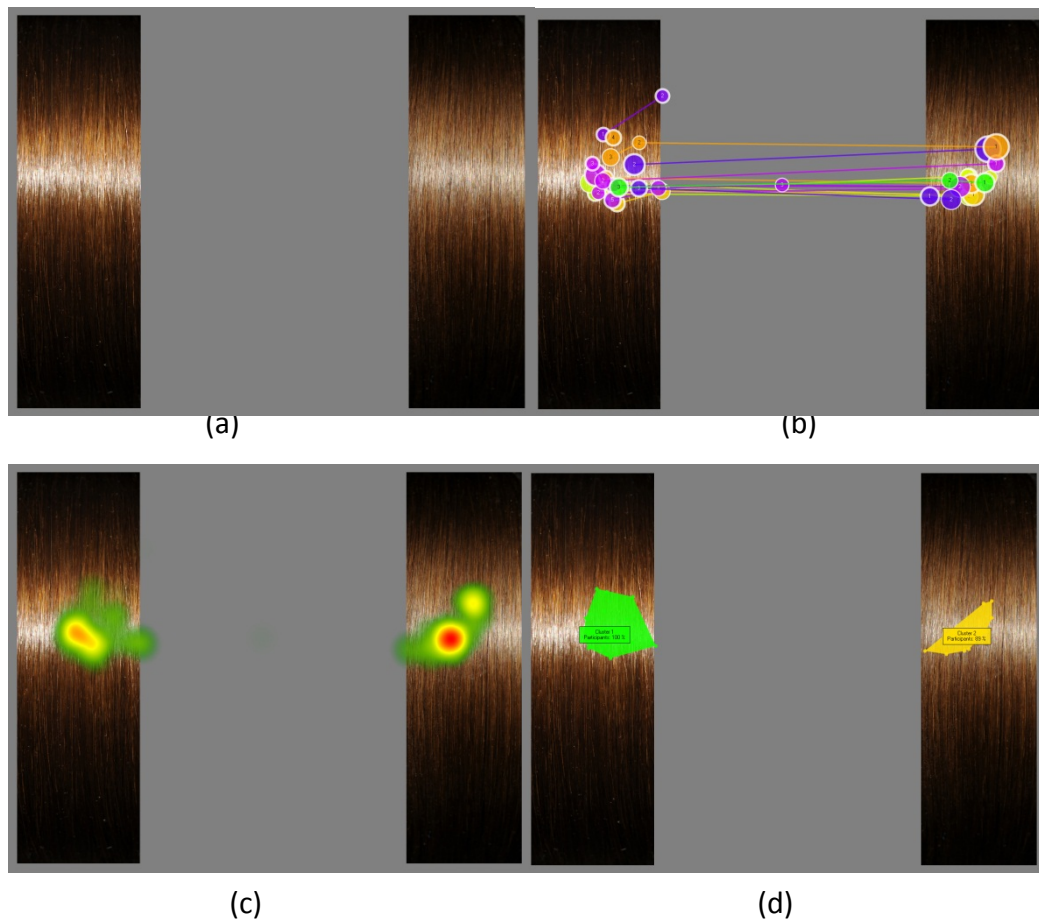


Figure 5-5 Screen shots of pair evaluation test (European-Brown Virgin tress on left and Wax treated tress on right) using the Tobii TX300 eye-tracker (a) Tress-Gloss 2.0 evaluation screen short (b) Gaze plot of all the participants for this evaluation, (c) heat map of the evaluation test, (d) Cluster plot of all the observers for this image

5.2.3.2 Area of interest

Tobii Studio collects the gaze data from the Tobii eye-tracking unit for the whole evaluation screen. This allowed a further dissection of the data. For example, if the frequency that a participant gazed in the Shine or Chroma areas is required. The Tobii Studio AOI definition tool was used to preselect areas for further analysis; this tool enables to user to define areas of interest (AOIs) within the image. Once the area of interest has been defined on the image, the analysis can be based on the frequency and time duration spent attending within the AOIs. The four AOIs selected for investigation on the human hair tress image areas were: (i) Shine area, (ii) Top Chroma area, (iii) Bottom Chroma area and (iv) Whole image. Figure 5-6 shows the AOIs on the screen shot of the Tress-Gloss 2.0.

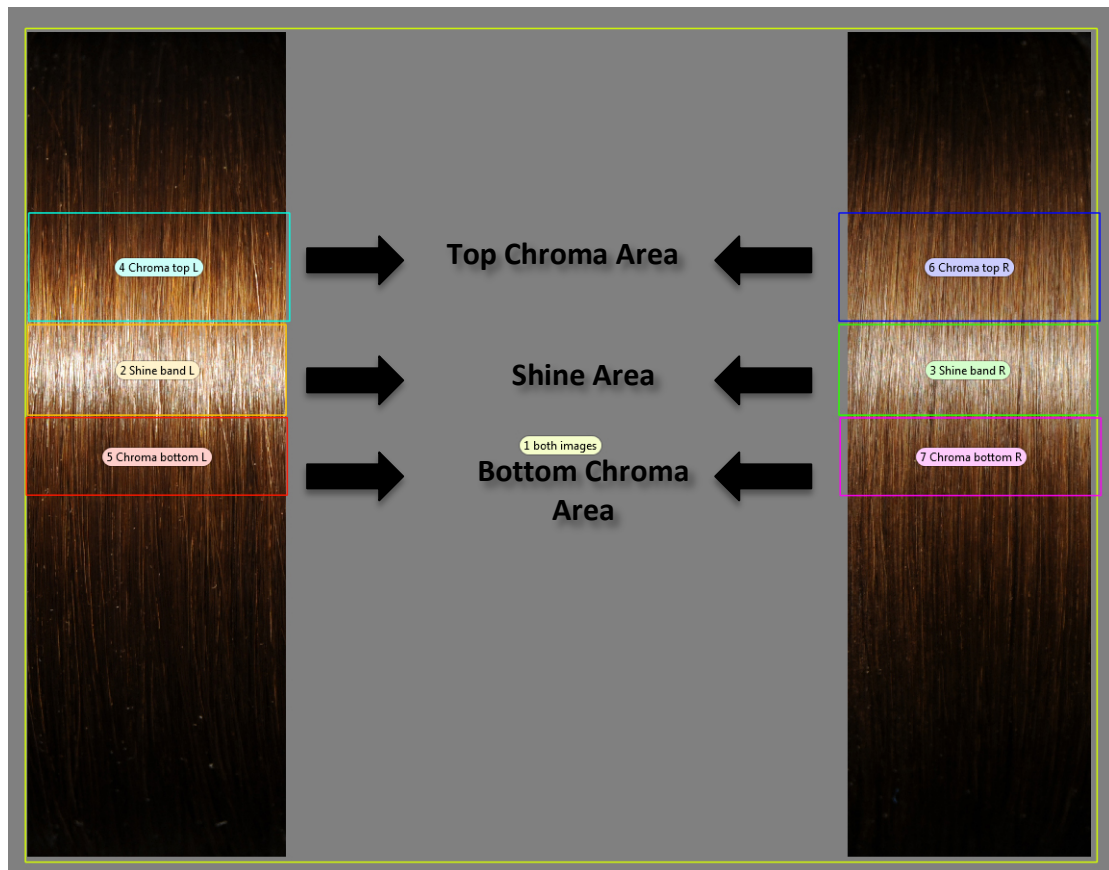


Figure 5-6 AOIs (Area of interest) defined on the GUI screen shot

5.2.4 Participants information

Eleven participants (7 males; 4 females; ages 21 – 40) participated in this research study. Three participants were farsighted and they used eyeglasses to help correct their vision. Out of the eleven, one participant was left-handed. Before the start of the experiment each participant was asked to sit in the room for at least half an hour in order to adapt to the ambient illumination. During this time they were briefed about the study by giving them an Experiment Information Sheet (see Appendix B). They were specifically asked to choose the shiniest hair tress out of two images, which appeared as a pair on the screen. If the subject thought the images looked the same, participants were encouraged to choose what they thought was the most visually pleasing of the two images. Figure 5-7 shows a participant using the Tobii eye-tracker system in the psychophysics laboratory at the University of Manchester.

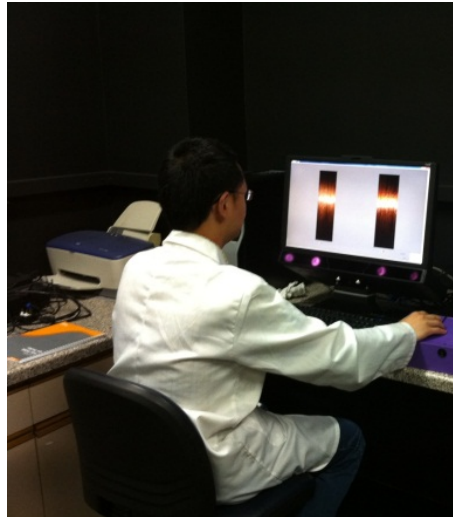


Figure 5-7 Participant performing the tress gloss psychophysical comparison experiment using the Tobii eye-tracker TX300

5.2.5 Evaluation selection of the Psychophysical experiment

Out of the sixty-six comparisons possible for each type of tress (Blonde, European-Brown, Oriental), twenty-one images, of each type of hair tress, will be discussed. The generic structure of the Tress comparisons selected for blonde hair tresses is described in Table 5-3.

Table 5-3 Generic structure of the tress comparisons analysed in this section

Evaluation type	Number of Evaluations
Virgin - Wax	3
Virgin – SLES	3
Virgin – Shine Spray	3
Virgin – Virgin	3
Wax – Wax	3
SLES – SLES	3
Shine Spray- Shine spray	3
Total Evaluations	21

5.3 Data analysis of Blonde hair tresses

5.3.1 Blonde Virgin – Blonde Wax

A pair of blonde hair tress images appeared on the screen. The tress on the left of the image was an untreated blonde hair tress (virgin) and the image on the right was of a tress treated with wax, Figure 5-8. Both tresses, even though they are of the same type, had a different visual appearance as the tress on right had a wax applied. Figure 5-8 shows the gaze plot of all the participants, on a screen shot captured from the Tress-Gloss 2.0 virgin-wax evaluation. It is evident from the gaze plot that the participants were predominantly interested in the central part of the hair tresses, which consists of the Shine and Chroma bands.

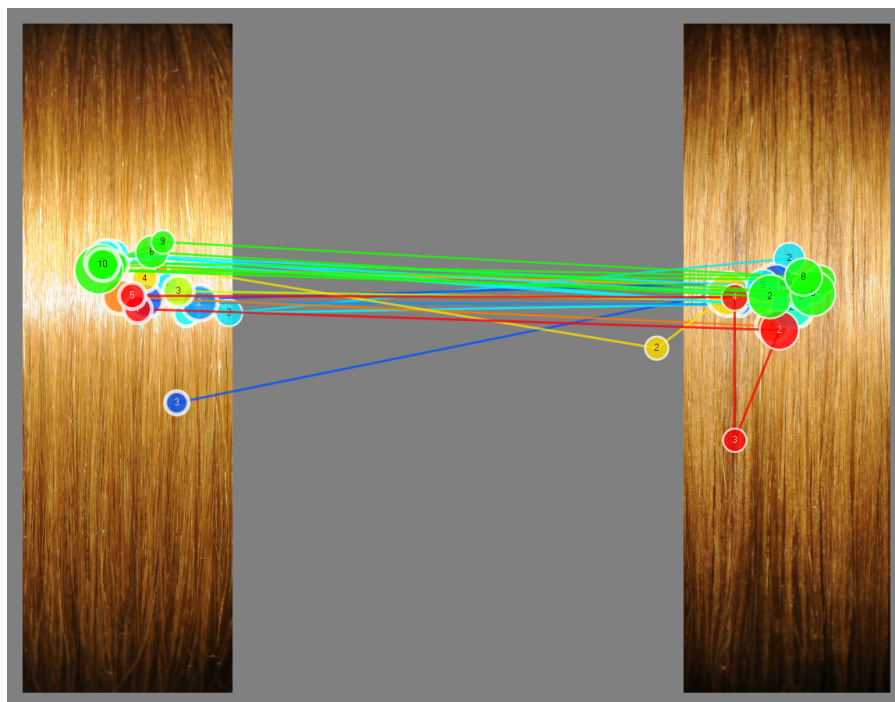


Figure 5-8 Gaze plot of all the participants (each colour is associated with a participant) on the Virgin tress (left) - Wax tress (right) evaluation screen.

Figure 5-9 shows a heat map of the same hair tress comparison. It is evident that the participants spent more time attending to the tress treated with wax than the image of virgin hair tress.

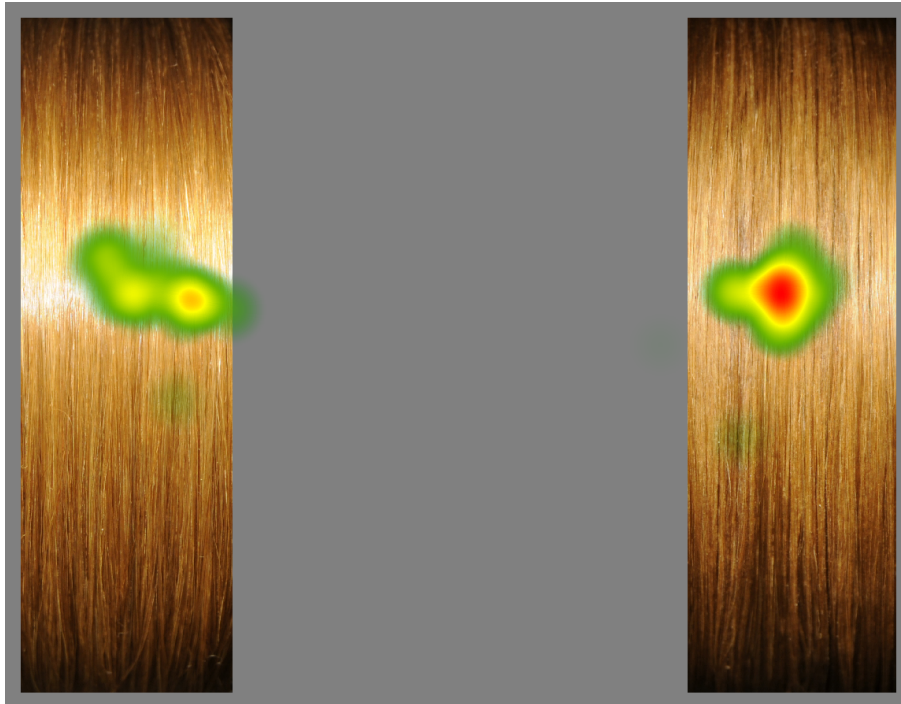


Figure 5-9 Heat map (time spent attending to AOIs, red represents high frequency, green low and yellow medium) of all the participants on Virgin-Wax evaluation screen of GUI

5.3.1.1 Time Taken and the number of fixations in the Evaluation process

The time taken to evaluate the shine varied from participant-to-participant. As the difference in terms of perceptual shine between wax and virgin tresses was high, it was believed that the participants would require less decision time in the virgin-wax evaluation. In this psychophysical study the data from three virgin-wax evaluations were analysed, the average time taken to record their choice, by each participant was 1.29 seconds, Figure 5-10 shows the average decision time taken by each participant.

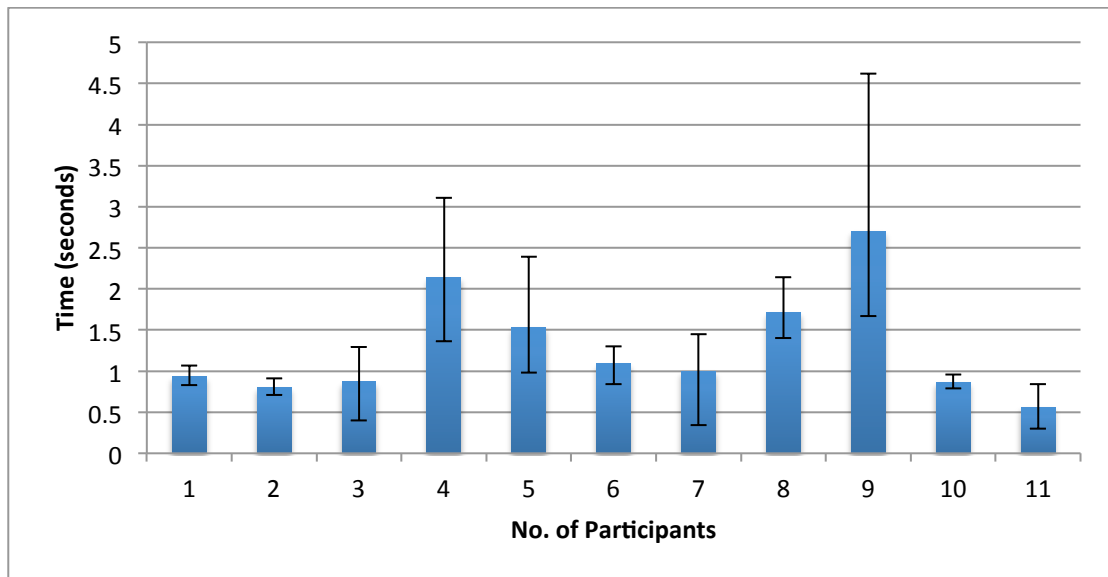


Figure 5-10 Average-time taken by each participant to record their decision, when the virgin (Blonde) – Wax (Blonde) hair tress appeared on the screen.

During the Blonde virgin-wax tress comparison, the number of times participants gazed at each of the tress images was calculated. Of the three evaluations on average each participant gazed approximately 4 times on the whole screen before recording their choice. Figure 5-11 shows the average fixation count of each participant.

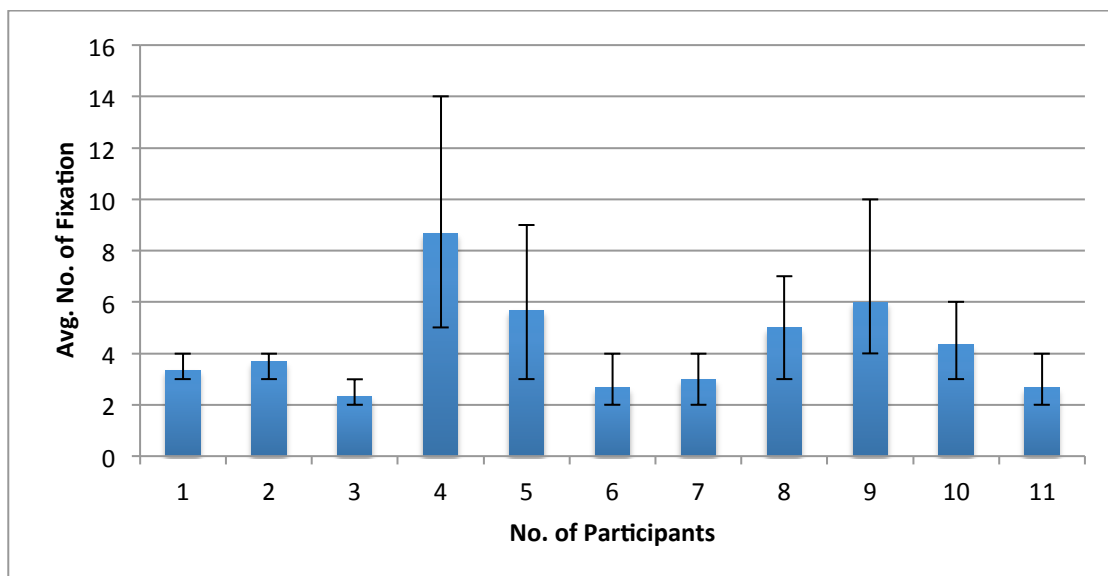


Figure 5-11 Average fixation-count of each participant during virgin-wax (blonde hair tresses) evaluation on the whole screen.

5.3.1.2 Time spent and number of fixation in the AOIs (Areas Of Interest)

As explained in Section 5.2.3.2, the Shine and Chroma areas (Top and bottom) were defined as AOIs on both tress images to determine the duration of fixation that participants were spending in a particular area. Of the three evaluations, the average time spent by the participant gazing at the shine area was approximately 0.48 seconds on left image and 0.62 seconds on right image, this suggests that the participants were spending more time attending to the right image, Figure 5-12 shows the average time spent by each participant gazing at the shine area of the hair tresses.

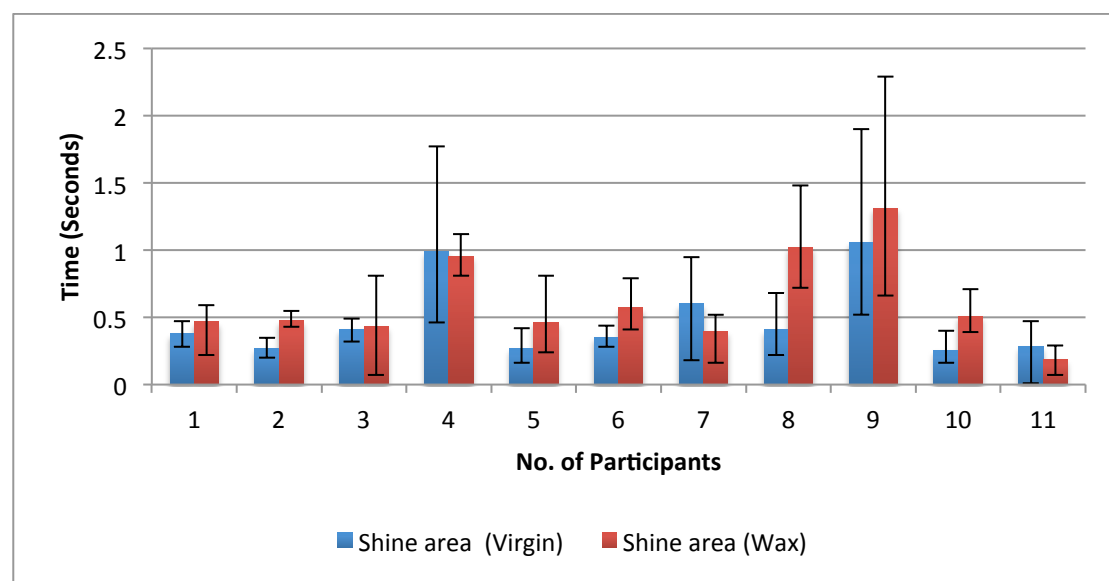


Figure 5-12 Average gaze duration spent by each participant attending to the shine area of the tresses

Of the three evaluations the average number of fixations in the shine area was approximately 1.5 times on the left image (virgin blonde) and 1.6 times on the right image (Wax blonde). Figure 5-13 shows the average number of gaze counts by the participants in the shine areas of the tresses.

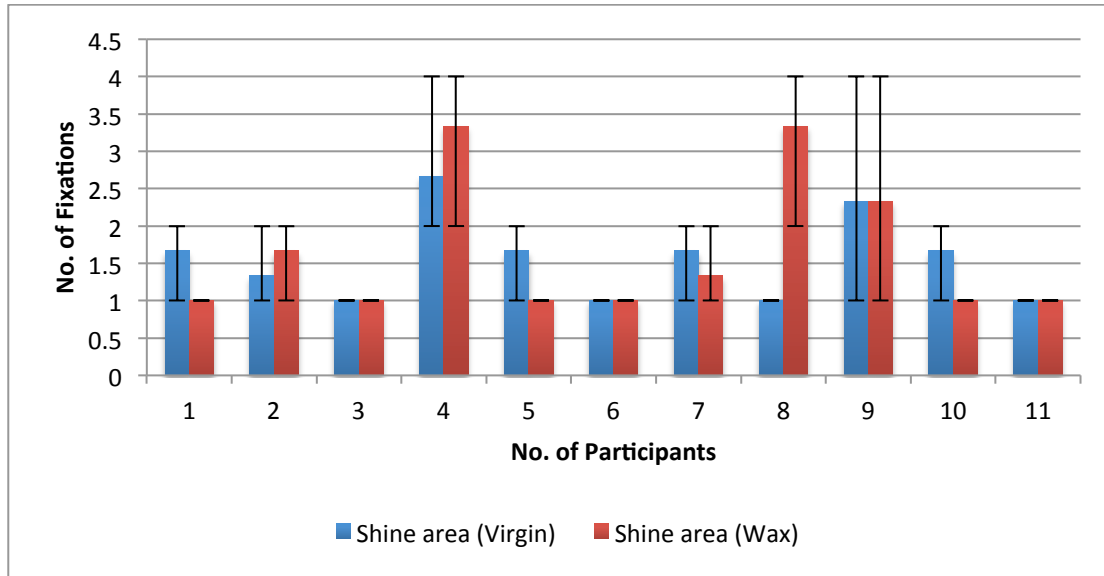


Figure 5-13 Average number of fixation counts of the participants in the shine areas of the Virgin-Wax blonde hair tress

The Chroma area of the hair tress was divided into two segments (1) the top Chroma area, which is above the shine area and (2) the Bottom Chroma area, which is below the shine area. Figure 5-6 (in the previous Section 5.2.3.2) shows the predefined Chroma regions selected on the hair tresses. In the Virgin-Wax comparison it was noted that the all participants did not attend to the Chroma areas of the tresses, out of eleven only two participants gazed in the top Chroma area of the virgin hair tress and one on the image of the wax hair tress. The total number of fixations in the Chroma-areas of both tress images was 28 times (15 on virgin hair tress and 13 on the wax treated tress image). It was noted that participants gazed three times more in the top-Chroma area then in bottom Chroma-area, this might be because top-Chroma area appears larger then bottom Chroma area. The difference in size of the Chroma-areas is because of the incident angle, as the light source is fixed at an angle of 20° relative to the sample holder (explained in Section 3.7.3) due to the angle of incident the bottom Chroma area appears smaller then top-Chroma area.

5.3.1.3 Decision and comparison with the formula

All of the participants chose virgin tress, as being the shinier of the two tresses, over the tress with wax applied on it. The values generated by all of the models showed the same trend although the ROC model was close to the participants' choices in terms of

sensitivity. The ROC₂ model predicted, on average, a 67% decrease in shine whereas the Modified Robbins model predicted an 18% decrease in shine. Table 5-4 shows the average shine values (three evaluations) generated by the different models and percentage difference in shine vales.

Table 5-4 Average values from different models and participants' choice. Highlighted value is the closest to the participants' choice

	Virgin	Wax	% Difference
Model type			
ROC ₁	893.23	291.46	-67.36 %
ROC ₂	657.04	217.81	-66.85%
Robbins*	262.55	214.78	-18.16%
Profile/width	96.55	84.35	-12.63%
User's choice	33	0	-100%

5.3.2 Blonde Virgin – Blonde SLES

In Virgin-SLES comparison, the difference in terms of perceptual shine between the tress images was low (i.e. both images exhibited a similar level of shine), in comparison with the virgin- wax pair. It was believed that the participants would require more decision time in Virgin-SLES than Virgin-Wax comparison. Figure 5-14 shows the gaze plot of the participants during the evaluation process and Figure 5-15 shows the durations of gaze spent by the participants on the screen as a heat map.

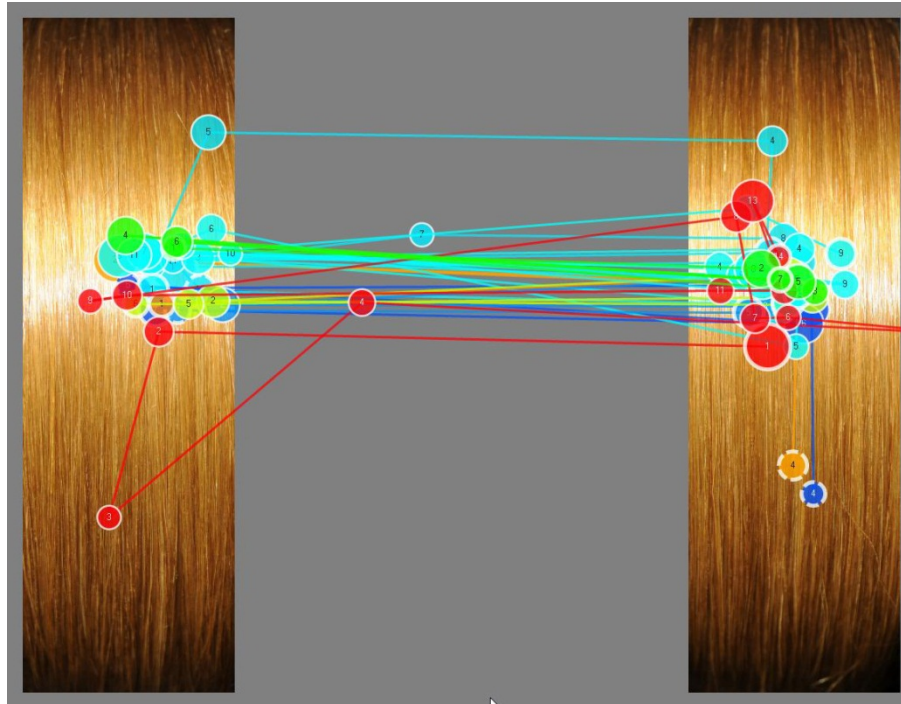


Figure 5-14 Gaze plots of all of the participants (each colour is associated with a participant) on the Virgin tress (left) - SLES tress (right) screen shot.

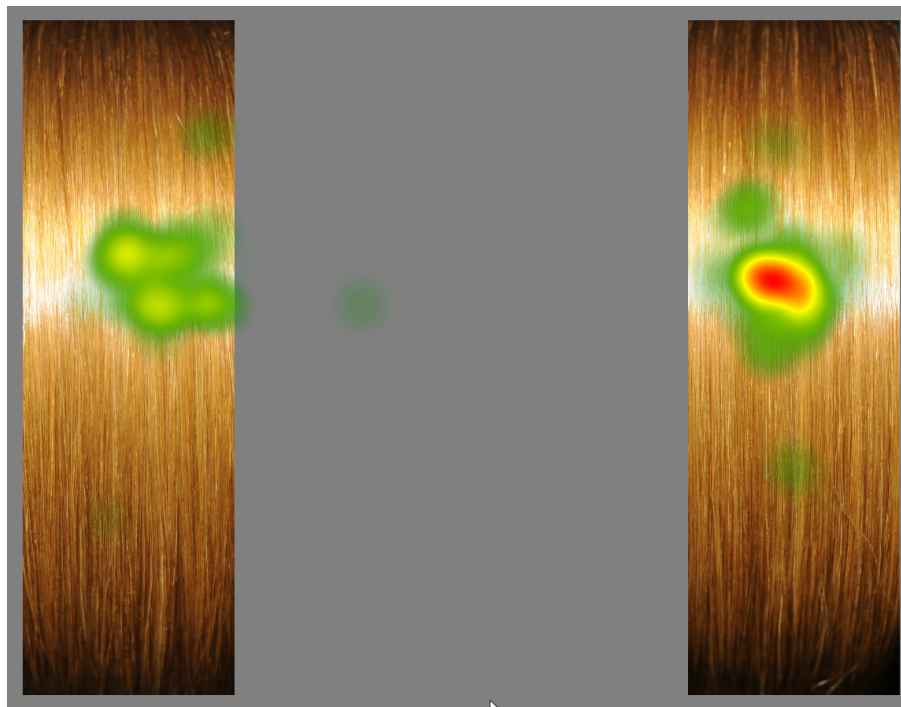


Figure 5-15 Heat map (time spent on the screen, red represents high frequency, green low and yellow medium) of all the participants on Virgin-SLES evaluation screen of GUI

5.3.2.1 Time Taken and number of fixation in the Evaluation process

The psychophysical study data from three Virgin-SLES comparisons showed that the average time taken by the participants to record the choice was doubled when

compared with average decision time of Virgin-Wax comparison Figure 5-16 shows the average duration taken by each user to record their decision. It was also noted the participants gazed twice as more in AOIs of Virgin-SLES comparison screen than Virgin-Wax AOIs Figure 5-17 shows the average number of fixations on the screen during the evaluation process by each participant.

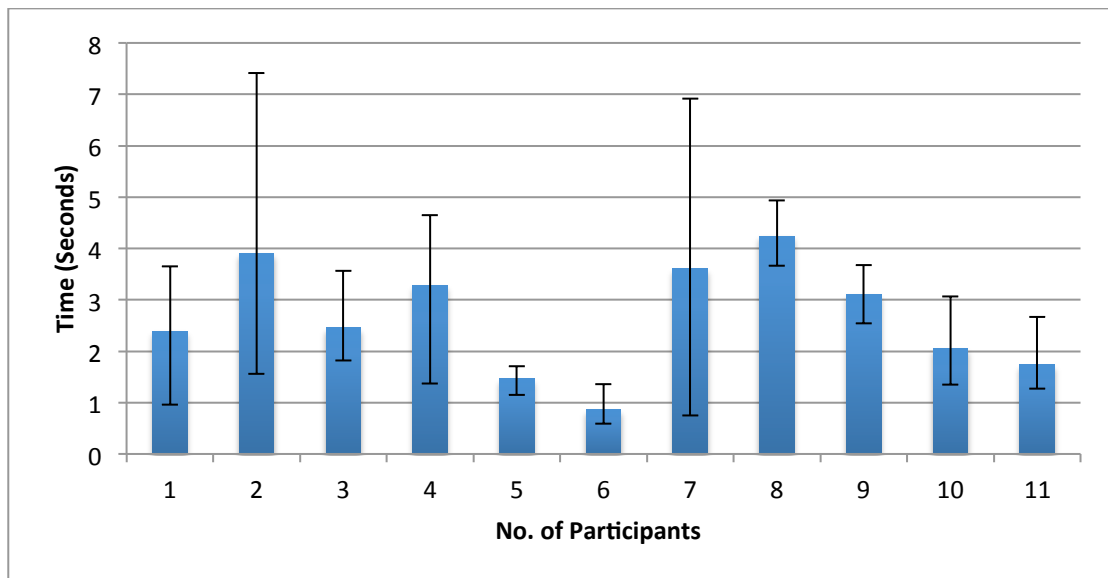


Figure 5-16 Average duration taken to record the decision by each participant during the Virgin-SLES (Blonde) evaluation process

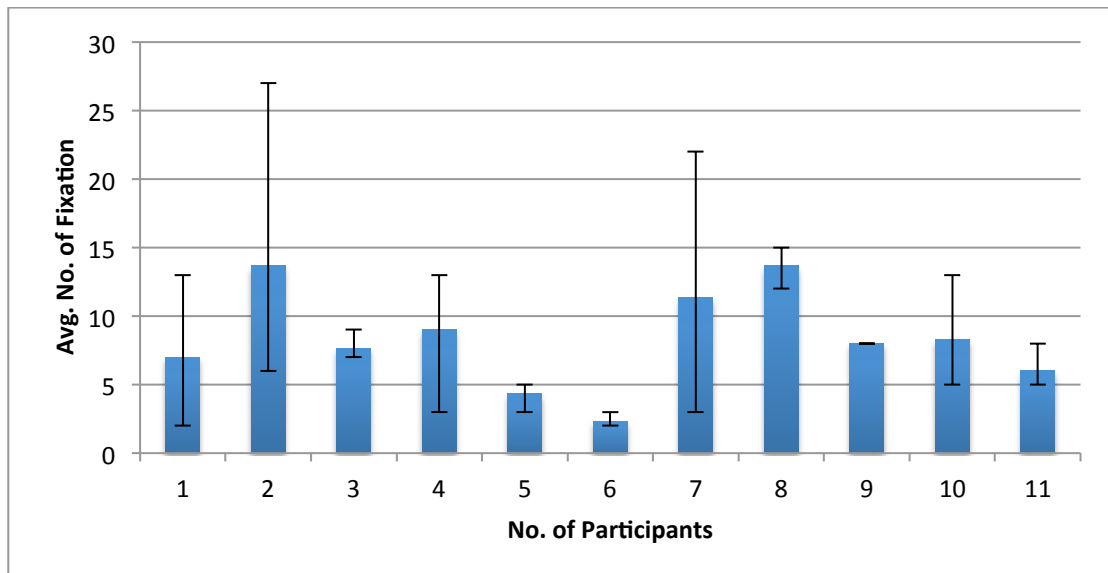


Figure 5-17 Average fixation count of each participant during Virgin-SLES evaluation process

5.3.2.2 Time spent and number of fixation in the AOIs (area of interest)

As explained in Section 5.3.2 the difference in terms of perceptual shine between the tress images was low in the Virgin-SLES comparison. It was expected that participant would spent more time, in making decision, in this comparison than Virgin-Wax comparison. Approximately 50% increase, from Virgin-Wax comparison, was noted in the average time spent by the participant in the shine areas of the tresses (0.75 seconds on left image and 1.05 seconds on right image). Figure 5-18 shows the average duration spent by each participant in the shine area of the hair tresses. Similarly higher number of fixations was recorded in the shine areas of the Virgin and SLES washed hair tress images, when compared with Virgin-Wax comparison. The average number of fixations in the shine area was approximately 2.3 times on the left image (virgin blonde) and 3 times on the right image (SLES blonde). Figure 5-19 shows the average gaze frequency by the participants in the shine areas of the tresses.

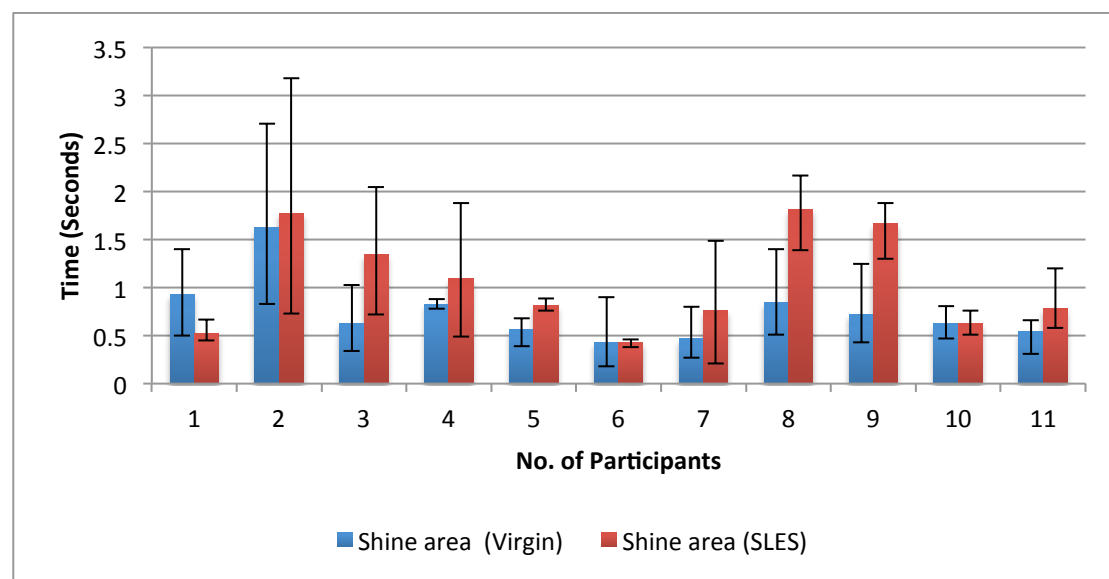


Figure 5-18 Average times spent by the participant within the Shine areas of the hair tress

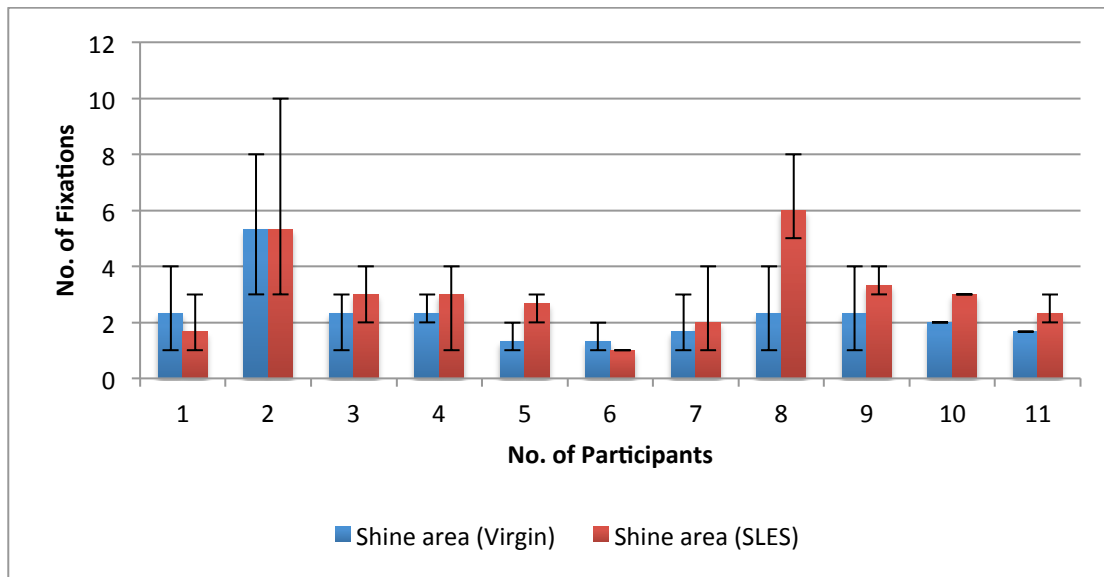


Figure 5-19 Average number of fixations within the Shine areas of the hair tresses

In the virgin-SLES comparisons it was noted that as the shine difference reduces between the hair tresses, some participants shifted their gaze from shine area to the Chroma areas. More than 100% increase in the number of fixations was recorded in the Chroma-areas of the Virgin-SLES comparison than Virgin-Wax comparison.

Out Of the 33 evaluations (11 participants x 3 repeats) the total number of fixations by the participants was 58 times in the Chroma-areas of the both tress images (28 times on the Virgin tress image and 31 on the SLES washed tress image). This shows how important Chroma-area is in evaluating the hair shine.

5.3.2.3 Blonde Virgin-SLES Decision and comparison with the formula

In this comparison the difference in shine was perceptually smaller (when compared with the virgin-wax shine difference), and the participants' decisions varied in the repeats. Overall, out of 33 evaluations the most popular choice was the tress washed with SLES, where 18 votes were recorded. The ROC_1 and ROC_2 models showed a positive change in shine differences of 13.61% and 13.84% respectively, which suggested that the SLES treated tresses were shinier. This can be directly related to the participants' choices. The Robins model showed a negative change in shine difference, which suggested that the Virgin Tresses were shinier, which was contrary to the panel decision. Table 5-5 shows the average shine values (out of three evaluations) generated by the different models.

Table 5-5 Average shine values of Virgin and SLES tresses generated by different models and participants' choice. Highlighted value is the closest to the participants' choice

	Virgin	SLES	% Difference
Model type			
ROC₁	893.23	1014.78	13.61%
ROC₂	657.05	747.98	13.84%
Robbins*	262.43	258.65	-1.44%
Profile/width	96.55	95.57	-1.01%
User's choice	15	18	20%

5.3.3 Blonde Virgin- Blonde Shine spray

Figure 5-20 shows the gaze plot of all of the participants on the virgin-shine spray comparison screen shot, the tress on the left of the image was an untreated blonde hair tress (Virgin) and the image on the right was of a tress treated with shine spray. Both tresses exhibited different visual appearance, tress treated with shine spray showed higher contrast between the shine band and the Chroma band when compared with the image of Virgin blonde hair tress. Figure 5-21 shows the duration spent in the AOIs on the screen in the form of a heat map.

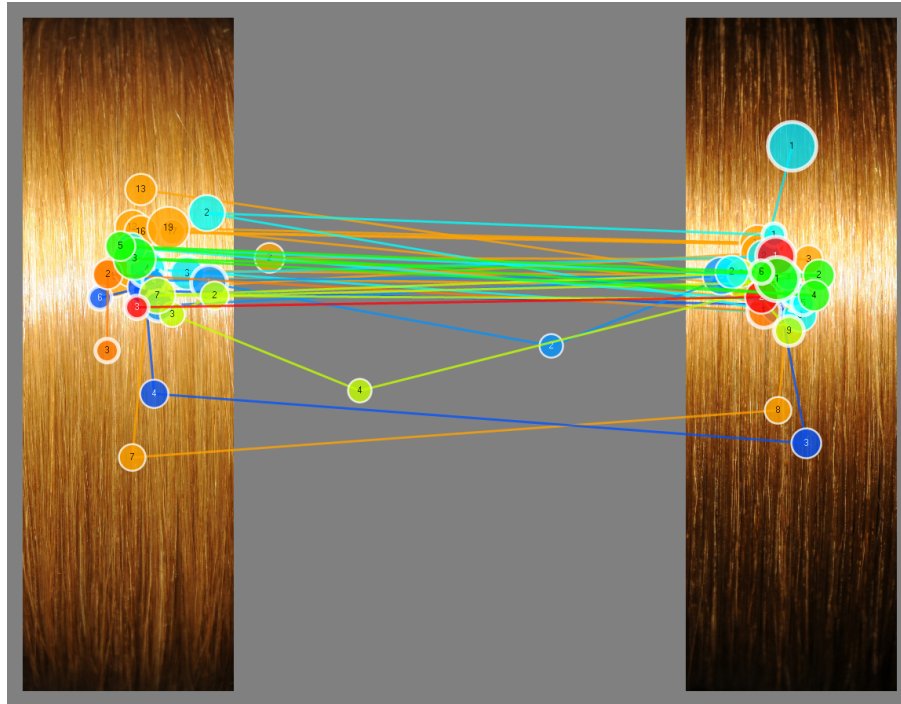


Figure 5-20 Gaze plot of all of the participants (each colour is associated with a participant) on the Virgin tress (left) - Shine Spray (right) screen shot.

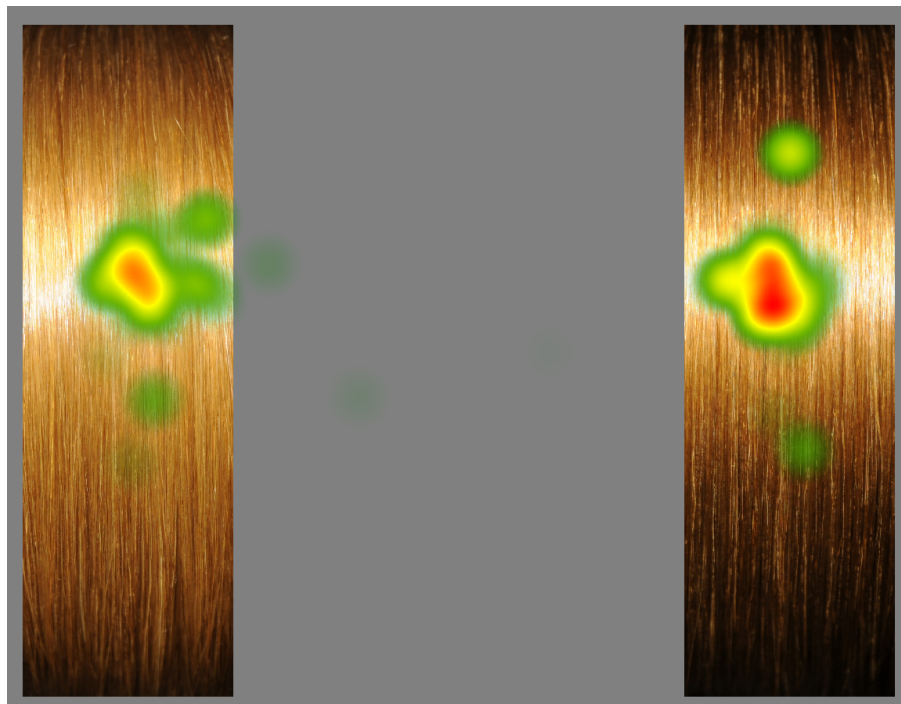


Figure 5-21 Heat map (duration spent gazing at AOIs on the screen, red represents high frequency, green low and yellow medium) of all the participants on Virgin-Shine spray evaluation screen of GUI

5.3.3.1 Time Taken and number of fixation in the Evaluation process

In Virgin-Shine spray comparison it was believed that the participants will spent less time to decide due to the higher visual appearance difference between the two tress images than Virgin-SLES comparison, the average decision time was approximately 20% lower than the Virgin-SLES comparison (average decision time in Virgin-Shine Spray was 2 seconds, out of three evaluations). Interestingly participants gazed approximately 7 times (on average) at the AOIs on the screen, which is similar to the Virgin-SLES comparison average gaze count (8) at the AOIs.

Most of the participant suggested that the tress treated with shine spray appear 'unhealthy' when compared with the image of Virgin hair tress, even though the shine-spray treated tress showed higher contrast. This might be the reason why participant gazed 75% more in Virgin –Shine spray comparison than Virgin-Wax comparison. Figure 5-22 shows the average time taken by each user to record their choices. Figure 5-23 shows the average number of fixations within AOIs on the screen during the evaluation process by each participant.

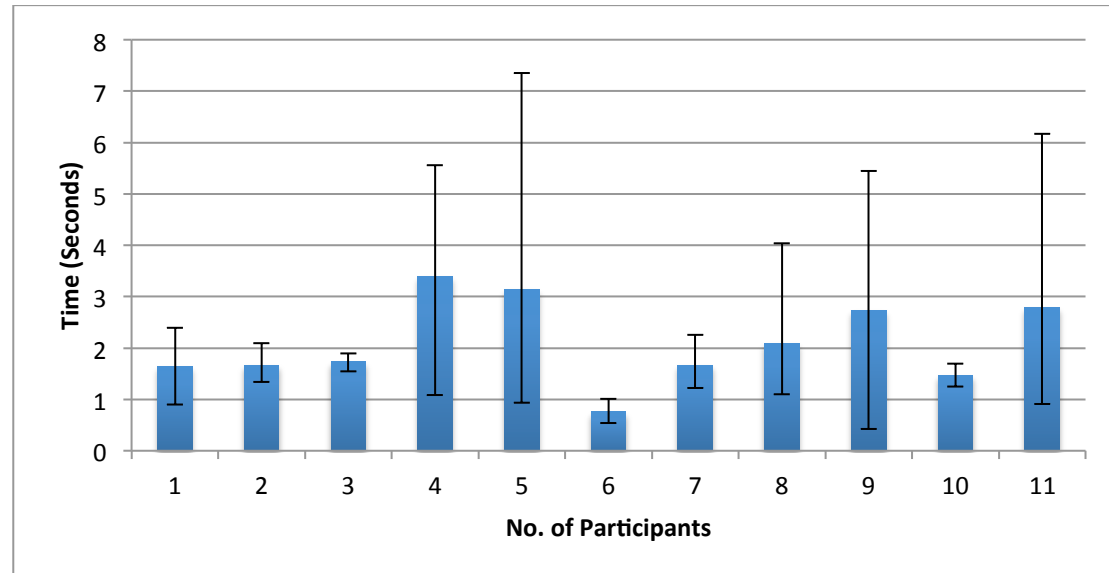


Figure 5-22 Average times taken to record the choice, by each participant during the Virgin-Shine Spray (Blonde) evaluation process

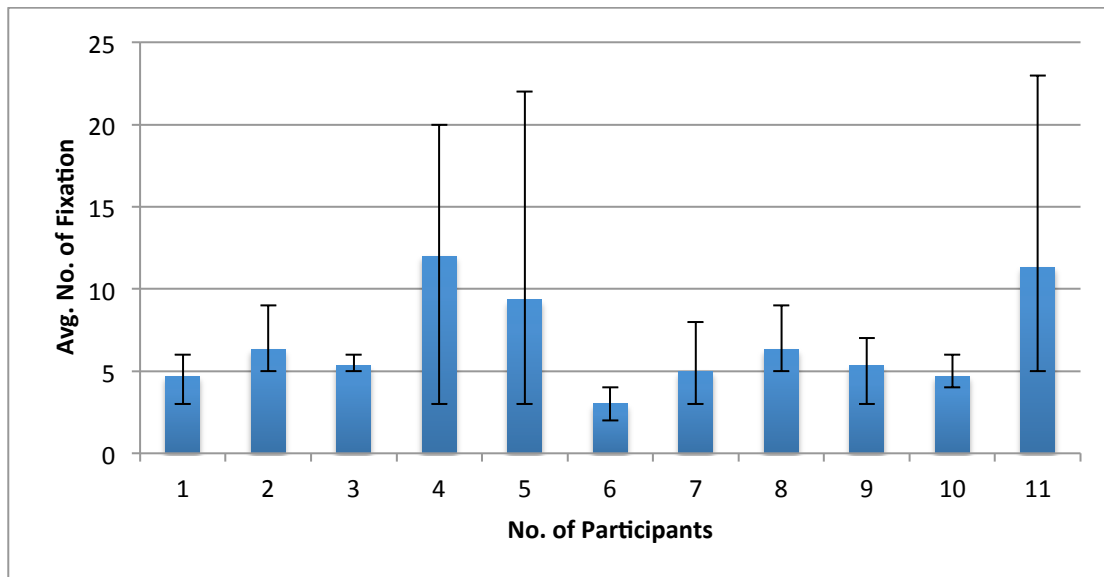


Figure 5-23 Average fixation count by each participant during Virgin-Shine Spray evaluation process

5.3.3.2 Time spent and number of fixation in the AOIs (area of interest)

Out of three evaluations average time spent by the participant in the shine areas was 0.62 seconds on left image and 0.94 seconds on right image. The average number of fixations in the shine area was approximately 2 times on the left shine-area and 2.6 times on the right shine-area. Figure 5-24 shows the average time spent by each participant attending to the shine area of the hair tresses and Figure 5-25 shows the average gaze frequency by the participants in the shine areas of the tresses.

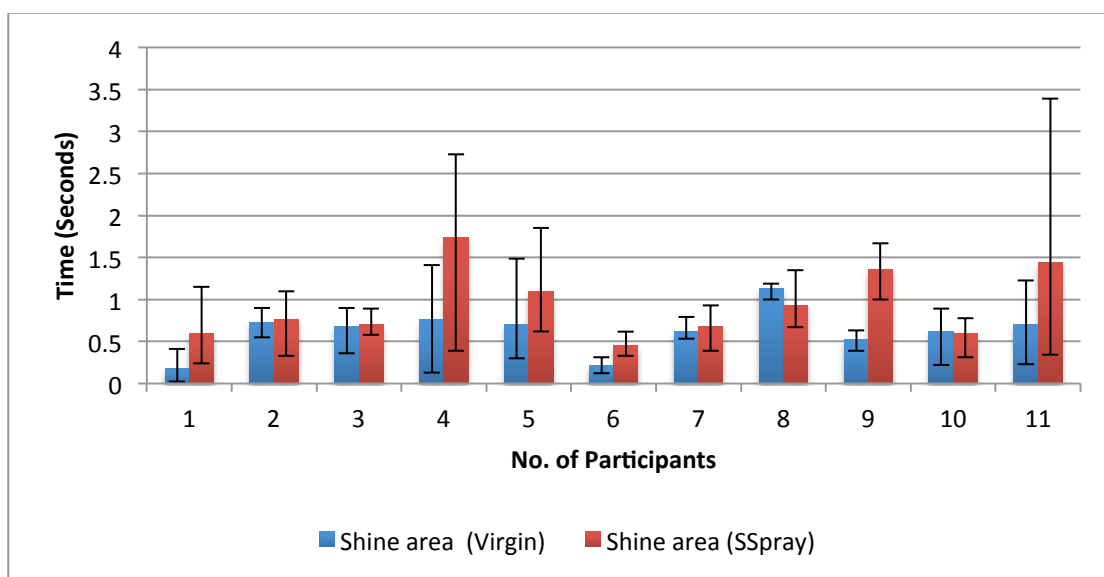


Figure 5-24 Average time spend by each participants in the Shine area of the tresses

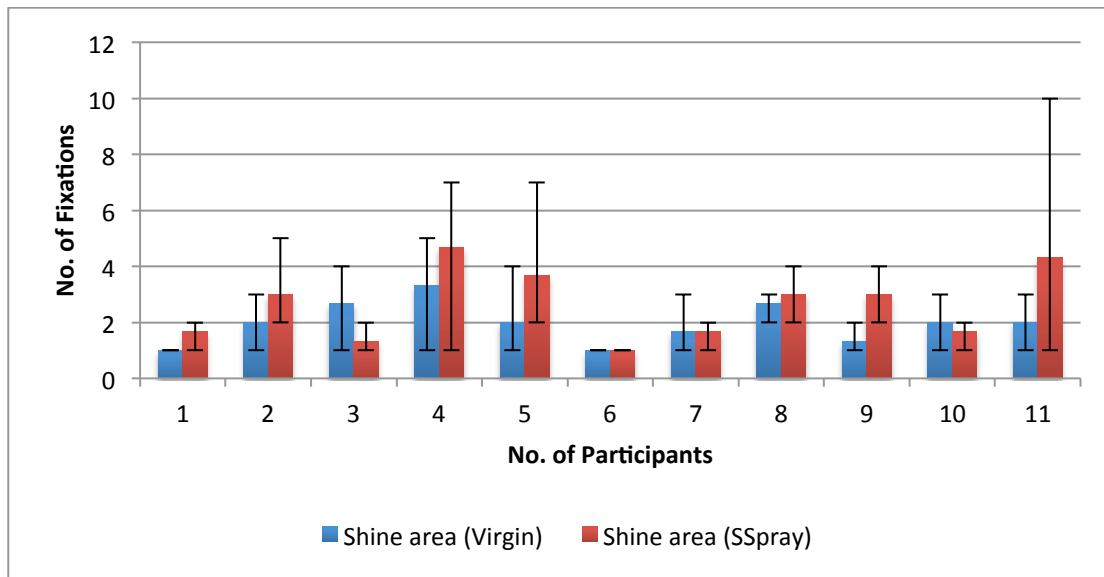


Figure 5-25 Average fixation frequency of the participants in the Shine areas of the Virgin-Shine Spray blonde hair tress

In the virgin-Shine spray comparisons it was noted that shine spray treated tress showed higher contrast between shine band and Chroma band but feedback from the participants suggested that the tress appeared to be ‘unhealthy’ due to this most of the participant shifted their gaze from shine area to the Chroma areas of the tresses. Out of the 33 evaluations (11 participants x 3 repeats) the total number of fixations recorded by the participants was 44 times in the Chroma-areas of the both tress images (25 times on the Virgin tress image and 19 on the Shine sprayed tress image). This shows how important Chroma-area is in evaluating the hair shine.

5.3.3.3 Blonde Virgin-Shine Spray Decision and comparison with the Models

Of the 33 evaluations 30 decisions were in favour of the Virgin hair tress over the tress sprayed with Shine Spray. The Models’ values varied in this comparison, the modified Robbins model and the Profile-width model showed positive differences, 10.35% and 12.24% respectively, suggesting that the Shine Spray was shinier. The ROC_1 and ROC_2 models produced negative differences, -19.62% and -16.85% respectively, suggesting that the Virgin Tress was Shinier, which more closely followed the participants’ choice. Table 5-6 shows the values generated by the models and participants’ choices.

Table 5-6 Average shine values of Virgin and SLES tresses generated by the different models and the participants' choices.

	Virgin	Shine Spray	% Difference
Model type			
ROC₁	893.23	717.94	-19.62%
ROC₂	657.04	546.32	-16.85%
Robbins*	262.55	289.73	10.35%
Profile/width	96.73	108.57	12.24
User's choice	30	3	-90%

5.3.4 Comparisons of Tresses treated with same products

As stated in the section 5.3.2.1 when the shine difference between the tresses was low (i.e. both tress images exhibited a similar level of shine), the average decision was time increased. In Virgin-SLES comparison average decision time was doubled when compared with Virgin-Wax comparison. The pair comparisons of tresses treated with similar products, for example Virgin-Virgin comparison, showed similar trend Figure 5-26 shows the gaze plots of all the participants in the Virgin-Virgin, Wax-Wax, SLES-SLES and Shine Spray-Shine spray comparisons and Figure 5-27 shows the duration spent on the screen in the form of heat map.

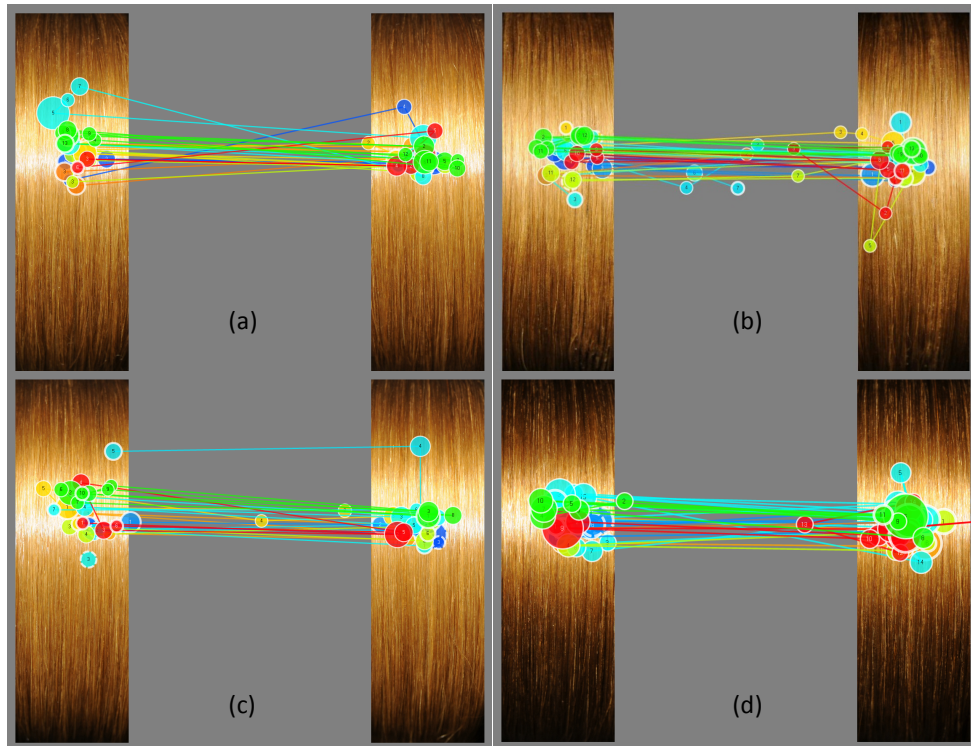


Figure 5-26 Gaze plots of all of the participants (each colour is associated with a participant) on the (a) Virgin – Virgin, (b) Wax-Wax, (c) SLES-SLES and (d) Shine Spray-Shine spray screen shot.

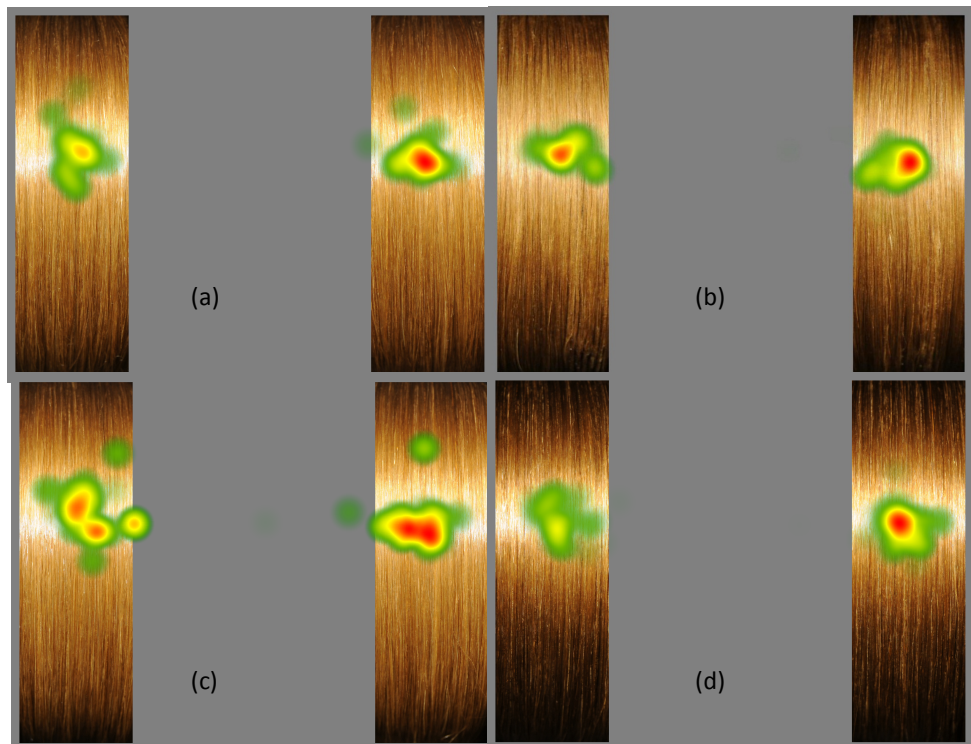


Figure 5-27 Heat map (time spent on the screen, red represents high frequency, green low and yellow medium) of all of the participants viewing areas on a (a) Virgin – Virgin, (b) Wax-Wax, (c) SLES-SLES and (d) Shine Spray-Shine spray screen shot.

5.3.4.1 Time Taken and number of fixations in the Evaluation process

The average time spent in making a decision depends upon the difference in the shine between the tresses. In the Virgin–Wax comparisons the average time taken to make a decision was 1.29 seconds, whereas tresses with similar visual appearance, in terms of shine, for-example Shine Spray–Shine Spray comparisons the average time taken to decide which one was shinier was 3.12 seconds. Figure 5-28 shows the average time taken by participants to record their decision.

Interestingly the average number of fixation in the AOIs during the similar tress comparisons were approximately the same, Figure 5-29 shows the average number of fixation by the participants during the pair comparison of tress treated with similar products. This suggests that, regardless of treatment type, participant behaved in a similar pattern while evaluating the shine of tresses exhibiting similar visual appearance.

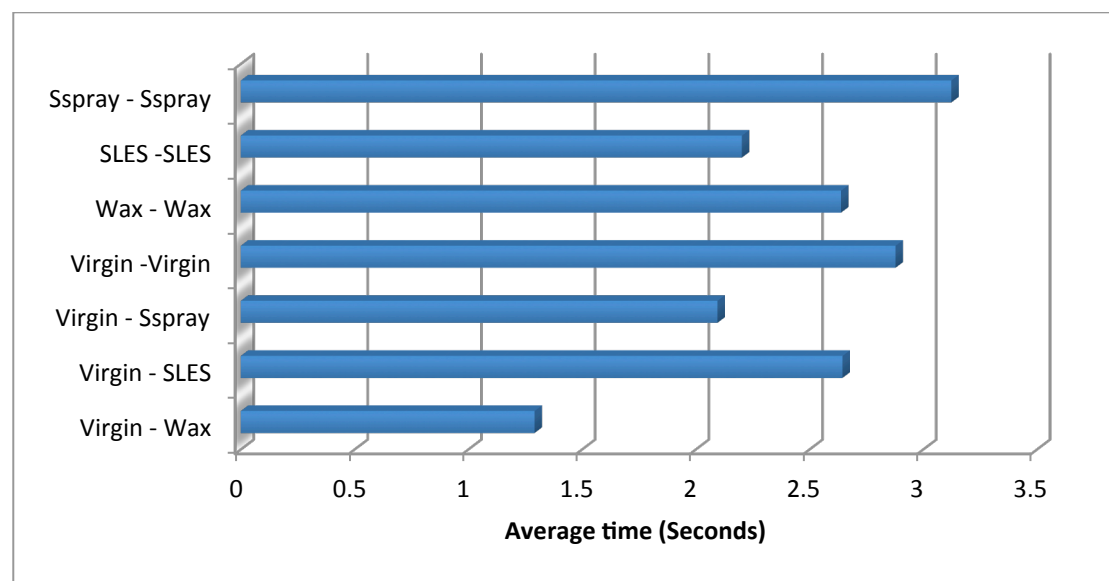


Figure 5-28 Average times taken by the participants to record their decision.

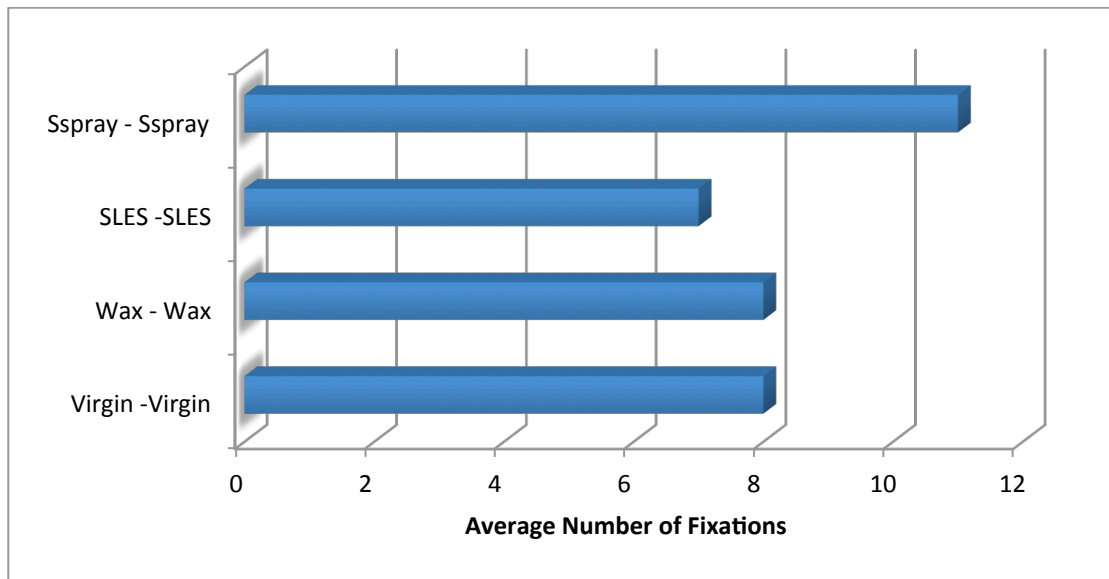


Figure 5-29 Average number of fixations by the participants in the AOIs on the screen shot of the pair tress comparison of similar tresses.

5.3.4.2 *Number of fixations in the Chroma-areas*

As explained in section 5.3.2.2 it was noted that as the shine difference reduces between the hair tresses, some participants shifted their gaze from shine area to the Chroma areas. This suggests that in pair comparison psychophysical test when the tress appears to be similar participant uses Chroma areas of the tresses to decide which tress appears to be shinier. Figure 5-30 shows the total number of fixation in the Chroma areas of the both images in 33 evaluations.

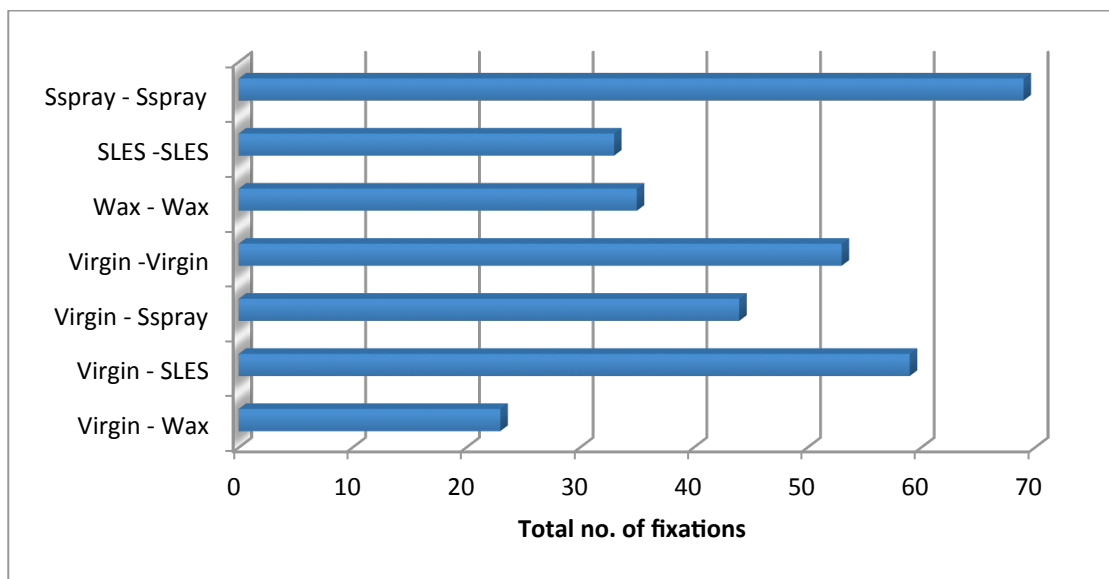


Figure 5-30 Total number of fixations in the Chroma areas of both images (top and bottom) in 33 evaluations.

5.3.4.3 Decision and comparison with the models

Unlike the other models, the ROC models uses information about both the Shine and Chroma bands to produce the hair shine values. The values generated by the ROC modes correlate well with the participants' panel decisions. Figure 5-31 shows the shine value percentage increase or decrease of the right image when compared with left image of the tress. Other than the Shine Spray–Shine Spray comparison the ROC model showed the same trend, with high sensitivity, when compared with the participants' panel choice, whereas other models were not sensitive enough.

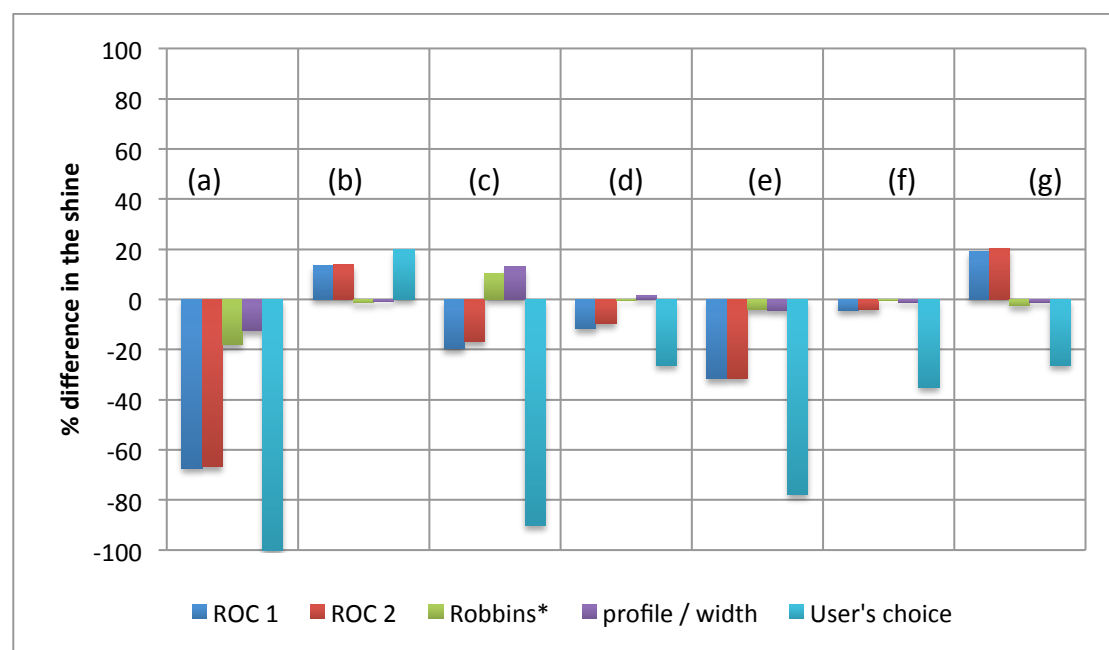


Figure 5-31 Percentage increase or decrease of shine value between the left image and right image. (a) Virgin-Wax comparison, (b) Virgin-SLES comparison, (c) Virgin-Shine spray comparison, (d) Virgin-Virgin comparison, (e) Wax-Wax comparison, (f) SLES-SLES comparison, (g) Shine Spray-Shine Spray comparison.

5.4 Data analysis of European Brown and Oriental hair tresses

To reduce the repetition of the analysis and to improve the readability of the thesis three main comparisons will be discussed: (a) Virgin-Wax (high difference in shine), (b) Virgin-SLES (medium difference), and (c) Virgin-Shine Spray.

5.4.1 Virgin-Wax comparison (European Brown and Oriental)

In the Virgin-Wax comparison the users behaved in a similar way to when they were evaluating the shine differences of the Blonde hair tresses. Thus, the participants only gazed in the shine and Chroma areas of the tresses. Figure 5-32 shows the gaze plots on the screenshot of the Virgin-Wax comparison of European-Brown and Oriental hair tresses. It can be noted there are similarities in the gaze plots for the different types of hair even though the tresses are different in colour. Figure 5-33 shows the area where participants spent more viewing time in the form of a heat map on the screen shots of the comparison GUI.

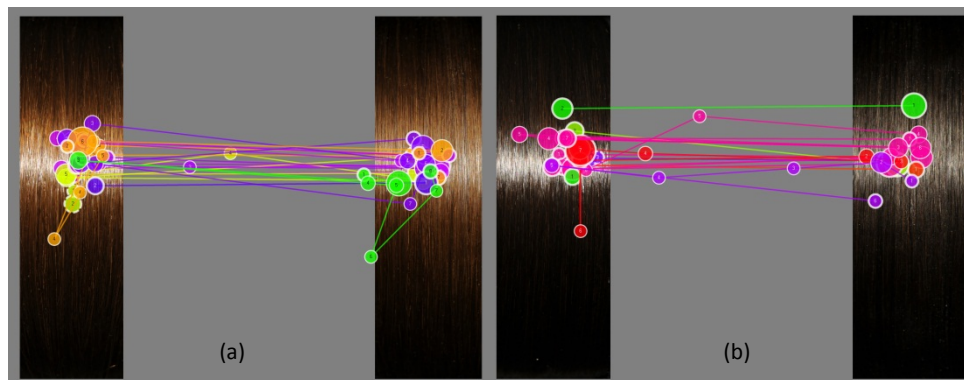


Figure 5-32 Gaze plots of all of the participants (each colour is associated with a participant) on the (a) Virgin-Wax comparison European Brown hair tress, (b) Oriental hair tress

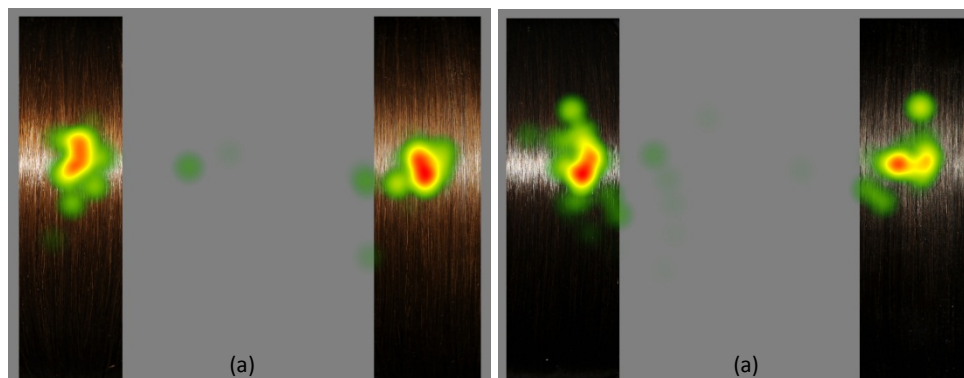


Figure 5-33 Time spent attending to the tresses by the participants in the form of heat maps (a) European Brown, (b) Oriental hair tress.

5.4.1.1 Decision Time Taken and number of fixation in the Evaluation process

In this comparison the shine band was prominent on only one hair tress (Virgin), on the second image (wax treated hair tress) the shine band was not visible. With the difference in shine easily noticeable, participants spent less time in deciding which tress was shinier. The average time taken to record the choice by the participants was 1.49 seconds for the European Brown tress (out of three evaluations) and 1.55 seconds in Oriental hair tress. The observer gazed approximately 5 times on both of the evaluation screens (EB and Oriental tresses) to evaluate the shine. Figure 5-34 shows the average time taken by each user to record their decision. Figure 5-35 shows the average number of fixations on the screen during the evaluation process by each participant.

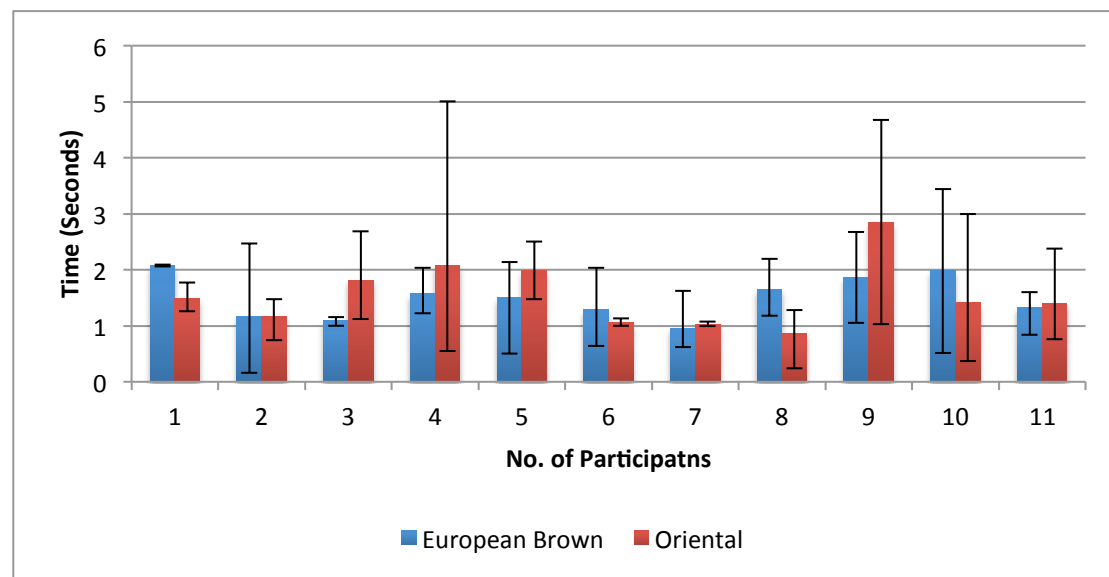


Figure 5-34 Average decision durations taken by each participant during the Virgin-Wax (for both European-Brown evaluations and Oriental hair tress evaluations) evaluation process

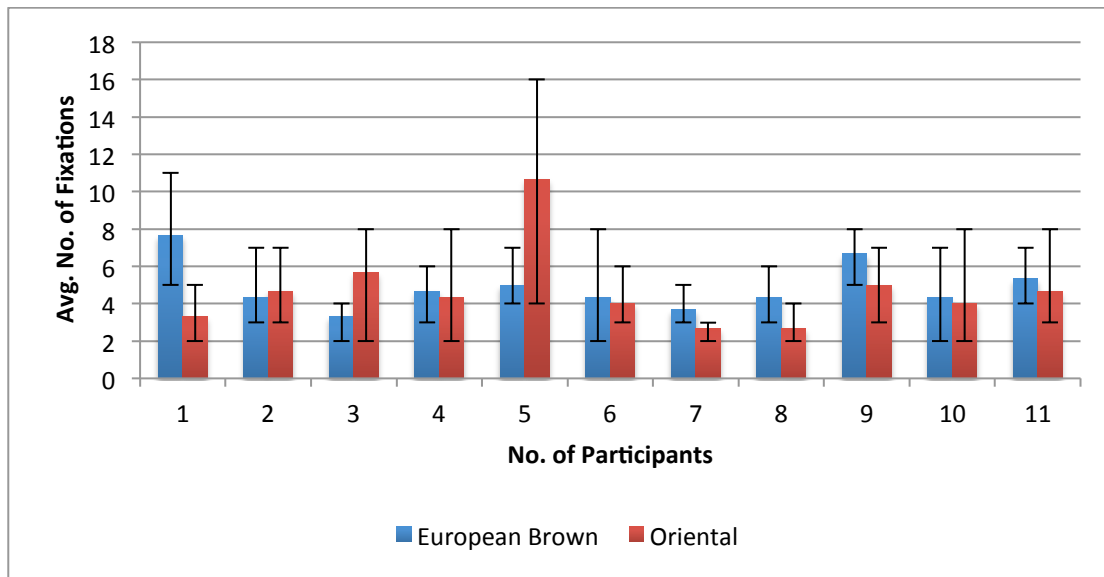


Figure 5-35 Average fixation counts for each participant during the Virgin-Wax evaluation process for European Brown and Oriental hair tresses

5.4.1.2 Fixation Duration and fixation frequency in the AOIs (areas of interest)

It was interesting to note that the average times spent by the participants attending to the shine areas of the Virgin tresses (European brown and Oriental) were the same, they spent 0.55 seconds (on average, out of three evaluations) attending to the left image of the evaluation screen and spent 0.7 and 0.78 seconds on the right image of the evaluation screen, for the European brown and Oriental comparisons respectively. Figure 5-36 and Figure 5-37 show the average time spent by each participant in the shine area of the European brown and Oriental hair tresses respectively.

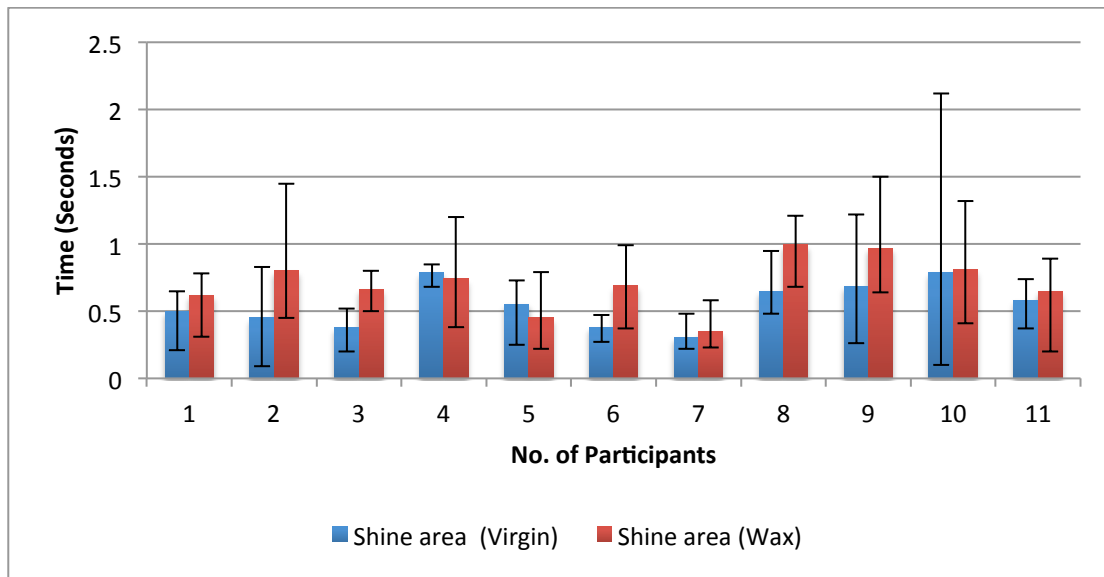


Figure 5-36 The average times spent by the participants fixating within the shine areas of the European Brown hair tresses (Virgin-wax comparison).

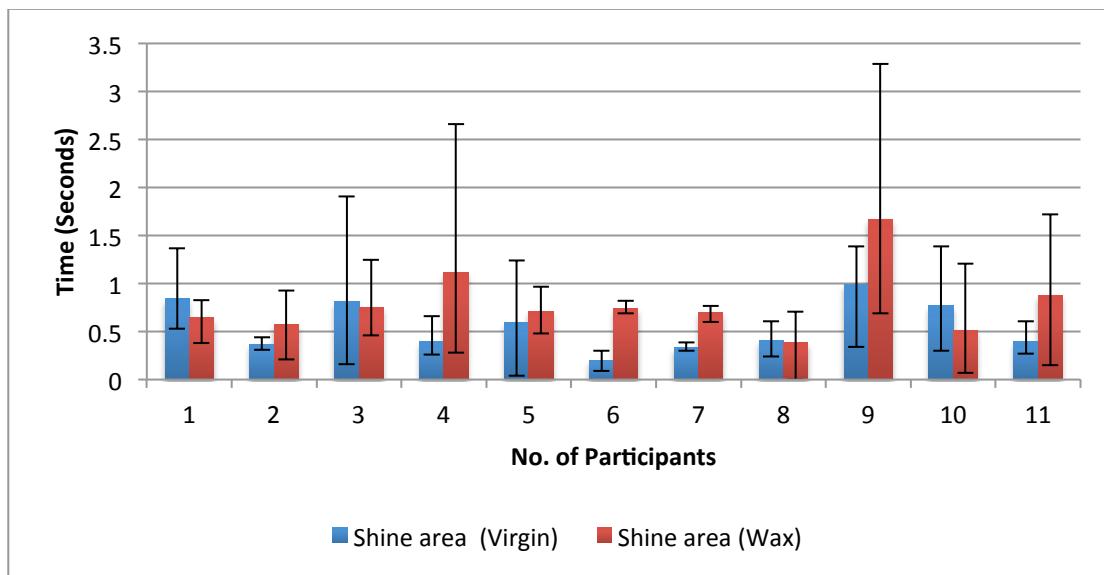


Figure 5-37 The average times spent by the participants fixating within the shine areas of the Oriental tresses (Virgin-Wax comparison)

The average numbers of fixations in the shine area of the virgin European brown and Oriental hair tress were 1.7 and 1.6 times respectively, whereas the average number of fixations recorded in the shine areas of right images (wax) were 2 times on European brown hair tress and 1.75 times on oriental hair tress. Figure 5-38 shows the average gaze frequency of the participants in the shine areas of the European Brown and Oriental hair tresses.

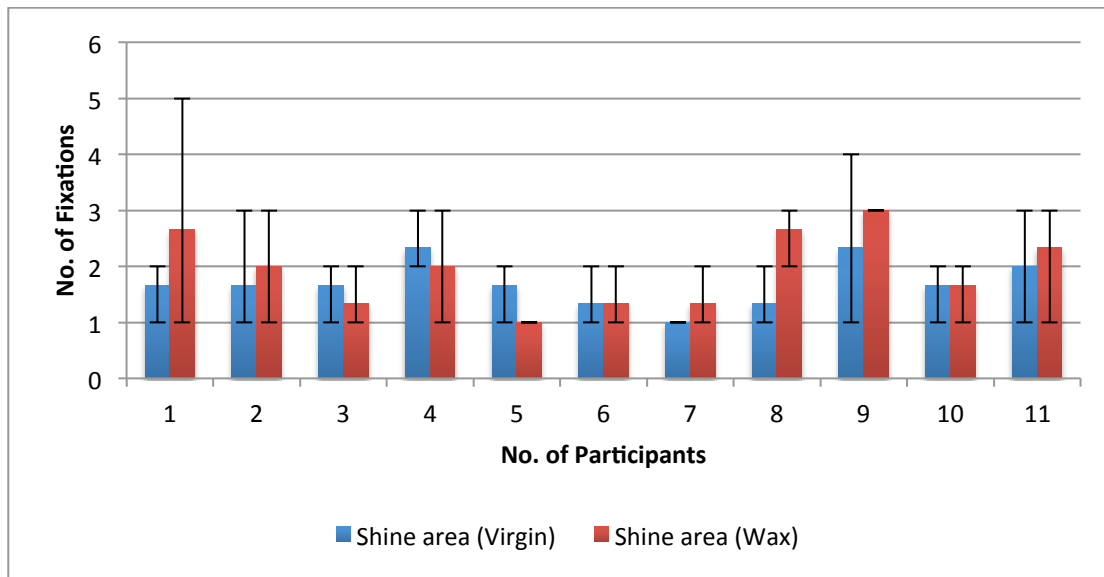


Figure 5-38 Average number of gaze count of the participants in the shine areas of the tresses.

In the Virgin-Wax comparison, participants do not appear to attend frequently to the Chroma-areas of the tresses. The observers gazed a total of 9 times (all repeats included) in the top Chroma area and two fixations were recorded out of 33 evaluations in the bottom Chroma area of the Virgin hair tress. In the top Chroma area of the right image (Wax), two participants' gazed in the Chroma top area (out of 33 evaluations) and three in the bottom Chroma area. This would suggest that when the difference between the tresses in terms of shine is easily noticeable, such as in the Wax and Virgin tress comparisons, that the majority of the participants would need only to gaze in the shine area in order to have enough information to make their decision.

5.4.1.3 Decision and comparison with the formula

All of the participants chose the Virgin tress, as being the shiniest, over the tress with wax applied. The values generated by the models showed the same trend as the Blonde analysis, with the ROC model being most closely correlated with the participants' choices in terms of sensitivity. The ROC₂ model produces, on average, a 66% decrease in shine whereas the Robbins model predicted a 23% decrease in shine. A similar trend was noted in the Oriental Virgin-Wax comparison as the ROC₂ model generated shine values that were closer to participants' choice. The percentage difference in shine values was -85% whereas the Robbins model showed a -41% reduction in shine on the tress treated with wax. Table 5-7 shows the average shine values of the European Brown tress

comparison (three evaluations). Table 5-8 shows the average shine values of the Oriental tress comparisons; generated by the different models and the percentage difference in shine vales.

Table 5-7 Average shine values of European Brown Virgin and Wax tresses generated by different models and participants' choice. The highlighted value is the closest to the participants' choice

	Virgin	Wax	% Difference
Model type			
ROC ₁	1814.92	617.38	-65.98%
ROC ₂	1119.50	383.66	-65.73%
Robbins*	285.59	217.97	-23.68%
Profile/width	107.40	83.08	-22.64%
User's choice	33	0	-100%

Table 5-8 Average shine values of Oriental Virgin and Wax tresses generated by the different models and the participants' choice. The highlighted value is the model closest to the participants' choice

	Virgin	Wax	% Difference
Model type			
ROC ₁	1181.17	337.59	-71.42%
ROC ₂	99.03	14.77	-85.09%
Robbins*	303.89	178	-41.43%
Profile/width	112.62	68.87	-37.96%
User's choice	33	0	-100%

5.4.2 Virgin-SLES Comparison

In the Virgin-SLES comparisons, the shine bands were prominent but in terms of intensity the shine band on the tresses washed with SLES appeared to be more intense. This may be a reason why participants spent more time evaluating the shine. Figure 5-39 shows the gaze plots of the participants on a screenshot of the comparison. Figure 5-40 shows the time spent by the participants in terms of a heat map on the screenshot.

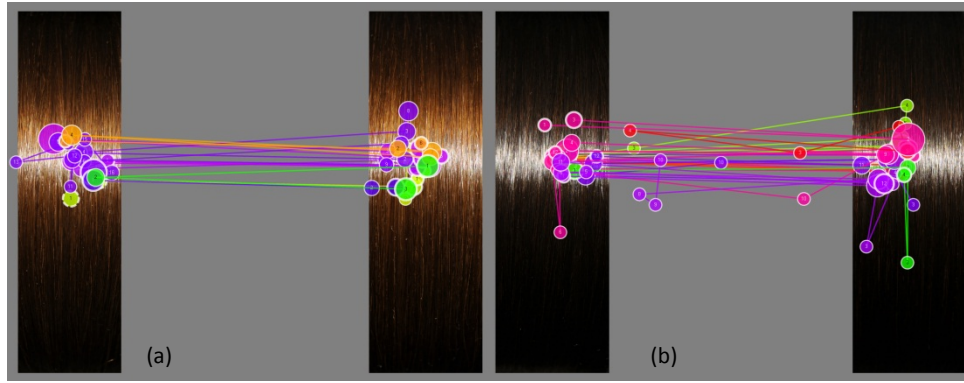


Figure 5-39 A gaze plot of all of the participants' gaze patterns (each colour is associated with a participant) on the Virgin tress (left)-SLES tress (right) screenshot. (a) European Brown hair tress paired comparison, (b) Oriental hair tress paired comparison

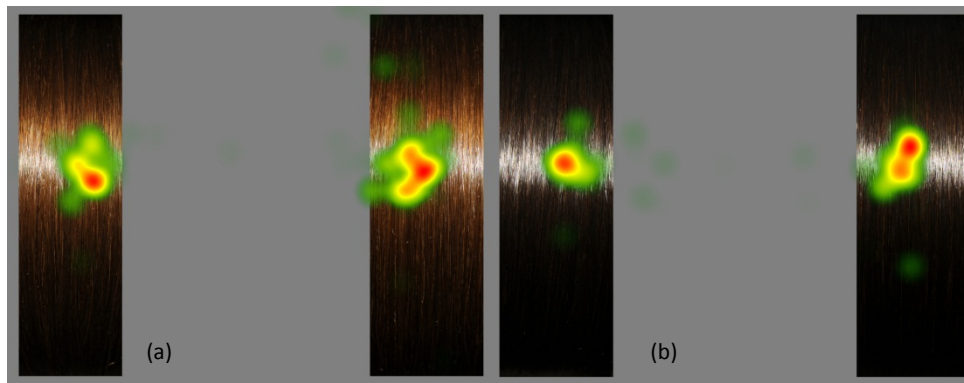


Figure 5-40 Heat map (time spent viewing areas of the screen, red represents high frequency, green low and yellow medium) of all of the participants, overlaying a Virgin-SLES evaluation screen. (a) European Brown hair tress paired comparison, (b) Oriental hair tress paired comparison

5.4.2.1 Decision durations and fixation frequency in the evaluation process

In the Virgin-SLES comparison the average time taken to record the decision was approximately 3 seconds in the European Brown tress comparison and approximately 2.6 seconds in the Oriental tress comparison. The numbers of fixations recorded were approximately 10 for the European Brown comparison screenshot and 8 on the Oriental tress comparison screenshot. Figure 5-41 shows the average decision time taken by each user and Figure 5-42 shows the average number of fixations captured during the evaluation process by each participant.

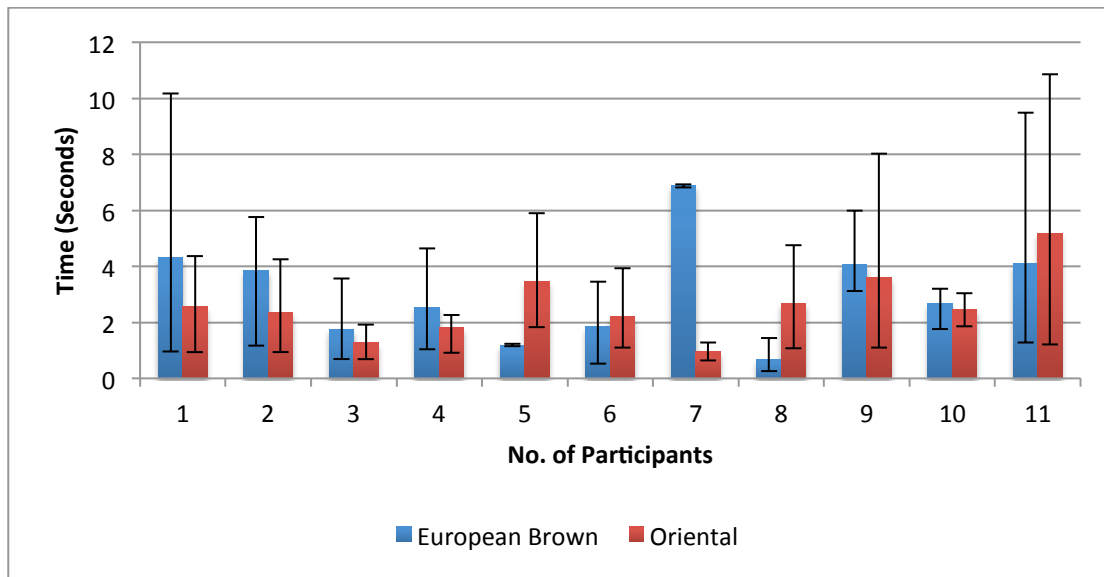


Figure 5-41 Average-decision time of each participant during the Virgin-SLES evaluation process

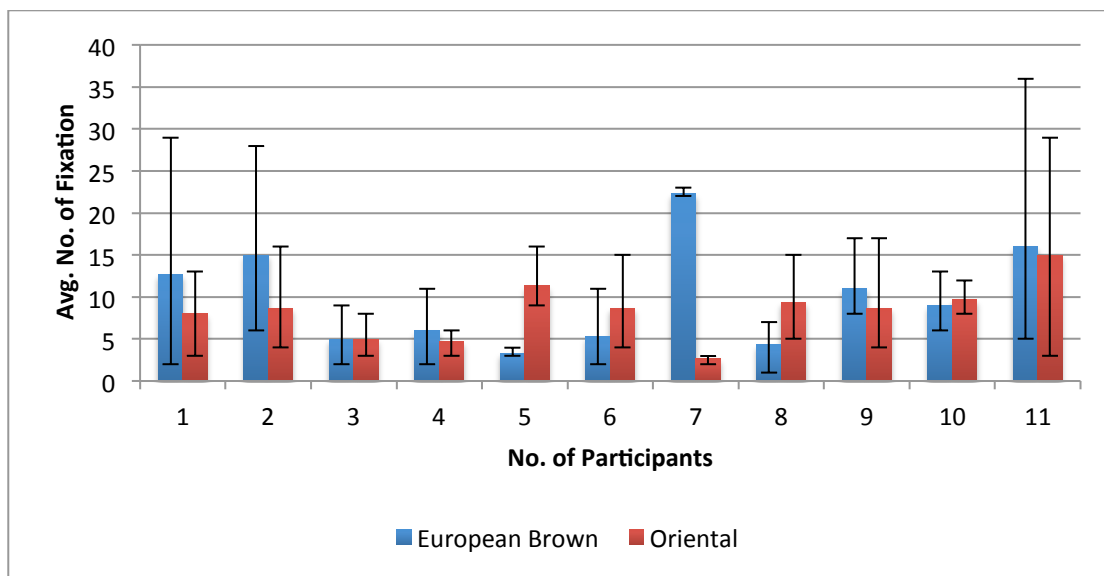


Figure 5-42 Average fixation counts by each participant during the Virgin-SLES evaluation process

5.4.2.2 Time spent and number of fixations in the AOIs (areas of interest)

Of the three evaluations, the average time spent by the participant viewing the shine area was 0.76 seconds on left image of the European Brown hair tress and 1.28 seconds on the right image. The average time spent by the participants assessing the Oriental hair tress was 0.73 seconds for the Virgin hair tress and 1.06 seconds for the SLES washed hair tress. Figure 5-43 and Figure 5-44 show the average time spent by each participant viewing the shine areas of the European brown and Oriental hair tresses.

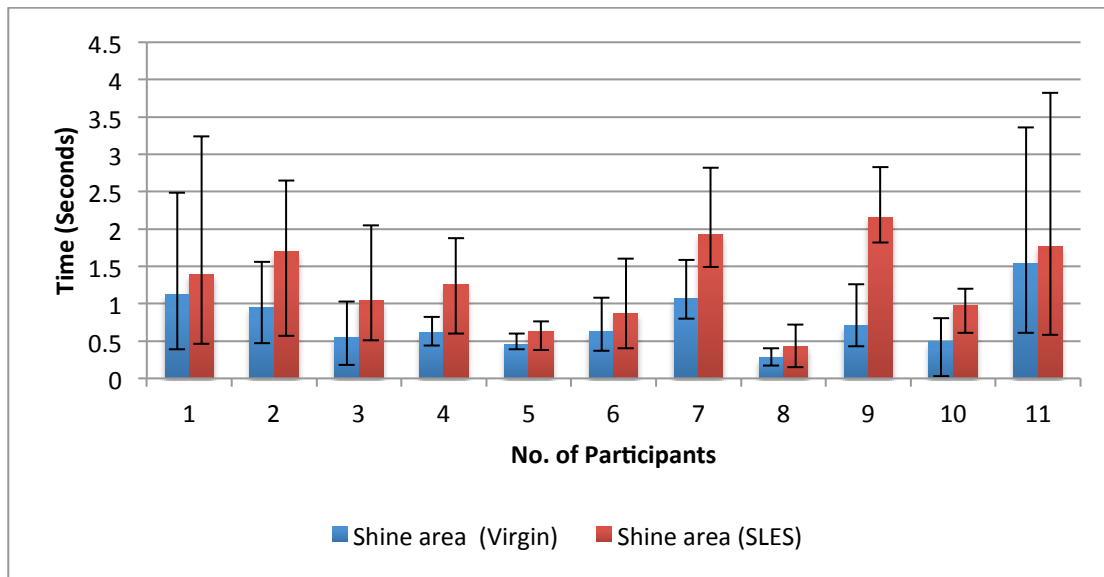


Figure 5-43 Average-time spent by the participants viewing the shine areas of the European Brown hair tresses (Virgin-SLES comparison).

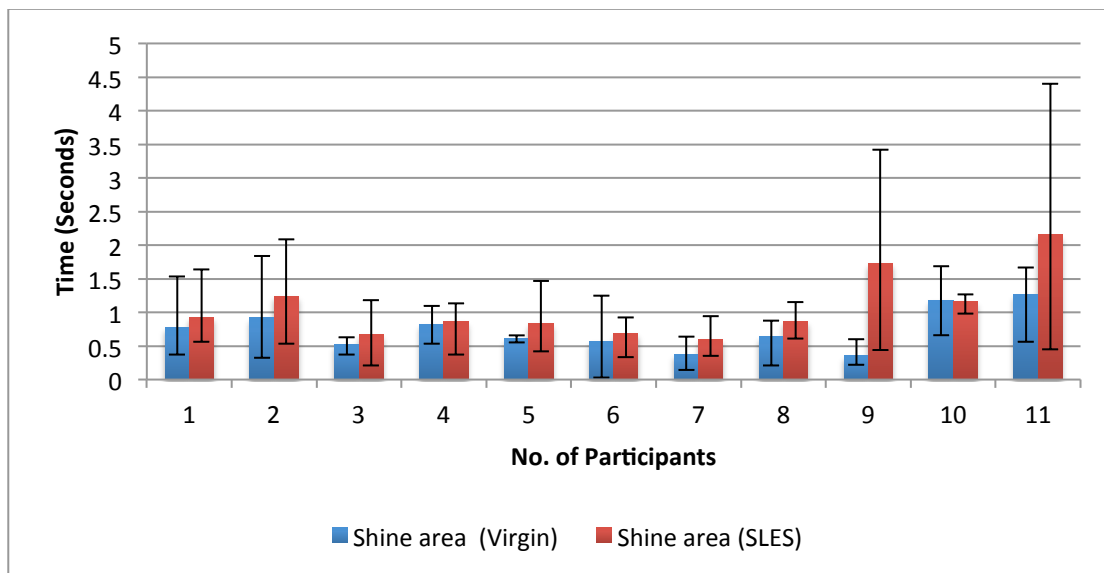


Figure 5-44 Average-time spent by the participants viewing the shine areas of the Oriental hair tresses (Virgin-SLES comparison).

The number of fixations recorded on the left image of the European Brown and Oriental tress evaluation screens were both approximately 2.3. The participants gazed approximately 3.5 times at the right image of the European Brown tress pair and 2.8 times on the Oriental hair tress. Figure 5-45 and Figure 5-46 show the average gaze frequencies of the participants in the shine areas for the European Brown and Oriental tresses respectively.

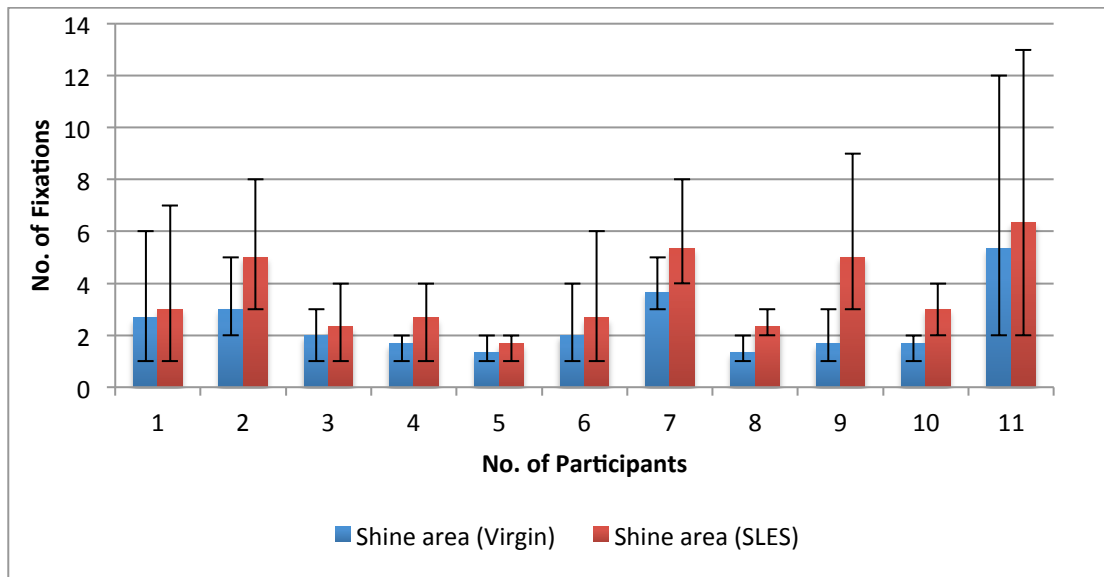


Figure 5-45 Average gaze frequency of the participants in the Shine areas of the European Brown tresses

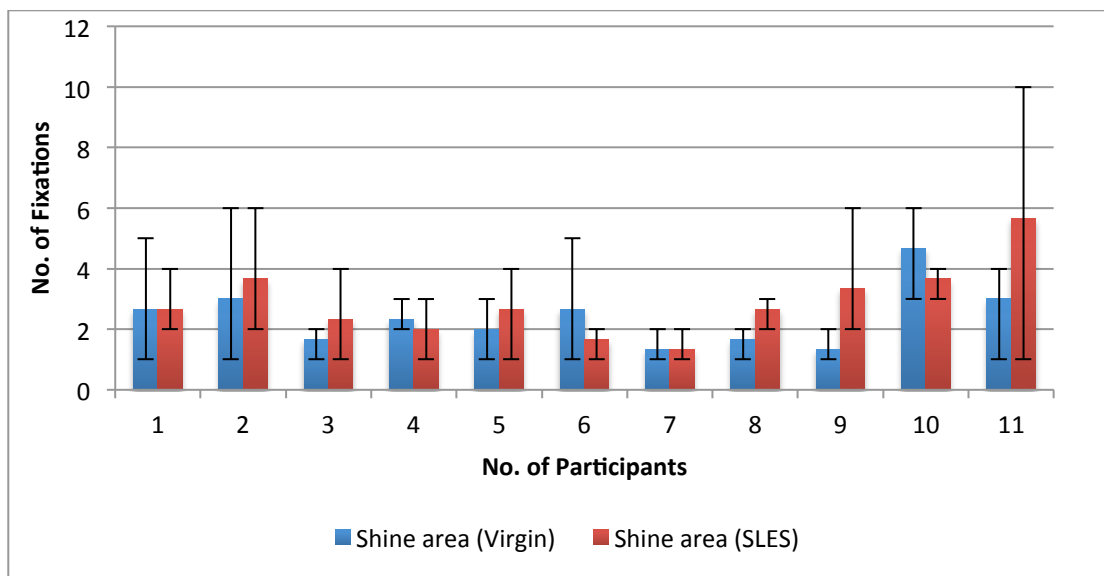


Figure 5-46 Average gaze frequency of the participants in the Shine areas of the Oriental tresses

Participant behaviour followed a similar trend to the way they gazed at the Virgin-SLES Blonde comparison. When the shine bands are clearly defined, and the comparison is between tresses of a similar appearance, some of the participants moved their gaze from the shine band to the Chroma bands on the hair tresses. Out of 33 evaluations, the participants gazed at the top Chroma area of the European Brown 13 times and Oriental Virgin hair tresses 12 times respectively. Participants gazed approximately 10 times at the top Chroma band for the European Brown tresses and 17 times at the Oriental

tresses washed with SLES. Some activity was also noted in the bottom Chroma area of these tresses.

5.4.2.3 Decision durations and comparison with the models

Of the 33 evaluated tresses, washed-with-SLES tresses were judged to be the shiniest. In both EB and Oriental tress evaluations participants picked SLES washed hair tresses 29 times (EB) and 25 times (Oriental). The ROC₂ model showed the highest sensitivity of all of the models as according to the ROC₂ model the shine, on the tress washed with SLES, increased in shine by 17% for the European Brown tress and 41% for the Oriental tress. Other models showed less of an increase in shine with the modified Robbins models suggesting a shine increase of 4%. Table 5-9 and Table 5-10 show the average shine values (three evaluations) generated by the different models. The ROC model indicates a better comparative sensitivity when compared to the panel results; as compared with other models.

Table 5-9 Average shine values of Virgin and SLES tresses generated by different models and the participants' choices. The highlighted value is the closest to the participants' choice

	Virgin	SLES	% Difference
Model type			
ROC ₁	1814.92	2036.64	12.22%
ROC ₂	1119.50	1316.13	17.56%
Robbins*	285.59	299.55	4.89%
Profile/width	107.40	111.18	3.52%
User's choice	29	4	86.20%

Table 5-10 Average shine values of the Virgin and SLES tresses generated by different models and the participants' choice. The highlighted value is the closest to the participants' choice

	Virgin	SLES	% Difference
Model type			
ROC ₁	1181.17	1436.88	21.65%
ROC ₂	99.03	140.02	41.38%
Robbins*	303.89	315.53	3.83%
Profile/width	112.62	115.48	2.53%
User's choice	25	8	68%

5.4.3 Virgin-Shine spray

Figure 5-47 shows the gaze plot for all of the participants on the Virgin-Shine spray comparison screenshot. Figure 5-48 shows the time spent viewing the paired comparison in the form of a heat map.

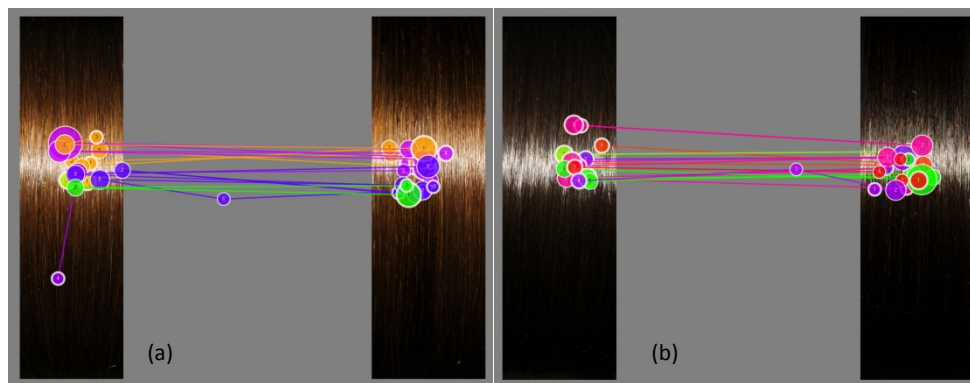


Figure 5-47 Gaze plot for all of the participants on the Virgin tress (left) – Shine Spray tress (right) screenshot (a) European Brown hair tress, (b) Oriental hair tress

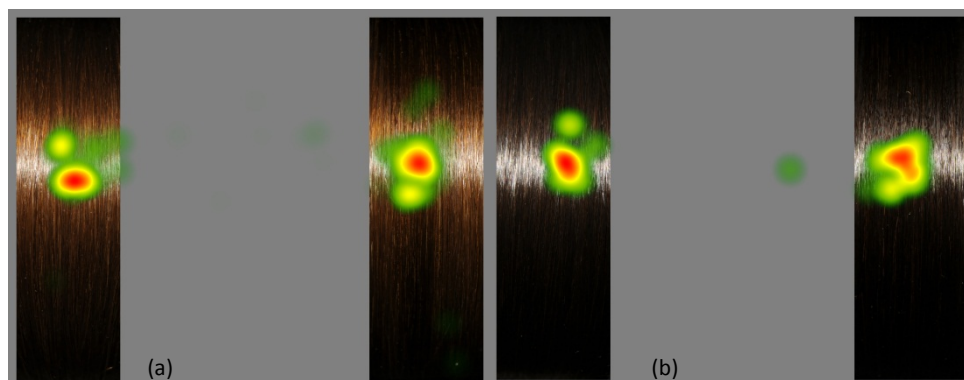


Figure 5-48 Heat map (time spent on the screen, red represents high frequency, green low and yellow medium) of all of the participants on Virgin-SLES evaluation screen of GUI (a) European Brown hair tress, (b) Oriental hair tress

5.4.3.1 Time Taken and number of fixations in the Evaluation process

In the Virgin-Shine Spray comparison, the average time taken to record the decision was approximately 3 seconds for European Brown and 2 seconds for the Oriental hair tress comparison. Participants gazed approximately 9 times at the screen to evaluate the shine of the European Brown tresses and 7 times to evaluate the shine of the Oriental hair tresses. Figure 5-49 shows the average time taken by each user to record their decision. Figure 5-50 shows the average number of fixations on the screen during the evaluation process by each participant.

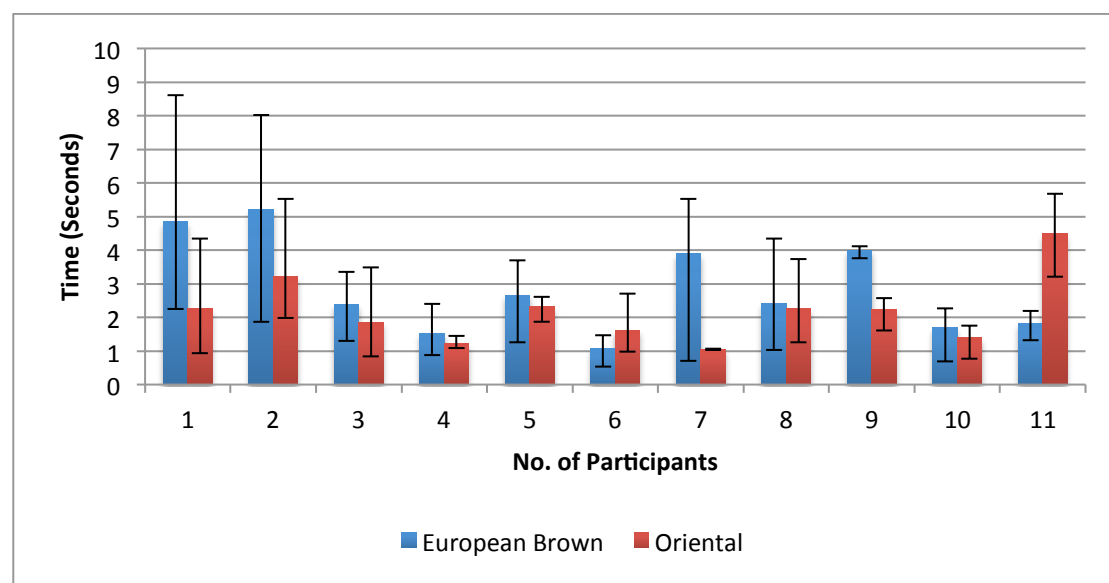


Figure 5-49 Average decision duration of each participant during the Virgin-Shine Spray (EB) evaluation process

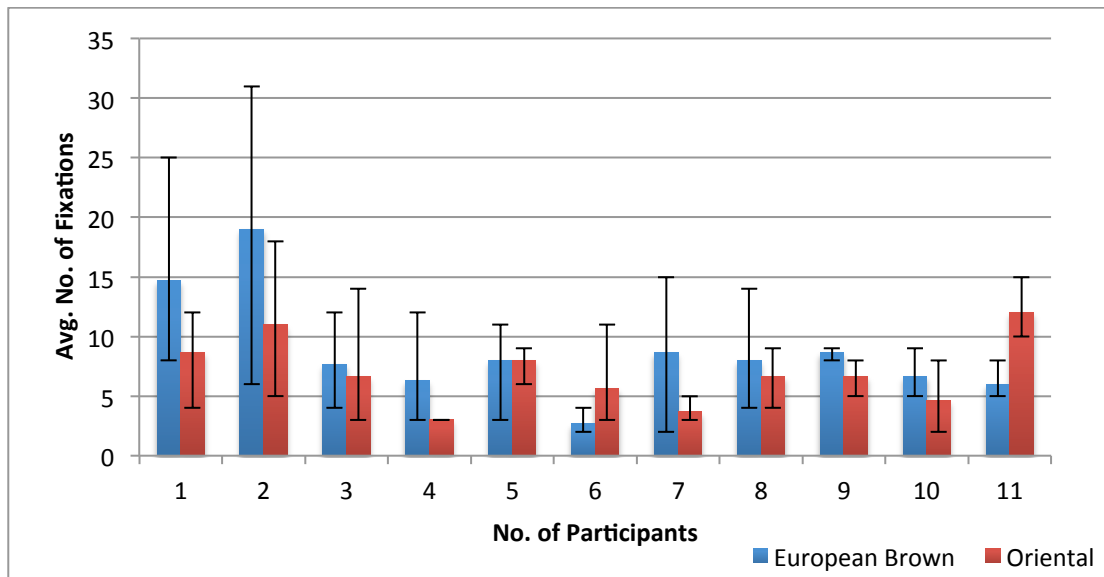


Figure 5-50 Average fixation count of each participant during the Virgin-Shine Spray evaluation process

5.4.3.2 Time spent and number of fixations in the AOIs (areas of interest)

Of the three evaluations, the average time spent by the participant viewing the shine areas of the left images were 0.86 seconds for the European Brown comparison and 0.67 seconds for the Oriental hair tress comparison. The average time spent by the participant attending to the shine areas of the right images were 1.26 seconds for the European Brown hair tress and 0.93 seconds for the Oriental hair tress. Figure 5-51 and Figure 5-74 show the average time spent by each participant viewing the shine area of the hair tresses for European Brown and Oriental paired comparisons of Virgin and Shine Spray.

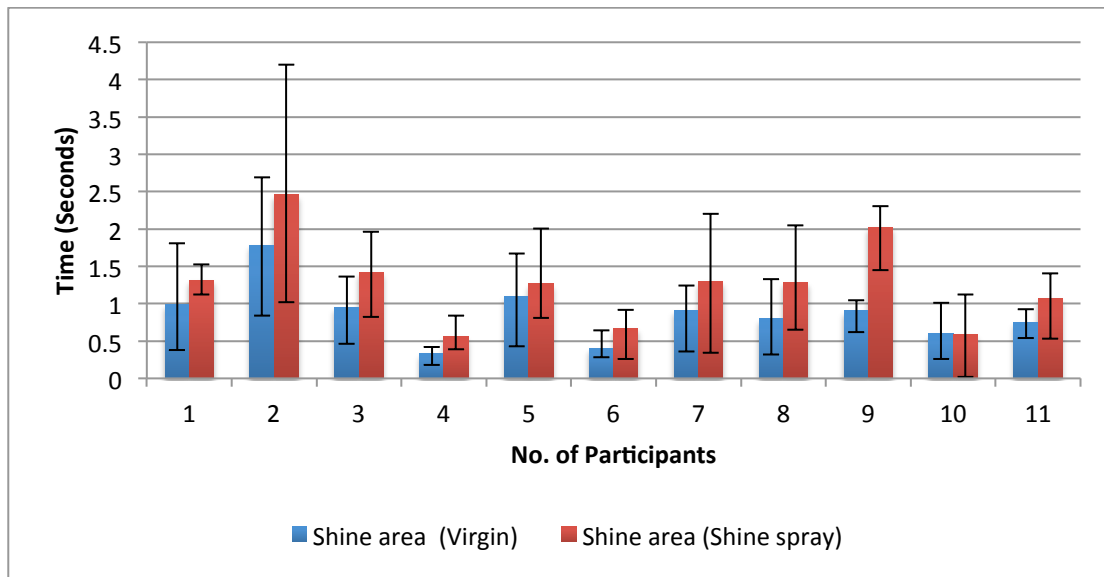


Figure 5-51 Average time spend by each participant viewing the shine area of the European Brown tresses

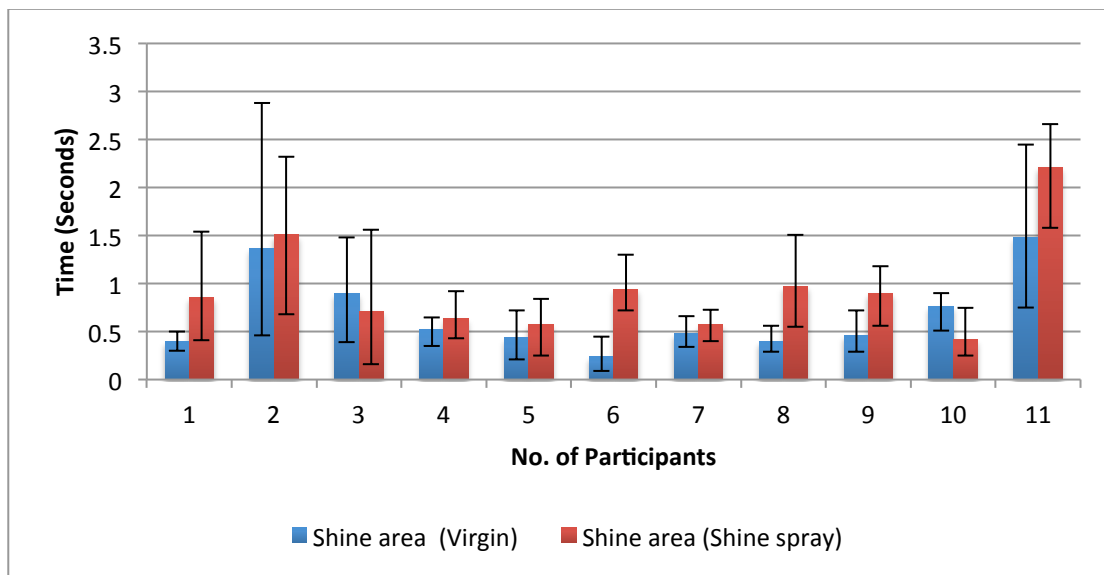


Figure 5-52 Average time spend by each participants in the shine area of the Oriental tresses

The average number of fixations in the shine areas were approximately 2.5 times on the left image of the European brown comparison and only 2 on the left image of the Oriental comparison. Whereas, the gaze frequency of the shine areas of the right images were 3.5 fixations on the European Brown and 2.7 fixations on the Oriental (right) tress image. Figure 5-53 and Figure 5-76 show the average gaze frequency of the participants in the shine areas of the tresses for European Brown and Oriental hair tress comparisons.

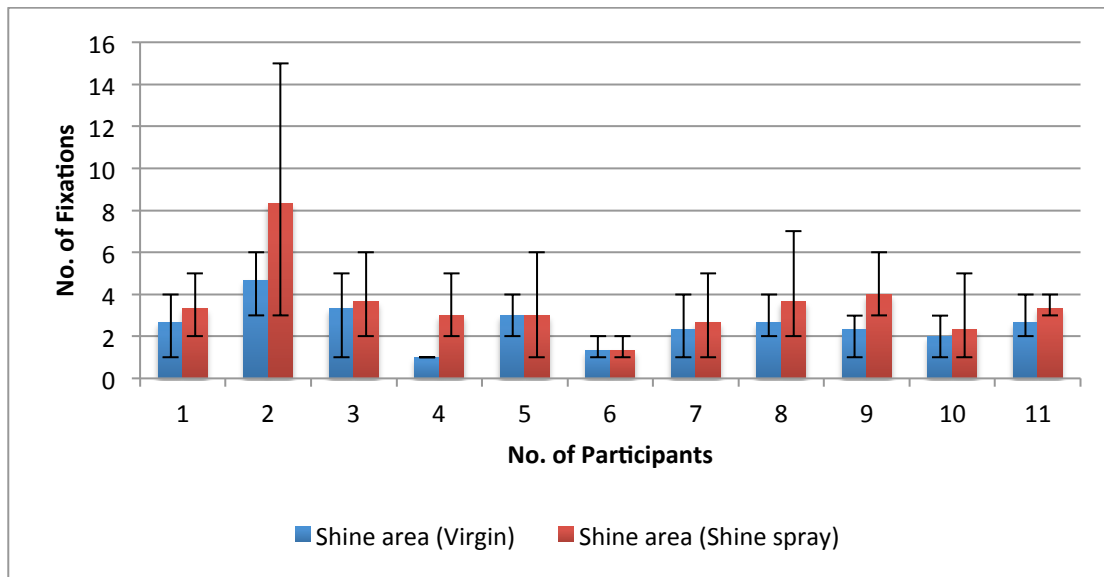


Figure 5-53 Average fixation count of the participants viewing the shine areas of the Virgin-Shine Spray (European Brown hair tress)

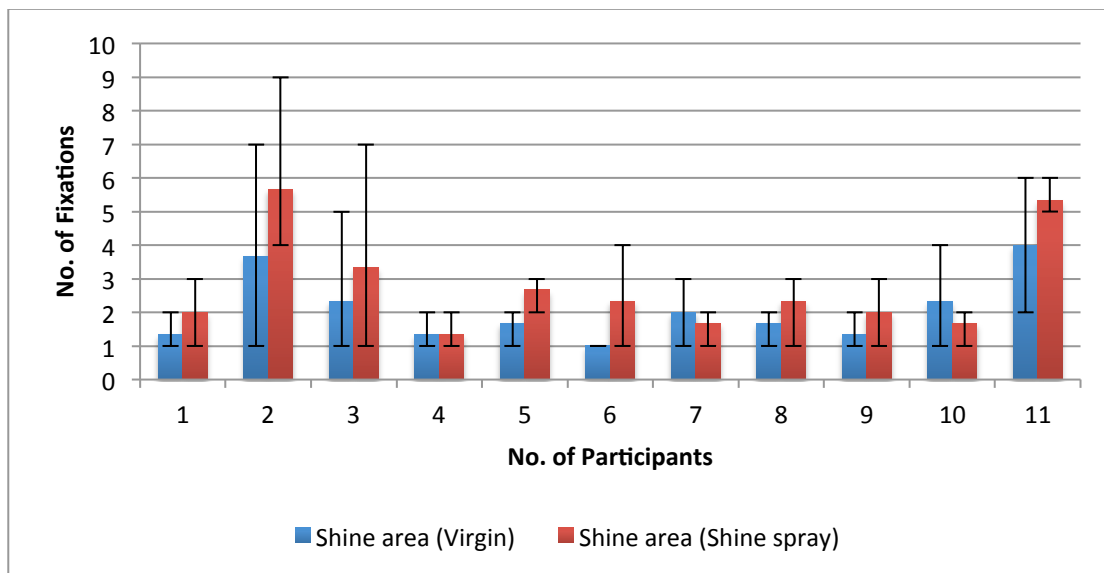


Figure 5-54 Average fixation count of the participants viewing the shine areas of the Virgin-Shine spray (Oriental hair tress)

In 33 evaluations (11 evaluation x 3 repeats) the total numbers of fixations recorded on the left image (Virgin) were 19 on the European Brown tress comparisons and 13 on the Oriental tress comparisons, respectively. Whereas, on the right image (Shine Spray) the total number of fixations recorded were 9 on the European Brown tresses and 15 on the Oriental tress comparison image. On the bottom Chroma areas the total fixations recorded were 11 times on the Virgin European Brown tresses and 7 times on the Virgin Oriental tress. On the right images, the total fixation frequencies were 15 on the bottom

Chroma area of the European Brown tress and 8 on the Oriental tress treated with Shine Spray.

5.4.3.3 Decision and comparison with the models

Of the 33 evaluations, 27 panellists selected the Virgin hair tress over the tress treated with Shine Spray. All of the models showed a decrease in shine, the ROC₂ model showed a -6% decrease in shine in the European Brown tress and a -18% decrease in the Oriental tress whereas the modified Robbins model showed an approximate -4% decrease in European Brown and a -18% decrease in shine in the Oriental tress. Table 5-11 shows the shine values of the European Brown hair tresses and Table 5-12 shows the shine values of the Oriental hair tresses, generated by the models and participants' choices.

Table 5-11 Average shine values of Virgin and Shine Spray tresses generated by different models and participants' choice. Highlighted value is the closest to the participants' choice

	Virgin	Shine Spray	% Difference
Model type			
ROC ₁	1814.92	1744.94	-3.86%
ROC ₂	1119.50	1050.23	-6.19%
Robbins*	285.59	274.24	-3.98%
Profile/width	107.40	103.18	-3.92%
User's choice	27	6	-77.77%

Table 5-12 Average shine values of Virgin and Shine Spray tresses generated by different models and participants' choice. Highlighted value is the closest to the participants' choice

	Virgin	Shine Spray	% Difference
Model type			
ROC ₁	1181.17	1012.81	-14.25%
ROC ₂	99.03	80.90	-18.31%
Robbins*	308.89	248.94	-18.08%
Profile/width	112.62	95.30	-15.38%
User's choice	28	5	-82.14%

5.4.4 Conclusion

In order to relate the values produced by the gloss evaluation models to human perception, a method of constant stimuli (forced-choice paired comparison) psychophysical test was conducted. To conduct the forced-choice paired-comparison test, images of Blonde, European Brown and Oriental hair tresses with different shine levels were captured using the Gonio Image Capture System. A GUI, Tress-Gloss 2.0 was developed by the author, which displayed two tress images side by side and a naïve panel of eleven participants were asked to select the image of the shinier tress (the GUI Tress-Gloss 2.0 is a modification of Tress-Gloss 1.0, developed by the author, details about the GUIs are described in Chapter 3 Section 3.5).

Twelve tress images of each hair type (Blonde, European-Brown and Oriental) were used in the psychophysical study. Each set of 12 images consisted of two repeats of four different shine levels (Virgin tress image, SLES washed tress image, Shine-Sprayed tress image and image of tress treated with Wax). The tress image presentation methodology is explained in Section 5.2.1. Each level of shine was compared with the others. The total number of evaluations performed by each participant was 198 (66 comparisons of the Blonde tress images, 66 comparisons of the EB tress images, and 66 comparisons of the Oriental tress images). The study was carried out in three sessions, one session for each hair type.

A group of eleven participants took part in the psychophysical study and to understand how each participant came to the decision (which tress appears the most glossy), the Tress-Gloss 2.0 GUI was developed and executed on an Eye-tracking system (Tobii TX300). The Tobii TX300 records the eyes movements of the participants. The eye-tracker has never been used in such studies. Thus, this was the first study to use eye-tracking equipment to collect the gaze data of the participants whilst they evaluated hair shine.

The analysis of the participants' gaze data gives an interesting insight into how a human observer evaluates the relative shine of a pair of hair tresses. It was noted that regardless of the hair type (Blonde, European-Brown or Oriental), all participants gazed in a similar pattern when the shine differences were large. Figure 5-55 shows the gaze

plot of all the participants on the Virgin-Wax comparisons of European-Brown, Oriental and Blonde hair tresses. The average time spent by the participants to register their decision showed similar pattern as well, regardless of hair type.

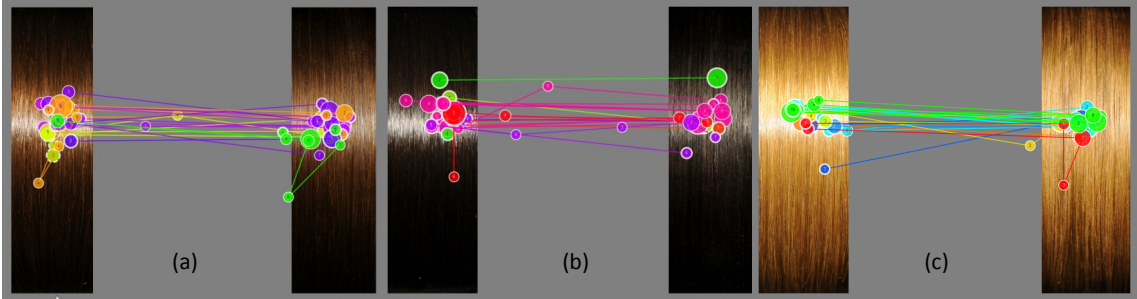


Figure 5-55 Gaze plots of all the participants on the Virgin-Wax comparison, (a) European-Brown, (b) Oriental, (c) Blonde.

In the Virgin-Wax comparison, the average time spent by the participant was 1.5 seconds for Oriental, 1.49 seconds for European Brown and 1.29 seconds for Blonde. When the comparison changes from Virgin-Wax to Virgin–SLES the average time spent increased, approximately 100% in the case of European Brown and Blonde, and 60% in oriental, as the difference in shine reduces. Figure 5-56 shows the average time spent by the participants viewing the screen to record the decision.

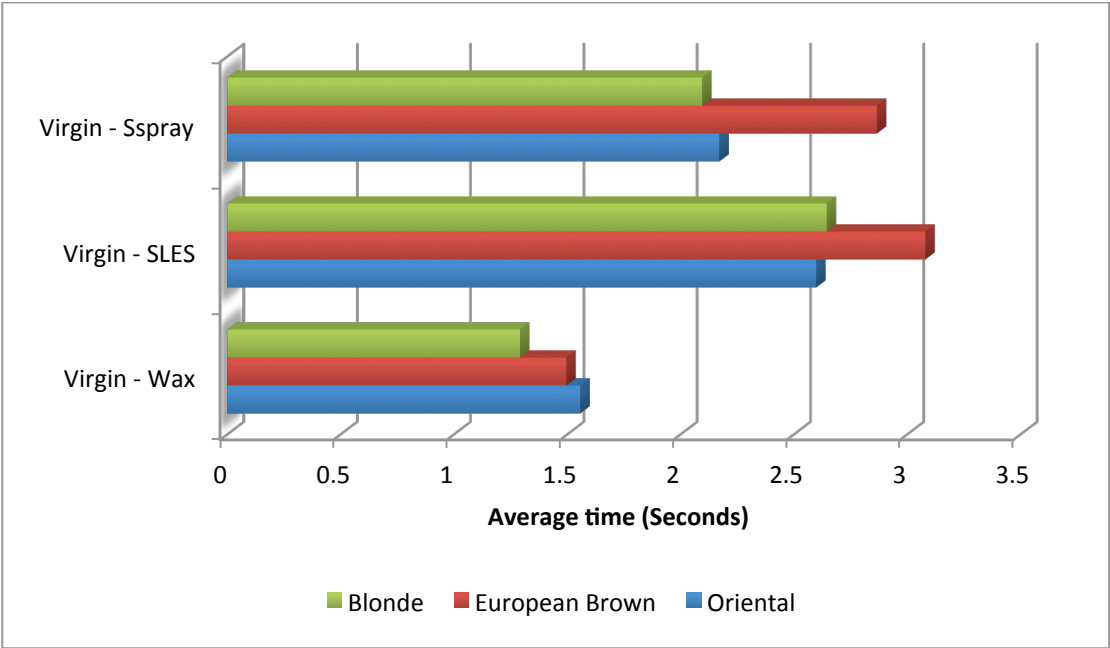


Figure 5-56 Average decision times taken by the participant panel.

It was noted that when the observers evaluated hair shine, the participant only gazed in the shine and Chroma areas of the tresses. The gazing patterns were similar for all types of hair tress comparison. This is an interesting finding, as the gaze pattern of the participants does not alter with a change in colour of the tresses. Figure 5-57 shows the screenshots of Tress-Gloss 2.0 and where, participants gazed most frequently are highlighted on the image.

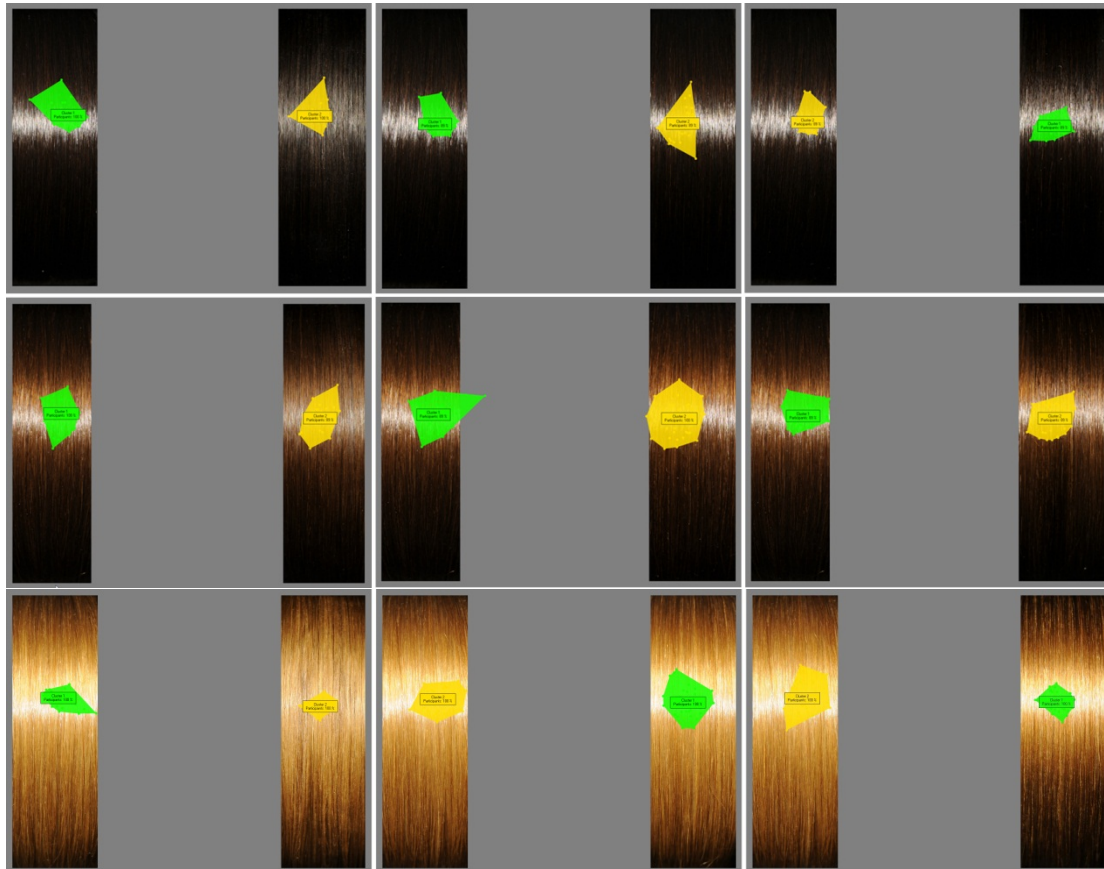


Figure 5-57 Screen shots of the paired comparisons; highlighted areas are where participants were most attentive, during the shine evaluation process

The gaze pattern of the participants suggests how important the Chroma area is in evaluating hair shine. If participants were treating all of the tresses equally, as the data suggests, the Chroma area of the hair tress would play a major factor in defining the shine as discussed in the previous section (Section 4.6: colour gradient).

With the above finding, the author has suggested a new interpretation of the reflection bands. By incorporating the Chroma-band into the model using the Chroma-Specular band, C_s , the author has developed a novel method to evaluate the hair shine of the

tress. The new models ROC_1 and ROC_2 (hair gloss evaluation models), use both the shine area and the Chroma areas to quantify the shine of the hair tress. The difference between the MFV (most frequent values) of L^* and C^* were incorporated in the model and this appears to increase the sensitivity of the model.

Comparisons were made between the participants' choices and the gloss values generated by the gloss evaluation models (ROC_1 , ROC_2 , Modified Robbins and Profile over width). The ROC_1 and ROC_2 models had the best overall correlation to the human evaluation system (participants' decisions). Although the other models showed a similar trend, in some cases, they appeared to lack sensitivity. Figure 5-58 shows the percentage difference in shine values generated by the different hair shine models and they are compared with participants' choice. For Blonde, European-Brown and Oriental hair tresses, with the current image capture system the ROC_1 and ROC_2 gloss values not only correlate to the participants decision but in some cases they can be related to visual preference (tentatively labelled as the health of the tress). For example, when the Blonde tress was treated with Shine-Spray it appeared unhealthy. 90% (30 out 33 evaluations) of the participants chose the Virgin blonde tress as the glossiest when compared with the Blonde hair tress sprayed with Shine-Spray. The ROC_1 and ROC_2 models showed the decrease in shine whereas all of the other models predicted an increase in shine when compared with a Virgin Blonde hair tress.

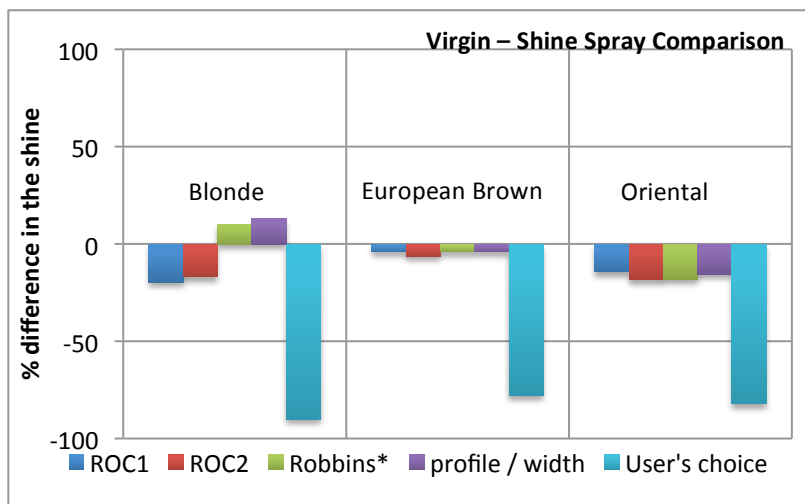
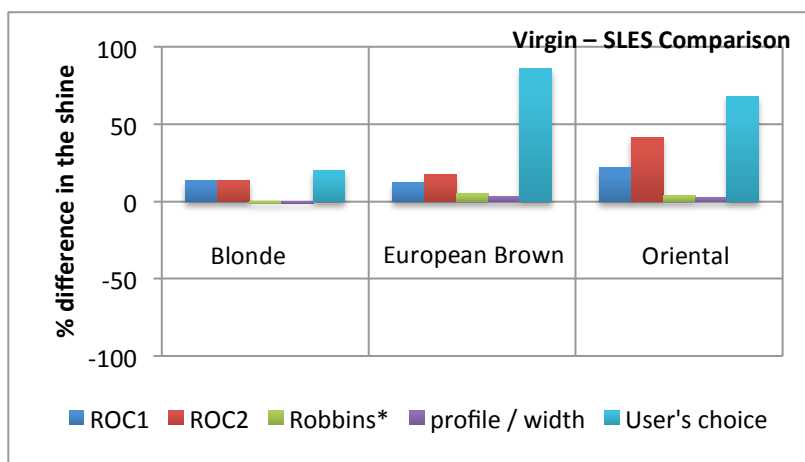
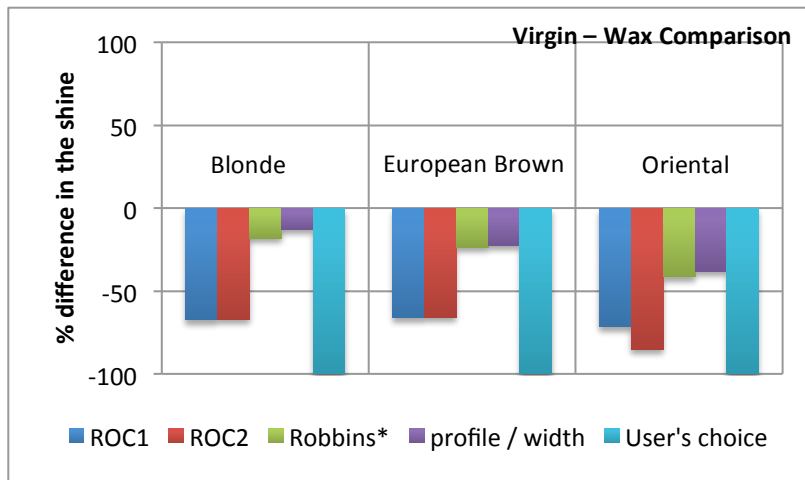


Figure 5-58 Percentage increase or decrease in shine values generated by different models and the participants' choice, between the left image and right image of the hair tresses.

Chapter 6

Conclusions and Further Work

6.1 Conclusions

The main aim of this study was to develop a gloss evaluation system for human hair tresses, which could quantify gloss in a similar way to a panel of human observers. The outputs of this system were to correlate with the human perception of gloss. Unfortunately, current computational modelling techniques are often found to be inconsistent when compared to the panel discriminations of human observers.

This thesis has made novel contributions in the following four main areas:

1. Sample Preparation
 - a. New Wax and Shine Spray application methods.
2. Gloss Image Capture and Processing
 - a. Development of a colour-calibrated Gonio Image Gloss capture system with a novel sample presentation stage featuring alignment and tensioning.
 - b. Diffuse and Gloss standards used to calibrate images.
 - c. A novel method of reflection band segmentation was developed to separate the different components of the reflection band from an image of a hair tress.
3. Gloss Models
 - a. A New part of the reflection band, the Chroma-Specular (C_s) band, was identified on the hair tress.
 - b. Two new gloss evaluation models ROC_1 and ROC_2 have been developed and assessed.
 - c. A comparative assessment of current gloss evaluation models with the ROC_1 and ROC_2 . A comparison with the results of a psychophysical panel.
4. Psychophysics
 - a. Development of two graphical user interfaces (GUI) using MATLAB, Tress-Gloss 1.0 and Tress-Gloss 2.0, for the psychophysical evaluation of the gloss differences of hair tresses.
 - b. A psychophysical experiment using the Tobii TX300 Eye Tracker to record which areas of the tress were important to human observers when discriminating between two tresses of varying gloss.

- c. Comparisons of the hair gloss models with participants' choices.

6.1.1 Development of methods to produce different hair tress shine levels

In order to develop an automated hair shine model, which can be related to the human perception of gloss, a dataset of hair tresses with different levels of hair shine was required. To achieve different levels of hair shine, tresses were treated with heat, chemical and mechanical techniques. A novel method was developed to heat treat the hair tress by dividing the hair tress into segments, where each segment's height was equal to that of the tongs height (hair-straightener). The tongs were then applied to each section for a particular duration. During chemical treatment the tresses were submerged in a 28% SLES solution for a defined duration and to create different level of hair using the UMIST Combing Tester mechanically treated shine tresses. Initially, it was predicted that with an increase in damage the shine of the hair tress would decrease. A panel evaluation by a group of naïve observers suggested that the range of hair tresses produced by different treatments (chemical, mechanical and heat) did not create a range of shine differences that could be detected by the participants.

To achieve different discriminable shine levels on the hair tresses a second approach was taken, where the tresses were treated with a series of commercial products. Due to the unavailability of commercial standards, with outline application methods, new application methods were developed in order to apply products to the hair tresses in a systematic and repeatable manner, which include applying wax to the tress. Applying a semisolid product to a tress evenly was achieved using a combination of a comb and a hair-dryer. This method is novel and has never been mentioned in the literature. Different commercial hair products were applied to hair tresses (listed in section 3.8.4). Of these products, the two selected produced the maximum difference in shine. These two tresses along with the Virgin and SLES-washed tresses were used in the gloss evaluation study.

6.1.2 Development of the hair tress Image Capture System

A Gonio Image Capture system has been developed, which consists of five main elements (light source, image capture device, sample holder, arc and tensioner). The sample holder and tress mounting techniques are novel and have never been mentioned

in the literature. For hair shine evaluation, the author has used HDR (high dynamic range) imaging, which is used for the first time that this technique has been used in such studies. A set of procedures was devised in order to capture a cropped image of a hair tress. These procedures included setting the camera and sample positions, camera calibration, exposure range determination, remote image capture, image alignment and cropping and finally image analysis. These steps are explained further in Section 3.10. A series of MATLAB scripts and functions were written in order to convert the sRGB image into the CIELAB colour space. The effect on each component of the CIELAB colour space on different shutter-speeds was examined. When the average L^* area under the curve of HDR images of hair tresses treated with wax, shine-spray and SLES were compared their difference remains the same throughout the HDR range; Section 3.11.1 explains the effect on the average L^* area of a hair tress image as the shutter speed increases.

6.1.3 Psychophysical study and development of the Graphical User Interfaces (GUIs) – Tress Gloss 1.0 and Tress Gloss 2.0

To relate the output of the automated gloss-evaluation system to those made by the human panel discriminations, a couple of psychophysical experiments were conducted. A GUI (graphical user interface) called Tress-Gloss 1.0 was developed by the author using MATLAB. Tress-Gloss 1.0 was based on a magnitude estimation test in which a single image of a hair tress appeared on the screen and the participants were asked to rate the gloss, initially on a scale of 1 to 9. It was noted that the participants were reluctant to give extreme values, as there was no anchor or standard on which to base their judgements. For this reason, the author changed the magnitude estimation psychophysical experiment to a method of constant stimuli (forced-choice paired-comparison) psychophysical experiment. The Tress-Gloss 1.0 GUI was modified to produce Tress-Gloss 2.0 in which a pair of images of hair tresses appeared on the screen and participants were asked to choose which hair tress looked shinier.

6.1.4 A new interpretation of the reflection band on the hair tress, Chroma-Specular (C_s)

A number of publications have been made on the subject of hair-shine, over the span of 30 years, as explained in Section 2.15.2. Even though these proposed models to evaluate hair-shine are different from one another they are based on principles outlined by

Stamm's three-component model. In this approach, the incident light reflected from a hair tress, or a hair fibre, can be broken into three discrete reflection bands (Specular, Chroma and Diffuse).

As these models do not always correlate to human judgements it may be suggested that the analysis of the light reflected from the hair tress is not as straightforward as that suggested by Stamm's three component-model. When an image of a hair tress is analysed it was noted that the Chroma band (coloured part of the reflection) is not uniform and it changes with a colour gradient; the concept of colour gradient is explained in Section 4.2. Using this information a new reflection band, in the Chroma band, was identified, and named Chroma-Specular (Cs). The new segment of the Chroma band (Chroma specular) can be related to digital special effects, where blur is required to create a glowing effect, for example the light-sabre from the movie Star-Wars.

6.1.5 Segmentation of the reflection bands of the human hair tress

Different techniques have been used by previous workers to separate the reflection bands as they appear on the hair tress. These techniques have included the use of polarizers, measuring reflectance at a certain angle and curve fitting. An ideal goal of a tress gloss system would be able to separate the reflection bands in a diffusely illuminated environment, which would replicate the viewing conditions of a normal observer in everyday life. This is not straightforward as there may be a number of different light sources and this would make the segmentation of the reflection band potentially problematic. Thus the separation of the Chroma-specular band may not be valid. Unfortunately, current separation methods do not identify the Chroma-specular band. To overcome this problem a new method has been developed. To separate the reflection bands from the image of the hair tress, the shine-area is selected in the image and the L^* and C^* limits of that area are calculated. These limits are then used to segment the tress image, which resulted in the separation of the shine band. Using the MATLAB scripts and functions, written during the study, allows the user to see a real-time confirmation, which shows the separated band overlaid on top the tress image in green. Figure 6-1 shows the separated reflection bands and overlaid on the image of a Virgin Blonde hair tress. The separation methods for the reflection-bands are explained in Section 4.8.

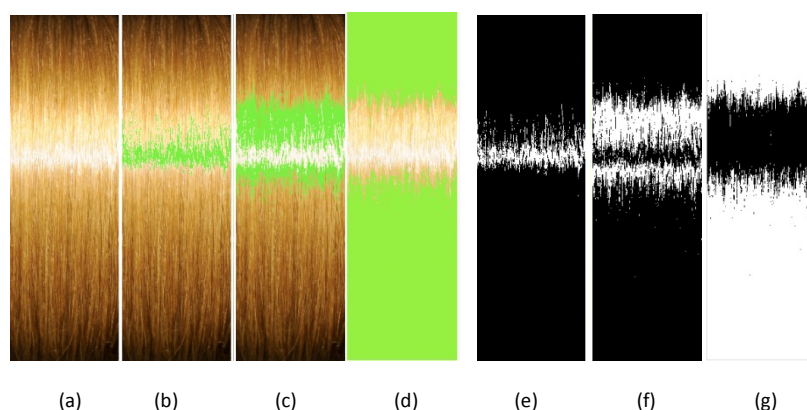


Figure 6-1 Reflection band separation of a virgin blonde hair tress. (a) Virgin blonde tress image, original image, (b) Shine-band separated and overlaid on the original image, (c) Chroma-specular-band separated and overlaid on the original image, (d) Chroma-diffuse-band separated and overlaid on the original image, (e) Separated shine-band, (f) Separated Chroma-specular-band, (g) Separated Chroma-diffuse-band.

6.1.6 Development of the novel human hair gloss models

Once the reflection bands were separated, each area was averaged horizontally and plotted as an intensity curve. The area under the curves was then calculated. The effects of different hair tress treatments on the areas of the reflection bands were examined. If the shine area increases, the common understanding is that the tress will appear shinier. It was interesting to note that the European Brown hair tresses appear shinier, if not the same, when compared with the Virgin hair tresses. This is contrary to the results of the shine areas as the calculated areas showed a 0.8% decrease when the SLES washed EB hair tress shine-area was compared with the Virgin EB hair tress. This suggests that the other reflection bands are also important to the sensitivity of the gloss evaluation system. The effects of the different tress treatments on the reflection bands are explained further in the Section 4.8.

To quantify the gloss of a human hair tress, two new formulas have been developed, the ROC formulas (Rizvi-Owens-Croda), which not only predict the correct level of shine, but are also sensitive enough to show a similar magnitude to changes in shine as those perceived by human observers. The formula consists of five main elements; the shine-area, Chroma-specular-area, Chroma-diffuse-area, width at half height (FWHM) of the shine curve and to increase the sensitivity difference in height of the L^* curve and the C^* curve, D_{LC} was also incorporated in the formula. Even though ROC showed the correct

level of shine, to increase the sensitivity of the model when using Oriental (black) hair tresses ROC was modified, where instead of using Chroma-diffuse, the difference between the profile and the Chroma-specular band was used.

6.1.6.1 Comparison of values generated by different gloss models using European-Brown hair tresses

ROC was compared with two conventional hair gloss models. Using the European-Brown hair tresses ROC₁ and ROC₂ predicted an 83% and a 71% decrease in the shine, respectively, whereas the modified Robbins model predicted only a 26% decrease when the SLES-washed hair tress was compared with the Wax-treated tress (3% wax). ROC₁ was most sensitive to shine differences between tresses when compared with the other models.

6.1.6.2 Comparison of values generated by different gloss models from Blonde hair tresses

When assessing the Blonde hair tresses it was interesting to note that when shine-spray was sprayed on the tress, even though the contrast between the shine and background increases the tress appeared to be visually less appealing (several observers labelled the tresses as looking “unhealthy”). Other than the ROC₁ and ROC₂ models, all of the other models showed an increase in shine when the Shine-Spray Blonde tress was compared with the Virgin Blonde hair tress. It is speculated that this is due to the inclusion of the Chroma-specular band. ROC₁ and ROC₂ may therefore be used not only to predict the shine but also to predict the visual appeal of the hair tress (tentatively this could relate to the “health of the hair tress”). Of the two models ROC₁ was the most sensitive to shine differences between the blonde hair tress images.

6.1.6.3 Comparison of values generated by different gloss models from Oriental hair tresses

In the Oriental hair tress comparisons, all of the models predicted the correct shine levels but ROC₁ and ROC₂ showed a maximum difference between the Virgin hair tress and Wax treated tress. ROC₁ showed a 65% decrease in the shine whereas ROC₂ showed an 82% decrease in shine. The modified Robbins model showed 37% decrease in shine. The ROC₂ model is the most sensitive to changes in shine for Oriental hair tress images.

6.2 Psychophysical study

In order to relate the values derived from the gloss evaluation models to human panel discriminations, a method of constant stimuli (forced-choice paired-comparison) psychophysical test was conducted. To conduct the paired-comparison test, images of Blonde, European-Brown and Oriental hair tresses with different shine levels were captured. A GUI, Tress-Gloss 2.0 was developed by the author, which displayed two tress images side by side and the participants were asked to choose which tress appeared shinier to them (details of the GUIs are described in Chapter 3 Section 3.5).

6.2.1 Paired image comparisons used in the psychophysical study

Twelve tress images of each hair type (Blonde, European-Brown and Oriental) were used in the psychophysical study. Each set of 12 images consisted of two repeats of four different shine levels (Virgin tress image, SLES washed tress image, Shine-Sprayed tress image and Wax treated tress image), tress image breakdown is explained in section 5.2.1. This means that there were three different Virgin tresses imaged, three different tresses treated with SLES imaged, etc. Each level of shine was compared with the others. The total number of evaluations performed by each participant was 198 (66 comparisons of blonde tress images, 66 comparisons of EB tress images, and 66 comparisons of Oriental tress images). The study was carried out in three sessions, one session for each hair type.

A group of eleven participants took part in the psychophysical study and to understand how each participant came to the decision (which tress appears most glossy), Tress-Gloss 2.0 was executed on the Eye-tracking system (Tobii TX300) at the University of Manchester. The Tobii TX300 records the eyes movements of the participants. An eye-tracking assessment of gloss has never been reported for such studies. This study introduces a novel application of eye-tracking technology to the collection of participant hair-shine gaze data.

6.2.2 Participants' gaze analysis

The analysis of the participants' gaze data gives an interesting insight into how a human evaluates the shine of a hair tress. It was noted that regardless of the hair type (Blonde, European-Brown or Oriental), that all participants gazed in a similar pattern. Figure 6-2

shows the gaze plots of all of the participants viewing the Virgin-Wax comparisons of European-Brown, Oriental and Blonde hair tresses.

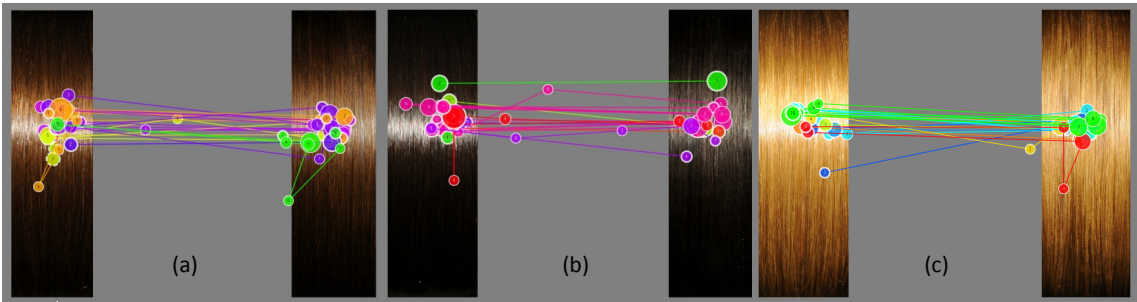


Figure 6-2 Gaze plots of all the participants viewing the Virgin-Wax comparison, (a) European-Brown, (b) Oriental, (c) Blonde.

6.2.3 Average decision duration of the participants

In the Virgin-Wax comparisons the average decision time for the participants was 1.5 seconds for Oriental, 1.49 seconds for European brown and 1.29 seconds for Blonde. The average decision times for Virgin–SLES were increased by approximately 100% in the cases of European Brown and Blonde, and 60% for Oriental, as the difference in shine difference between the two images reduces. Figure 6-3 shows the average time spent by the participants viewing the pair of images before they recorded their decision.

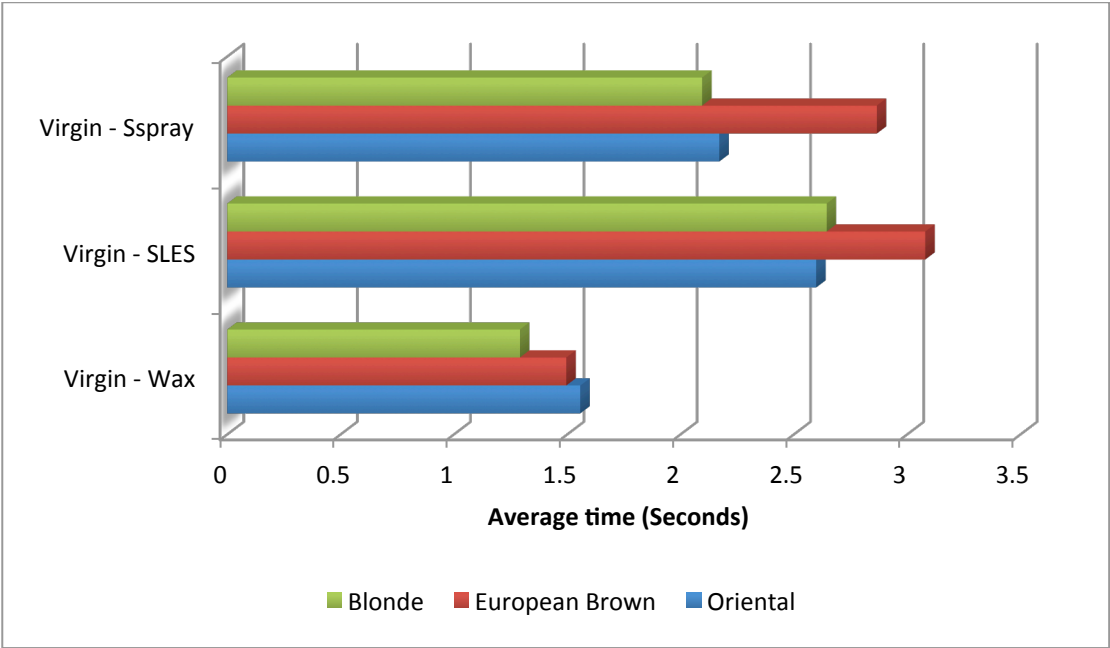


Figure 6-3 Average times taken by the participants to record their decision.

6.2.4 Areas on the tress images used by the participants to evaluate hair shine and the importance of the Chroma area

It was noted that when evaluating hair shine, the participant only gazed within the shine and Chroma areas of the tresses. The gazing patterns were similar for all types of the hair tresses used in this study. The gaze pattern of the participants does not change with change in colour of the tresses. Figure 6-4 shows some screenshots of the Tress-Gloss 2.0 GUI and where the participants gazed most frequently is highlighted on the image.

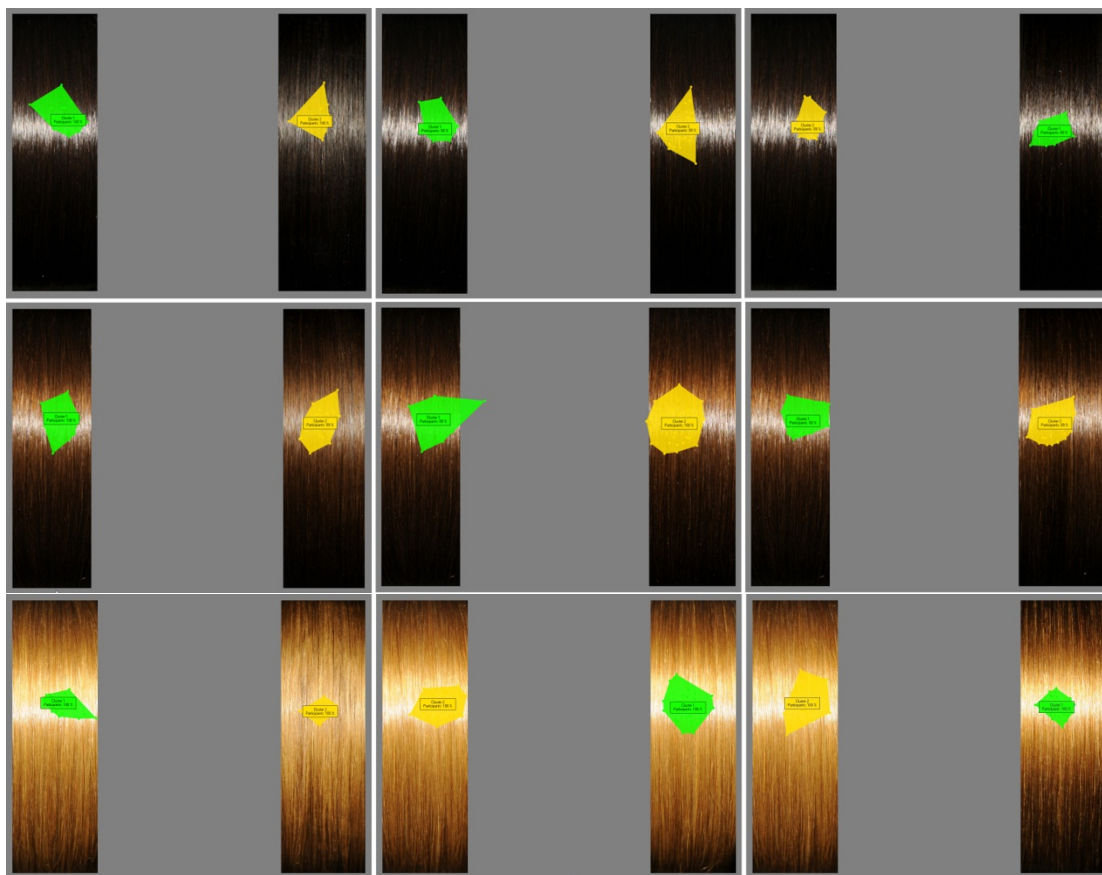


Figure 6-4 Screen shots of the pair comparison images; the highlighted areas are where participants most frequently fixated during the shine evaluation process

The gaze patterns of the participants confirm the importance of the Chroma area in evaluating the hair shine. If the participants were treating all of the tresses equally, as the data suggests, the Chroma area of the hair tress plays a major part in defining the shine as discussed in previous section (Section 4.6: colour gradient).

6.3 Comparison between the participant's choices and the gloss evaluation models

The new models ROC_1 and ROC_2 (Hair gloss evaluation models), use both the shine and Chroma areas to quantify shine of the hair tress. The difference between the MFV (most frequently occurring values) of L^* and C^* were incorporated in the models as they appear to increase the sensitivity of the results produced by the model.

Comparisons were made between the participants' choices and the gloss values generated by the gloss evaluation models (ROC_1 , ROC_2 , Modified Robbins and Profile over width). ROC_1 and ROC_2 gave the closest representation of the human panel evaluations (participants' decisions). Although the other models predicted the same decisions in some cases, they lacked sensitivity. Figure 6-5 shows the percentage difference in shine values generated by the different models and the participants' choices are included for completeness. For the Blonde, European-Brown and Oriental hair tresses the ROC_1 and ROC_2 gloss values not only replicate the participants' decisions but in some cases they can be related to the "health" of the tress. For example when Shine-Spray was applied to the Blonde hair tress it appeared unhealthy; 90% (30 out of 33 evaluations) participants chose the Virgin Blonde tress as the glossiest when compared with the Shine-Spray Blonde hair tress. ROC_1 and ROC_2 showed this decrease in shine whereas the other models predicted an increase in shine, which was contrary to the panel result.

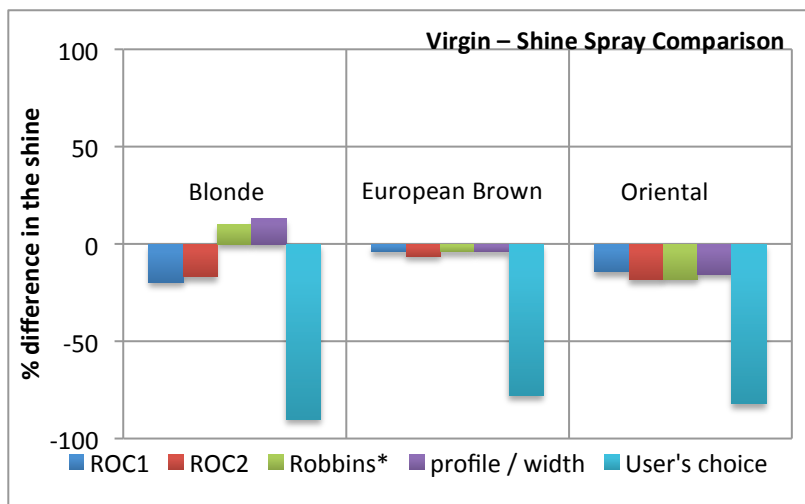
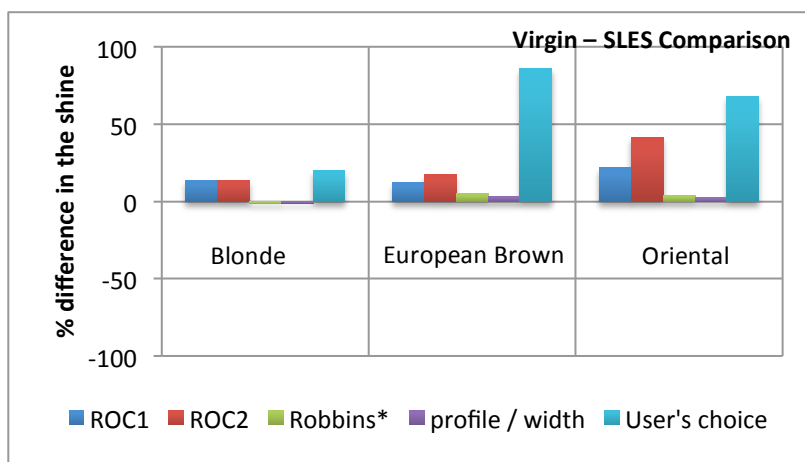
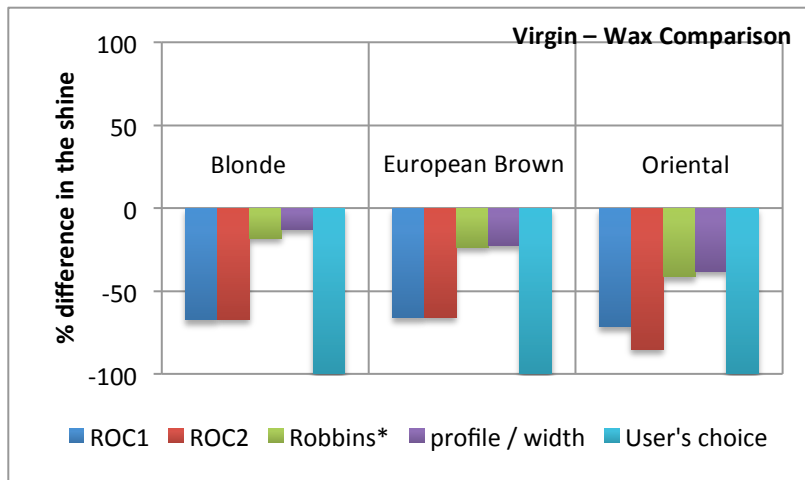


Figure 6-5 Percentage increase or decrease in shine values generated by the different models and participants' choice, between the left and right images of the hair tresses.

6.4 Future work

6.4.1 Tress Preparation

Applying different commercial products to virgin hair tresses produced four different levels of shine in this study. The shine range could be extended by increasing the range of hair products applied to the tresses. This could provide a more complete gloss scale for human hair tresses and hence be used to provide an indication of the sensitivity for each of the models. For a further increase in the perceived shine level, an oil based gloss treatment could be used.

6.4.2 Tress Evaluation Models

It was interesting to determine that the ROC_1 and ROC_2 models were identifying the difference between greasy looking hair and healthy hair. The Blonde tresses treated with Shine Spray were reported as looking “unhealthy” but the ROC models generated lower shine values when compared to the Virgin Blonde tress images (whereas other models showed an increase in shine). Further research is required to determine whether hair gloss correlates with perceived health.

The gloss evaluation models reported in the literature to date generate hair gloss values either from a single hair fibre, multiple hair fibre arrays or from a hair tress. Hair gloss evaluation in the Cosmetics Industry generally relies on panel studies or image analysis of hair tresses. Currently there is little work in the literature correlating the gloss evaluations of hair tresses to more complete models of a full head of human hair. Thus, it would be interesting to determine whether the hair tress gloss evaluations correlate to full hair gloss evaluation.

The ROC equations were tested on Blonde, European-Brown and Oriental hair tresses and the gloss values generated by these models showed a similar decision trend to human perception. The models should be tested on a wider set of natural hair types including red or grey. It would be interesting to determine what gloss values the ROC equations generate when the hair colour changes to red or grey.

The ROC models have not been assessed with dyed or bleached hair. It would be interesting to analyse the Chroma-specular bands of these types of hair and relate them to what is seen in natural hair types. This could potentially be used to design better colourants that would replicate the colour gradients observed in natural hair. It would be interesting to investigate how observers perceived the dyed/bleached hair and determine what factors contribute to the visual preference of hair and how this relates to “health”.

The ROC models have not been assessed with Negroid hair samples and although the sample presentation may need to be modified this should be tested.

Although research into hair tress gloss has been active for over thirty years the capture instrumentation has remained very similar. This suggests that the physical attributes of the hair tresses are being captured effectively but the models still fail to relate to human panel discriminations. One area of further research would be to use more extensive models of human visual processing. Vision Science has provided many models of visual processing but none specifically related to gloss. The evaluation of gloss could then be improved if we could model the visual experience of the panellist. The use of spatiochromatic models of human visual processing could be used to assess colour, texture, surround, ambient illumination and luminance of the visual stimulus. These models are currently predominantly used to assess colour differences in complex scenes and it would be interesting to investigate whether colour and gloss difference evaluation are intrinsically linked. Finally, it should be determined whether a more suitable set of standard gloss surfaces (a gloss scale) for hair gloss could be produced.

6.4.3 Tress Gloss Capture System

The Gonio image capture system developed in this study captures images of human hair tresses. It was designed to have flexibility of image capture in terms of angle of illumination and angle of image capture. It was also designed to be large enough to be able to take full head measurements of a mannequin head. As this was not performed during this study, further enhancements are needed to accommodate a full mannequin head. Measurements could then be used to simulate the natural appearance of a full head of hair. It would be interesting to compare the values generated from the hair tresses with values generated from hair attached to a mannequin ahead.

Further, analysis could be performed on the discrimination sensitivity of the image capture system and whether the system can effectively be used to capture full head hair data.

6.4.4 Virtual Tress Presentation

There is a body of literature that has not been examined in detail during this thesis. This is the computer graphics body of work that attempts to simulate photo-realistic images in terms of hair, fur and feathers. Using techniques such as Ray Tracing a simulation/prediction of the appearance of a full head of hair treated with a particular product could be produced onscreen. This could be validated against the images captured by the Gonio Image Capture System.

6.4.5 Psychophysical Evaluations of Gloss

This study used images of hair tresses to quantify the amount of gloss exhibited by hair tresses in a constrained imaging environment. Although the models produced results that correlate well to the psychophysical experiment, a further experiment to determine whether expert observers behave the same way as naïve observers when evaluating the shine of hair tresses would be valuable. The eyes tracking results could then be compared with the results obtained from the naïve observers.

The validity of judging hair tress gloss from digital images could be assessed by undertaking an eye-tracking study of real tresses. Although the number of hair tress samples needed would be extensive and the setup presentation time also significant this would produce a definitive dataset that could be used by the entire Industry and perhaps lead to an agreed assessment of hair gloss for the Cosmetics Industry.

References

6.5 References:

- Acharya, R., Tan, W., Yun Li, W., Ng, K. Y., Eddie, Min Choo, L., Chee, C., Gupta, M., Nayak, J. and Jasjit, S. S. (2008) 'The Human Eye' in U, R. A., Ng, E. Y. K. and Suri, J. S., eds., *Image Modeling of the Human Eye*, USA: Artech House inc.
- Barkas, W. W. (1939) 'Analysis of light scattered from a surface of low gloss into its specular and diffuse components', 51(274-295),
- Bayer, E. B. (1976) *Color imaging array*, US patent 3,971,065.
- Beigel, H. (1869) *The Human Hair : Its Structure, Growth, Diseases, and their Treatment*, London: Henry Renshaw.
- Berivan, E., Hasan, H., Sebnem, A. and Nuriye, K. (2008) 'Biomechanical properties of human hair with different parameters', *Skin Research and Technology*, 14(2), (147-151).
- Berns, R. S., Saltzman, M. and Billmeyer, F. W. (2000) *Billmeyer and Saltzman's principles of color technology*, John Wiley.
- Bloch, C., Bethke, D., Vogl, B. and Steinmuller, U. (2007) *The HDRI Handbook: High Dynamic Range Imaging for Photographers and CG Artists*, USA: Rocky Nook Inc.
- Bustard, H. K. and Smith, R. W. (1990) 'Studies of factors affecting Light-Scattering by individual Human Hair fibers', *International Journal of Cosmetic Science*, 12(3), (121-133).
- Bustard, H. K. and Smith, R. W. (1991) 'Investigation into the Scattering of Light by Human Hair', *Applied Optics*, 30(24), (3485-3491).
- Christie, J. S., Jr (1979) 'Review of geometric attributes of appearance', *Journal of coatings technology*, 51(653), (64-73).
- Czepluch, W., Hohm, G. and Tolkiehn, K. (1993) 'Gloss of Hair surfaces – Problems of visual Evaluation and possibilities for Goniophotometric measurements of treated strands.', *Journal of the Society of Cosmetic Chemists*, 44(6), (299-317).
- David A, A. and George, S. (2000) *Optics of the Human Eye*, Edinburgh: Butterworth-Heinemann.
- Derham W (1713) Chapter XII, of animals clothing. In: *Physico-theology: Or, a demonstration of the being and attributes of god, from his works of creation*. W. Innys, London
- Draelos, Z. D. (2008) 'Hair Cosmetics' in Blume-Peytave, U., Tosti, A., Whiting, D. A. and Trüeb, R. M., eds., *Hair Growth and Disorders*, Germany: Springer.

- Dutcher, T. F. (1951) 'Iron, Copper and Ash Content of Human Hair of Different Colors¹', *The Journal of Investigative Dermatology*, 17(2), 65.
- Erik, B., Havitcioglu, H., Aktan, S. and Karakus, N. (2008) 'Biomechanical properties of human hair with different parameters', *Skin Research and Technology*, 14(2), 147-151.
- Fairchild, M. D. (2005a) 'Human Color Vision' in *Color Appearance Models*, Second ed., England: John Wiley & Sons Ltd.
- Fairchild, M. D. (2005b) 'Psychophysics' in *Color Appearance Models*, Second ed., England: John Wiley & Sons Ltd.
- Fan, J. and Gijbels, I. (1996) 'Local Polynomial Modelling and its Applications', London: Chapman & Hall
- Fechner, G. T. (1966). Elements of psychophysics (Vol. 1). (H. E. Adler, Trans.). New York: Holt, Rinehart & Winston. (Original work published 1860).
- Gao, T., Moses, C. and Landa, P. (2010) 'Hair Vibrance Factor', (PDF. Presentation provided by CRODA)
- Gao, T., Pereira, A. and Zhu, S. (2009) 'Study of hair shine and hair surface smoothness', *International Journal of Cosmetic Science*, 60, 10.
- Gonnet, J.-F. (1998) 'Colour effects of co-pigmentation of anthocyanins revisited—1. A colorimetric definition using the CIELAB scale', *Food Chemistry*, 63(3).
- Guioulet, A., Garson, J. C. and Levecque, J. L. (1987) 'Study of the Optical-properties of Human-Hair', *International Journal of Cosmetic Science*, 9(3), 111-124.
- Guthrie, J. C., Morton, D. H. and Oliver, P. H. (1954) 'An investigation into Bending and Torsional Rigidities of some Fibers', *Journal of the Textile Institute*, (45).
- Halal, J. (2002) 'Hair Structure and Chemistry Simplified', New York, Delmar Cengage Learning.
- Harrison, V. G. W. (1945) *Definition and Measurement of Gloss : A survey of published literature*, London: The Printing and Allied Trades Research Association.
- Hashimoto, K. (1988) 'The structure of human hair', *Clinics in Dermatology*, 6(4).
- Hill, A. R. (1997) 'How we see colour' in McDonald, R., ed. *Colour Physics for Industry*, Second ed., Society of Dyers and Colourists.
- Howell, H. G., Mieszkis, K. W. and Tabor, D. (1959) 'Friction in textiles', 263p.

- Hunt, R. W. G. (1998) 'Colour Vision' in *Measuring Colour*, Third ed., England: Fountain Press England.
- Hunt, R. W. G. (2004) *The Reproduction of Colour*, 6th ed. ed., Chichester, England: John Wiley & Sons.
- Hunter, R. S. (1937) 'Methods of determining gloss', *Journal of Research, NBS*.
- Hunter, R. S. (1975a) 'Instruments for the Geometric Attributes of Object Appearance' in *The Measurement of Appearance*, USA: John Willy & Sons.
- Hunter, R. S. (1975b) 'Scales for Gloss and other Geometric attributes' in *The Measurement of Appearance*, USA: John Willy & Sons.
- Ingersoll, L. R. (1914) 'A means to measure the glare of paper.', *Electr. World* 63, (645-647)
- Ingersoll, L. R. (1921) 'The Glarimeter: An instrument for measuring the gloss of paper', *Journal of the Optical Society of America*, V(3), 213-217.
- Johnson, G. M. and Fairchild, M. D. (2003) 'Visual Psychophysics and color appearance' in Sharma, G., ed. *Digital Color Imaging Handbook*, USA: CRC Press.
- Jones, L. N. (2001) 'Hair structure anatomy and comparative anatomy.', *Clinics in Dermatology*, 19(2).
- Kantowitz, B. H., Roediger III, H. L. and Elmes, D. G. (2008) 'Psychophysics' in *Experimental Psychology*, 9th ed., USA: Wadsworth.
- Kaplan, P. D., Park, K., Qi, J. and Yang, K. (2010) 'The shine problem in hair: Review of imaging methods and measures for luster', *International Journal of Cosmetic Science*, 32(2), 155-155.
- Keis, K., Ramaprasad, K. R. and Kamath, Y. K. (2004a) 'Effect of hair color on luster (vol 55, pg 423, 2004)', *Journal of Cosmetic Science*, 55(6), 568-568.
- Keis, K., Ramaprasad, K. R. and Kamath, Y. K. (2004b) 'Studies of light scattering from ethnic hair fibers', *International Journal of Cosmetic Science*, 26(4), 218.
- Kittler, R. (2007) 'Daylight Prediction and Assessment: Theory and Design Practice', *Architectural Science Review*, 50(2), 94-99.
- Kumar, P. and MacDonald, L. (2006) *Measuring gloss by digital photography*, translated by Eschbach, R. M., Gabriel G., San Jose, CA, USA: SPIE.

- Lefaudeux, N., Lechocinski, N., Clemenceau, P. and Breugnot, S. (2008) 'New luster formula for the characterization of hair tresses using polarization imaging', *International Journal of Cosmetic Science*, 32(2), 157.
- Lindstrand, M. (2002) *Gloss: measurement, characterization and visualization-in the light of visual evaluation*, unpublished thesis Institute of Technology Linkopings Univeristy (Sweden).
- Liu, Y., Hong, L., Wakamatsu, K., Ito, S., Adhyaru, B., Cheng, C.-Y., Bowers, C. R. and Simon, J. D. (2005) 'Comparison of Structural and Chemical Properties of Black and Red Human Hair Melanosomes', *Photochemistry and Photobiology*, 81(1).
- Lu, R., Koenderink, J. J. and Kappers, A. M. L. (1998) 'Optical Properties (bidirectional reflection distribution functions) of Velvet', *Applied Optics*, 37(25).
- Luo, W. (2008) *Assessment of Tooth Colour using Digital Imaging*, unpublished thesis University of Leeds.
- Marschner, S. R., Westin, S. H., Lafortune, E. P. F. and Torrance, K. E. (2000) 'Image-Based Bidirectional Reflectance Distribution Function Measurement', *Journal of Applied Optics*, 39(16), 2592.
- McDonald, R. (1997) *Colour Physics for Industry*, Second Edition ed., Society of Dyers and Colourists.
- McMullen, R. and Jachowicz, J. (2003) 'Optical properties of hair: Effect of treatments on luster as quantified by image analysis', *Journal of Cosmetic Science*, 54(4), 335-351.
- McMullen, R. and Jachowicz, J. (2004) 'Optical properties of hair - Detailed examination of specular reflection patterns in various hair types', *Journal of Cosmetic Science*, 55(1), 29-47.
- Mendoza, F., Dejmek, P. and Aguilera, J. M. (2010) 'Gloss measurements of raw agricultural products using image analysis', *Food Research International*, 43(1), 18-25.
- Nakamura, J. (2006) 'Basics of Image Sensors' in Nakamura, J., ed. *Image sensors and signal processing for digital still cameras*, USA: Taylor & Francis.
- Nickerson, D. (1957) 'A New Cotton Lustermeter for Yarns and Fibers', *Textile Research Journal*, 27(2), 111.
- Nicodemus, F. E. (1965) 'Directional Reflectance and Emissivity of an Opaque Surface', *Applied Optics*, 4(7).

- Nikiforidis, G. (1992) 'Mechanical parameters of human hair: possible application in the diagnosis and follow-up of hair disorders', *Clinical physics and physiological measurement*, 13, 281.
- Palmer, J. M. and Grant, B. G. (2010) *Art of Radiometry*, USA: SPIE.
- Ramanath, R., Snyder, W. E., Yoo, Y. and Drew, M. (2005) 'Color image processing pipeline', *Signal Processing Magazine, IEEE*,
- Ratliff, F. (1984) 'Why Mach Bands are not seen at the edges of a step', *Vision Research*, 24(2).
- Reich, C. and Robbins, C. R. (1993) 'Light-Scattering and Shine measurements of Human hair – A sensitive probe of the Hair surface ', *Journal of the Society of Cosmetic Chemists*, 44(4), 221-234.
- Reiger, M. M. (2000) *Harry's Cosmeticology*, 8 ed., Chemical Publishing Company Inc.
- Reinhard, E., Ward, G., Pattanaik, S. and Debevec, P. (2006a) *High Dynamic Range Imaging : Acquisition, Display, and Image-Based Lighting*.
- Reinhard, E., Ward, G., Pattanaik, S. and Debevec, P. (2006b) 'Light and Color' in *High Dynamic Range Imaging : Acquisition, Display, and Image-Based Lighting*, USA: Morgan Kaufmann Publishers.
- Rennie, J. H., Bedford, S. E. and Hague, J. D. (1997) 'A model for the shine of hair arrays', *International journal of cosmetic science*, 19(3), 131-40.
- Rigg, B. (1997) 'Colorimetry and the CIE system' in McDonald, R., ed. *Colour Physics for Industry*, Second Edition ed., Society of Dyers and Colourists.
- Robbins, C. R. (2002a) 'Chemical Composition' in *Chemical and Physical Behavior of Human Hair*, 4th Edition ed., New York: Springer - Verlag.
- Robbins, C. R. (2002b) 'Morphological and Macromolecular Structure' in *Chemical and Physical Behavior of Human Hair*, 4th Edition ed., New York: Springer - Verlag.
- Robbins, C. R. (2002c) 'The Physical and Cosmetic Behavior of Hair' in *Chemical and Physical Behavior of Human Hair*, 4th Edition ed., USA: Springer-Verlag.
- Rook, A. (1965) 'Endocrine Influences on Hair Growth', *British Medical Journal*, 1, 16.
- Roy, B. (2000) 'Defining Color' in *Principles of Color Technology*, Third edition ed., USA: John Wiley & Sons.

- Rushton, H. (2006) 'Hair Structure', *Society of Cosmetic Scientists, Distance Learning*, Unit 12)
- Schueller, R. (1999) *Conditioning Agents for Hair and Skin*, New York: Marcel Dekker, INC.
- Scott, G. V. and Robbins, C. R. (1978) 'Stiffness of human hair fibers', *Journal of The Society of Cosmetic Chemists*, (29), 17.
- Silvennoinen, R., Peiponen, K.-E. and Myller, K. (2007) 'Specular Gloss' in *Specular Gloss*, Finland: Elsevier.
- Sinclair, R. S. (1997) 'Light, light sources and light interactions' in McDonald, R., ed. *Colour Physics for Industry*, Society of Dyers and Colourists.
- Stamm, R. F., Garcia, M. L. and Fuchs, J. J. (1977a) 'Optical-Properties of Human hair. 1. Fundamental considerations and Goniophotometer curves', *Journal of the Society of Cosmetic Chemists*, 28(9), 571-599.
- Stamm, R. F., Garcia, M. L. and Fuchs, J. J. (1977b) 'Optical-Properties of Human hair. 2. Luster of Hair fibers', *Journal of the Society of Cosmetic Chemists*, 28(9), (601-609).
- Swift, J. A. (1997) *Fundamentals of human hair science*, Wewymouth: Micelle Press.
- Tobii Technology AB (2010) ', Tobii Studio, User Manual, Manual release 1.0, september 2010 URL: www.tobii.com
- Tomes, C. (2008) 'The Effect of Chemical Derivatives on Hair Processing', *Thesis, The University of Manchester*.
- Toomey, M. B., Butler, M. W., Meadows, M. G., Taylor, L. A., Fokidis, H. B. and McGraw, K. J. (2010) 'A novel method for quantifying the glossiness of animals', *Behavioral Ecology and Sociobiology*, 64(6), 1047-1055.
- Toyoda, K. (2006) 'Digital Still Cameras at a Glance' in Nakamura, J., ed. *Image sensors and signal processing for digital still cameras*, USA: Taylor & Francis.
- Tribble, A. C. (2000) *Fundamentals of Contamination Control*, Washington: SPIE - The International Society for Optical Engineering.
- Vogt, A., McElwee, K. J. and Blume-Peytavi, U. (2008) 'Biology of the Hair Follicle' in Blume-Peytavi, U., Tosti, A., Whiting, D. A. and Trüeb, R. M., eds., *Hair Growth and Disorders*, Germany: Springer.
- Ward, G. J. (1992) 'Measuring and modeling anisotropic reflection', *SIGGRAPH Computer Graphics*, 26.

- Wolfram, L. J. (2003) 'Human hair: A unique physicochemical composite', *Journal of the American Academy of Dermatology*, 48(6), S106.
- Wortmann, F. and Schulze, E. (2003) 'Analyzing the laser-light reflection from human hair fibers. I. Light components underlying the goniophotometric curves and fiber cuticle angles', *Journal of Cosmetic Science*, 54(3), 301-316.
- Zaraga, F. and Langfelder, G. (2010) 'White balance by tunable spectral responsivities.', *The Journal of the Optical Society of America*, 27.
- Zviak, C. (1986) *The science of hair care*, New York: M. Dekker.

Appendix A

International standards connecting to the evaluation of appearance of surface	
AS/NZS 1580.481.1.2:1999	Paints and related materials, method of test, coatings, exposed to weathering and change in gloss
AS/NZS 1580.602.2:1995	Paints and relating materials: method of test and measurement of specular gloss of non-metallic paint films at 20 ⁰ , 60 ⁰ and 85 ⁰
AS/NZS 3750.10:1994	Paints for steel structures and full gloss epoxy
ASTM C346-87 (2004)e1	Standard test method for 45 ⁰ specular gloss of ceramic materials
ASTM C584-81 (1999)	Standard test method for of glazed ceramic whitewares and related products
ASTM D1003-92	Test method for haze and luminous transmittance of transparent plastics
ASTM D1223-93 (1998)	Standard test method for specular gloss of paper and paperboard at 75 ⁰
ASTM D1455-87 (2002)	Standard test method for 60 ⁰ specular gloss of emulsion floor polish
ASTM D1834-90	Test method for 20 ⁰ specular gloss of waxed paper
ASTM D2457-03	Standard test method for specular gloss of plastic films and solid plastic
ASTM D3134-97 (2003)	Standard practice for establishing colour and gloss tolerances
ASTM D3928-00a (2005)	Standard test method for evaluation of gloss or sheen uniformity
ASTM D4039-93(2004)	Standard test method for reflection haze of high-gloss surfaces
ASTM D4449-90 (2003)	Standard test method for visual evaluation of gloss differences between surfaces of similar appearance
ASTM D985-93	Test method for brightness of pulp, paper and paperboard (directional reflectance at 457 nm)
ASTM D523-89 (1999)	Standard test method for specular gloss
ASTM D5767-95(2004)	Standard test method for instrumental measurement of distinctness of image gloss of coating surfaces
ASTM D7163-05	Standard test method for specular gloss of printed matter
ASTM E167 91	Practice for goniophotometry of object and materials
ASTM D 179 91a	Guide for selection of geometric conditions for

	measurement of reflection and transmission properties of materials
ASTM E275-93	Practice for describing and measuring performance of ultraviolet, visible and near infrared spectrophotometers
ASTM E284-93a	Terminology of appearance
ASTM E1331-04	Standard test method for reflectance factor and colour by spectrophotometry using hemispherical geometry
ASTM E1349-90 (1998)	Standard test method for reflectance factor and colour by spectrophotometry using bidirectional geometry
ASTM E284-05a	Standard terminology of appearance
ASTM D429-91	Test method for measurement and calculation of reflecting characteristics of metallic surfaces using integrating sphere instruments
ASTM E430-05	Standard test method for measurement of gloss of high-gloss surfaces by abridged goniophotometry
DIN EN 12373-11	Aluminium and aluminium alloys, anodizing: measurement of specular reflectance and specular gloss of anodic oxidation coatings at angles 20°, 45°, 60° or 85°
DIN EN 12373-12	Aluminium and aluminium alloys, anodizing: measurement of reflectance characteristics of aluminium surfaces using integrating sphere instruments
DIN EN 12373-13	Aluminium and aluminium alloys, anodizing: measurement of reflectance characteristics of aluminium surfaces using a goniophotometer or an abridged goniophotometer
DIN EN 13523-2	Coil-coated metals, test methods, part 2: specular gloss
DIN EN 13722	Furniture and assessments of the surface gloss
DIN EN 14086	Paper and board, measurement of specular gloss and 45° gloss with a parallel beam (DIN method)
GB/T 11420-1989	Measurement of specular gloss of vitreous and porcelain enamels
GB/T 12032-1989	Paper and board preparation of a offset print for test gloss
GB/T 13891-1992	Test methods of specular gloss for decorative building materials
GB/T 15614-1995	Method for measuring the glossiness of ceramic pigment
GB/T 3295-1996	Standard test method for 45° specular gloss of ceramic ware

GB/T 8686-1988	Textile fabrics: test method of gloss
GB/T 9754-1988	Paints and varnishes: measurement of specular gloss of non-metallic paint films at 20°, 60° and 85°
ISO 2813:1994	Paint and varnishes: determination of specular gloss of non-metallic paint films at 20°, 60° and 85°
ISO 6719: 1986	Anodized aluminium and aluminium alloys: measurement of reflectance characteristics of aluminium surfaces using integrating sphere instrument
ISO 7668: 1986	Anodized aluminium alloys: measurement of specular reflectance and specular gloss at angles of 20°, 45°, 60° or 85°
ISO 7759: 1983	Anodizing of aluminium and its alloys: measurement of reflectivity characteristics of aluminium surfaces using abridged goniophotometer or goniophotometer
ISO 8254-1:1999	Paper and board, measurement of specular gloss, part 1: 75° gloss with a parallel beam, DIN method
ISO 8254-2:2003	Paper and board, measurement of specular gloss, part 2: 75° gloss with a converging beam, TAPPI method
ISO 8254-3:2004	Paper and board, measurement of specular gloss, part 3: 20° gloss with a converging beam, TAPPI method
JIS K 5600-4-7:1999	Testing method for paints, part 4: visual characteristics of film; Section 7: specular gloss
JIS Z 8741:1997	Specular glossiness: method of measurement

Appendix B

Visual Assessment

There are three sets of hair tresses,

Set A contains the heat treated tresses

Set B contains the mechanically treated tresses and

Set C contains the chemically treated tresses.

You will be asked to rank the tresses depending upon the shine, in each set (1 is least Glossy).

A Remarks column has been added if you want to add your thoughts.

University of Manchester

Participant's Details

Name		
Gender	<input type="checkbox"/> Male <input type="checkbox"/> Female	
Age-band	<input type="checkbox"/> 10-19 <input type="checkbox"/> 20-29 <input type="checkbox"/> 30-39 <input type="checkbox"/> 40-49 <input type="checkbox"/> 50-59	
Colour Vision	<input type="checkbox"/> Normal <input type="checkbox"/> Colour-Blind	
Vision	<input type="checkbox"/> 6/6 <input type="checkbox"/> Near-sighted <input type="checkbox"/> Far-sighted	
Eye-Correction	<input type="checkbox"/> Glasses <input type="checkbox"/> No-Glasses <input type="checkbox"/> Contact lens	
<input type="checkbox"/> Left Handed	<input type="checkbox"/> Right Handed	

Tress Gloss evaluation test (Created by Syed Rizvi, Supervisor: Dr. Huw Owens)

Tress ID	Ranking (1 to 6)	Remarks
101		
102		
103		
104		
105		
106		

Tress Set A (Heat treated tresses)

Tress ID	Ranking (1 to 6)	Remarks
108		
109		
110		
111		

Tress Set B (Mechanically treated tresses)

Tress ID	Ranking (1 to 5)	Remarks
112		
113		
114		
115		
116		

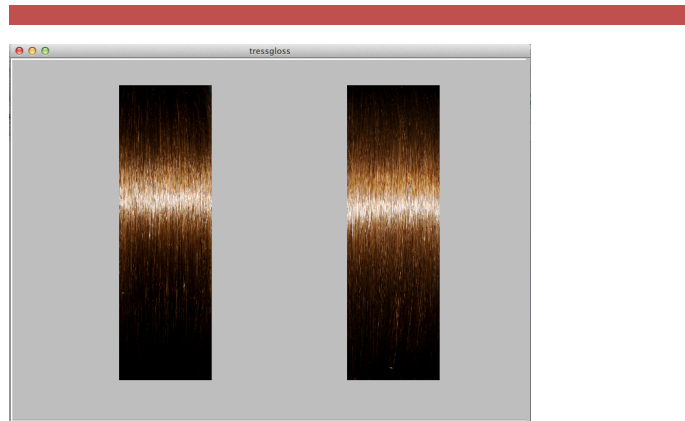
Tress Set C (Chemically treated tresses)

Appendix C

UID	Name	Gender	Age-Band	Colour-Vision	Vision	Eye-Correction	Hand	File name	Rank	Rank 2nd	Rank 3rd	Average
6b21d6a7-6f48-4d5e-bb30-f4316ab4eae3	M****	Male	20-30	Normal Vision	6/6 Vision	NO Glasses	Right Handed	DSCN3511daylight.JPG	8	9	9	8.67
6b21d6a7-6f48-4d5e-bb30-f4316ab4eae3	M****	Male	20-30	Normal Vision	6/6 Vision	NO Glasses	Right Handed	DSCN3514daylight.JPG	8	8	7	7.67
6b21d6a7-6f48-4d5e-bb30-f4316ab4eae3	M****	Male	20-30	Normal Vision	6/6 Vision	NO Glasses	Right Handed	DSCN3844daylight.JPG	8	8	6	7.33
6b21d6a7-6f48-4d5e-bb30-f4316ab4eae3	M****	Male	20 to 30	Normal Vision	6/6 Vision	NO Glasses	Right Handed	DSCN3847daylight.JPG	8	7	8	7.67
6b21d6a7-6f48-4d5e-bb30-f4316ab4eae3	M****	Male	20 to 30	Normal Vision	6/6 Vision	NO Glasses	Right Handed	DSCN3850daylight.JPG	3	2	2	2.33
602cf818-9fa3-4bc6-b34b-428302a38f1e	P****	Female	20 to 30	Normal Vision	Farsighted	Glasses	Right Handed	DSCN3511daylight.JPG	7	8	8	7.67
602cf818-9fa3-4bc6-b34b-428302a38f1e	P****	Female	20 to 30	Normal Vision	Farsighted	Glasses	Right Handed	DSCN3514daylight.JPG	8	6	5	6.33
602cf818-9fa3-4bc6-b34b-428302a38f1e	P****	Female	20 to 30	Normal Vision	Farsighted	Glasses	Right Handed	DSCN3844daylight.JPG	5	5	5	5
602cf818-9fa3-4bc6-b34b-428302a38f1e	P****	Female	20 to 30	Normal Vision	Farsighted	Glasses	Right Handed	DSCN3847daylight.JPG	4	4	4	4
602cf818-9fa3-4bc6-b34b-428302a38f1e	P****	Female	20 to 30	Normal Vision	Farsighted	Glasses	Right Handed	DSCN3850daylight.JPG	3	2	4	3
0fcacff4-112c-46b3-a2fd-0db40869305b	S****	Male	20 to 30	Normal Vision	Farsighted	Glasses	Left Handed	DSCN3511daylight.JPG	9	9	9	9

*Border and column names have been added for the ease of reading

Appendix D



Pair Comparison (Forced Choice) Psychophysical Experiment

Instruction Sheet

In this experiment two images of the hair tresses will appear on the screen. Your task is to choose the shiniest one out of two. This test is a Pair comparison (forced choice) test, which is part of Psychophysical experiment. We have developed a MATLAB program Tress-Gloss 2.0, which will collect your details (related to the experiment) and display tress images on the screen. You can register your choice by pressing a number key. Number key 1 represents left image and number key 2 represents right image. As soon as you register your choice another pair will appear on the screen and it will keep on going till all the comparison have been done. In this study 12 images have been used and there will be 66 pair comparisons in total.

To understand how people behave, when they evaluate shine, we are running this program on an eye-tracker. The eye-tracker will record your eye movements and save it as a movie. During this experiment only your eye-movements have be captured, no voice or videos are recorded. I will do a live demo and will go through each step of the experiment. If you want to know more about the study I will be happy to give you more information about it. My email id is syed.n.rizvi@postgrad.manchester.ac.uk and my desk is in Mezz 3, Sackville street building.

Thanks for being part of the experiment.